Sheffield Hallam University

Interaction and Functional Impact of Colorectal Cancer Extracellular Vesicles on Escherichia coli

MAANI, Rawan

Available from the Sheffield Hallam University Research Archive (SHURA) at:

https://shura.shu.ac.uk/35645/

A Sheffield Hallam University thesis

This thesis is protected by copyright which belongs to the author.

The content must not be changed in any way or sold commercially in any format or medium without the formal permission of the author.

When referring to this work, full bibliographic details including the author, title, awarding institution and date of the thesis must be given.

Please visit https://shura.shu.ac.uk/35645/ and http://shura.shu.ac.uk/information.html for further details about copyright and re-use permissions.

Interaction and Functional Impact of Colorectal Cancer Extracellular Vesicles on *Escherichia coli*

Rawan Maani

A thesis submitted in partial fulfilment of the requirements of
Sheffield Hallam University
for the degree of Doctor of Philosophy

October 2024

Candidate Declaration

I hereby declare that:

1. I have not been enrolled for another award of the University, or other academic or professional organisation, whilst undertaking my research degree.

2. None of the material contained in the thesis has been used in any other submission for an academic award.

3. I am aware of and understand the University's policy on plagiarism and certify that this thesis is my own work. The use of all published or other sources of material consulted have been properly and fully acknowledged.

4. The work undertaken towards the thesis has been conducted in accordance with the SHU Principles of Integrity in Research and the SHU Research Ethics Policy.

5. The word count of the thesis is 35,000

Name	Rawan Maani
Award	PhD
Date of Submission	2nd October 2024
Research Institute	Biomolecular Sciences Research Centre
Director(s) of Studies	Dr Nicholas Peake

Dedication

To my people, **to my beloved homeland**, **to PALESTINE**.

I dedicate this to you with all my heart. I wish for each of you to have the opportunities I've had—to follow your dreams, receive the education you deserve, and live safely and happily.

Table of Contents

List of Tables

List of Figures

Acknowledgement

Completing PhD journey has been a profound experience, and it would not have been possible without the support, encouragement, and guidance of many remarkable individuals.

First and foremost, I would like to express my deepest gratitude to my supervisors, Nick Peake, Mel Lacey, and Sarah Forbes. Thank you for your guidance and belief in my potential. Your expertise, support, and encouragement have been instrumental in shaping this research.

A special thanks to Celine, your expertise and assistance have been crucial to the successful completion of this work. Your meticulous attention to detail and your willingness to help at every step have been greatly appreciated.

To all the collaborators who played a pivotal role in the success of this work. A special thank you to Prof. Chris Hill, NanoFCM team, and Dr. Lewis Quayle for their collaboration and contributions, which were instrumental in the advancement of this research. I would also like to express my sincere gratitude to the NHS staff and blood donors.

To my husband, Ahmed, who has been my constant source of strength and inspiration. Your unwavering belief in me and your endless support have carried me through every challenge.

To my daughter, Lamar, you have been my source of joy. Your bright smiles and boundless energy have given me the motivation to persevere, even on the most challenging days. I hope this achievement will inspire you to follow your dreams with passion and determination.

I would like to express my deepest gratitude to my family. Especially my mum who has been my constant source of strength and inspiration.

I am also deeply thankful to my colleagues, Rob, Sonia, Charlotte, Chloe, Lucy, Kelly, Sam, and Sarah. Your support has been invaluable, and I am fortunate to have worked alongside such talented individuals.

To my friends, especially Dallal, thank you for your unwavering support. Your friendship has been a source of comfort and joy, and I am grateful for the laughter, encouragement, and moments we have shared throughout this journey.

Abstract

The human gut microbiota plays a vital role in regulating various physiological processes, and alterations in the composition and function of the microbial community (dysbiosis) are associated with the pathogenesis of colorectal cancer (CRC). Although the causative link between CRC and microbiota is widely investigated, the underlying microbiota-tumour interactions are not well understood, yet. It is evident that CRC-derived extracellular vesicles (EVs) have an impact on various oncogeneses processes, however, their impact on the surrounding microbiota is not clear. Therefore, this project hypothesises that EVs have an impact on the microbiota, supporting the disease-linked interactions between host and microbiota, and contributing to dysbiosis.

CRC cell lines (SW480, SW620) were cultured in CELLine AD 1000 bioreactor flasks, blood was collected from CRC patients and healthy individuals, and colon tissue was collected from CRC patients. EVs were isolated from CRC-cell line culture media, blood plasma, and digested tissues by size-exclusion chromatography (SEC) and characterised by nanoparticle flow cytometry (NanoFCM), western blotting, ELISA, and transmission electron microscopy (TEM). Confocal microscopy, TEM, Flow cytometry, and EVs-enzymatic treatments were performed to assess the interactions between EVs and *E. coli* strains (*E. coli* MG1655 (Laboratory strain) and *E. coli* 11G5 (CRC-associated strain)). Also, the impact of the EVs on *E. coli* phenotypic characteristics, growth and biofilm formation, and bacterial transcriptome were assessed by turbidimetric assay, microtiter plate assay, and transcriptomic analysis, respectively.

NanoFCM analysis showed a high yield of EVs with characteristic size profiles, EV markers detection confirmed the presence of EVs, and TEM revealed the double-membranous structure of EVs. TEM analysis indicated an interaction between the EVs and *E. coli* with clear surface binding. Flow cytometry analysis showed that *E. coli*-EVs interactions are disease-stage specific and bacterial-strain specific. EV treatment had an impact on bacterial phenotypic characteristics; an increase in *E. coli* growth and a decrease in the ability of the bacteria to form biofilm were observed. It also resulted in an upregulation of genes which are involved in bacterial motility, the flagella structure of *E. coli* such as *fliA*, and a downregulation of genes involved in the zinc-ion uptake system such as *ZinT*. Overall, EVs appeared to be capable of mediating CRC-microbiome interactions and altering bacterial phenotypes; bacterial growth and ability to form biofilm.

Abbreviation

AMPs	Antimicrobial peptides
APC	Adenomatous polyposis coli
B. fragilis	*Bacteroides fragilis*
BEVs	Bacterial extracellular vesicles
BSA	Bovine serum albumin
C. parvum	*Cryptosporidium parvum*
CAFs	Cancer-associated fibroblasts
c-di-GMP	Cyclic-diguanylic-acid
CIMP	CpG island methylator phenotype
CIN	Chromosomal instability
CM	Culture medium
CPDs	CRC patient donors
CRC	Colorectal cancer
CSC	Colon stem cells
DGC	Density gradient centrifugation
DMEM	Dulbecco's modified Eagle's medium
E. coli	*Escherichia coli*
ECM	Extracellular matrix
EGFR	Epidermal growth factor receptor
EoCRC	Early-onset colorectal cancer
EPS	Extracellular polymeric substances
F. nucleatum	*Fusobacterium nucleatum*
FAP	Familial adenomatous polyposis
FBS	Foetal bovine serum
FMT	Faecal microbiota transfer
GO	Gene ontology
HDs	Healthy blood donors

HRP	Horseradish peroxidase
IBD	Inflammatory bowel disease
InDel	Insertion-deletion
ISEV	International Society of Extracellular Vesicles
LB	Luria-Bertani
miR, miRNA	microRNA
MISEV	Minimal information for studies of extracellular vesicles
MMPs	Matrix metalloproteases
MMPsi	Matrix metalloproteases inhibitor
MSH2	DNA mismatch repair protein
MSI	Microsatellite instability
NanoFCM	Nano-flow cytometry
OD	Optical density
OMVs	Outer membrane vesicles
P. aeruginosa	*Pseudomonas aeruginosa*
P/S	Penicillin and streptomycin
PBS	Phosphate buffered saline
PK	Proteinase-k
pks	Polyketide synthase
RNAase	Ribonuclease
SCFAs	Short-chain fatty acids
SEC	Size exclusion chromatography
SEM	Standard error of the mean
SNV	Single nucleotide variant
TEM	Transmission electron microscopy
TGF-β	Transforming growth factor-beta
TGF-β	Tumour growth factor beta
TME	Tumour microenvironment
TMN	Tumour-node-metastasis
TP53	Tumour protein 53
TRF	Time-resolved fluorescence

Tryp	Trypsin
UC	Ultracentrifugation
VEGF	Vascular endothelial growth factor
WNT	Wingless/Integrated

1 Introduction

1.1 Colorectal cancer

CRC is a tumour that develops in the tissues of the large intestine, specifically, in the colon (colon cancer) or rectum (rectal cancer). The colon's main functions are water and certain nutrient absorption, and faeces storage and excretion. The rectum's main function is defecation, along with the absorption of small amounts of water, salt, glucose, and some drugs (Duan et al., 2022). Common symptoms of CRC include abdominal pain, diarrhoea, constipation, blood in the stool, weight loss, fatigue, and low iron levels. Many people do not exhibit symptoms in the early stages of the disease (Skalitzky et al., 2023).

1.1.1 CRC incidence and epidemiology

CRC is one of the most prevalent cancer types worldwide, ranking as the third most common malignancy and the second leading cause of cancer-related mortality. It accounts for approximately 10% of all cancers diagnosed annually, with the highest incidence observed in developed countries, where the rate is nearly four times higher than in developing countries (Sung et al., 2021). Also, incidence and mortality in women are approximately 25% lower than in men (Dekker, Tanis, Vleugels, Kasi, & Wallace, 2019). In 2020, nearly two million new cases and one million deaths were estimated to have occurred, and the incidence is predicted to rise to 2.5 million new cases by 2035 (Dekker, Tanis, Vleugels, Kasi, & Wallace, 2019; Sung et al., 2021). CRC can be classified as either hereditary or sporadic, hereditary CRC is linked to inherited gene mutations and accounts for 10-16% of CRC cases. Inflammatory/sporadic CRC is often associated with inflammatory bowel diseases and accounts for more than 80% of all CRC cases (Hampel, Kalady, Pearlman, & Stanich, 2022).

CRC is one of the cancers that most commonly spreads to the liver, lungs, ovaries, and other parts of the gastrointestinal tract. More than 70% of CRC-related deaths are caused by metastases to the liver (Neo et al., 2010). Although new treatments have improved the outcome and surgery can be curative, less than 25% of cases are operable. Inoperable cases, recurrent and metastatic CRC, are generally treated with palliative chemotherapy (Munro, Wickremesekera, Peng, Tan, & Itinteang, 2018). While the early stages of CRC are potentially curable, 50% of the cases are diagnosed at later stages. In stages I and II, where the tumour is confined to the wall of the intestine, the 5-year

survival rate is 70-90%. However, the 5-year survival rate of regional-stage (nodal; stage III) and distant-stage (metastatic; stage IV) is approximately 50-70% and 10-14%, respectively. This decline is due to the tumour's invasive behaviour, as it penetrates the intestinal wall and spreads via the lymphatics to lymph nodes and distant organs through the bloodstream (Fabregas, Ramnaraign, & George, 2022; Munro, Wickremesekera, Peng, Tan, & Itinteang, 2018). Nearly 50% of CRC patients experience tumour recurrence (Gupta, Bhatt, Johnston, & Prabhavalkar, 2019).

The incidence and mortality of CRC significantly vary between countries worldwide, this is due to differences in genetic factors, socioeconomic status, geographical characteristics, and exposure to various risk factors. Despite these variations in incidence among countries, the overall incidence has decreased due to effective early screening, early intervention, and treatment improvement (Baidoun et al., 2021). However, alarming rising trends show a rising incidence rate among younger individuals (<50 years old), with an increase of 1-2% each year. Approximately 11% of CRC occur in patients younger than 50 years for whom early screening typically is not recommended (Fabregas, Ramnaraign, & George, 2022; Kasi et al., 2019). It is projected that the incidence of colon and rectal cancers may increase by 90% and 124%, respectively, for the 20-34 years age group by 2030, though the causal link has yet to be established (Bailey et al., 2015). This alarming trend highlights the need for new preventative strategies.

1.1.2 CRC risk factors

Unlike many cancers, multiple factors are linked to the increased incidence of CRC (Baidoun et al., 2021; Brenner, Kloor, & Pox, 2014; Feizi et al., 2023; Song, Chan, & Sun, 2020). These factors include:

I. **Family history**: Some families with a history of CRC carry genetic mutations associated with the disease, accounting for 5-10% of CRC cases (Kastrinos, Samadder, & Burt, 2020).
II. **Age**: There is a linear relationship between age and CRC incidence, with the likelihood of developing CRC increasing markedly after the age of 50 (Gupta, Bhatt, Johnston, & Prabhavalkar, 2019).

III. **Gender**: The incidence rate of CRC is higher in males compared to females, regardless of age group (Patel, Karlitz, Yen, Lieu, & Boland, 2022).

IV. **Body weight:** Obesity has a significant effect on the carcinogenesis process, and patients with a high body mass index have a higher risk of developing CRC (Patel, Karlitz, Yen, Lieu, & Boland, 2022).

V. **Diet**: A high-fat diet and red meat consumption correlate with an increased risk of CRC. Conversely, higher intakes of dietary fibre, green leafy vegetables, folate, and calcium have been reported to be protective against CRC. A study showed an inverse correlation between high calcium consumption and CRC, as calcium activates immune cells and T cells, which are crucial in the immune defence against CRC (Zhang, Xuehong et al., 2016).

VI. **Alcohol intake**: Alcohol consumption has been linked to CRC as it causes damage to colon mucosa and stimulates pathogenic cellular proliferation (Keum & Giovannucci, 2019).

VII. **Smoking**: Smoking is considered a leading cause of many preventable cancers, including CRC. Interestingly, studies showed that smoking could modulate the gut microbiota (Bai, Xiaowu et al., 2022).

VIII. **Inflammatory bowel disease (IBD)**: Ulcerative colitis and Crohn's disease, the predominant forms of IBD, are linked to an increased risk of CRC (Birch et al., 2022).

IX. **Diabetes**: Type 2 diabetes has been identified as a high-risk factor for CRC through several potential pathophysiological and molecular mechanisms, including hyperinsulinemia, insulin-like growth factor axis, obesity, cytokines, and chronic inflammation (Yu, G., Li, Wei, & Jiang, 2022).

X. **Bacterial infections**: Pathogenic bacteria, such as certain strains of *Escherichia coli* (*E. coli*) and *Bacteroides fragilis* (*B. fragilis*), are linked to CRC. *E. coli* produce toxins, such as cytolethal distending genotoxin, that can disrupt cell differentiation and proliferation, apoptosis, and induce DNA damage (Wang, Y. & Fu, 2023). *B. fragilis*, found in CRC patients at higher levels compared to healthy individuals, is a critical pathogen that remodels the gut microbiota to promote CRC through interleukin-mediated inflammatory responses and toxin production, leading to adenoma development which can then be colonised with other pathogenic bacteria like *Fusobacterium nucleatum* (*F. nucleatum*) which

then further drive CRC tumorigenesis process (Wu, N. et al., 2022; Yusuf, Sampath, & Umar, 2023).

XI. **Altered gut microbiome (Dysbiosis)**: Dysbiosis of microbial gut communities is proposed to disrupt the mucosal barrier of the digestive tract, leading to chronic inflammation and eventually CRC (Quaglio, Grillo, De Oliveira, Di Stasi, & Sassaki, 2022).

1.1.3 CRC pathogenesis

The luminal surface of the colon is composed of a single layer of epithelial cells that are folded to form finger-like protrusions into the lumen, the spaces between these folds are defined as crypts (Figure 1.1). The normal gastrointestinal tract contains approximately 10^7 crypts, each housing small, normal colon stem cells (CSC) located at the base of the crypts within the stem-cell niche. These CSCs divide slowly and asymmetrically, generating transit-amplifying cells that migrate up the crypt, proliferate, and differentiate into goblet cells, enterocytes, enteroendocrine, and Paneth cells (Anderson, Hessman, Levin, Monroe, & Wong, 2011; Onfroy-Roy, Hamel, Foncy, Malaquin, & Ferrand, 2020; Pino & Chung, 2010). Accumulating evidence suggests that CSCs are pivotal in the initiation of CRC. They are immortal and can self-renew, studies proposed that CSCs can generate tumour cells with different phenotypes, leading to the regrowth of the original tumour and the development of a new tumour (Gupta, Bhatt, Johnston, & Prabhavalkar, 2019; Munro, Wickremesekera, Peng, Tan, & Itinteang, 2018).

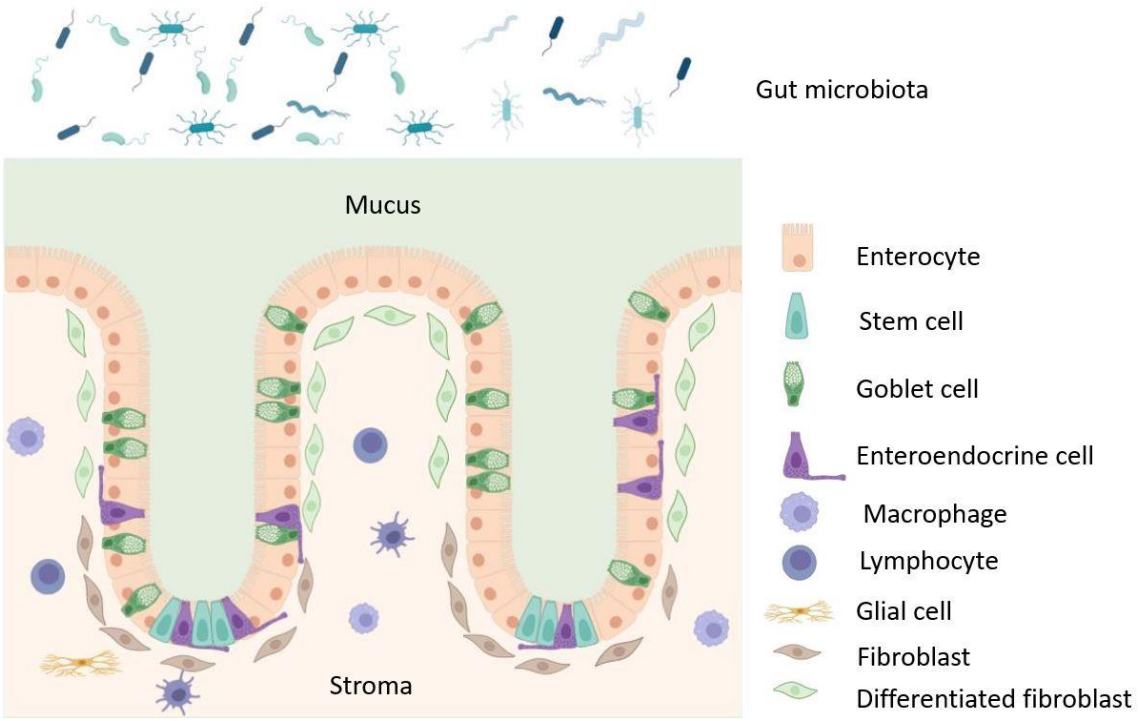

Figure 1.1: Schematic representation of the colonic crypt structure. The colonic epithelium (enterocyte) is organised as a continuous layer of columnar epithelial cells arranged into distinct crypt-like structures. Colon stem cells reside at the base of the crypts, giving rise to transit-amplifying cells that migrate along the crypt. These stem cells rapidly divide and differentiate into the functional cells of the colon, such as goblet cells and enteroendocrine cells. The underlying mucosal layer (stroma) consists of stromal cells, including immune cells and fibroblasts. The mucus layer forms a barrier separating the gut microbiome and colon epithelial cells.

CRC develops through a multistep carcinogenic process involving a series of histological, morphological, and genetic changes that accumulate over time (Simon, 2016). Mutations in specific genes can lead to the development of CRC, these mutations can occur in oncogenes, tumour suppressor genes, and genes involved in DNA repair mechanisms (Mármol, Sánchez-de-Diego, Pradilla Dieste, Cerrada, & Rodriguez Yoldi, 2017). In the adenoma-carcinoma model, consecutive point mutations in the tumour protein 53 (TP53), epidermal growth factor receptor (EGFR), wingless/integrated (WNT), and transforming growth factor-beta (TGF-β) signalling pathways lead to the initiation and progression of the tumour (Sedlak, Yilmaz, & Roper, 2023).

Cancers derived from point mutations are known as sporadic cancers and account for 70% of all CRC cases. The pathogenesis of sporadic CRC is heterogenous, as mutations

can occur in different genes. However, approximately 70% of CRC cases follow a specific sequence of mutations that leads to a particular morphological sequence, starting with adenoma and developing into carcinoma. The first mutation occurs in the tumour suppressor gene adenomatous polyposis coli (*APC*), which triggers the development of non-malignant adenomas, also called polyps. It was reported that around 15% of these polyps develop into carcinoma within ten years (Fearon & Vogelstein, 1990). The initial mutation in *APC* happens in CSC, leading to $APC^{+/-}$ mutant stem cells. The mutant cells can then colonise the base of the crypt and replace the non-mutant stem cells, once the second allele of *APC* is mutated, the crypt is filled with $APC^{-/-}$ cells, leading to the formation of a mono-cryptal adenoma. Subsequent mutations in oncogenes and tumour suppressor genes occur within this CSC population (Pino & Chung, 2010).

On the other hand, inherited cancers account for 5% of all CRC cases. They are caused by inherited mutations in one of the alleles of specific genes, and a subsequent point mutation in the second allele triggers tumour development. Inherited CRC is classified into two groups: polyposis and non-polyposis. Polyposis includes familial adenomatous polyposis (FAP), which is characterised by the formation of multiple malignant polyps in the colon (Lynch & de la Chapelle, 2003). Hereditary non-polyposis CRC, Lynch syndrome, is caused by mutations associated with DNA repair mechanisms genes, such as MSH2 (DNA mismatch repair protein). Lynch syndrome accounts for 2%-3% of all CRC cases (Stoffel & Kastrinos, 2014).

Genomic instability is a key feature of CRC and can be classified into three different pathogenic pathways; chromosomal instability (CIN), microsatellite instability (MSI), and CpG island methylator phenotype (CIMP). CIN refers to an accelerated rate of gains or losses of whole or large portions of chromosomes, resulting in karyotypic variability from cell to cell. It represents 80%-85% of all sporadic CRC cases and is characterised by chromosomal imbalance, leading to aneuploidy, sub-chromosomal genomic amplifications, and loss of heterozygosity (Pino & Chung, 2010).

The second pathway, MSI, results from defects in the DNA mismatch repair system and is characterised by instability in stretches of DNA microsatellites. Tumours with microsatellite instability have a decreased ability to repair short DNA chains or tandem repeats (two to five base-pair repeats). Finally, the CIMP pathway is characterised by gene silencing due to hypermethylation of CpG islands-short sequences rich in the CpG

dinucleotide found at the 5' region of about half of all human genes. Cytosine methylation within the 5' CpG region is associated with loss of gene expression, particularly of tumour suppressor genes in cancer (Pino & Chung, 2010; Toyota et al., 1999).

1.1.4 CRC screening and stages

The clinical presentation of CRC depends on the stage and location of the tumour (Buccafusca, Proserpio, Tralongo, Rametta Giuliano, & Tralongo, 2019). Early detection of CRC is crucial for reducing mortality. Various screening tools are available, with colonoscopy established as the gold standard due to its high specificity and sensitivity. However, colonoscopy has limitations, including high costs and the need for specialist training. Therefore, the development of new molecular techniques is essential. Several biomarkers of CRC have been explored, including proteins, DNA (mutations), RNA (mainly microRNAs (miRNAs or miRs)), volatile organic compounds, and changes in gut microbiome composition (Loktionov, 2020; Wu et al., 2020; Zygulska & Pierzchalski, 2022).

The tumour-node-metastasis (TMN) classification of the American Joint Committee on Cancer is the internationally recognised protocol for CRC staging. Tumours are classified according to local invasion depth (T stage), lymph node involvement (N stage), and presence of distant metastases (M stage) (Edge & Compton, 2010; Kekelidze, D'Errico, Pansini, Tyndall, & Hohmann, 2013). These stages are (Figure 1.2):

- **Stage 0**: Hyperproliferation causes a benign polyp or adenoma. About 10% of these adenomatous polyps can progress to malignancy, forming adenocarcinoma that invades the muscularis propria.
- **Stage I**: The tumour grows in volume and invades the tissue of the serosa.
- **Stage II**: The tumour further invades the visceral peritoneum.
- **Stage III**: The tumour can metastasise to blood or lymphatic vessels.
- **Stage IV**: The cancer spreads to distant organs (Hossain et al., 2022).

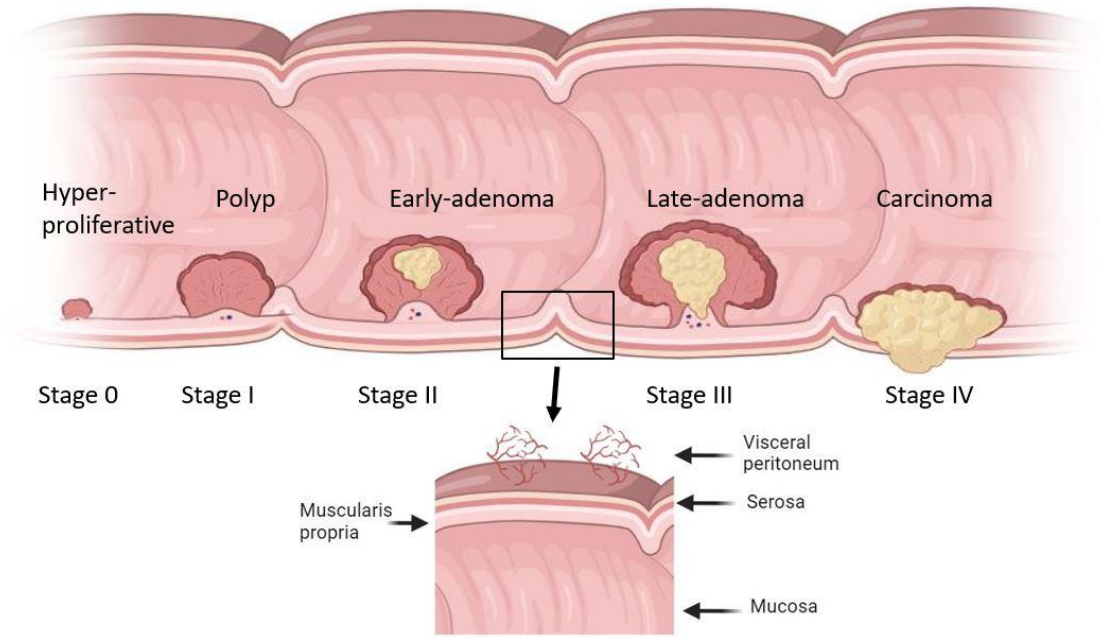

Figure 1.2: CRC stages and development. There are four stages in the development of CRC: Stage 0 (initiation): involves the earliest changes in the cells leading to the formation of benign polyps or adenomas. Stage I (promotion): at this stage, the benign adenomas grow and may develop into malignant adenocarcinoma that invades the muscularis propria of the colon or rectum. Stage II (progression): the tumour continues to grow and invade surrounding tissues including the serosa and potentially the visceral peritoneum. Stage III and IV (metastasis): in these stages, the cancer spreads to nearby lymph nodes (Stage III) and potentially to distant organs through the blood or lymphatic system (Stage IV).

1.2 Microbiome

1.2.1 Gut microbiome

The human body contains more than a hundred trillion microbes (Ursell, Metcalf, Parfrey, & Knight, 2012), most of them colonise the gut forming the so-called gut microbiome and are currently considered to be a new organ that is strongly associated with the host health and various diseases (Cho & Blaser, 2012). The healthy human gut harbours hundreds to thousands of microbial species including viruses, bacteria, and fungi that are acquired at birth from the mother and then shaped through feeding and other environmental factors. The human adult gut harbours approximately 10^{14} bacteria, which is about 1:1 microbial cell to human cell ratio, belonging to more than a thousand different bacterial species (Compare, D., Nardone,G., 2013; Kho & Lal, 2018;

Tlaskalová-Hogenová et al., 2011). They colonise the gut epithelial barrier surfaces with the largest number in the distal ileum and colon, it has been estimated that the colon contains approximately 70% of the estimated human microbiome. Notably, the colon is more susceptible to developing cancer, with cancer incidence 12-fold higher in the colon compared to the small intestine (Gagnière et al., 2016).

A few dominant bacterial phyla compose most of the gut microbiome such as *Bacteroidetes*, *Firmicutes*, *Actinobacteria*, and *Proteobacteria* (Sedlak, Yilmaz, & Roper, 2023). They mainly reside within the outer mucus layer which is unattached to the epithelium and acts as a physical barrier against pathogens, however, certain strains may infiltrate the inner mucus layer and epithelium. The inner mucus layer is attached and adjacent to the epithelial barrier and denser than the outer layer, it is also renewed every hour by goblet cells and is nutrient-rich (Johansson, Sjövall, & Hansson, 2013).

Host-gut interactions are dynamic and controlled by various genetic and environmental factors such as age, lifestyle, and geography (Engen, Green, Voigt, Forsyth, & Keshavarzian, 2015; Yadav, Ghosh, & Mande, 2016). These interactions are essential for maintaining body homeostasis, a beneficial gut microbiome plays functional roles in human physiology and metabolism including the synthesis of vital vitamins (vitamin K), digestion of indigestible carbohydrates such as pectin, and immunity through modulation of the immune system and prevention of colonisation of enteropathogenic bacteria (Bull & Plummer, 2014; Jandhyala et al., 2015)(Figure 1.3). On the other hand, these commensal bacteria benefit from the gut environment (oxygen, pH, and nutrients) (Geuking, Köller, Rupp, & McCoy, 2014; Krishnan, Alden, & Lee, 2015; Ursell, Metcalf, Parfrey, & Knight, 2012).

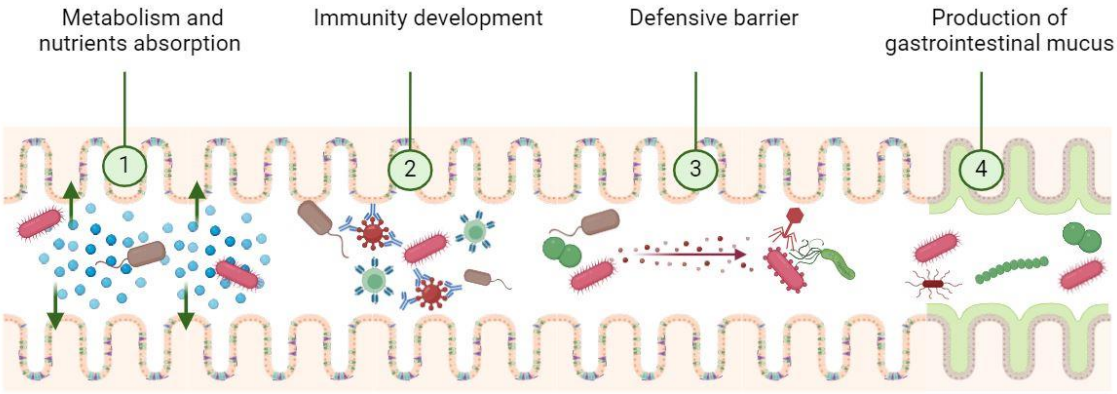

Figure 1.3: Functions of the gut microbiome. Metabolism and nutrient absorption: gut bacteria provide vital biochemical pathways for metabolising non-digestible carbohydrates. Immunity development: continuous and dynamic interactions between the host's immunity and intestinal microbiota are essential for immunity development. Defensive barrier: many bacteria produce antimicrobial compounds and compete with pathogens for nutrients and attachment sites in the gut lining to prevent pathogens from gut colonisation by pathogens. Production of gastrointestinal mucus: the gut microbiota contributes to the structural development of the gut mucosa through the induction of the transcription factor angiogenin-3, which has been implicated in the development of intestinal microvasculature.

1.2.2 Associations between gut microbiome and CRC

Back in 1863, it was initially stated that cancer could be a result of a chronic inflammatory process triggered by a toxic environment, including infection (Virchow, 1989). Various studies looked at this infectious origin of cancer context, such as the close association between *Helicobacter pylori* and gastric cancer (de Martel & Franceschi, 2009), *Salmonella typhi* with gallbladder cancer (de Martel & Franceschi, 2009). In the last years, a growing body of evidence has indicated the involvement of gut microbiota in the CRC carcinogenesis process, bacteria can either protect against or promote CRC. For example, *Fusobacterium nucleatum* (*F. nucleatum*), genotoxic *pks*$^{+}$ *E. coli*, and enterotoxigenic *B. fragilis* are closely associated with the development and progression of CRC (Pleguezuelos-Manzano, Puschhof, & Clevers, 2022).

1.2.3 Dysbiosis and CRC

Given the key roles of gut microbiome in various physiological processes, alterations and disruption of gut microbiome structure, a condition known as dysbiosis, has been closely

associated with many pathological conditions (Zhang, Yu-Jie et al., 2015). Various factors have been identified as a cause for dysbiosis including antibiotics and some types of diet (David et al., 2014), a large body of evidence suggests that dysbiosis could be considered a cause of IBD (Nagao-Kitamoto, Kitamoto, Kuffa, & Kamada, 2016; Schippa & Conte, 2014) and CRC (Clay, Fonseca-Pereira, & Garrett, 2022; Tomasello et al., 2014). One of the hypotheses to explain the role of dysbiosis in carcinogenesis is the driver-passenger model, according to this model, indigenous intestinal bacteria (the driver bacteria) trigger DNA damage in epithelial cells, resulting in tumour initiation. Then, ongoing tumorigenesis alters the surrounding microenvironment, favouring the proliferation of opportunistic bacteria (the passenger bacteria) (Saus, Iraola-Guzmán, Willis, Brunet-Vega, & Gabaldón, 2019).

Moreover, it has been proposed that inflammation is a contributory mechanism to dysbiosis leading to CRC, as alterations in the gut microbial structure result in the activation of the immune system inducing chronic inflammation that is linked to various types of cancer including CRC (Hung et al., 2015). Production of secondary metabolites, such as reactive oxygen species and toxins is another mechanism by which dysbiosis is proposed to lead to CRC (Borges-Canha, Portela-Cidade, Dinis-Ribeiro, Leite-Moreira, & Pimentel-Nunes, 2015; Sobhani et al., 2013). Notably, it is still unknown whether an action of a single bacterium, an action of microbial consortia, or both is the cause of CRC. Moreover, the causes of dysbiosis are poorly understood, and understanding the contribution of CRC to its symbiotic environment could facilitate the development of preventative strategies.

Short-chain fatty acids (SCFAs) are the most abundant microbial metabolites in the colonic lumen that are mainly produced by the microbial fermentation of prebiotics, such as dietary fiber (Kim, 2023). SCFAs, such as butyrate and propionate, contribute to gut health through various processes such as maintenance of intestinal barrier integrity, mucus production, and protection against inflammation, thus decreasing the risk for CRC (Silva, Bernardi, & Frozza, 2020). In CRC, butyrate decreases pro-inflammatory cytokine expression by inhibiting nuclear factor-κB activation in human colonic epithelial cells. Numerous studies have reported that butyrate metabolism is impaired in the intestinal mucosa of CRC patients (Canani et al., 2011).

Many studies have identified *E. coli*, *Streptococcus bovis*, enterotoxigenic *B. fragilis*, *F. nucleatum*, *Enterococcus faecalis*, and *Peptostreptococcus anaerobius* as CRC candidate pathogens (Cheng, Ling, & Li, 2020). Using next-generation sequencing methods based on 16s rRNA, many screening studies revealed enrichment in proinflammatory bacteria, such as *Fusobacterium*, and a lower abundance of butyrate producers, such as *Bifidobacteria*, in CRC patients compared to healthy individuals (Wang, T. et al., 2012; Wu, N. et al., 2013). These changes in the microbiome could be considered biomarkers for early detection of CRC, to complement the current screening strategies. It has been shown that the changes in the microbiome occur during the early stages of CRC carcinogenesis (Song, Chan, & Sun, 2020), therefore these changes could be used to identify people at higher risk of developing adenoma, the precursor lesion of CRC.

1.2.4 Role of *E. coli* in CRC

E. coli species can be divided into four phylotypes: A, B1, B2, and D. Commensal *E. coli* frequently belong to phylotype A and are mainly found in the gut, while phylotype B2 and D are mainly virulence genes carriers and have been linked to CRC as they produce bacteriocins that cause cellular and molecular damage (Kohoutova et al., 2014). They also produce various virulence factors including toxins (cyclomodulins), such as cytolethal distending toxins, cytotoxic necrotising factor, cycle inhibiting factor, and colibactin. Colibactin is one of the most well-studied *E. coli* bacteriocins (Figure 1.4A), it is a hybrid non-ribosomal peptide-polyketide encoded by the 54 kDa polyketide synthase (*pks*) genotoxic island and causes DNA-double strand breaks and chromosomal instability (Figure 1.4B) (Bonnet et al., 2014; Dougherty & Jobin, 2021).

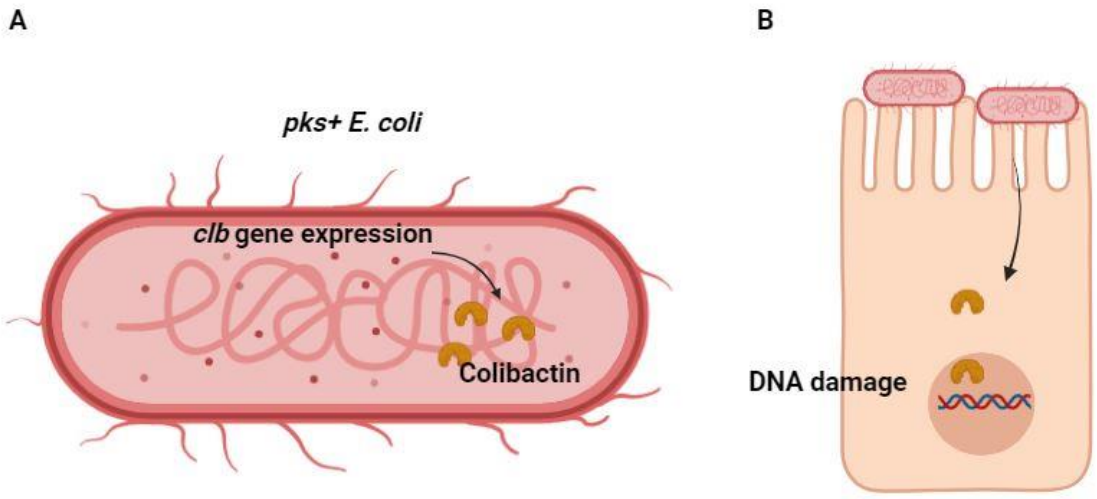

Figure 1.4: Colibactin-induced mutagenesis. (A) pks+ E. coli expresses colibactin genotoxin. (B) genotoxin colibactin alkylates DNA leading to DNA damage inducing tumorigenesis in gut epithelial cells.

The proposed link between *E. coli* and CRC has been established as it was repeatedly found to colonise CRC lesions and neighbouring epithelium (Bonnet et al., 2014; Buc et al., 2013; Martin et al., 2004; Raisch et al., 2014). The earliest study, in 1998, detected *E. coli* by polymerase chain reaction, PCR, in 62% of adenoma and 77% of carcinoma biopsy samples, compared to 12% positive biopsies from symptomatic, and only 3% from asymptomatic controls (Swidsinski et al., 1998). Subsequent studies showed a high prevalence of mucosa-associated *E. coli* in IBD and CRC patients, compared to healthy individuals (Wassenaar, 2018). Particularly, *E. coli* harbouring *pks* gene cluster (*pks*$^{+}$ *E. coli*) has been found more often in biopsies from CRC (67%) and IBD patients (40%) than in biopsies from healthy controls (21%) (Shah & Itzkowitz, 2022). Other studies have shown the cytotoxicity effect of *E. coli* (phylogenetic group B2) on colonic epithelial cells. When incubated *in vitro*, they cause cells to elongate, arrest their cell cycle, and force them to enter senescence (Cougnoux et al., 2014; Maddocks, Short, Donnenberg, Bader, & Harrison, 2009; Nougayrède et al., 2006; Secher, Samba-Louaka, Oswald, & Nougayrède, 2013).

Around 10-12% of healthy individuals were found to have *pks+ E. coli*, however, it appeared to be significantly over-presented in patients with CRC and IBD, when compared to healthy controls (Addington, Sandalli, & Roe, 2024; Buc et al., 2013; Dejea et al., 2014). The link between this genotoxin and CRC carcinogenesis is well

investigated, particularly with the identification of a distinct colibactin mutational signature in CRC following exposure of epithelial cells to *pks+ E. coli* (Dziubańska-Kusibab et al., 2020; Pleguezuelos-Manzano et al., 2020). It can induce DNA damage such as interstrand links, double-strand breaks, single base pair substitutions, and insertion and deletion mutations (Bossuet-Greif et al., 2018; Cougnoux et al., 2014; Nougayrède et al., 2006; Secher, Samba-Louaka, Oswald, & Nougayrède, 2013).

1.2.5 *E. coli*-induced mutagenesis in CRC a cause or effect of tumour

Chronic intestinal inflammation is an established driver for CRC development as seen in colitis-associated CRC, and is essential for colibactin-induced tumorigenesis, as *pks+ E. coli* fail to produce CRC in inflammation-free murine models (Arthur et al., 2012, 2014). It was proposed that the carcinogenic microenvironment and the accompanying intestinal inflammation may provide a favourable niche for *E. coli* which can utilise inflammation-derived nitrate and formate for their growth (Cevallos et al., 2019; Winter et al., 2013). It has been shown that the transcription of *pks* gene is significantly upregulated in response to the inflammatory and carcinogenic environment in mice (Arthur et al., 2014). Notably, the relationship between cancer development and its accompanying carcinogenic microenvironment with *E. coli* prevalence has not been investigated yet and requires further investigation.

pks+ E. coli is found in large numbers in healthy individuals as well as CRC patients (Lee-Six et al., 2019). However, studies have shown that commensal *pks+ E. coli* may only exert carcinogenic influence under specific conditions such as transcriptional activation of all *clb* genes and cell-to-cell contact, i.e., a close association between colonising *pks+ E. coli* strain and host epithelial cells (Dougherty & Jobin, 2021). Thus, understanding how mutagenesis of *pks+ E. coli* is regulated under specific environmental conditions is critical to assess whether CRC is involved in the mutagenic shift of *E. coli*.

1.2.6 Bacterial biofilm and CRC

Bacteria can adhere to surfaces to form microcolonies (a small aggregate of bacteria covered in a simple matrix), these microcolonies then may progress to larger colonies called biofilms. Biofilm formation enables the survival of bacterial cells living in challenging environments, such as the gut. The colonic mucosa is comprised of two distinct layers: a loose outer mucus layer that is rich in bacteria (Li, H. et al., 2015) as it

acts as a natural habitat for the commensal bacteria, and a stratified inner mucus layer which is firmly attached to the underlying epithelium, free from bacteria with a thickness that prevents the penetration of the bacteria to the epithelial cells (Johansson, Larsson, & Hansson, 2011). It is believed that the crosstalk between the microbiota, epithelium, and immune system is crucial for maintaining mucosal organisation and architecture (Peterson & Artis, 2014).

Bacterial biofilm has been recognised to contribute to chronic infection and diseases in humans. Dysbiosis and an abnormal inflammatory environment predispose the colonic mucosa to bacterial biofilm formation (Tytgat, Nobrega, van der Oost, & de Vos, 2019). Various studies have suggested that the formation of biofilm appears to play a vital role in the development and progression of CRC (Dejea et al., 2014; Raskov, Kragh, Bjarnsholt, Alamili, & Gögenur, 2018; Tomkovich et al., 2019). Biofilm-positive CRC cases have also shown poorer prognosis as they may have an additional epithelial injury and intestinal inflammation (Li, S., Konstantinov, Smits, & Peppelenbosch, 2017). Interestingly, a study has revealed that human colon mucosa biofilms, whether from CRC cases or healthy individuals, are carcinogenic (Tomkovich et al., 2019). These findings raise a key question; are cancer-associated biofilms and their microbial members induced or altered by cancer-associated signals?

1.3 Host-control mechanisms of microbiome

Previous findings revealed the symbiotic relationship between the host and gut microbiome that helps to maintain host homeostasis and provide the microbiota with a suitable environment for their growth (Yan, 2020). Therefore, the host-microbiota relationship is typically characterised as cooperation and mutualism, where both sides receive benefits. Notably, gut microbiota composition is unique in each human individual and varies substantially between different people, and it is not understood yet what leads to and what regulates this variation, however, it is known that changes in the microbiome are correlated to various diseases including IBD and cancer (Gilbert et al., 2018). Moreover, the microbial communities vary across animal species (de Jonge, Carlsen, Christensen, Pertoldi, & Nielsen, 2022). This suggests a strong host-natural selection mechanism that controls the composition of microbiota.

In humans and other species, there is extensive evidence suggesting that hosts exert some control over their microbiota (Rawls, Mahowald, Ley, & Gordon, 2006; Sharp & Foster, 2022; Suzuki et al., 2004; Weiland-Bräuer et al., 2015). In the gut, intestinal epithelial cells act as a physical barrier between microbes and the host's body and mediators of immune responses, through direct sensing of the microbiota. Whereas the host suppresses pathogenic and harmful microbiota through the immune system, various studies suggested that the host can have positive selective control mechanisms that influence the species composition at the gut epithelium, host-secreted specific nutrients that have an impact on microbiota composition is one of these mechanisms (Kashyap et al., 2013; Schluter & Foster, 2012). Affecting microbial adhesion to epithelial cells is another mechanism for both positive and negative selection of microbiota, a study showed that positive selection of microbiota via adhesion could be transformed into negative selection if the host secretes large quantities of matrix material such as mucus (McLoughlin, Schluter, Rakoff-Nahoum, Smith, & Foster, 2016).

Moreover, microbial reverting following the faecal microbiota transplant procedure (FMT) is another evidence of the host control mechanism on microbiota composition. FMT is the transfer of microbiota from healthy donors into a recipient's gut to treat a disease associated with gut microbiota alterations. Recently, FMT attracted the interest of scientists and clinicians, however, studies have shown a shift in the donated microbiota after a while. A study reported that proinflammatory species and species with immune modulation potential are more likely to engraft in the recipient's gut (Ianiro et al., 2022). It was reported that five ulcerative colitis patients were followed up for three months after FMT, their gut microbiota was changed in the first three days of FMT, however, it was shifted to the original dysbiotic state after one to four weeks of the FMT procedure (Angelberger et al., 2013). It has also been reported that IBD patients require several FMTs to stabilise the altered intestinal microbiota (Kunde et al., 2013). Notably, the efficacy of FMT after remission is significantly lower than the initial FMT (Dang, Yin, Sun, & Yang, 2020).

This FMT reverting could suggest control mechanisms that could be driven by the host to promote the inflammatory diseased state of the gut. Therefore, under a diseased state, the tumour could shape its surrounding microbiota through control mechanisms promoting their progression under an inflammatory and dysbiotic environment. Many

studies have focused on how the microbiota affects human health and the microbial contribution to disease, this project proposes that there are other effects (host-to-microbiota) that explain the functions and modulation of the microbiome and their involvement in various diseases. Although the correlation between CRC and microbiota is widely investigated, the underlying microbiota-gut interactions are not understood yet. EVs, cell-derived membranous structures released by tumour cells could be considered as mediators of gut-microbiome interactions. Therefore, this project aims to introduce and explore other potential host control mechanisms.

1.4 Extracellular vesicles

EVs are heterogeneous groups of cell-derived lipid bilayer particles that can be produced by most organisms including bacteria. Also, they can be released from various cells such as fibroblasts, tumour cells, and immune cells, and found in all body fluids such as urine, blood, and breast milk. They contain proteins, lipids, and nucleic acids (Figure 1.5). Proteins that are often used as EV biomarkers are also involved in their biogenesis, such as Alix, TSG101, and tetraspanin family members, in particular, CD9, CD81, and CD63 (Kimiz-Gebologlu & Oncel, 2022).

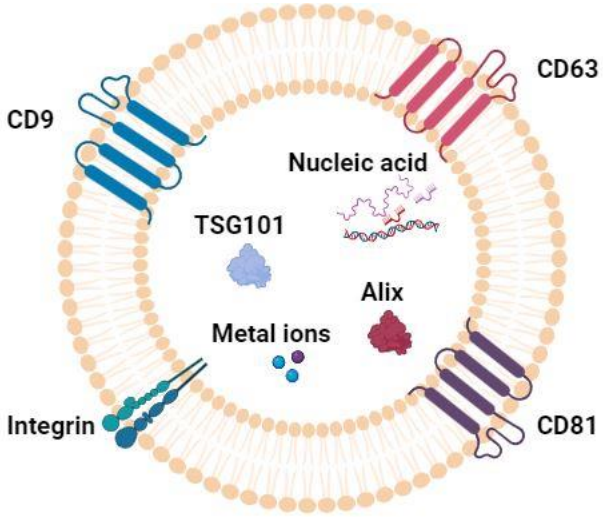

Figure 1.5: Schematic diagram of EVs. EVs are nanovesicles membranous structures released by all cell types, their surface covered with various molecules that are involved in their biogenesis and interactions with other cells, such as tetraspanin proteins (CD9, CD63, and CD81), and integrin receptors. Their cargoes include nucleic acids such as DNA, RNA and miRNA, and cytosolic proteins such as Alix and TSG101. These surface receptors and cytosolic proteins are considered markers of EVs. They also carry various metal ions such as zinc and iron (Jeppesen et al., 2019; Piacenza et al., 2018).

In humans, they are produced by all cell types and generally classified according to their size and origin into three subtypes: exosomes (50-200 nm), ectosomes (microvesicles) (100-1,000 nm), and apoptotic bodies (50-5000 nm) (Figure 1.6). Initially, they were considered as a route for the elimination of proteins, lipids, and RNA from cells, however, they are now projected as a mode of intercellular communication (Xiao et al., 2020). The biogenesis of exosomes, ectosomes (microvesicles), and apoptotic bodies varies, exosomes are generated within the endosomal system as intraluminal vesicles and secreted during the fusion of multivesicular bodies (MVBs) with the cell surface. Ectosomes (microvesicles) originate from an outward budding at the plasma membrane, whereas apoptotic bodies are formed during cellular apoptosis (Urabe et al., 2020; van Niel, D'Angelo, & Raposo, 2018).

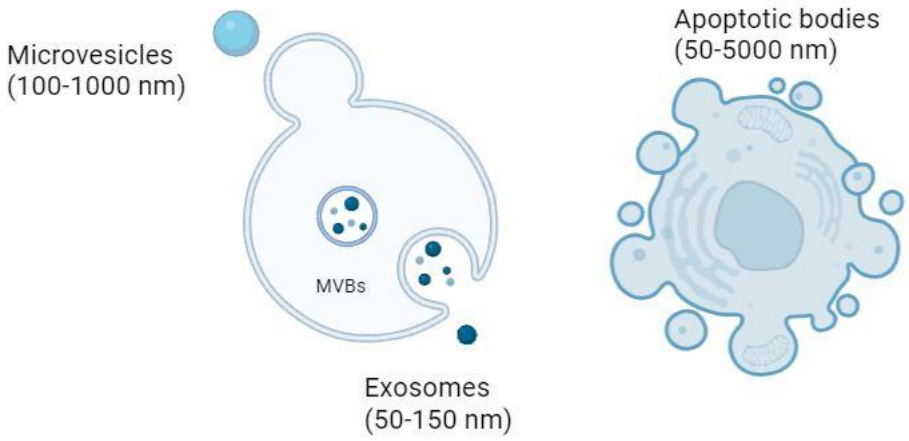

Figure 1.6: EVs types and biogenesis. EVs are classified according to their size and origin into three subtypes: exosomes (50-150 nm) that originate from the inward budding of the endosomal membrane and are secreted when MVBs fuse with the plasma membrane, ectosomes (microvesicles) (100-1000 nm) that are directly secreted from the plasma membrane through budding under normal circumstances or as a response to stimuli, and apoptotic bodies (50-5000 nm) that are formed during cellular apoptosis.

Once the EVs are released to the extracellular space, they can reach recipient cells and deliver their contents to evoke functional and phenotypic changes. The nature and abundance of the EV cargoes are cell-type-specific and are influenced by the physiological or pathological state of the donor cell. EVs-mediated intercellular communication requires docking at the plasma membrane (EV-cell contact) leading to the activation of surface receptors and signalling pathways, vesicle internalisation, or the transfer of secreted molecules, such as cytokines, chemokines, and growth factors. EVs can travel through body fluids and deliver functional cargoes to distant sites in the body (Mulcahy, Pink, & Carter, 2014; Urabe et al., 2020).

1.4.1 EVs in CRC

Cancer cells produce and release more EVs than normal cells, and their cargoes are significantly different from those released by normal cells (Xiao et al., 2020). Various studies have shown that proteins and miRNA, small non-coding RNA molecules capable of mediating gene expression at the post-transcriptional level (Zhou, G., Zhou, & Chen, 2017), carried by tumour-derived EVs could be considered as potential markers for CRC (Cha, Park, & Park, 2020). During tumour development, the production of EVs increases and they have been reported to play crucial roles in tumour development, survival,

progression, and modifying the tumour microenvironment (TME). The malignant properties of tumours are not limited to tumour cells but also various non-tumour surrounding cell types such as fibroblasts, immune cells, endothelial cells, and extracellular matrix. These TME cells have been reported as crucial regulators of tumour progression, the crosstalk between TME cells may influence tumour progression and metastasis. This involved direct cell-cell contact across TME and paracrine signalling between malignant and non-malignant cells within the TME (Tao & Guo, 2020).

Tumour-derived EVs can alter TME homeostasis by directly targeting fibroblasts, endothelial, and immune cells or by changing the structure and composition of the extracellular matrix (ECM) (Figure 1.7). The TME is rich in various immune cells, such as lymphocytes, monocytes and dendritic cells, tumour cells can regulate these immune cells turning them into immunosuppressive entities to promote tumour survival. There is a growing body of evidence suggesting that tumour-EVs are involved in the immune-regulatory process through various mechanisms, they deliver tumour growth factor-β (TGF- β) to T cells suppressing their proliferation in response to interleukins and enhance the production of TGF-β-producing myeloid immunosuppressive cell subsets which then suppress T lymphocyte proliferation (Valenti et al., 2006).

Tumour-associated fibroblasts, also known as cancer-associated fibroblasts, comprise a large part of the TME, these reprogrammed fibroblasts are involved in tumour development and progression, and EVs have been reported to influence these fibroblasts, they transform fibroblasts into myofibroblasts, triggering vascularisation and tumour invasion through the delivery of TGF- β (Webber, Steadman, Mason, Tabi, & Clayton, 2010). Moreover, EVs are involved in tumour angiogenesis, a process that is defined as the formation of new blood vessels under specific physiological conditions such as a response to tissue damage, and EVs with their vascular endothelial growth factor (VEGF) content, pro-angiogenic factor, trigger endothelial infiltration via ECM, therefore enhance tumour angiogenic tumour activity (Tao & Guo, 2020). EVs are rich in ECM-degrading enzymes such as matrix metalloproteases (MMPs). MMPs are a family of proteins implicated in ECM remodelling and thus cancer invasion and migration (Karampoga, Tzaferi, Koutsakis, Kyriakopoulou, & Karamanos, 2022). Overall, revealing the precise mechanism of EV-mediated communications in cancer patients may provide

a novel strategy for cancer treatment (Minciacchi, Freeman, & Di Vizio, 2015; Urabe et al., 2020).

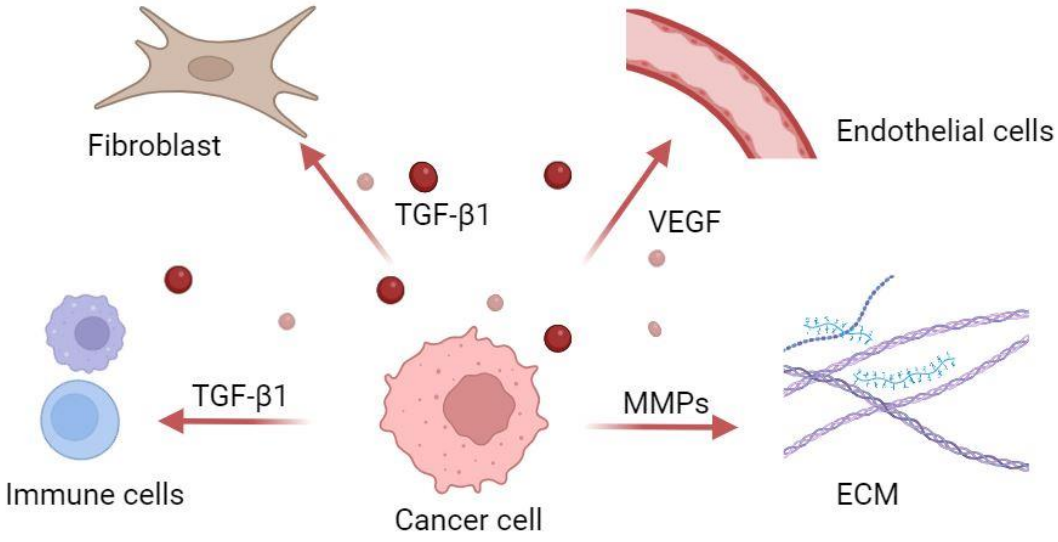

Figure 1.7: Tumour-derived EVs can alter the tumour microenvironment. EVs content induces the formation of a supportive tumour microenvironment; TGF-β1 induces immune suppression and differentiation of fibroblasts into cancer-associated fibroblasts. VEGF enhances endothelial cell invasion and MMPs mediate the ECM remodelling to promote cancer invasion.

1.4.2 EVs-mediated interactions within the gut microenvironment

EVs have been proposed to contribute to gut homeostasis. Studies have shown that EVs contribute to the interactions between host and microbiota in the gut microenvironment promoting microbial community reconstruction and immune responses under gut dysbiosis conditions. Previously, studies have shown that metabolites (Shoaie & Nielsen, 2014), proteins (de Vos, Tilg, Van Hul, & Cani, 2022) and nucleic acids mediate the host-microbiome interactions (Liu et al., 2016) The major host-gut microbiome interactions occur through metabolites including short-chain fatty acids that have an impact on the host physiology since 60-90% of these metabolites are absorbed by the epithelial cells, thus regulating cellular energy supply, controlling the pH in the colon, and provide resistance to pathogen growth. The abundance of these metabolites depends on the microbial composition therefore subject to modulation by diet and environmental factors, and abnormalities in the production of these fatty acid

chains are linked to various diseases such as type 2 diabetes and CRC (Shoaie & Nielsen, 2014).

Indole is a metabolite produced by commensal *E. coli* that could reduce the motility and adherence of pathogenic *E. coli* to host intestinal epithelial cells. Studies have shown that exposure to indole could up-regulate genes associated with mucosal barrier reinforcement, therefore it could serve as a beneficial signalling molecule for intestinal epithelial cells (Lin & Zhang, 2017). Moreover, sensing of gut flora DNA is found to have an immunostimulatory effect, unmethylated cytosine and guanine (CpG) motifs in prokaryotes are known to be 20 times more enriched than those in mammalian DNA, these motifs can induce immune response by activating toll-like receptor 9 (Krieg, 2002).

Notably, EVs and outer membrane vesicles (OMVs) (Toyofuku, Nomura, & Eberl, 2019) derived from host cells and microbiota, respectively, also participate in these host-gut interactions in the gut microenvironment. Many studies reported that dysbiosis of gut microbiota in IBD patients is associated with higher abundance in cargoes of EVs and OMVs, the latter contain cargoes of various lipoproteins, DNA, RNA, and peptidoglycan that initiate proinflammatory signalling cascades in the gut (Shen, Q., Huang, Yao, & Jin, 2022). For example, OMVs from enterohemorrhagic *E. coli* were found to stimulate the production of interleukin 9 in intestinal epithelial cells (Chang et al., 2020). Also, OMVs from commensal *E. coli* can enter epithelial cells through endocytosis and trigger DNA damage (Cañas et al., 2016).

On the other hand, host-EVs are involved in immunomodulatory functional cargo transfer, including proteins and nucleic acids between immune cells. It has been shown that EVs induce the production of tumour necrosis factor and immunoglobins by macrophages leading to their activation in IBD models. Macrophages are essential for intestinal homeostasis and their activation is linked to the pathogenesis of IBD (Shen, Q., Huang, Yao, & Jin, 2022; Wong, W. et al., 2016). Moreover, macrophages can regulate the intestinal mucosa and are involved in the epithelial barrier function (Bui, Mascarenhas, & Sumagin, 2018).

Regulatory miRNAs are probably the best-characterised EV cargo. It has been shown that gut epithelial cell miRNAs are abundantly present in the gut lumen and alter the abundance of the gut microbiome. These miRNAs can enter bacterial cells and directly bind to DNA based on sequence similarity resulting in altered bacterial gene expression

and growth. For example, miRNAs, such as miR-515-5p and miR-1226-5p, can enter *F. nucelatum* and *E. coli* and alter bacterial gene expression, 16srRNA of *F. nucleatum* and *yegH* gene in *E. coli*, resulting in an increased bacterial growth (Liu et al., 2016).

Moreover, a study showed intestinal epithelial exosomes were taken up by *E. coli* resulting in a decrease in *tnaA* gene expression that encodes the tryptophanase enzyme, leading to altered metabolism processes (Kumar, A. et al., 2021). Reciprocally, studies have investigated the transfer of regulatory signals (bacterial metabolites) to CRC cells and their impact on CRC development and progression (Pleguezuelos-Manzano et al., 2020). For example, it has been shown that *F. nucleatum*, which is a key player in CRC progression, appears to play a role in microbial regulation of CRC-associated miRNAs, it induces the production of miR-21 that is responsible for the enhanced CRC cell proliferation and invasion (Yang et al., 2017).

1.5 Hypothesis and aims

Dysbiosis is closely correlated with CRC (Gagnière et al., 2016), and the causative link between microbiome and CRC has been established, however, the underlying microbiome-tumour interactions have not been investigated yet (Saus, Iraola-Guzmán, Willis, Brunet-Vega, & Gabaldón, 2019). Therefore, this project aims to test the novel hypothesis that CRC-EVs alter the gut microbiome leading to dysbiosis and tumour progression, through the following objectives (Figure 1.8):

A. To isolate and characterise EVs from the culture medium of CRC-cell lines, CRC cases blood, and CRC cases tissue.
B. To assess the CRC-EVs-*E. coli* cross-kingdom interactions; binding and uptake of EVs by *E. coli*.
C. To assess the impacts of CRC-derived EVs on the bacterial phenotypic characteristics, such as growth rate and biofilm formation, and on bacterial transcriptomic to examine gene expression upregulation and downregulation.
D. To reveal mechanisms of EV-impact on *E. coli*.

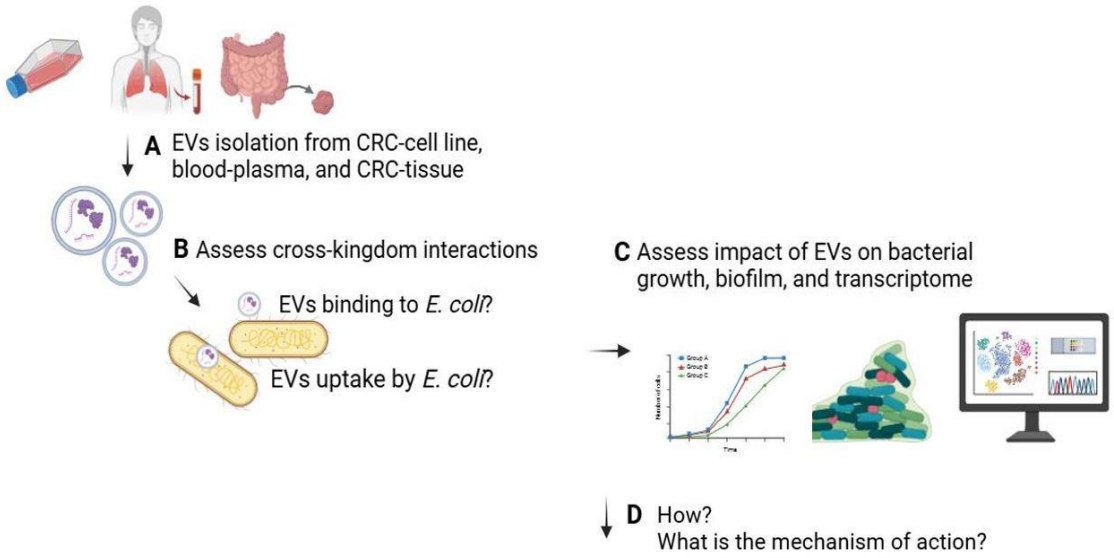

Figure 1.8: Schematic of the experimental plan to achieve project objectives. To assess the project hypothesis, the following experimental plan will be followed; (A) isolate and characterise EVs from CRC-cell lines, CRC patients' blood plasma, and CRC tissues, (B) assess the binding and uptake of EVs by E. coli, (C) assess the functional impact of EVs on the bacterial phenotypic characteristics; growth, biofilm formation, and changes in the bacterial genes expression, (D) investigate the mechanisms of EVs impact on E. coli.

2 Methods

2.1 Methods

2.1.1 Cell culture

Isotypic human CRC cell lines SW480 (derived from a primary tumour) and SW620 (derived from a metastatic tumour) from the same patient (ATCC, USA) were used (Hewitt et al., 2000). Cells were initially cultured in 175 cm2 flasks in Dulbecco's modified Eagle's medium (DMEM) (Lonza, Slough, UK) supplemented with 10% (v/v) foetal bovine serum (FBS) and 1% (v/v) Penicillin and Streptomycin (P/S) (Thermo Fisher Scientific, USA) at 37˚C in a humidified atmosphere with 5% CO2. Cells were then seeded into the lower cell cultivation chamber of a CELLine AD-1000 bioreactor flasks, at a concentration of 2.5×10^7 cells/ml in 15 ml DMEM supplemented as above (Sigma Aldrich, USA) and 500 ml of the same media was added to the upper chamber as described previously (Suwakulsiri et al., 2019). After ten days, cells in the cultivation chamber were washed twice with 10 ml of DMEM, and 15 ml of supplemented DMEM with 10% EV-depleted FBS (Thermo Fischer Scientific, USA) and without P/S was added, while the media chamber was replaced with 500 ml of DMEM supplemented with 5% FBS (Thermo Fisher Scientific, USA). Media in both chambers was refreshed every 7 days, and the cell chamber-conditioned media (CM) was collected and centrifuged at 300x g for 10 minutes, and 2000x g for 10 minutes and stored at -80 °C before EV isolation.

2.1.2 Blood samples collection and processing

Peripheral blood samples from healthy blood donors (HDs) and CRC patient donors (CPDs) were collected for the isolation of EVs (Table 2.1). Samples were provided by Sheffield Teaching Hospitals (Northern General Hospital, Sheffield) after approval from the local research ethics committee (REC reference number: 19/NI/0221) (Appendix 7.3). None of the HDs had colon disease, and all donors gave written informed consent. Blood was collected in EDTA vacutainers and processed into platelet-depleted plasma. First, blood was centrifuged at 1,000x g for 10 minutes to obtain plasma, the plasma was then diluted with an equal volume of phosphate-buffered saline (PBS) and centrifuged at 1,500x g for 15 minutes, and the resulting supernatant was centrifuged at 2,500x g for fifteen minutes before being stored at -80 °C as described previously (Baranyai et al., 2015).

Table 2.1: Demographic and clinical characteristics data of blood donors.

	Healthy controls [n= 11]	CRC-patients [n=18]
Age		
Median	40	73
Range	26-58	46-89
Mean ± SD	40.3 ± 9.11	72.3 ± 10.98
Sex		
Male	2	8
Female	9	10
Grade		
T2/T3 (M0)	-	11
T3/T4 (M1)	-	8

2.1.3 Tissue samples collection and processing

Tumour-adjacent bowel tissues from 4 patients with a confirmed diagnosis of CRC were collected from consenting patients undergoing surgical tumour resection at the Northern General Hospital, Sheffield. Ethics permission was granted from the local research ethics committee (REC reference number: 19/NI/0221) (Appendix 7.3). Tissue samples were processed before EVs isolation, samples were incubated with type-1 collagenase (5 mg/ml) for 2 hours at 37 °C to digest the tissues. Enzymatic digestion was inhibited by adding a protease inhibitor cocktail, centrifugation was performed at 10,000x g for 30 minutes and supernatant was stored at -80 °C for EVs isolation.

Table 2.2: Demographic and clinical characteristics data of bowel tissue donors.

	CRC-patients [n= 4]
Age	
Median	68
Range	43-79
Mean ± SD	64.5 ± 16.28
Sex	
Male	2
Female	2
Grade	
T2/T3 (M0)	4 (1 N1)
T3/T4 (M1)	0

2.1.4 EVs isolation and characterisation

2.1.4.1 Size exclusion chromatography

Initially, the stored CM was reduced to 0.5 ml using a Vivaspin-20 (100 kDa molecular weight cut-off) column (SLS, Nottingham, UK). EVs were then isolated from reduced CM, stored plasma, and tissue digests by SEC using Sepharose CL-2B (GE Healthcare, Uppsala, Sweden) stacked in disposable Econo-Pac columns (Bio-Rad, Watford, UK) and eluted in PBS. First, sepharose was washed 3 times with PBS before running CM, plasma and tissue digest, and 20 fractions of 0.5 ml volume were collected. Where required, EVs-rich fractions were pooled by ultracentrifugation (UC) at 95,994x g for 1 hour at 4 °C.

2.1.4.2 Protein quantification

Protein concentration in the SEC fractions was determined using Pierce™ BCA Protein Assay Kit (Fisher Scientific, Loughborough, UK), following the manufacturer's protocol.

2.1.4.3 Immunoblotting

EVs samples were lysed in Laemmli sample buffer (3:1) (100 mM Tris HCl, 20% glycerol, 4% SDS, 10% β-mercaptoethanol, 0.2% bromophenol blue) and heated for 2 min at 95°C,

equal volumes of EV fractions were then separated by SDS-polyacrylamide gel electrophoresis (PAGE; 4-20% precast polyacrylamide gel, Bio-Rad, Watford, UK) and transferred to PVDF membranes (Millipore) using a Trans-Blot Turbo Transfer System (Bio-Rad, Watford, UK), following the manufacturer protocol. To prevent non-specific binding, membranes were incubated with a blocking solution, 5% non-fat milk powder in Tris-buffered saline containing 0.1% Tween-20, TBST, for 1 hour. Membranes were immunoblotted with anti-CD9 (ab2215) and anti-CD63 (ab193349) primary antibody (1:1000, Abcam, Cambridge, UK) overnight at 4°C, followed by either goat anti-mouse IgG, horseradish peroxidase labelled (HRP) (926-80010), and goat HRP-labelled anti-rabbit IgG secondary antibody (926-80011) (1:10,000, LICOR, USA). Finally, using the Bio-Rad enhanced chemiluminescence-HRP system, the signal of bound antibody was visualised by Odyssey Infrared Imaging System (LI-COR, USA), following the manufacturer's protocol.

2.1.4.4 DELFIA-ELISA

As shown in Figure 2.1, EVs were incubated overnight in Nunc-Immuno 96-Microwell plates (Sigma Aldrich, USA) at 4°C. After 3x washes, non-specific sites were blocked with 300 µl of 1% bovine serum albumin (BSA) in PBS at room temperature for two hours. EVs were then incubated with primary antibodies; CD9 (ab2215), CD63 (ab193349) (Abcam, Cambridge, UK), CD81 (MCA1847) (Bio-rad, Watford, UK), and TSG101 (sc-7964) (Santa Cruz Biotechnology, USA) that were diluted (1:5000) with 0.1% BSA in PBS and incubated at room temperature for 2 hours. EVs were incubated then with a secondary antibody, biotinylated anti-mouse IgG (NEF823001EA, 1:2500, PerkinElmer, USA), for 1 hour at room temperature. Lastly, the plate was incubated with DELFIA Europium-labelled streptavidin (PerkinElmer, USA) for 45 minutes in assay buffer (50mM Tris-HCl, 0.9% NaCl, 0.2% BSA, 0.1% Tween-20, 20 µM DTPA, pH 7.8), followed by DELFIA enhancement solution (PerkinElmer, USA) for 5 minutes at room temperature. Time-resolved fluorescence (TRF) was measured on a Wallac Victor plate reader (excitation at 320 nm and emission at 615 nm).

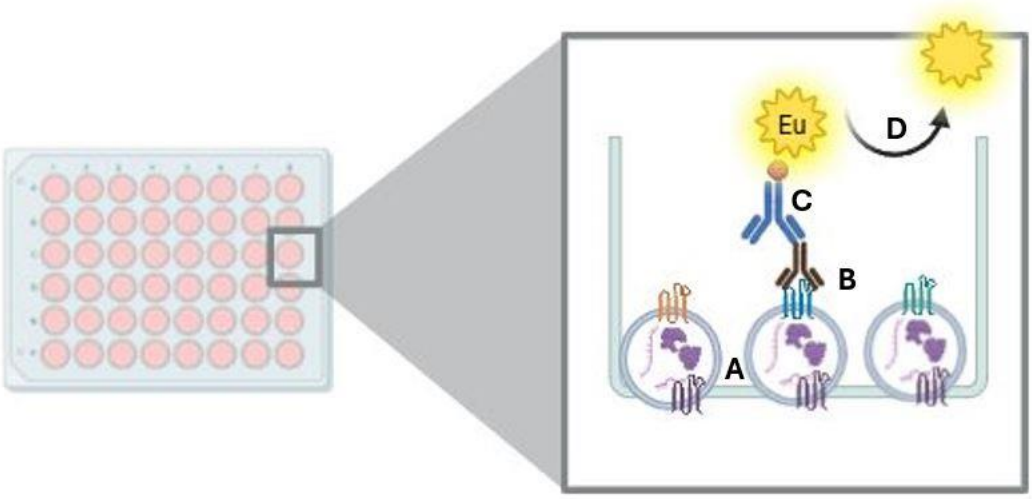

Figure 2.1: Basis of DELFIA-ELISA for EVs' markers detection. The main four steps for DELFIA-ELISA EVs' markers detection are: (A) plate coating; binding of EVs to polystyrene treated 96-well plate, (B) primary antibody binding to EVs' surface markers, (C) binding of biotinylated secondary antibody to the primary antibody, (D) binding of DELFIA Europium-streptavidin to biotin, and dissociation of Europium due to enhancement solution action, then the Europium fluorescence is measured by time-resolved fluorometry.

2.1.4.5 Transmission electron microscopy

TEM was done at the University of Sheffield. Negative staining TEM of EVs was conducted by adsorption onto carbon-coated copper grids for 1 minute. Excess liquid was removed with filter paper before placing the grid sequentially into 2 separate drops of water briefly, the copper grid was then transferred to 20 µl of filtered 2% uranyl acetate for 2 minutes. Excess liquid was removed with filter paper, and the grid was allowed to dry for 10 minutes. Then, the grids were stained in uranyl formate and visualised on an FEI Tecani G2 Spirit BioTwin (PennState, USA) TEM. Images were recorded using a Gatan Orius 1000B CCD camera and Gatan Digital Micrograph software (Gatan, USA).

2.1.4.6 NanoFCM

EVs size/concentration profile and markers were assessed by a Nano-analyser instrument based on nanoflow cytometry (NanoFCM) (MediCity, Nottingham). Briefly, EVs were diluted in PBS (1:2000) to analyse particle count and size, they were compared

to quality control beads (250 nm silica standard) and size beads (68, 91, 113, and 155 nm). To detect EV markers, EVs were labelled with FITC/APC conjugated antibodies for CD9, CD81, and CD63 (1:10) and incubated at room temperature for 30 minutes before being detected by the Nano-analyser.

2.1.5 Bacterial identification and culture

Two strains of *E. coli* were used in the investigation: *E. coli* MG1655, a laboratory-characterised strain, and *E. coli* 11G5, a CRC-associated strain, the latter was generously donated by Guillaume Dalmasso, University Clermont Auvergne, Clermont-Ferrand, France (Pleguezuelos-Manzano et al., 2020). Bacteria were routinely cultured on Luria-Bertani (LB) agar and incubated at 37 °C.

Bacterial genomic sequencing was performed to confirm the identity of both strains; DNA was extracted using PureLink Genomic DNA kit (ThermoFisher Scientific, UK), following the manufacturer's protocol. Illumina whole genome sequencing was performed by Microbes NG (Microbes NG, UK).

Parental *E. coli* MG1655 and motility-mutant strains: *Δpdeh E. coli* (Aono, 2013), *ΔFliC E. coli* (Schwan, Flohr, Multerer, & Starkey, 2020), and *ΔFlh E. coli* (Fahrner & Berg, 2015) were also used in the investigation of altered gene expression (Table 2.3). Bacteria were routinely cultured on LB agar supplemented with 50 µg/ml kanamycin (Sigma-Aldrich, UK) and incubated at 37 °C.

Table 2.3: Characteristics of motility-deficient E. coli MG1655 strains

E. coli MG1655 strain	Mutated gene function	Mutation effect
Δpdeh E. coli	c-di-GMP-degrading phosphodiesterase	Higher level of c-di-GMP promote sessile growth
ΔFliC E. coli	Encodes the flagellin subunit	Failure of flagella biosynthesis, loss of swimming motility and adhesion
ΔFlh E. coli	Encode transcription factor that initiate flagellar synthesis	Failure of flagella biosynthesis and loss of swimming motility

2.1.6 CRC-EVs-*E. coli* interactions

2.1.6.1 Transmission electron microscopy

An overnight culture of *E. coli* MG1655 was treated with 50 µg/ml of SW620-EVs for 1 hour at 37 °C, bacterial cells were collected by centrifugation at 3000x g for 5 minutes, then washed twice with 1x PBS and centrifuged at 3000x g for 5 minutes after each wash.

The collected bacterial cells were fixed with 2.5% Glutyryl aldehyde and negative staining TEM was then conducted, as previously described in section 2.1.4.5.

2.1.6.2 Confocal microscopy

EVs were labelled with CellTrackerTM Red CMTPX dye (20 μM) (Fisher Scientific, Loughborough, UK), and *E. coli* was labelled by SYTO 9 Green Fluorescent Nucleic Acid stain (Fisher Scientific, Loughborough, UK), according to the manufacturer's protocol. Labelled-EVs and labelled-*E. coli* were then co-incubated in DMEM at 37 °C for 1 hour. Interactions were visualised using LSM 800 laser scanning confocal microscope (Zeiss, Germany).

2.1.6.3 Flow cytometry

For quantitative assessment of *E. coli*-EVs interactions, EVs were labelled with Memglow 700 TM (Cytoskeleton, USA) according to the manufacturer's instructions, and incubated with *E. coli* at 37 °C for 18 hours. Bacterial cells were collected after 1, 2, 4, 6, and 18 hours of incubation, then fixed with 4% paraformaldehyde (Sigma-Aldrich, UK) for 20 minutes and washed with PBS. Fluorescent bacteria were quantified using Cytoflex flow cytometer (Beckman Coulter), and results were analysed by FlowJo software (BD Life Sciences, USA).

2.1.6.4 EVs-enzymatic treatment

For de-glycosylation of EVs-surface glycans, EVs were treated with a mixture of de-glycosylases using de-glycosylation mix II (New England Biolabs, UK), following the manufacturer protocol of denaturing reaction conditions. EVs were then washed with an equal volume of 1x PBS and collected by UC at 95,994x g for 1 hr at 4 °C.

To digest EV's surface proteins, EVs were treated with 25 μg/ml of proteinase-k (PK) (New England Biolabs, UK) and incubated at 37 °C for 1 hour. The reaction was then stopped by adding a protease inhibitor cocktail (Sigma-Aldrich, UK), EVs were then washed with an equal volume of 1X PBS and collected by UC at 95,994x g for 1 hour at 4 °C.

EVs were also treated with 1 μg/ml of trypsin (Tryp) (Fisher Scientific, UK), and incubated at 37 °C for 1 hour, the reaction was then stopped by adding a protease inhibitor cocktail

and EVs were then washed with an equal volume of 1x PBS, and collected by UC at 95,994x g for 1 hour at 4 °C.

2.1.6.5 EVs lysis

EVs were treated by volume (1:10) with supernatant of an overnight culture of *E. coli* MG1655 (1:10) (EVs: supernatant) and were incubated overnight at 37 °C. Initially, the supernatant was centrifuged at 300 x g for 5 minutes to clear the pellet containing bacterial cells, then UC at 95,994x g to clear bacterial OMVs. EVs were also treated with RIPA lysis buffer (Sigma-Aldrich, UK) (1:10) (EVs: RIPA buffer) and kept on ice for 5 minutes then stored at 4 °C. EV's integrity was then assessed by NanoFCM, as described in section 2.1.4.6.

To investigate potential EVs-functional cargoes, EVs were lysed with RIPA buffer, then were treated with PK as described in section 2.1.6.4, ribonucleases A (RNAase) (Sigma-Aldrich, UK) at a working concentration of 20 µg/ml, and matrix metalloproteases inhibitor (MMPsi), GM6001 (EMD Millipore Corporation, USA).

2.1.7 Impact of CRC-EVs on *E. coli*

2.1.7.1 Growth curve-turbidimetric assay

To assess bacterial growth under aerobic and anaerobic growth conditions, overnight cultures of *E. coli* strains were diluted to an Optical density of 0.011 at 600 nm (OD_{600}) in phenol red-free DMEM. Bacteria were treated with EVs and incubated in 96-well microtiter plates at 37 °C for 18 hours in phenol-red free DMEM. OD_{600} was determined at 30-minute intervals by a Clariostar plate reader (BMG Labtech).

2.1.7.2 Biofilm formation assay-batch microtiter plate-based system

To assess the impact of EVs on the ability of *E. coli* to form biofilm under aerobic and anaerobic growth conditions, overnight cultures of *E. coli* strains were diluted to an OD600 of 0.011. In a 96-well plate, bacteria were treated with EVs, and a Nunc Immuno TSP lid (Fisher Scientific, Loughborough, UK) was placed into each 96-well plate, then incubated at 37 °C for 24 hours. Batch biofilm growth was assessed as described previously (Harrison et al., 2010), in brief, peg lids were removed from the base plate and washed twice with PBS to remove loosely attached cells. Biofilm on pegs was disrupted by sonication for 10 minutes with a water bath sonicator, dissociated cells

were serially diluted and grown on LB agar plates at 37 °C overnight, and CFU/ml was quantified.

2.1.7.3 Bacterial training

To assess the prolonged-term impact of EVs on *E. coli*, *E. coli* was initially grown from a single colony overnight to initiate the experiment. Long-term serial passages were performed every 24 hours by diluting the culture 1:10 in a 96-well plate, *E. coli* was passaged with 50 µg/ml of EVs for 10 days followed by 5 days without EVs treatment under anaerobic growth conditions at 37°C. Planktonic cells of each passage were stored with 50% glycerol (1:1) (Sigma-Aldrich, UK) at -80 °C for future analysis (Figure 2.2).

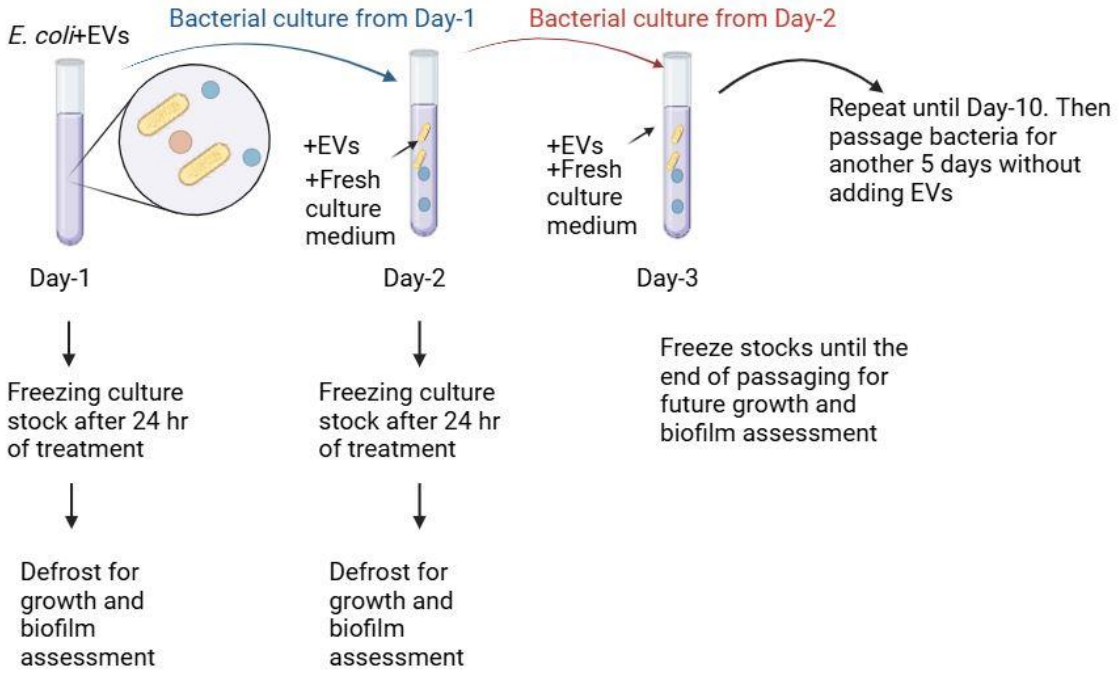

Figure 2.2: Schematic diagram of the bacterial training experiment. E. coli was passaged for 10 days in the presence of EVs, then passaged for 5 days without EVs treatment. After each day of passaging, bacterial culture was stored at -80C for future bacterial growth and biofilm formation assessment without any further treatment with EVs.

2.1.7.4 Total-RNA extraction and transcriptomic analysis

Overnight culture of *E. coli* MG1655 was diluted to an OD_{600} of 0.011 and treated with 50 µg/ml of SW620-EVs in a 96-well plate, incubated at 37 °C overnight for 24 hours. Planktonic cells were centrifuged at 3,000x g for 5 minutes and then resuspended with 800 µl of DNA/RNA protection reagent before RNA isolation using Monarch Total RNA

Miniprep kit (New England Biolabs, UK), following the manufacturer's protocol. RNA quantity and quality were assessed by nanodrop and gel-electrophoresis (1% agarose in Tris-borate-EDTA buffer), respectively. Isolated RNA samples were stored at -80 °C for transcriptomic analysis by Azenta (Azenta, UK) using Illumina NovaSEq, PE 2x 150. Ribosomal RNA was depleted first, then RNA was fragmented and primed randomly. cDNA was then synthesised, and sequence end-repair was performed (5´ phosphorylation and 3´ dA-tailing). Adapter ligation, PCR enrichment, and sequencing were lastly performed.

Bioinformatics analysis was then performed; sequence quality was first evaluated, and reads were trimmed to remove possible adapter sequences and nucleotides with poor quality using Trimmomatic v.0.36. The trimmed reads were mapped to the reference genome (*E. coli*_k12_MG1655_GCF_904425475.1) available on ENSEMBL using the STAR aligner v.2.5.2b, to generate hit counts for genes/exons. Gene hits were then compared, and gene ontology analysis was performed. Lastly, the Wald test was used to determine p-value and log2 fold changes. Genes with a p-value <0.05 and absolute log2 fold change >1 were called differentially expressed genes.

2.1.7.5 Alignment analysis

A list of miRNAs of SW480-EVs and SW620-EVs was obtained from a previous study (Chen et al., 2019). miRNA list was sorted depending on their expression in both types of EVs and enrichment in SW620-EVs. miRs sequences were obtained from the miRbase website (https://www.mirbase.org/) that were then aligned individually against the *E. coli* MG1655 genome using the standard nucleotide BLAST tool, BLASTN (https://www.ncbi.nlm.nih.gov/).

2.1.7.6 Bacterial invasion assay

To prepare cells, SW480-cells and SW620-cells were seeded in a 24-well plate at $2*10^5$ cell density and incubated at 37 °C with 10% FBS-supplemented DMEM overnight to reach 70% confluency. To prepare bacteria, an overnight culture of *E. coli* MG1655 was diluted to an OD_{600} of 0.011, and then bacteria were treated with 50 µg/ml of SW620-EVs and incubated at 37 °C overnight. SW480-cells and SW620-cells were then incubated with EV-treated *E. coli* MG1655 and non-treated *E. coli* MG1655 at a ratio of 1:100 (Cells: *E. coli*) at 37 °C with DMEM only for 4 hours. Cells were washed twice with PBS and

incubated with Gentamicin (50 mg/ml) containing DMEM for 1 hour at 37 °C to remove non-invaded bacterial cells. Cells were then washed with PBS and lysed with RIPA lysis buffer. The lysed cell suspension was serially diluted and plated on LB agar plate to determine the total number of CFU/ml of invaded bacterial cells.

2.1.8 Impact of EV-treated *E. coli* on CRC cells-Alamar-blue assay

Overnight cultures of *E. coli* MG1655 and *E. coli* 11G5 were diluted to an OD_{600} of 0.011 then treated with 50 µg/ml SW620-EVs and incubated at 37°C for 24 hours. To obtain supernatant, bacterial culture was centrifuged at 3000x g for 5 minutes and supernatant was collected to treat CRC-cells. SW480- and SW620-cell lines were seeded into 96-well plates at 5000 cell/ml cell density and incubated at 37°C with complete DMEM (10% FBS, 1% P/S) for 24 hours. Cells were then washed with PBS and DMEM was replaced by bacterial supernatant and DMEM at 1:3 ratio and incubated at 37°C for 48 hours. Media was then removed and replaced by DMEM with resazurin sodium salt (Sigma, UK) at 1:100 dilution of 3 mg/ml stock concentration, plates were then incubated at 37°C for 4 hours and fluorescent intensity was measured at 570 nm wavelength.

2.1.9 Statistical analysis

GraphPad Prism 7.0 (GraphPad Software) was used for data analysis. The data were presented as values with standard error of the mean (mean ± SEM). The significance of differences in mean values between the two groups was analysed using the student's t-test (two-tailed). In cases of more than two groups, differences between individual groups were analysed via one-way ANOVA and two-way ANOVA, Brown-forsythe and Welch tests were used as post-hoc tests. Differences were considered significant when the P-value was less than 0.05.

3 Colorectal cancer extracellular vesicles interact with *Escherichia coli*

3.1 Abstract

Overview: Cellular crosstalk is an important mechanism for maintaining organismal homeostasis and is involved in the pathogenesis of various diseases including cancer. In CRC, tumour cells communicate with their surrounding stromal cells through EVs, to promote their progression and metastasis. The gut microbiome is a major contributor to gut function and health, interacting with colon cells through OMVs and contributing to tumour initiation and progression. However, the interactions of CRC cells with the gut microbiome through EVs are not fully explored yet, therefore, this chapter hypothesises that CRC-EVs mediate the interaction between CRC and gut microbiome, and the gut microbiome uptake host-derived EVs.

Methods: EVs were isolated from two CRC-cell lines SW480 and SW620 (patient-matched cell lines), obtained at the early and later metastatic stages of CRC, respectively. EVs were isolated by SEC from a culture medium of AD-1000 CELLine adhere bioreactors and characterised following the International Society of Extracellular Vesicles (ISEV) guidelines (Théry et al., 2018). Two strains of *E. coli* were chosen to investigate the host-microbiome interactions, *E. coli* MG1655 (laboratory-strain), and *E. coli* 11G5 (CRC-associated strain) (Pleguezuelos-Manzano et al., 2020). Interactions were assessed by TEM, fluorescent microscopy, flow cytometry, enzymatic disruption of EVs surface proteins and glycans, and EV lysis.

Results: TEM showed the binding of EVs to the surface and the motility-structure of *E. coli*, flagella. Fluorescent microscopy showed the co-localisation of *E. coli* and EVs fluorescent signals, indicating the interaction and uptake of EVs by *E. coli*. Flow cytometry data showed that EVs-*E. coli* interactions increase over time, and it is stage-specific with higher interaction observed between SW620-EVs and *E. coli*, compared to SW480-EVs- *E. coli* interactions. EVs-enzymatic treatment analysis showed that these interactions are largely protein-mediated. Lastly, EV lysis analysis showed that *E. coli* has an impact on CRC-EV's integrity, appearing to secrete substances that lyse EVs.

3.2 Introduction

Communication between cells is crucial to maintain body homeostasis and health. Cells communicate with adjacent and distant cells and tissues through the secretion of soluble substances, such as cytokines and growth factors (Majka et al., 2001). Recently, an additional means by which cells can communicate is through EVs, which are considered mediators of cell-cell communication by transferring bioactive molecules including proteins, lipids, and miRNA from donor to recipient cells. These cellular crosstalk communications are crucial to various physiological and pathological conditions including cancer. The role of EVs in many health conditions is well established and EVs are now considered potential diagnostic biomarkers and therapeutic tools for several diseases. In CRC, several EV-associated miRNAs have been highly expressed in the serum of patients compared to healthy controls, thereby, they could be novel diagnostic markers (Ogata-Kawata et al., 2014).

3.2.1 EVs-mediated tumour crosstalk mechanisms

EVs are critical mediators of cell-cell crosstalk, facilitating the communication between the tumour and its microenvironment, to support cancer progression (Webber, Steadman, Mason, Tabi, & Clayton, 2010). Tumour-derived EVs carry bioactive messengers that participate in tumorigenesis processes including oncoproteins, oncogenic miRNAs, and immunomodulating molecules. A large body of evidence suggests that tumour cells release a higher amount of EVs compared to normal cells, particularly in patients with CRC which supports their pathological contribution (Titu et al., 2023; Valter, Verstockt, Finalet Ferreiro, & Cleynen, 2021).

Studies have shown the interaction and uptake of CRC-EVs by surrounding stromal cells (Wang, M., Su, & Amoah Barnie, 2020), such as tumour-associated macrophages (Liang, Z. et al., 2019; Yin et al., 2022; Zhao, S. et al., 2020), hepatic cells to promote metastasis to the liver (Zhao, S. et al., 2022), and cancer-associated fibroblasts (Wang, D. et al., 2022). It was further shown that the interaction of CRC-derived EVs and immune cells results in the activation of cytokine secretion and enhanced inflammatory response, which in turn promotes tumour progression (Popēna et al., 2018). Moreover, it was shown that CRC-derived EVs mediate the transfer of cancer miRNA into stromal fibroblasts, resulting in their activation and transformation into cancer-associated

fibroblasts (CAFs) (Abdouh et al., 2019). On the other hand, EVs from stromal cells were also shown to be taken up by CRC cells to deliver their functional contents and promote tumour progression, such as EVs from carcinoma-associated fibroblasts (Ren et al., 2018), tumour-associated platelet (Contursi et al., 2023), and macrophages (Lan et al., 2019).

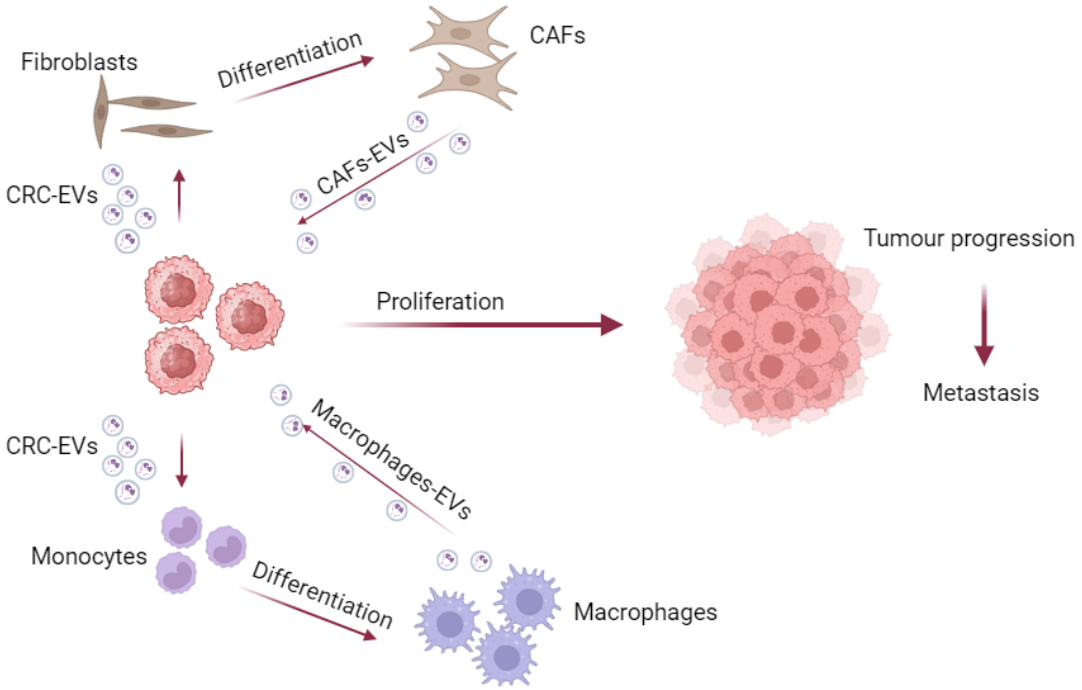

Figure 3.1: CRC-tumour and stromal cells crosstalk through EVs. To promote cancer progression, CRC cells release EVs to surrounding stromal cells, such as fibroblasts and monocytes, to stimulate their differentiation into CAFs and macrophages, respectively. On the other hand, these activated CAFs and macrophages release EVs containing chemokines and interleukins that lead to the progression of the tumour, promoting metastasis.

3.2.2 EVs in host-gut microbiome interkingdom communications

Gut homeostasis depends on complex and dynamic interactions between the microbiota, the gut epithelium, and the host immune cells. Bacteria are the most studied component of the gut microbial community, these microorganisms are physically separated from the host cells of the intestinal mucosa by the gut barrier, therefore, interkingdom communications do not involve direct physical contact but are facilitated by mediators such as EVs, microbial metabolites, and proteins that can cross the mucus layer (Díaz-Garrido, Badia, & Baldomà, 2021).

It is evident that intra- and inter-kingdom crosstalk is mediated by EVs released from the gut microbiota, and from intestinal epithelial cells (Figure 3.2). Bacterial EVs (BEVs), defined as OMVs, are also involved in the host-gut interactions. It was 1967 when BEVs were discovered, they were initially considered needless, however, further studies established them as active mediators for cellular communications. OMVs are spherical bilipid nanostructures, they range from 20 to 300 nm in size and are released by both gram-positive and gram-negative bacteria. They carry various bacterial molecules such as lipopolysaccharides, lipids, peptidoglycan, proteins, and nucleic acid. Pathogenic-derived BEVs carry toxins and virulence factors that contribute to bacterial pathogenicity (Díaz-Garrido, Badia, & Baldomà, 2021).

These bacterial OMVs interact with host cells, OMVs from commensal *E. coli* were found internalised by epithelial cells through endocytosis. OMVs from the probiotic *E. coli* Nissle 1917 were internalised by gut epithelial cells and induced DNA double-strand breaks in epithelial cells. This could be due to the ability of this *E. coli* strain to produce the genotoxic compound, colibactin (Cañas et al., 2016). Another study has shown the interaction between another major gut commensal bacteria, *Bacteroides thetaiotaomicron*, and epithelial cells through OMVs, it showed the internalisation of the bacterial OMVs by the intestinal epithelial cells and the transmigration of these bacterial OMVs via the paracellular route to reach other tissues such as the liver (Jones et al., 2020).

On the other hand, EVs released from intestinal epithelial cells interact with the gut microbiota. It was shown that an intestinal infection with the protozoan parasite *Cryptosporidium parvum* (*C. parvum*) resulted in an increased release of epithelial-EVs, and the EV release resulted in the activation of Toll-like receptor which recognises pathogens and activates several intracellular kinases, thus mediating epithelial antimicrobial defence mechanisms. These EVs also carry antimicrobial peptides of epithelial cell origin, including cathelicidin-37 and beta-defensin 2, and the exposure of *C. parvum* to these EVs decreased their viability and infectivity. Moreover, electron microscopy revealed the binding of epithelial-derived EVs to the surface of *C. parvum* (Hu et al., 2013). Other studies have shown the uptake of epithelial cell-derived miRNA (Liu et al., 2016) and epithelial cell-derived exosomes by *E. coli* (Kumar, A. et al., 2021). Therefore, host-EVs could be considered mediators of cross-kingdom interactions.

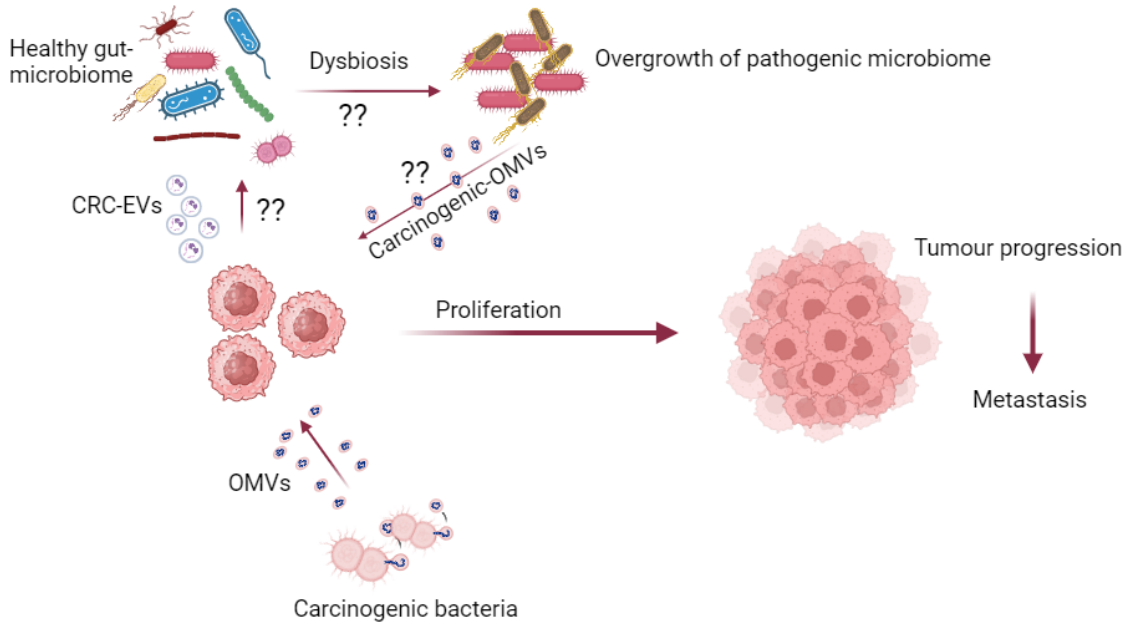

Figure 3.2: Host-gut microbiome cross-kingdom interactions. Carcinogenic bacteria such as pks+ E. coli release OMVs that carry carcinogenic contents, these OMVs are delivered into colon cells, promoting the tumorigenesis process. On the other hand, CRC-EVs could interact with gut microbiota, disrupting the healthy microbiome structure, and leading to dysbiosis which is highly associated with tumour initiation and progression.

3.2.3 Hypothesis and aims

This chapter hypothesises that CRC-derived EVs are mediators of host-microbiome kingdom interactions. As shown in (**Figure 3.3**). To investigate these interactions, potential functional routes will be assessed: binding interactions and uptake mechanisms (A), and content delivery mechanisms (B).

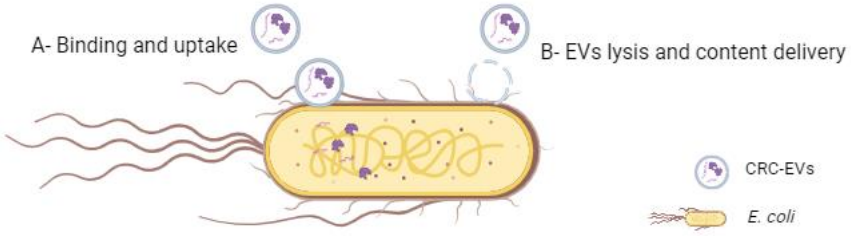

***Figure 3.3. Potential mechanisms of host-microbiome interactions**. Two potential mechanisms of EVs-E. coli interactions to be assessed: (A) binding of CRC-EVs to the surface of E. coli, and uptake of EVs by E. coli. (B) EV content delivery through EV lysis and release of contents.*

3.3 Results

3.3.1 Bacterial identification

To first confirm the identity of *E. coli* strains used, *E. coli* MG1655 and *E. coli* 11G5, the genome of both strains was sequenced and aligned to the reference genome of *E. coli k-12* MG1655 using data from GenBank. The variant calling analysis showed that *E. coli* MG1655 has higher similarities to the reference genome with only 2 mutations, 1 single-nucleotide variant (SNV) and 1 insertion-deletion (InDel). Whereas *E. coli* 11G5 has 2034 mutations, 2032 SNV, 2 InDel, (Table 7.1).

3.3.2 High-yield generation and isolation of EVs from CRC-cell lines using continuous cell culture and SEC approaches

A continuous cell culture approach was applied to obtain a high and reproducible yield of SW480- and SW620-cell line-derived EVs. EVs were isolated and separated from free proteins in the CM of CELLine bioreactor flasks by SEC, as previously described (Jamaludin et al., 2019; Suwakulsiri et al., 2019). Protein and particle concentrations in the collected SEC fractions were assessed by BCA and nanoparticle flow cytometry (NanoFCM), respectively, to determine EV-rich fractions. As shown in (Figure 3.4A), protein and particle quantification analysis showed no proteins and particles in fractions 1 to 5, and a peak of high protein and particle concentration was observed in fractions 7, 8, and 9. This indicates that SW480- and SW620- EVs are eluted in fractions 7, 8, and 9 (EVs-rich fractions) due to the aligned peaks of protein and particle concentrations. Fraction 8 contained the highest protein and particle yield, around 500 µg/ml proteins and $2.5*10^{11}$ particles/ml, respectively, for isolated SW480-EVs isolate. Around 500 µg/ml proteins and $1.5*10^{11}$ particles/ml, respectively for SW620-EVs isolate, therefore, fractions 7 to 9 were pooled for further use as EVs. However, lower particle and higher protein concentrations were observed in fractions 10 to 15.

Pooled EVs were then characterised following the ISEV guidance (Théry et al., 2018); TEM imaging was performed to investigate the size and morphology of isolated EVs, (Figure 3.4B) shows round double membranous structures, between 80-100 nm in diameter for SW480- and sW620- EVs, which is by the typical morphology/size of EVs (Kurtjak et al., 2022). Also, particle size and concentration profile in the pool fractions

(7-9) were assessed by NanoFCM (Figure 3.4C), and the average diameters of EVs secreted by SW480- and SW620-cell lines were confirmed as 77.37 nm and 72.64 nm, respectively.

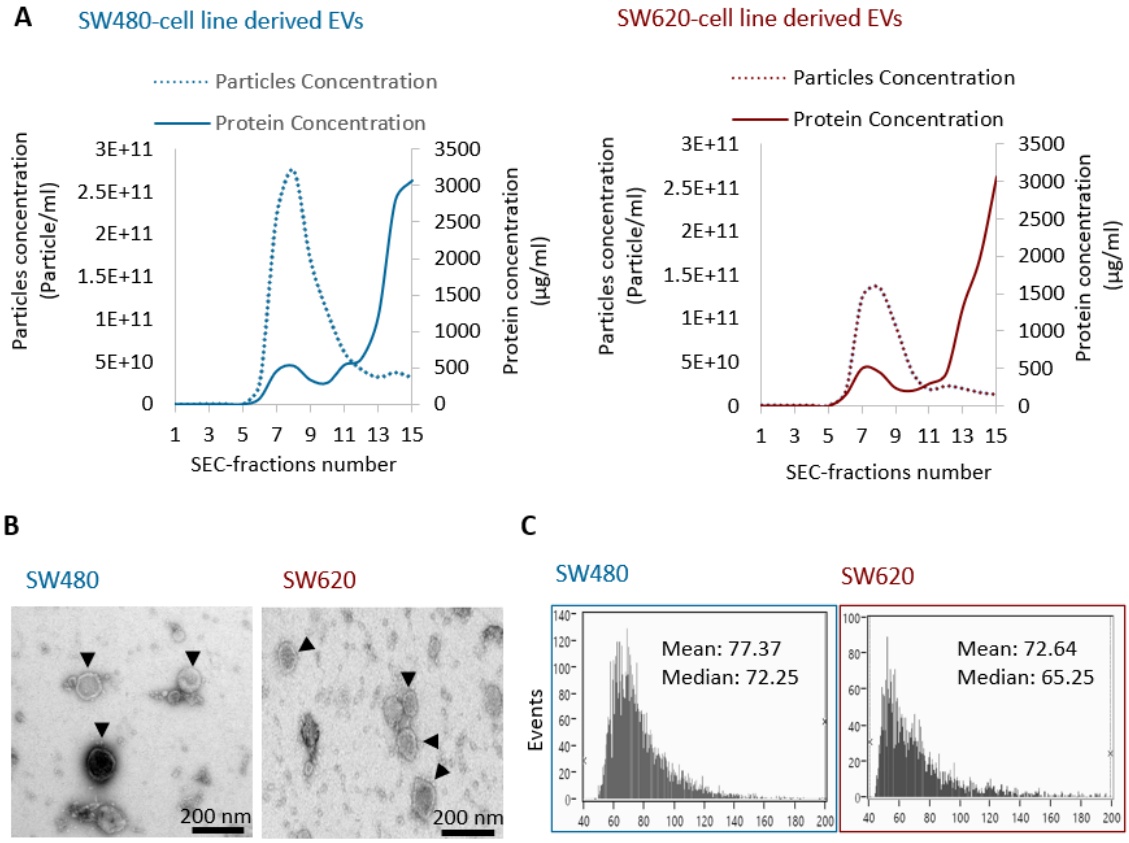

Figure 3.4: High-yield purification of CRC cell lines derived-EVs. (A) protein and particle concentrations in SEC fractions (Fractions 1-15) of SW480- and SW620- EVs isolates. (B) TEM-image of SW480- and SW620- EVs in the pool fractions (7-9) at 11500x magnification, black arrows indicate the round-double membranous structure, scale bar= 200 nm. (C) NanoFCM analysis showing particle size and concentration profile in the pool fractions (Fractions 7-9) of SW480- and SW620- EVs isolates. Representative replicates.

Finally, EV surface and cytosolic protein markers were detected by Western blot, NanoFCM, and ELISA (Figure 3.5). Western blot confirmed the presence of EVs in fractions 7-9 (Figure 3.5A), showing strong positivity of CD63 and CD9 in both SW480- and SW620- EVs SEC fractions. NanoFCM analysis showed the percentage of CD9- and CD63- positive particles, as shown in Figure 3.5B, around 20% and 40% of isolated SW480- and SW620-EVs, respectively, were CD9 positive. Also, around 10% of isolated SW480- and SW620- EVs were CD63 positive. ELISA was also performed to detect CD9,

CD63, CD81, and TSG101 in the pooled fractions (Figure 3.5C), high fluorescent signal was detected for CD81, CD63, and CD9 of both SW480- and SW620- EVs isolate, and a low signal was detected for the cytosolic TSG101 marker. Overall, NanoFCM, western blot, and ELISA revealed the classical SW480-EVs and SW620-EVs markers, indicating that the isolated particles were indeed EVs. Therefore, EVs were successfully isolated from defined fractions and pooled for further functional studies.

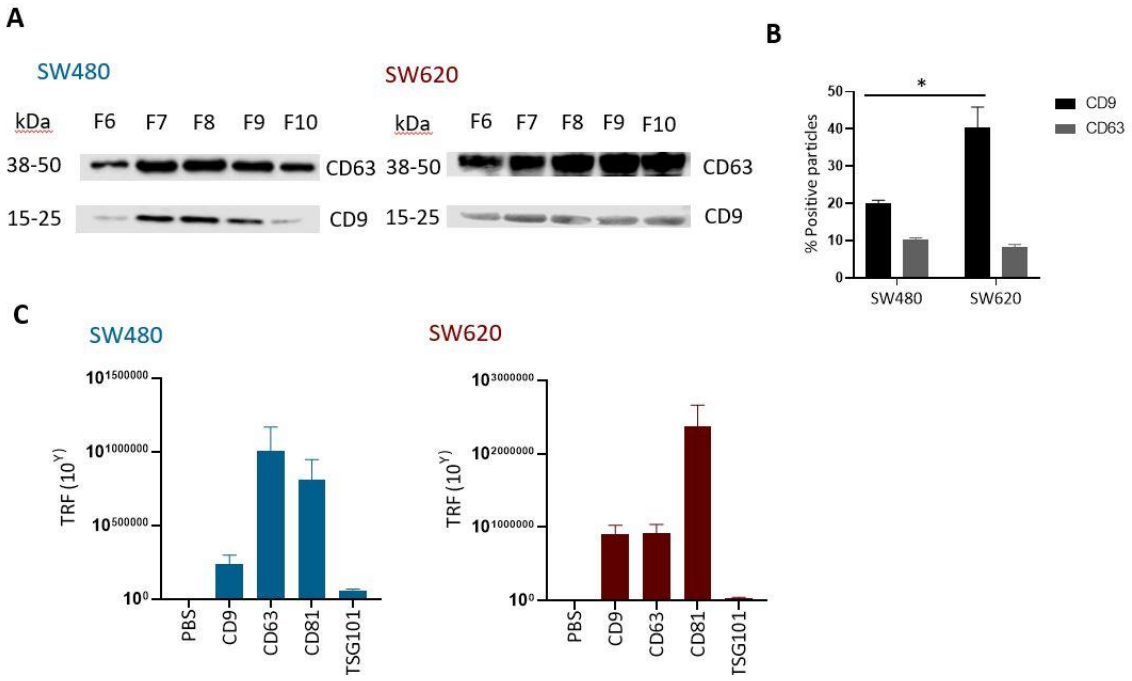

Figure 3.5: EVs classical markers detection of the isolated SW480-EVs and SW620-EVs. (A) Western blot analysis using anti-CD63 and anti-CD9 in SEC fractions (6-10) of SW480- and SW620-EV isolates. (B) NanoFCM analysis of the CD9 and CD63 positive particles in the pool fractions (F7-F9). (C) ELISA, the TRF signal (320 nm/615 nm) of DELFIA Europium-streptavidin in the pool fractions (F7-F9) of CD9, CD63, CD81 and TSG101 EVs-markers. Plots show mean ± SEM, n=3.

3.3.3 CRC cell lines derived-EVs interact with *E. coli.*

To investigate the interaction between *E. coli* and CRC-cell line-derived EVs, *E. coli* was co-cultured with SW620-EVs and observed by TEM and confocal microscopy. As shown in Figure 3.6, TEM imaging shows the structure of *E. coli* MG1655 (Figure 3.6A) without evidence of membrane vesicles presence. Figure 3.6B shows SW620-EVs only, as a control. Images of *E. coli* MG1655 co-cultured with SW620-EVs indicated the binding of

SW620-EVs to the surface (Figure 3.6 C, E, F) and the fimbriae structure of *E. coli* MG1655 (Figure 3.6D).

This interaction was further observed by confocal microscopy, SYTO-9 green labelled *E. coli* MG1655 (Figure 3.6G) and Cell-Tracker CMTPX red labelled SW620-EVs (Figure 3.6H) were co-cultured (Figure 3.6I), the co-localisation of the fluorescent signals confirmed the binding of CRC-cell line EVs to the surface of *E. coli* MG1655 and the possible uptake of EVs by *E. coli* MG1655. Overall, TEM and confocal microscopy revealed the interaction of CRC-EVs with *E. coli* and the potential uptake of EVs by *E. coli*, revealing the cross-kingdom interaction of human EVs and *E. coli*.

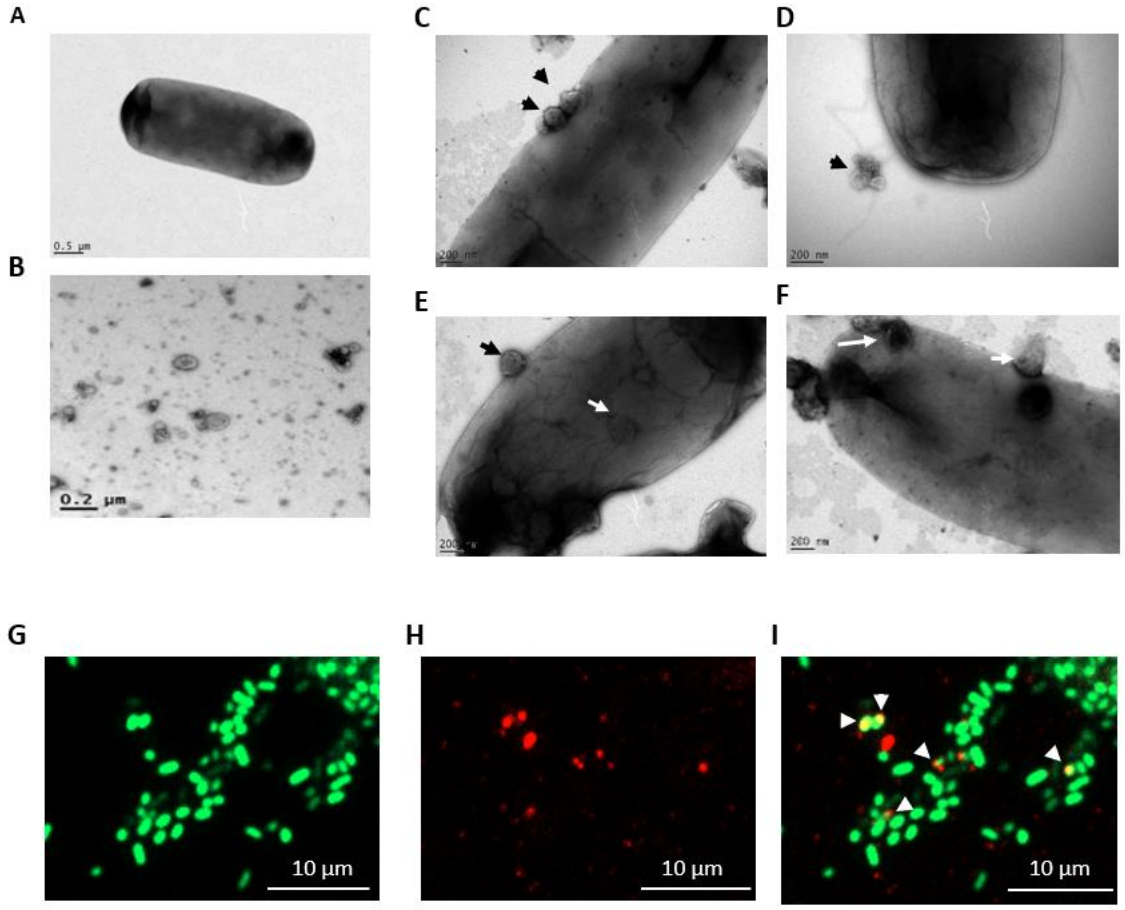

Figure 3.6: CRC-cell lines derived EVs interact with E. coli. TEM images of untreated E. coli MG1655 *at 4800x (A), SW620-EVs at 11500x (B), and E. coli* MG1655-*SW620-EVs co-culture at 9300 x (C, D, E, F), black arrows indicate the presence of EVs on the surface (C) and fimbriae of E. coli* MG1655 *(D). White arrows indicate the potential uptake of EVs by E. coli (E), and degradation of EVs on the surface of E. coli (F). Confocal microscopy images showing SYTO-9 green labelled E. coli* MG1655 *(G), Cell-Tracker CMPTX red labelled SW620-EVs (H), and fluorescently labelled E. coli* MG1655-*SW620-EVs co-culture (I), white arrows indicate for the co-localisation of the fluorescent signal. Representative images.*

3.3.4 EVs-*E. coli* interaction is disease-stage specific

Flow cytometry analysis was performed to quantify the uptake of CRC-cell line-derived EVs by *E. coli*, Memglow-700-labelled CRC-cell lines EVs were co-cultured with un-labelled *E. coli*, and the fluorescent bacterial cells were detected by flow cytometry. As shown in Figure 3.7, control non-florescent *E. coli* MG1655 (Figure 3.7A) were first gated and selected from a forward scatter-area vs side scatter-area dot plot to identify non-

fluorescent control bacteria depending on their size and complexity. After 18 hours of EVs-*E. coli* co-culturing, the percentage of Memglow-700 positive *E. coli* MG1655 was detected and gated, with 3.74% of *E. coli* cells being memglow-700 positive following co-culturing with labelled SW480-EVs (Figure 3.7B) and 11.3% of fluorescent *E. coli* following co-culturing with labelled SW620-EVs (Figure 3.7C).

Similarly, control non-fluorescent *E. coli* 11G5 (Figure 3.7D) were first gated and selected from a forward scatter-area vs side scatter-area dot plot, and the percentage of Memglow-700 positive *E. coli* 11G5 were detected and gated after 18 hours of co-culturing with labelled SW480- and SW620-EVs, 2.66% (Figure 3.7E) and 6.8% (Figure 3.7F), respectively. Therefore, interactions of both *E. coli* strains with SW620-EVs are significantly greater than interactions with SW480-EVs, indicating that these cross-kingdom interactions are disease-stage specific (Figure 3.8).

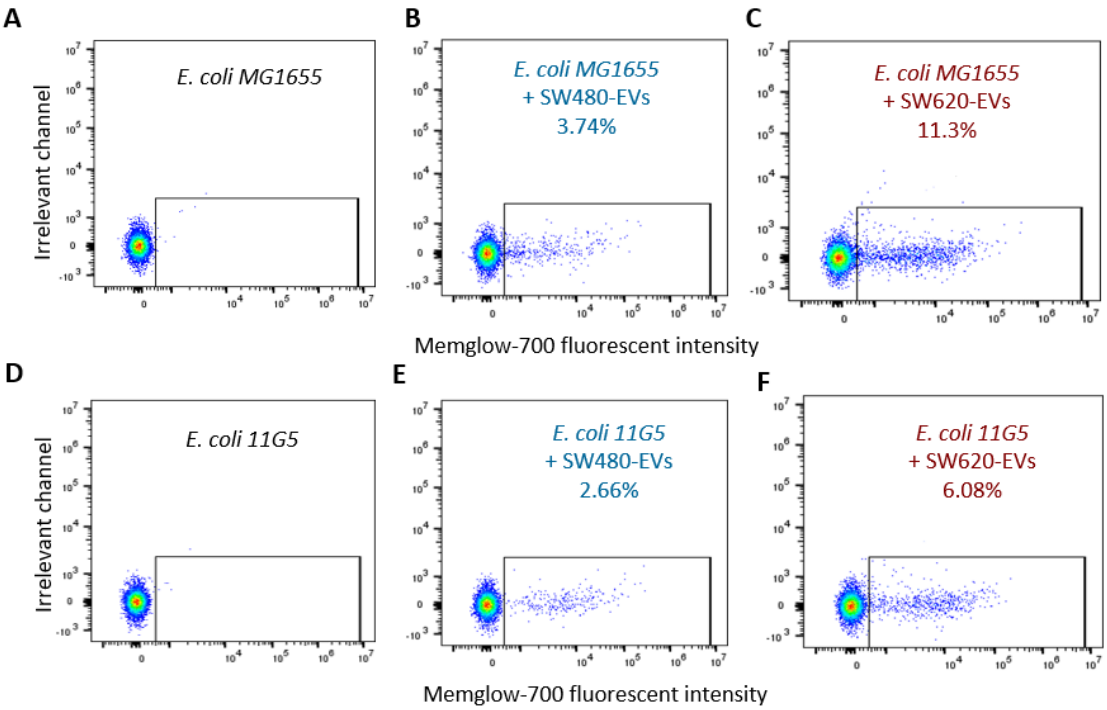

Figure 3.7: EVs- E. coli interaction is disease-stage specific. Flow cytometry analysis of untreated E. coli MG1655 *cells (G) and untreated E. coli* 11G5 *cells (J), and Memglow-700 red positive E. coli cells were sorted containing memglow-700 labelled SW480-EVs (H, K), and memglow-700 labelled SW620-EVs (I, L). The percentage of Memglow-700 positive E. coli* MG1655 *(M) cells and E. coli* 11G5 *(N) at 18 hours of co-culturing. N=3, representative replicate.*

Moreover, the dynamics of *E. coli*-EVs interactions were observed over time. As shown in Figure 3.8, the percentage of Memglow-700 positive *E. coli* MG1655 cells (Figure 3.8A) and Memglow-700 positive *E. coli* 11G5 cells (Figure 3.8B) increased over time.

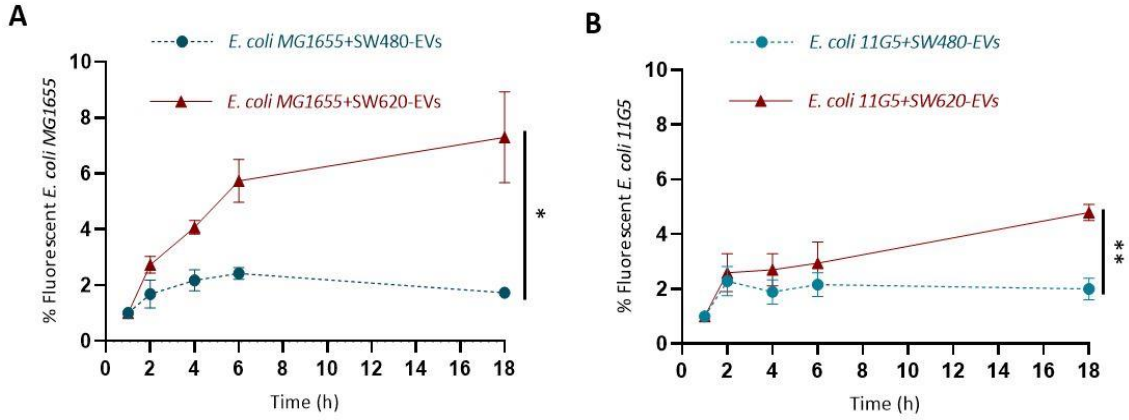

Figure 3.8: CRC cell line-derived EVs-E. coli interactions are strain-specific. Flow cytometry analysis of E. coli MG1655 *cells and E. coli* 11G5 *cells co-cultured with Memglow-700 labelled SW480- and SW620-EVs. The percentage of Memglow-700 positive E. coli* MG1655 *(A) cells and E. coli* 11G5 *(B) over 18 hours of co-culturing. Flow cytometry data were normalised to the first time point (1 hour of co-culturing). Error bars represent mean ± SEM, statistical analysis by t-test to the end-time point, * p<0.05, ** p<0.01, n=3.*

In comparison between *E. coli* MG1655 and *E. coli* 11G5, interactions between EVs and *E. coli* MG1655 are significantly greater, indicating that these interactions are also bacterial strain-specific (Figure 3.9).

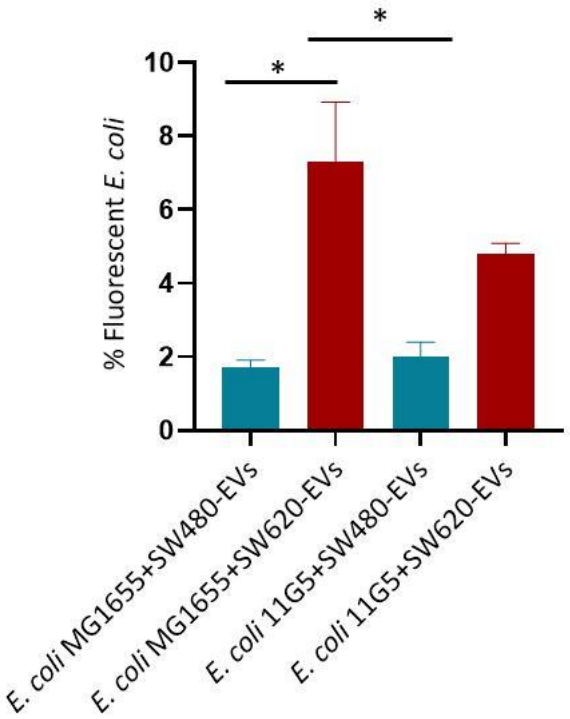

*Figure 3.9: Interactions between E. coli MG1655 and CRC cell line-derived EVs are greater than their interactions with E. coli 11G5. Flow cytometry analysis of E. coli MG1655 cells and E. coli 11G5 cells co-cultured with Memglow-700 labelled SW480- and SW620-EVs. The percentage of Memglow-700 positive E. coli MG1655 cells and E. coli 11G5 over 18 hours of co-culturing. Error bars represent mean ± SEM, statistical analysis by t-test to the end-time point, * p<0.05, ** p<0.01, n=3.*

To assess whether EV integrity is essential for *E. coli*-EVs interactions, Memglow-700 labelled EVs were degraded using Triton-X. Initially, Triton-X-treated SW620-EVs were analysed by NanoFCM, as shown in Figure 3.10, the particle concentration significantly decreased following Triton-X treatment (Figure 3.10A) and the particle size/concentration profile was also changed, with decreasing particle size and concentration (Figure 3.10B). Flow cytometry data showed that EV's integrity is essential for *E. coli*-EV interactions, the percentage of fluorescent bacterial cells also decreased when co-cultured with Triton-X treated SW620-EVs, in comparison to the percentage of fluorescent bacterial cells that were treated with intact SW620-EVs. Therefore, the loss of fluorescent bacterial cells suggests that EV's integrity is needed for *EVs-E. coli* interactions.

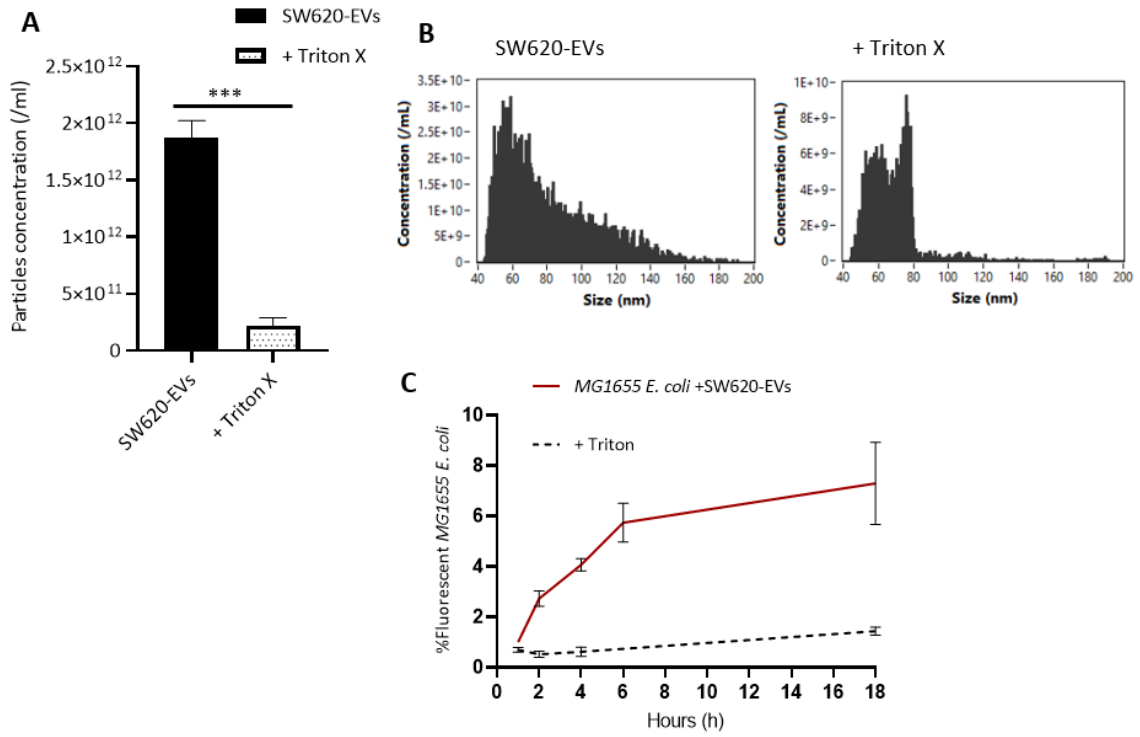

Figure 3.10: EV's integrity is essential for EVs-E.coli interactions. NanoFCM analysis showing the particle concentration (A) and particle size/concentration profile (B) of SW620-EVs treated with Triton-X. Flow cytometry analysis showing the percentage of Memglow-700 fluorecsent E. coli that was co-cultured with Memglow-700 labelled SW620-EVs, and Memglow-700 labelled and Triton-X treated SW620-EVs (C).

3.3.5 Clearing EV-surface proteins has no impact on EV's integrity

To investigate the possible binding mechanisms of these interactions, EV-surface sugars and proteins were digested to assess whether they are involved in the EVs binding to *E. coli* and the possible EVs uptake by *E. coli*. Initially, EV integrity and surface markers were examined following the enzymatic treatments, de-glycosylation and deproteination. Following de-glycosylation treatment (Figure 3.11), particle concentration was assessed by NanoFCM and showed no significant change in the particle concentration, a slight trend towards lower particle counts was observed (Figure 3.11A), and particle size/concentration profile (Figure 3.11B) also showed no change. EV markers were also assessed (Figure 3.11C), and there was an increase in the fluorescent signals of CD9, CD63, and CD81, indicating an increase in the sensitivity of markers detection following the de-glycosylation treatment of EVs. Overall, the de-glycosylation step had no impact on EV's integrity.

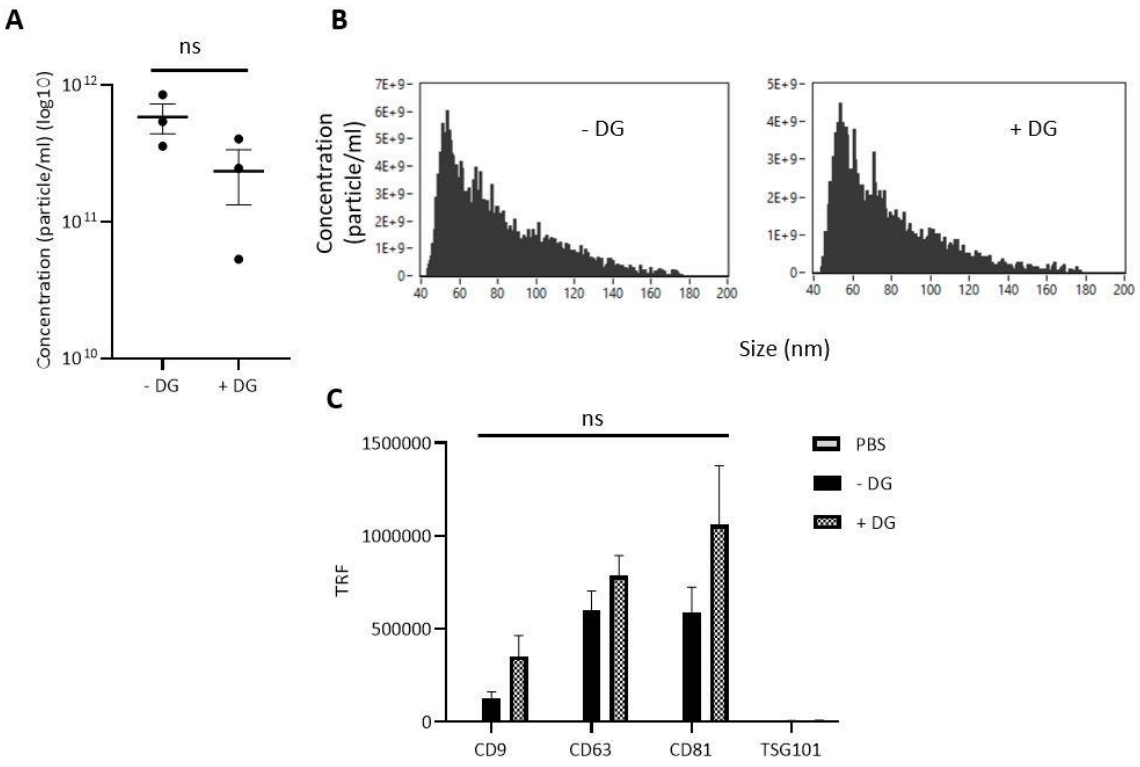

Figure 3.11: De-glycosylation enzymatic treatment had little impact on EV's integrity. Following the enzymatic treatment, nanoFCM particle concentration analysis showed no significant change in the particle concentration following the enzymatic treatment. (A). Particle size/concentration profile showing no change (B). (C) DELFIA-ELISA, the TRF signal (320 nm/615 nm) of DELFIA Europium-streptavidin showing the detection of EVs protein markers, CD9, CD63, CD81 and TSG101. Error bars represent mean ± SEM, representative replicate of particle size/concentration profile, n=3.

Similarly, as shown in Figure 3.12, particle concentration was assessed by nanoFCM and showed no significant change in the particle concentration (Figure 3.12A), particle size/concentration profile (Figure 3.12B) also showed no change following the de-proteination treatment by proteinase-k. EV protein markers, CD9, CD63, CD81, and TSG101, were assessed by ELISA (Figure 3.12C), and no CD9, CD81, and TSG101 signals were detected following protein digestion, however, a CD63 signal was detected indicating the presence of CD63 following protein digestion. Overall, the proteinase-k de-proteination reaction had no impact on EVs integrity.

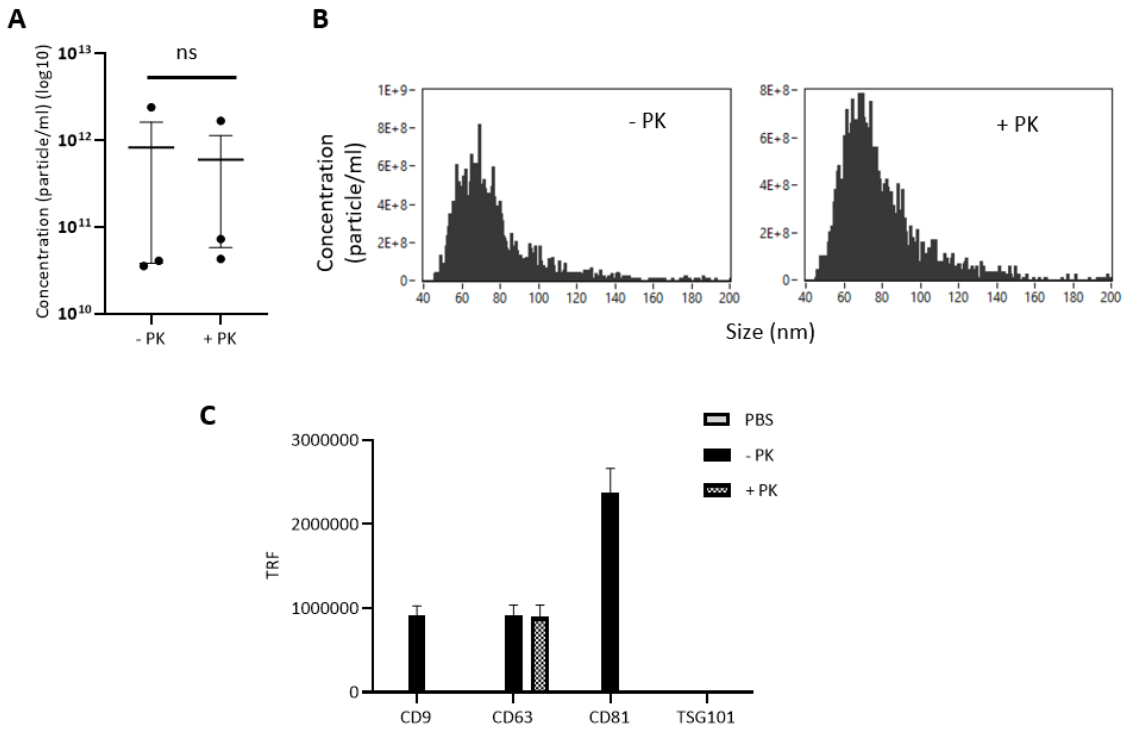

Figure 3.12: De-proteination enzymatic treatment had little impact on EV's integrity. (A) nanoFCM particle concentration analysis showed no significant change in the particle concentration following enzymatic treatment by proteinase-k. Also, (B) particle size/concentration profile by NanoFCM is showing no change. (C) DELFIA-ELISA, the TRF signal (320 nm/615 nm) of DELFIA Europium-streptavidin showing the detection of EV protein markers, CD63 and loss of signal for CD9 and CD81. Error bars represent mean ± SEM, representative replicate of particle size/concentration profile, n=3.

Lastly, EVs-proteins were digested by trypsin as not all proteins are sensitive to proteinase-k. As shown in Figure 3.13, particle concentration was assessed by NanoFCM and showed no significant change in the particle concentration (Figure 3.13A), and particle size/concentration profile (Figure 3.13B) also showed no change following the de-proteination treatment by trypsin. EV's protein markers were also assessed (Figure 3.13C), data showed a reduction in the fluorescent signal for CD9, CD63, and CD81, and no change for the TSG101 marker. ELISA detection of co-enzyme digestion of EV proteins (Figure 3.13D) showed no fluorescent signal for CD9, CD81 and TSG101 markers, and a reduction in the fluorescent signal for CD63 marker. Therefore, trypsin digestion did not affect EV's integrity and suggested that EV-surface markers are less sensitive to trypsin digestion. Proteinase-k and trypsin co-digestion reaction improved the sensitivity of EVs-surface marker to enzymatic digestion.

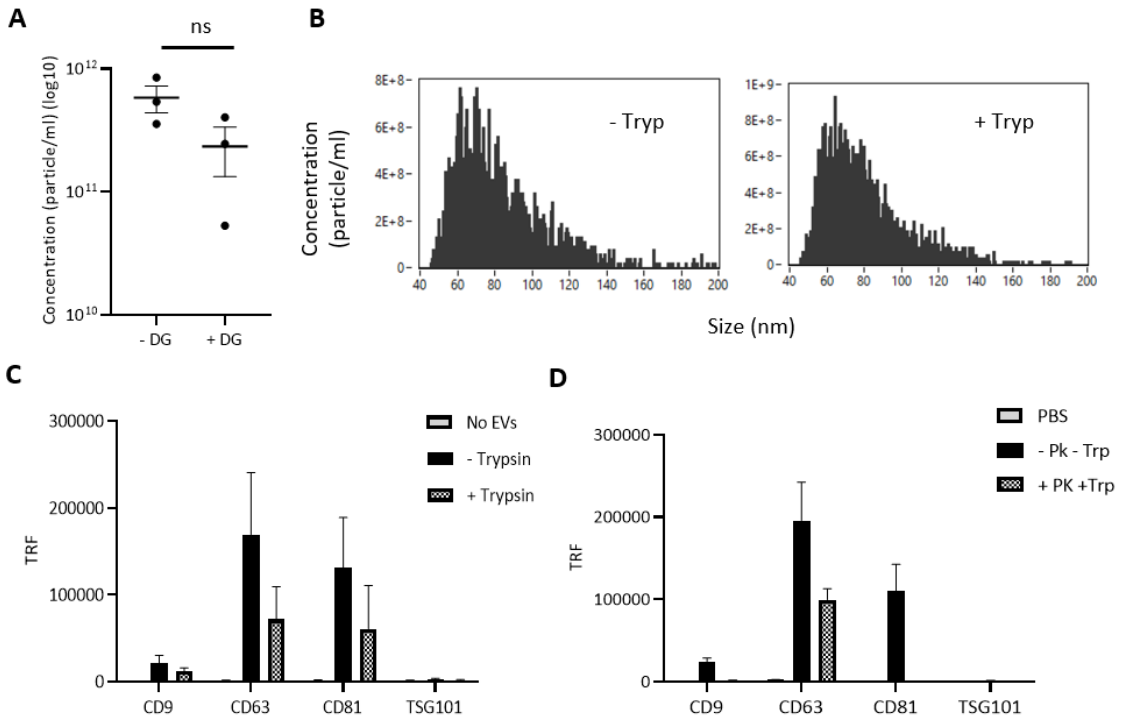

Figure 3.13: De-proteination treatment had little impact on EV's integrity. (A) NanoFCM particle concentration analysis showed no significant change in the particle concentration after trypsin treatment of EVs. Also, the particle size/concentration profile showed no change (B). DELFIA-ELISA, the TRF signal (320 nm/615 nm) of DELFIA Europium-streptavidin showing the detection of EVs-markers, CD9, CD63, CD81 and TSG101, following trypsin-enzyme digestion (C), and proteinase-k-trypsin co-digestion (D). Error bars represent mean ± SEM, representative replicate of particle size/concentration profile, n=3.

3.3.6 EVs-surface proteins mediate the *E. coli*-host EVs interactions

Following the assessment of enzymatic treatment on EV's integrity, treated SW620-EVs were labelled with Memglow-700 and co-cultured with unlabelled *E. coli* MG1655 to investigate mechanisms of interactions. As shown in Figure 3.14, flow cytometry analysis (Figure 3.14A) showed no change in the percentage of fluorescent *E. coli* MG1655 cells co-cultured with deglycosylated-SW620-EVs for six hours. However, a reduction in the percentage of fluorescent *E. coli* MG1655 cells was observed due to incubation with PK-treated SW620-EVs (Figure 3.14B). At 6 hours co-incubation, de-glycosylation of surface EVs-proteins showed no impact on *E. coli*-EVs interaction (Figure 3.14C), deproteination showed an impact on *E. coli*-EVs interactions (Figure 3.14D), proteinase-k, trypsin, and co-digestion of surface-EVs protein had an impact on this interaction, a significant

reduction in the percentage of fluorescent *E. coli* was observed, indicating disruption of interaction between CRC-EVs and *E. coli* following the lysis of EVs-surface proteins.

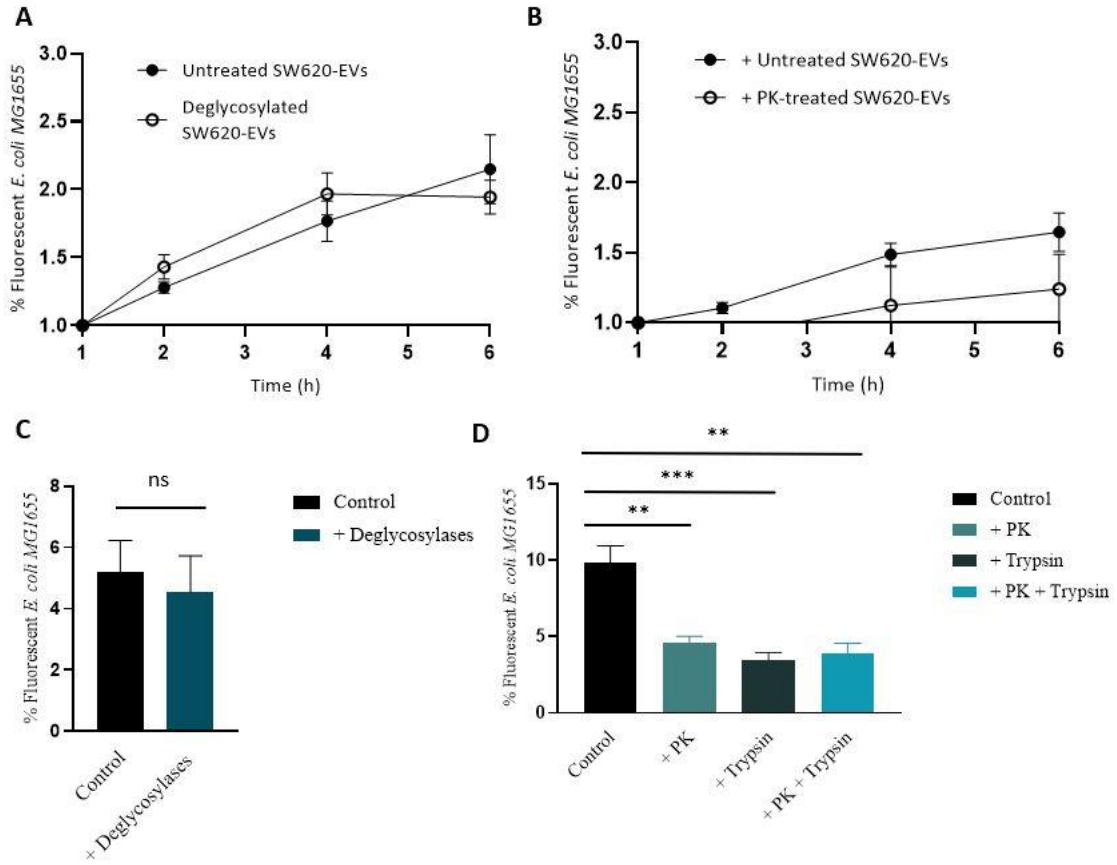

Figure 3.14: EVs-surface proteins are involved in E. coli-EVs interactions. Flow cytometry analysis of fluorescent E. coli MG1655 co-cultured with (A) de-glycosylated/ labelled SW620-EVs, and (B) proteinase-k/labelled SW620-EVs for six hours. At a six-hour co-culture time-point, the percentage of fluorescent E. coli MG1655 was assessed when co-cultured with de-glycosylated and labelled SW620-EVs (C), and with deproteinated and labelled SW620-EVs that were treated with proteinase-k, trypsin, and proteinase-k-trypsin co-enzymes (D). Error bars represent mean ± SEM, n=3, and statistical analysis was performed using a student t-test.

3.3.7 CRC cell line-derived EVs lysed by *E. coli* degrading enzymes

To investigate whether bacteria could degrade EVs without direct interaction, EVs were treated with bacterial-cell-free supernatant (S) of an overnight culture of *E. coli* MG1655. EVs were also treated with RIPA-lysis buffer (R) as a control for degraded EVs. As shown in Figure 3.15, the particle size/concentration profile of untreated EVs (Figure 3.15A), EVs treated with S (Figure 3.15B), and EVs treated with R (Figure 3.15C) showed

a reduction in the particle concentration and a shift in the size profile due to bacterial supernatant and RIPA buffer treatment. Particle concentration analysis (D) showed a significant reduction in the particle's concentration of SW620-EVs treated with bacterial supernatant and RIPA lysis buffer. Therefore, *E. coli* had an impact on EV's integrity, appearing to secrete substances that lyse EVs.

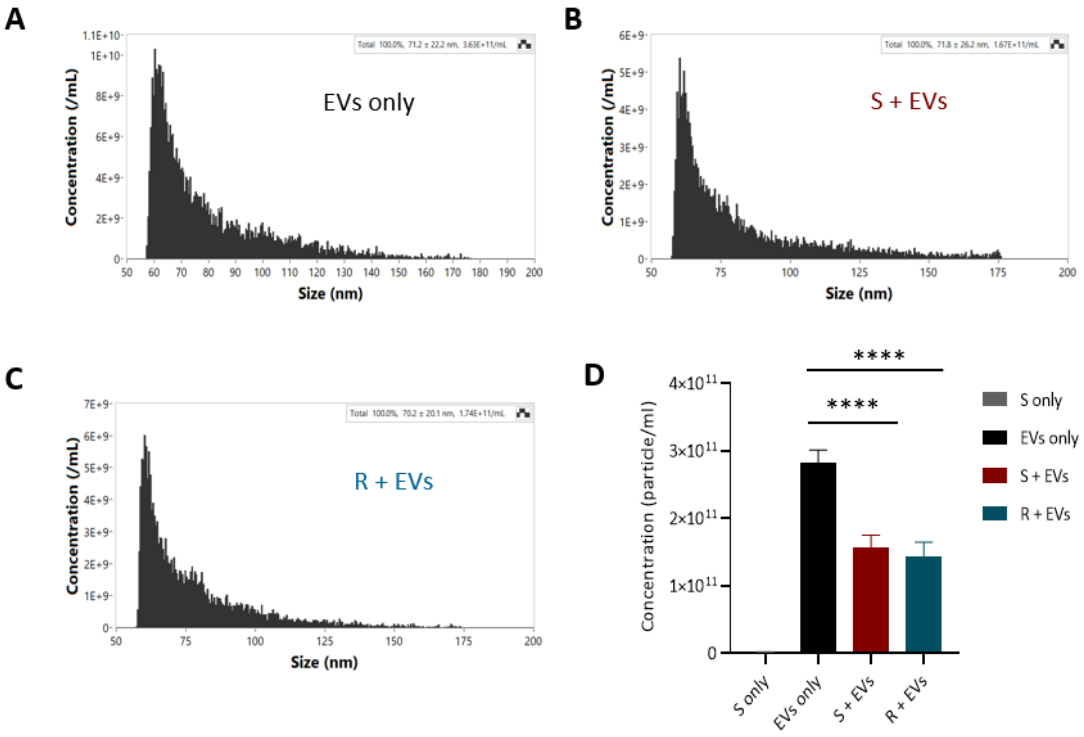

Figure 3.15: E. coli lyses CRC-derived EVs. NanoFCM particle size/concentration profile of untreated SW620-EVs (B), SW620-EVs treated with bacterial supernatant (S) (B), and SW620-EVs treated with RIPA lysis buffer ®(C). Particle concentration analysis of EVs treated with S and R buffer (D). Error bars represent mean ± SEM, representative replicate of particle size/concentration profile, n=3, and statistical analysis was performed using student t-test.

3.4 Discussion

CRC is the second most common cause of cancer death in the UK, more than 16,800 people die from CRC in the UK each year (Morgan et al., 2023). Notably, the incidence of CRC in the younger age group (<50 years old), for whom early screening is not recommended, has risen and is estimated to increase by more than 140% by 2030 (Hofseth et al., 2020; Siegel, Jakubowski, Fedewa, Davis, & Azad, 2020). With only 10-15% of CRC cases being hereditary, new primary prevention strategies are crucial to reduce the disease incidence rate.

In the past decade, CRC development and progression have been linked to the gut microbiome (Wong, S. H. & Yu, 2019) and gut dysbiosis which results in the decreased diversity and abundance of commensal bacteria that have been closely linked to CRC (Rebersek, 2021). It has been reported that pathogenic intestinal bacteria such as *F. nucleatum*, *E. coli*, and *B. fragilis* play a vital role in CRC progression (Cheng, Ling, & Li, 2020; Zhou, P., Yang, Sun, & Zhou, 2022). Many studies have revealed the differences in the abundance of these gut microbiota species at various stages of CRC; the number of these pathogenic species increases during the development and progression of the disease (Liang, J. Q. et al., 2021; Yachida et al., 2019; Zhang, Xinyu et al., 2019). These variations in the bacterial composition between healthy and CRC patients suggest underlying host-control mechanisms contributing to gut dysbiosis that have not been investigated yet. Therefore, this chapter hypothesises that CRC-EVs interact with *E. coli* and mediate gut microbiome alterations.

3.4.1 CRC-EVs isolation and characterisation

In CRC, EVs have been considered functional entities that play crucial roles in tumour progression through functional cell-cell cargo transfer and cell-EV interactions, activating various tumorigenic signalling pathways. It is also evident that CRC cells release EVs into the tumour microenvironment to modulate the surrounding cells for cancer promotion and progression (Glass & Coffey, 2022). EVs could also mediate the tumour-gut microbiome homeostasis, therefore, their role in this possible cross-kingdom interaction was investigated. CRC-cell lines, SW480 and SW620, were utilised as a model of various stages of CRC and the progression of the tumour, they were

cultured in bioreactor flasks for large-scale purification of EVs, as previously described (Suwakulsiri et al., 2019)

A high yield of isolated SW480- and sW620- EVs was obtained; around 0.75 m per weekly isolate. Also, EVs were characterised by multiple complementary techniques, following the MISEV 2018 guidance (Minimal information for studies of extracellular vesicles) (Théry et al., 2018). Data showed specific characteristics of the isolated SW480-EVs and SW620-EVs, such as their morphology, the double membranous structure, density, and size distribution. The presence of surface and cytosolic proteins (CD9, CD63, CD81, and TSG101) in SW480-EVs and SW620-EVs isolates was confirmed by Western blot, NanoFCM, and ELISA. Since ELISA is a cell surface-antigen detection method (Bishop & Hwang, 1992), signal for TSG101, cytosolic protein, was not detected, indicating that EVs were intact. Overall, bioreactor-cell culture and SEC isolation approaches are reliable procedures to generate high yields of EVs.

3.4.2 CRC-EVs interact with *E. coli*

Studies have shown the uptake of colon epithelial cells-derived EVs by gut bacteria (Kumar, A. et al., 2021). In this chapter, TEM images showed that CRC-cell line-derived EVs interact with *E. coli*. EVs bind to the surface and surface motility structures (fimbriae) of *E. coli*, revealing cross-kingdom communication and interactions between *E. coli* and CRC. Also, flow cytometry analysis showed that these cross-kingdom interactions are specific, they vary depending on the *E. coli* strain type and EVs-type, data showed that the interactions and binding between *E. coli* and SW620-EVs are greater than their interactions with SW480-EVs. It also showed that the interactions between EVs and the *E. coli* MG1655 strain are greater than their interactions with the *E. coli* 11G5 strain. Lastly, the intensity of these interactions increases over time.

One explanation for these selective interactions could be that CRC cells actively select the microorganisms that support their progression, EVs could have receptors that can bind to specific species, and the expression of these receptors could also be disease-stage-dependent. These selective interactions could lead to an altered gut environment and shift the balanced gut towards an inflammatory and disease-driven state. A previous finding showed an abnormally higher prevalence of *E. coli* in biopsies of CRC, compared to healthy patients (Bonnet et al., 2014). These findings provide a foundation for future

studies to investigate the mechanism of interaction that illustrates the variation in the level of interactions.

3.4.3 Disruption of surface-EVs proteins and glycan had no impact on EV's integrity

Enzymatic disruption of surface-EVs glycans and proteins did not affect the EV's integrity, NanoFCM analysis confirmed that the particle concentration is similar to the control, non-treated EVs. However, there was a difference in the EV markers (CD9, CD63, and CD81) detection profile by ELISA; de-glycosylation of surface-proteins enhanced their detection whereas proteinase-k treatment changed the marker detection profile, signals for CD9 and CD81 were lost due to the enzymatic degradation, but no change was detected for CD63 as it is not sensitive to proteinase-k treatment due to high level of glycosylation, as shown previously (Bonsergent et al., 2021; Diaz et al., 2018).

To enhance surface-protein degradation, EVs were treated with trypsin only, and with a combination of both enzymes, proteinase-k and trypsin. Trypsin treatment had no impact on EV's integrity, as particle concentration did not change compared to the control non-treated EVs. By contrast with proteinase-k treatment, signals for CD9, CD63 and CD81 were all reduced, compared to marker detection of the control non-treated EVs. Previous studies have shown the differences between trypsin and proteinase-k treatment, including the insensitivity of CD81 to trypsin (Choi, Dongsic et al., 2020), and CD9 sensitivity to proteinase-k treatment and insensitive to trypsin treatment (Tang et al., 2019). Proteinase-k/trypsin co-enzymatic digestion changed the markers detection profile, no signal was detected for CD9 and CD81, and a reduction of CD63 signal was observed.

3.4.4 EVs-surface proteins mediate the EVs-*E. coli* cross-kingdom interactions

Tumour-derived EVs are enriched with tumour-associated glycans. Glycosylation, the post-translation modification of proteins, has been identified as a key process involved in the biosynthesis and function of EVs (Wu, L. & Gao, 2023). Numerous proteins at the surface of EVs have been identified as highly glycosylated, it has been shown that EV surface receptors are involved in cellular crosstalk mechanisms (Isaac, Reis, Ying, & Olefsky, 2021). Many studies have shown that EV glycans are involved in the EV uptake

process, a study showed that integrin beta chain 3 (glycoprotein) mediates the uptake of EVs by tumour cells by activating integrin-mediated endocytosis as it interacts with heparan sulfate proteoglycans (Fuentes et al., 2020). It has been also shown that EV-surface proteins play a role in the fusion and uptake of EVs by recipient cells such as EVs surface tetraspanin, CD9 and CD81 (Mulcahy, Pink, & Carter, 2014).

Moreover, other findings showed the reduction in the uptake of EVs by recipient cells following enzymatic treatment with proteinase-k (Inder et al., 2014; Smyth, Redzic, Graner, & Anchordoquy, 2014) and de-glycosylases (Williams et al., 2019) which strongly supports the role of protein and glycans in EV uptake. This chapter aimed to assess whether EVs-surface proteins are involved in cross-kingdom interactions, and data showed that the disruption in EVs-surface glycans has no impact on the interaction, however, disruption of surface-proteins interfered with the EVs-*E. coli* interactions. There was no change by flow cytometry in the percentage of Memglow-700 fluorescent *E. coli* co-cultured with de-glycosylated labelled SW620-EVs for six hours. However, a reduction in the percentage of fluorescent *E. coli* was observed when *E. coli* was incubated with deproteinated Memglow-700 labelled, SW620-EVs. As a comparison between proteinase-k and trypsin, treatment with both enzymes individually and co-digestion with both enzymes significantly reduced the flow cytometry signal, indicating disruption of binding and uptake of EVs by *E. coli*.

3.4.5 *E. coli* degrades EVs

In terms of the EV-mediated host cell-cell crosstalk, many studies have revealed the internalisation of EVs by recipient cells and delivery of their contents into the cytosol (Mulcahy, Pink, & Carter, 2014), it was also shown that EVs release their content upon their interactions with the plasma membrane (Bonsergent & Lavieu, 2019), and this mechanism is not explored in EV-bacteria interactions. Therefore, to investigate another potential mechanism of *E. coli*-EVs interaction, the degradation and lysis of EVs by bacterial degrading enzymes were assessed. Treating EVs with a supernatant of bacterial overnight culture resulted in a significant reduction of particle concentration, and this impact is comparable to the positive control of EVs-lysis by RIPA buffer. This suggests that external degradation of EVs by *E. coli* degrading enzymes is a possible approach for *E. coli* to uptake EV contents.

3.5 Future work

This chapter has shown the binding of EVs to the surface of *E. coli*, and future work would involve finding EVs-surface receptor/s that is/are involved in this binding. Previous studies have undertaken comprehensive surface membrane protein analysis of EVs secreted by SW480-cell line and SW620-EVs (Suwakulsiri et al., 2024). Therefore, identifying EVs-surface proteins by proteomic analysis and blocking potential receptors would be a future experiment to find a binding receptor of EVs to *E. coli*. 140 surface membrane proteins of SW480-EVs that were sensitive to proteinase-k treatment were identified previously (Xu et al., 2019), and only 25 of these proteins were found to be enriched in SW620-EVs compared to SW480-EVs (Choi, Dongsic et al., 2020). Since the interaction between SW620-EVs and *E. coli* is greater than between SW480-EVs and *E. coli*, it is feasible to investigate these 25 proteins first. Literature review showed that 6 out of the 25 could potentially be linked to interactions with *E. coli* including tetraspanin CD81 (Ramachandran et al., 2018), low-density lipoprotein receptor, LDLR (Runova & Golubkov, 2002), and transferrin receptor protein, TFRC (Jennifer et al., 2020).

Moreover, cargo transfer to *E. coli* through EVs could be investigated. Previous studies showed that EVs are more efficient at cellular drug delivery compared to free drugs (Chandler et al., 2023). Therefore, loading labelled EVs with Oxaliplatin, a chemotherapy drug for CRC treatment, and tracking cargo delivery to *E. coli* could reveal whether EVs could be used as therapeutic tools for treating bacterial infection and CRC.

3.6 Conclusions

To conclude, CRC-EVs mediate host-gut interactions. EVs interact with *E. coli*, and CRC-EVs attach to the surface and motility structure of *E. coli*. These interactions are disease-stage specific; greater interaction was observed between *E. coli* and EVs derived from metastatic-cell lines, compared to EVs derived from non-metastatic early-stage CRC. Also, the interaction between CRC-cell line-derived EVs and non-pathogenic *E. coli* (*E. coli* MG1655) is greater than their interactions with CRC-associated *E. coli* (*E. coli* 11G5). Lastly, EVs binding and uptake by *E. coli* is not the only mechanism of interaction, *E. coli* lyses EVs to, potentially, facilitate the uptake of the EVs content.

4 Colorectal cancer extracellular vesicles reduce the ability of *Escherichia coli* to form biofilm

4.1 Abstract

Overview: CRC accounts for about 10% of all new cancer cases worldwide. The gut microbiome comprises a large population of microorganisms and has been identified as an etiological factor for CRC. Dysbiosis is closely related to tumour development and progression. A large body of evidence reveals differences in gut microbial composition between CRC patients and healthy individuals, and a high prevalence of pro-inflammatory and pro-carcinogenesis microbes have been found in CRC patients. The previous chapter (Chapter 3) showed that CRC interacts with *E. coli* through EVs, and this chapter hypothesises that CRC-derived EVs alter the phenotypic characteristics of *E. coli* and contribute to microbial shifts towards dysbiosis.

Methods: EVs were isolated by SEC from CRC-cell lines, CRC patient blood, healthy individual blood, and CRC tissues. EVs were characterised following the MISEV guidance; NanoFCM, TEM, western blot, and ELISA were performed to confirm the EV presence in the EV isolates. The impact of EVs on *E. coli* MG1655 (laboratory strain) and *E. coli* 11G5 (CRC-associated strain) growth was performed using turbidimetric assay and on the bacterial ability to form biofilm using batch microtiter plate-based system The impact on bacterial growth was assessed under aerobic and anaerobic growth conditions. Lastly, the impact of short and long-term exposure to EV on bacterial phenotypic characteristics, growth and biofilm formation, was investigated.

Results: CRC cell line derived-EVs altered the phenotypic characteristics of *E. coli*; SW620-EVs increased the growth of *E. coli* MG1655, and both types of cell line derived-EVs decreased the ability of both *E. coli* strains to form a biofilm with higher impact observed due to SW620-EVs treatment, compared to SW480-EVs. The impact of blood-derived EVs and tissue-derived EVs mirror the impact of cell line-derived EVs, they increased the growth of *E. coli* and decreased its ability to form biofilm. Overall, CRC-EVs have a functional impact on the bacterial phenotypic characteristics; increased bacterial growth and decreased its ability to form a biofilm.

4.2 Introduction

A healthy human body consists of about 30 trillion human cells and about 38 trillion bacteria. The colon has a higher number of bacteria and is more susceptible to developing cancer, compared to the small intestine (Sender, Fuchs, & Milo, 2016). It is evident that gut dysbiosis is involved in the initiation and progression of CRC as well as its response to different treatment strategies (Rebersek, 2021). Therefore, analysis of gut microbiome structure provides important information for screening and early detection of CRC, and potentially a prediction of treatment outcome. Moreover, revealing mechanisms by which CRC contribute to gut dysbiosis could provide new preventative strategies for CRC.

4.2.1 Gut dysbiosis and CRC

Eubiosis is defined as the healthy balanced state of the gut microbiome and is characterised by diverse bacterial structure, a balance between pro-inflammatory and anti-inflammatory cytokines, a balance between immune cells and IgA secretion, and an intact healthy mucosal barrier and mucus layer of the gut. This balanced healthy state is maintained through constant crosstalk between the host and microbiome, and between the microbiome community. Contrarily, under dysbiosis, these characteristics are disturbed, and the balance shifts in favour of pathogens that are normally suppressed by beneficial members of the gut microbiome, this results in an increased gut vulnerability to pathogenic and carcinogenic bacterial toxins, hence promoting the initiation and progression of CRC (Koliarakis et al., 2019; Rebersek, 2021).

It was initially proposed that CRC is linked to individual bacteria such as *Helicobacter pylori* (Strofilas et al., 2012) and *E. coli* (Arthur et al., 2012). Various studies have investigated the alterations in the gut bacterial structure in CRC patients, compared to healthy subjects, and demonstrated variations in the bacterial profile between healthy subjects, and patients with adenomas and CRC, suggesting a continuous shifting mechanism of the microbiota during CRC progression (Figure 4.1) (Cheng, Ling, & Li, 2020), a decrease in beneficial species that contribute to gut homeostasis, such as Bifidobacterium, and an increase in pathogenic and pro-inflammatory species have been observed in CRC patients, compared to healthy individuals. Recent studies have identified *B. fragilis*, *Streptococcus bovis*, *Enterococcus faecalis*, *E. coli*, *F. nucleatum*, and

Peptostreptococcus anaerobius as CRC-associated pathogens. This suggests that the initiation of CRC is correlated to the modification of the balanced interaction between the host and microbiome, promoting the prevalence of pathogenic bacterial profile (Cheng, Ling, & Li, 2020; Flemer et al., 2017; Koliarakis et al., 2019). However, mechanisms involved in this shift have not been investigated yet.

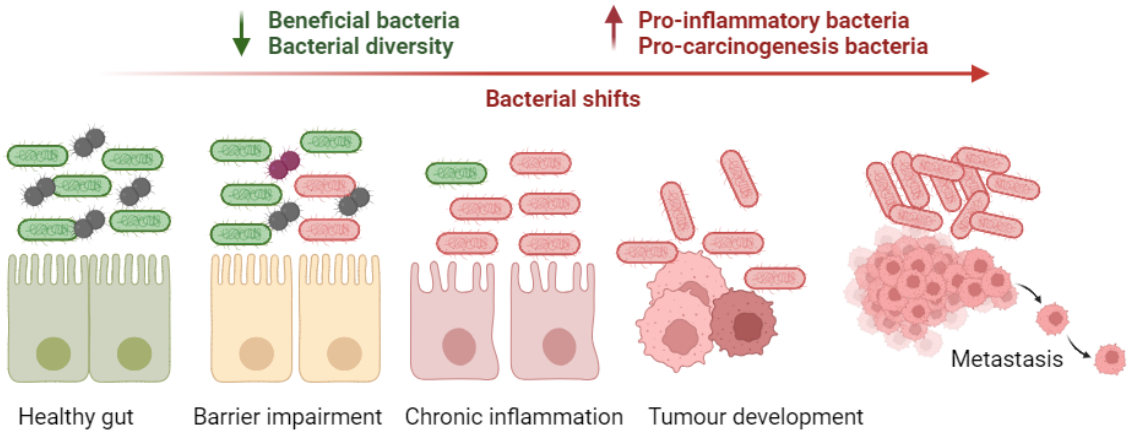

Figure 4.1: Intestinal dysbiosis in CRC development. A bacterial shift in favour of pro-inflammatory and pro-carcinogenesis bacteria is linked to the development of CRC, and a continuous shift leads to the overgrowth of pathogenic bacteria and loss of beneficial bacteria, overgrowth of pathogenic and adherent bacteria leads to loss of barrier integrity and chronic inflammation, and ultimately tumour development and progression.

4.2.2 Mechanisms of gut microbiome in CRC

Bacteria can directly be involved in the carcinogenesis process, and these pro-carcinogenic strains can be involved in CRC through different mechanisms including inflammation, bacterial genotoxins, metabolites and biofilm (Cheng, Ling, & Li, 2020; Ranjbar et al., 2021). Compared to healthy individuals, a higher abundance of pro-carcinogenesis strains has been detected in CRC patients. On the other hand, a decrease in the abundance of beneficial bacteria has been involved in CRC development (Quaglio, Grillo, De Oliveira, Di Stasi, & Sassaki, 2022). For example, *Faecalibacterium prausnitzii* is one of the most abundant beneficial bacteria in the gut, it has anti-inflammatory and immunomodulatory properties due to its butyrate production, and a decrease in its abundance has been reported in CRC patients (Nishida et al., 2018).

F. nucleatum leads to increased expression of inflammatory mediators (Proença et al., 2018), it acts at the early steps of CRC carcinogenesis as it adheres to and induces CRC through its *Fusobacterium adhesin A* that binds to E-cadherin and activates inflammatory and oncogenic signalling pathways (Rubinstein et al., 2013). Also, it inhibits T cell activation and natural cell cytotoxicity, protecting the tumour from immune cell attack (Gur et al., 2015), and induces secretion of pro-inflammatory cytokines that promote CRC migration (Casasanta et al., 2020). *E. coli* produces genotoxin that leads to DNA damage (Pleguezuelos-Manzano et al., 2020; Pleguezuelos-Manzano, Puschhof, & Clevers, 2022), *B. fragilis* secretes toxins that disrupt the colonic barrier (Wu, S., Rhee, Zhang, Franco, & Sears, 2007), and *Peptostreptococcus anaerobius* induces a pro-inflammatory microenvironment to promote tumorigenesis (Long et al., 2019).

4.2.3 Eubiosis-dysbiosis shift mechanisms

The mechanisms that lead to an increase in the abundance of the pathogenic and inflammation-inducing strains in CRC have not been investigated yet. However, one mechanism by which this shift could occur is the oxygen hypothesis which proposes a reduction in obligate anaerobes and an increase in facultative anaerobes such as *E. coli* in gut inflammation. Under homeostasis, epithelial cells mediate the depletion of oxygen through beta-oxidation processes to generate anaerobic conditions, contrarily, a reduction in beta-oxidation processes has been observed under inflammation, which is associated with increased availability of oxygen, thus altering the bacterial community structure promoting dysbiosis (Rizzatti, Lopetuso, Gibiino, Binda, & Gasbarrini, 2017). It was also hypothesised that inflammation-induced nitrate production could promote the overgrowth of *E. coli* (Winter et al., 2013).

Notably, studies showed that these shifts vary at different stages of CRC (Wu, J. et al., 2023) (Figure 4.2). For example, it has been shown that the relative abundance of *F. nucleatum* in CRC was higher compared to adenoma, with a significant linear trend of increase during CRC development and progression (Liang, J. Q. et al., 2020). Given the fact that the tumour modulates its surrounding microenvironment in favour of its progression, this suggests that the tumour could modulate the gut microbiome and promote the balanced gut homeostasis-dysbiosis shift in favour of its progression.

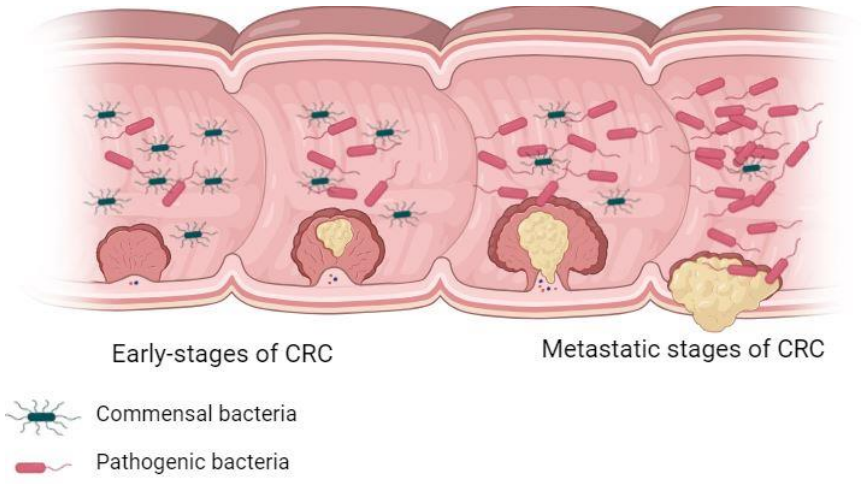

Figure 4.2: Gut homeostasis-dysbiosis shift during cancer progression. The abundance of several CRC-associated strains increases at later and metastatic stages of the disease, compared to the early stages of CRC.

Accumulating evidence suggests that EVs are essential for gut homeostasis, they have been involved in immunity and inflammation regulation in the gut, as well as regulation of intestinal mucosa and epithelial barrier function (Jiang et al., 2016; Ocansey et al., 2020; Shen, Q., Huang, Yao, & Jin, 2022). Numerous studies have shown that EVs from host cells could play a role in microbial reconstruction and dysbiosis (Liu et al., 2016; van Bergenhenegouwen et al., 2014; Zhao, L. et al., 2021). Indeed, EVs-mediated gut microbial shaping is a potential strategy for manipulating the microbiome which may become an important application in CRC and other intestinal disease therapies. However, EV's role in CRC-associated dysbiosis has not been investigated yet.

4.2.4 Hypothesis and aims

This chapter hypothesises that CRC contributes to the shift of the gut microbiome towards dysbiosis through EVs, and CRC-EV contents have a functional impact on the phenotypic characteristics of the gut microbiome (Figure 4.3). To test this hypothesis, the following aims will be investigated:

- To assess the impact of CRC-cell line-derived EVs, CRC patients' blood-derived EVs, healthy individual's blood-derived EVs, and CRC tissue-derived EVs on the growth and ability of *E. coli* to form biofilm under aerobic and anaerobic growth conditions.
- To assess the impact of CRC-cell line-derived EVs on *E. coli* growth and ability to form biofilm following short- and long-term exposure of *E. coli* to EVs.
- To assess the impact of EV-treated *E. coli* on CRC-cell line proliferation.

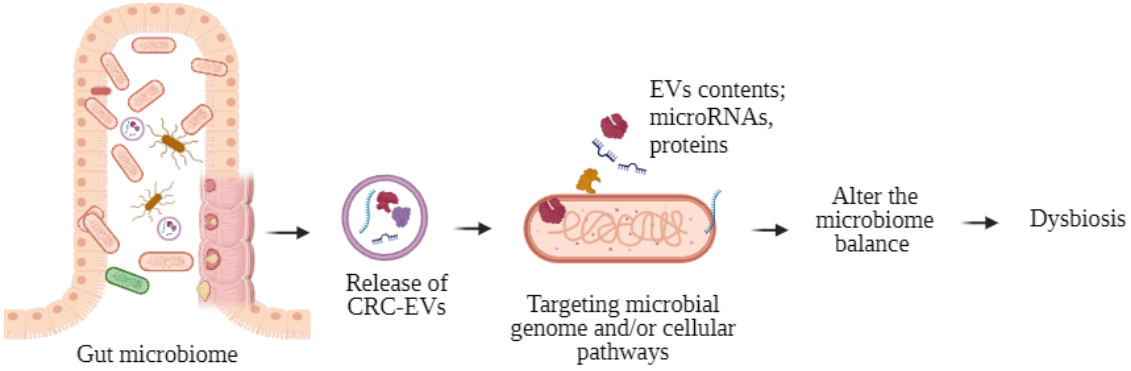

Figure 4.3: CRC could be involved in the eubiosis-dysbiosis shift of the gut microbiome. CRC could modulate the gut microbiome through EVs. Functional contents of CRC-EVs could target the gut bacteria, and alter their phenotypic characteristics, thus promoting dysbiosis.

4.3 Results

4.3.1 SW480-cell line derived-EVs increased the growth of *E. coli* MG1655 under anaerobic growth conditions

To assess the impact of SW480-cell line derived-EVs on bacterial growth under aerobic and anaerobic growth conditions, *E. coli* MG1655 were treated with different concentrations of SW480-EVs (5 ng/ml, 50 ng/ml, 500 ng/ml, 5 µg/ml, and 50 µg/ml). Bacterial growth was not affected following treatment by any concentration of SW480-EVs as demonstrated by measuring absorbance at 600 nm (Figure 4.4).

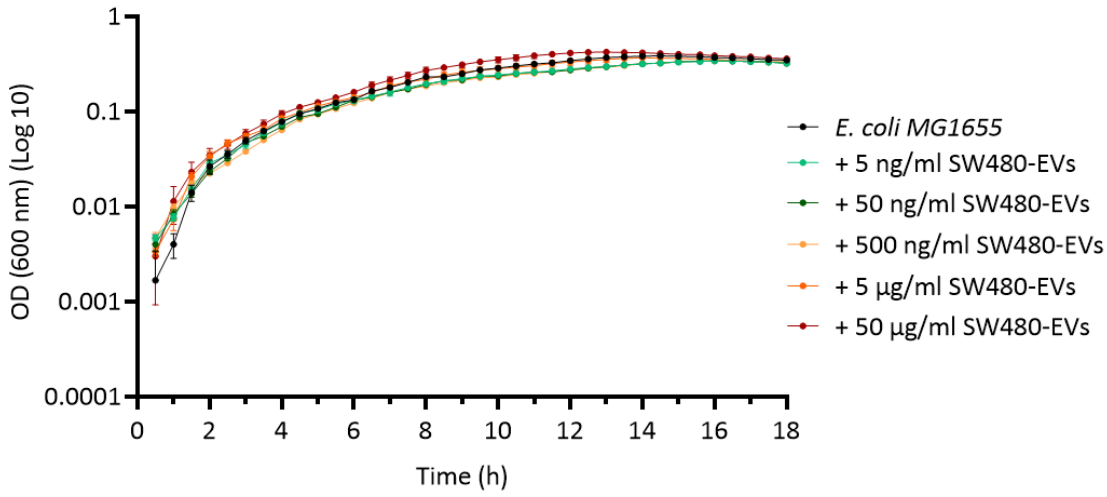

Figure 4.4: Growth curve of E. coli MG1655 under aerobic growth conditions. Absorbance at 600 nm of E. coli MG1655 culture treated with different concentrations of SW480-EVs (5 ng/ml, 50 ng/ml, 500 ng/ml, 5 µg/ml, and 50 µg/ml) under aerobic growth conditions for 18 hours. Error bars represent mean ± SEM, n=3.

However, mimicking physiologically relevant conditions, under anaerobic growth conditions, treating *E. coli* MG1655 with 50 µg/ml of SW480-EVs increased the bacterial growth but low-dose of EVs, 5 µg/ml, had no impact on the bacterial growth (Figure 4.5). This indicates that SW480-EVs increase bacterial growth under physiologically relevant growth conditions.

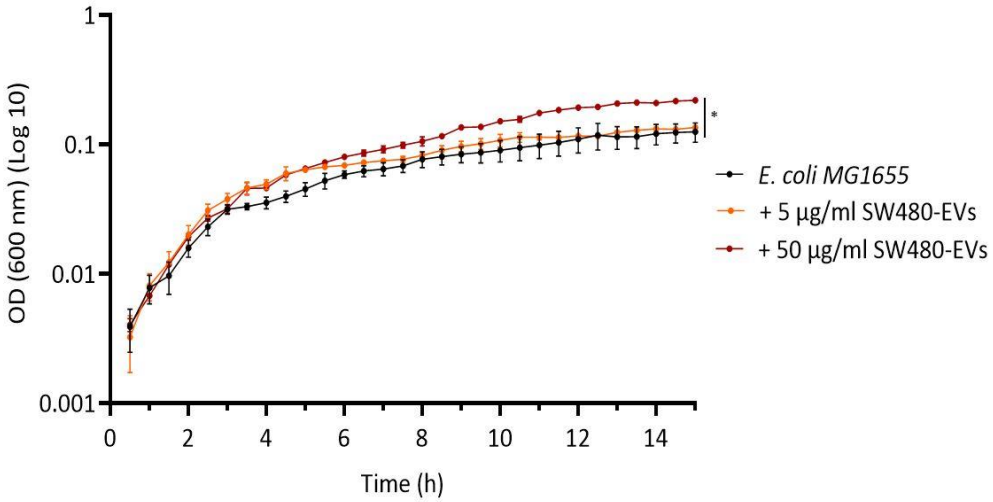

Figure 4.5: Growth curve of E. coli MG1655 treated with SW480-cell line derived EVs under anaerobic growth conditions. Absorbance at 600 nm of E. coli MG1655 culture treated with 5 µg/ml and 50 µg/ml SW480-EVs under anaerobic growth conditions for 15 hours. Error bars represent mean ± SEM, p<0.05, n=3.

4.3.2 SW620-cell line derived-EVs increased the growth of *E. coli* MG1655 under aerobic and anaerobic growth conditions

A modest increase in *E. coli* MG1655 growth was observed when treated with different concentrations of SW620-EVs under aerobic growth conditions (Figure 4.6). Lower doses of SW620-EVs (5 ng/ml, 50 ng/ml, 500 ng/ml, and 5 µg/ml) had no impact on bacterial growth, and a high dose of 50 µg/ml of SW620-EVs increased bacterial growth.

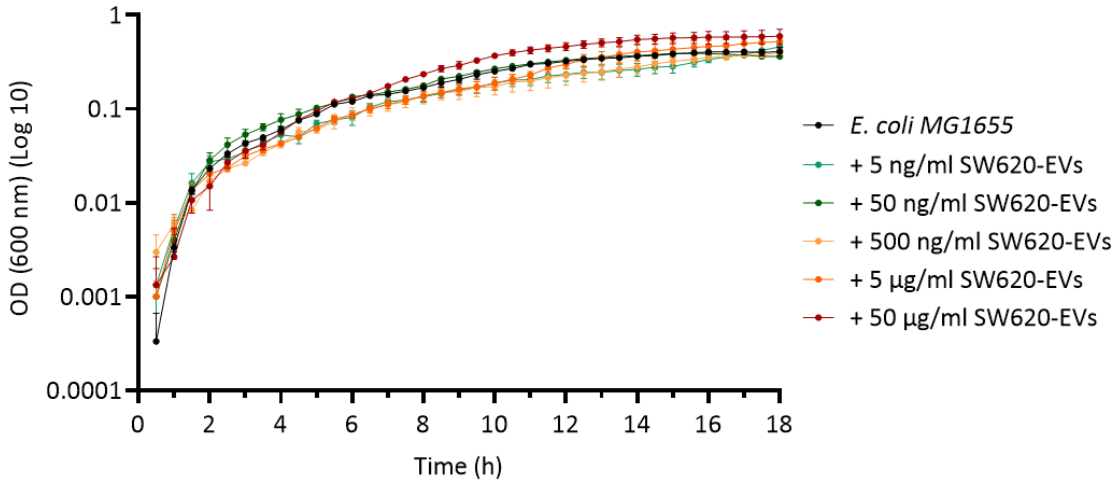

Figure 4.6: Growth curve of E. coli MG1655 under aerobic growth conditions. Absorbance at 600 nm of E. coli MG1655 culture treated with different concentrations of SW620-EVs (5 ng/ml, 50 ng/ml, 500 ng/ml, 5 µg/ml, and 50 µg/ml) under aerobic growth conditions for 18 hours. Error bars represent mean ± SEM, n=3.

A non-significant increase was observed after 6 hours of co-incubation with SW620-EVs; OD_{600nm} reading increased from 0.126 to 0.128 (Figure 4.7A). However, there was a significant increase in *E. coli* MG1655 growth after 12 hours (Figure 4.7B) and 18 hours (Figure 4.7C) of incubation with 50 µg/ml SW620-EVs, the OD_{600nm} reading increased from 0.331 to 0.461, and from 0.376 to 0.590, respectively.

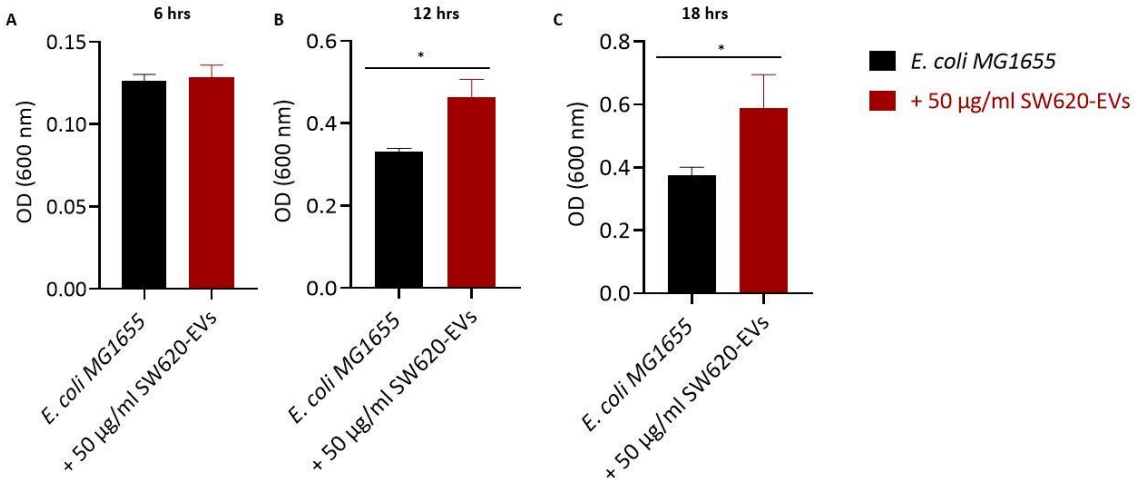

*Figure 4.7: SW620-EVs significantly increased the growth of E. coli MG1655 under aerobic growth conditions. Bar charts representing the absorbance (OD) readings at 600 nm of the bacterial growth after 6 hrs (A), 12 hrs (B), and 18 hrs (C) incubation of E. coli MG1655 with 50 µg/ml of SW620-EVs. Error bars represent mean ± SEM, n=3. Statistical analysis by T-test, * p<0.05.*

However, both high-dose and low-dose SW620-EVs (5 µg/ml and 50 µg/ml) increased the growth of *E. coli* MG1655 under anaerobic growth conditions (Figure 4.8). The impact of 50 µg/ml dose is higher than 5 µg/ml, at 6 hrs time-point of incubation, the OD_{600nm} increased from 0.051 to 0.075 and from 0.051 to 0.117 when *E. coli* MG1655 was co-cultured with 5 µg/ml and 50 µg/ml of SW620-EVs, respectively.

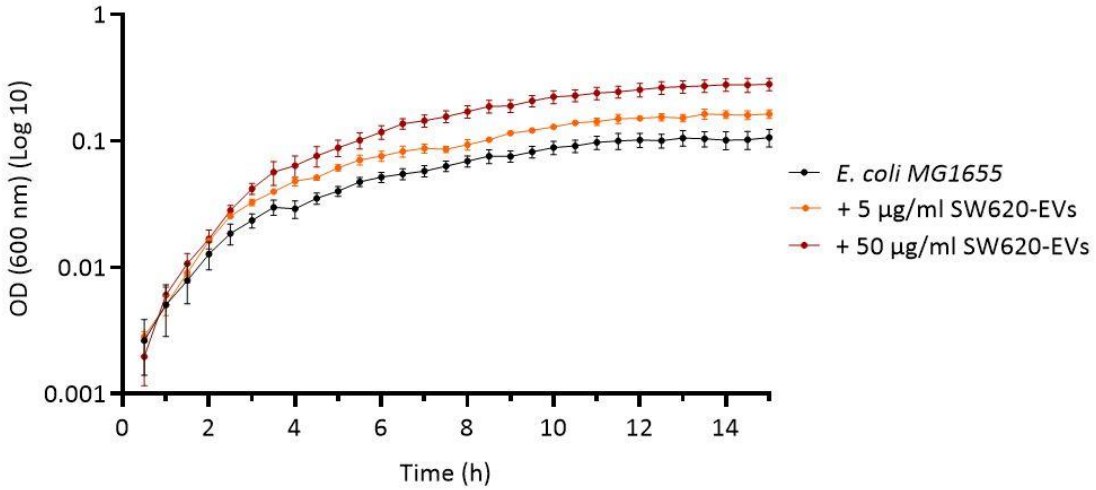

Figure 4.8: Growth curve of E. coli MG1655 treated with SW620-EVs under anaerobic growth conditions. Absorbance at 600 nm of E. coli MG1655 culture treated with SW620-EVs (5 µg/ml and 50 µg/ml) under anaerobic growth conditions for 15 hours. Error bars represent mean ± SEM, n=3.

There was a significant increase in *E. coli* MG1655 growth after 6 hrs, 12hrs, and 15 hrs of incubation with 50 µg/ml SW620-EVs, the OD_{600nm} reading increased from 0.051 to 0.117 (Figure 4.9A), from 0.101 to 0.253 (Figure 4.9B), and from 0.106 to 0.281 (Figure 4.9C), respectively. Therefore, SW620-EVs increased the growth rate of *E. coli* MG1655 throughout the incubation period under anaerobic growth conditions.

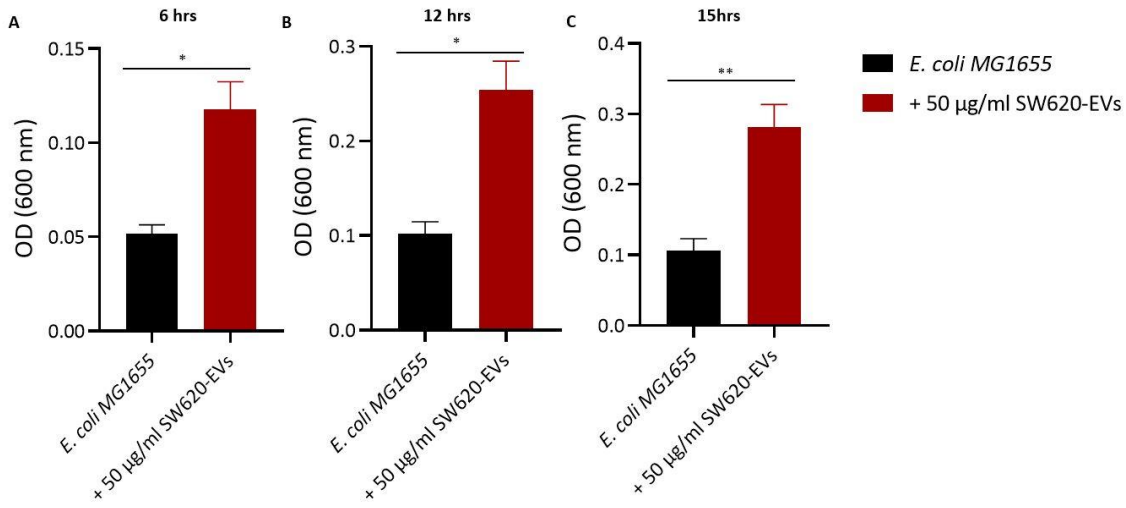

*Figure 4.9: SW620-EVs significantly increased the growth of E. coli MG1655 under anaerobic growth conditions. Bar charts representing the OD readings at 600 nm of the bacterial growth after 6 hrs (A), 12 hrs (B), and 15 hrs (C) incubation of E. coli MG1655 with 50 µg/ml of SW620-EVs. Error bars represent mean ± SEM, n=3. Statistical analysis by T-test, * p<0.05, **<0.01.*

In comparison between EV types, SW620-EVs had a significantly higher impact on bacterial growth compared to SW480-EVs (Figure 4.10), after 12 hours of bacterial incubation with EVs under anaerobic growth conditions, OD_{600nm} increased from 0.105 to 0.192 and from 0.105 to 0.253 when bacteria were incubated with 50 µg/ml SW480-EVs and 50 µg/ml SW620-EVs, respectively. Overall, these data indicate that SW620-EVs can induce bacterial growth under both anaerobic and anaerobic growth conditions, and their impact on bacterial growth is higher than SW480-EVs, however, this difference is not statistically significant.

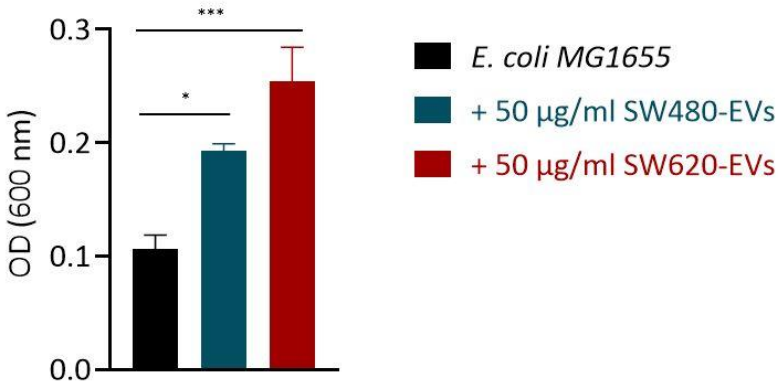

*Figure 4.10: Growth of E. coli MG1655 treated with CRC-cell line derived EVs under anaerobic growth conditions. Absorbance at 600 nm of E. coli MG1655 culture treated with 50 µg/ml of SW480-EVs and SW620-EVs after 12 hours of culturing under anaerobic growth condition. Error bars represent mean ± SEM, n=3. Statistical analysis by one-way ANOVA test, Brown-forsythe and Bartlett's tests, * p<0.05, *** p<0.001.*

4.3.3 CRC cell line derived-EVs reduced the ability of *E. coli* MG1655 to form a biofilm

To assess the impact of CRC cell line derived-EVs on the ability of *E. coli* MG1655 to form a biofilm, bacteria were treated with different concentrations (5 ng/ml, 50 ng/ml, 500 ng/ml, 5 µg/ml, and 50 µg/ml) of SW480-EVs and SW620-EVs and incubated for 24 hrs at 37 °C under aerobic growth conditions, the formed biofilm was then assessed. SW480-EVs significantly decreased the ability of *E. coli* MG1655 to form a biofilm with the highest impact observed due to 50 µg/ml of SW480-EVs treatment, the number of CFU/ml of biofilm cells decreased from $7.66*10^7$ CFU/ml to $8*10^5$ CFU/ml (Figure 4.11A). Similarly, SW620-EVs significantly decreased the ability of *E. coli* MG1655 to form a biofilm with the highest impact observed due to 50 µg/ml of SW620-EVs treatment, the number of CFU/ml of biofilm cells decreased from $8*10^7$ CFU/ml to $1.6*10^5$ CFU/ml (Figure 4.11B). The inhibitory impact of SW620-EVs on the ability of *E. coli* MG1655 to form biofilm was significantly higher than the impact of SW480-EVs (Figure 4.11C).

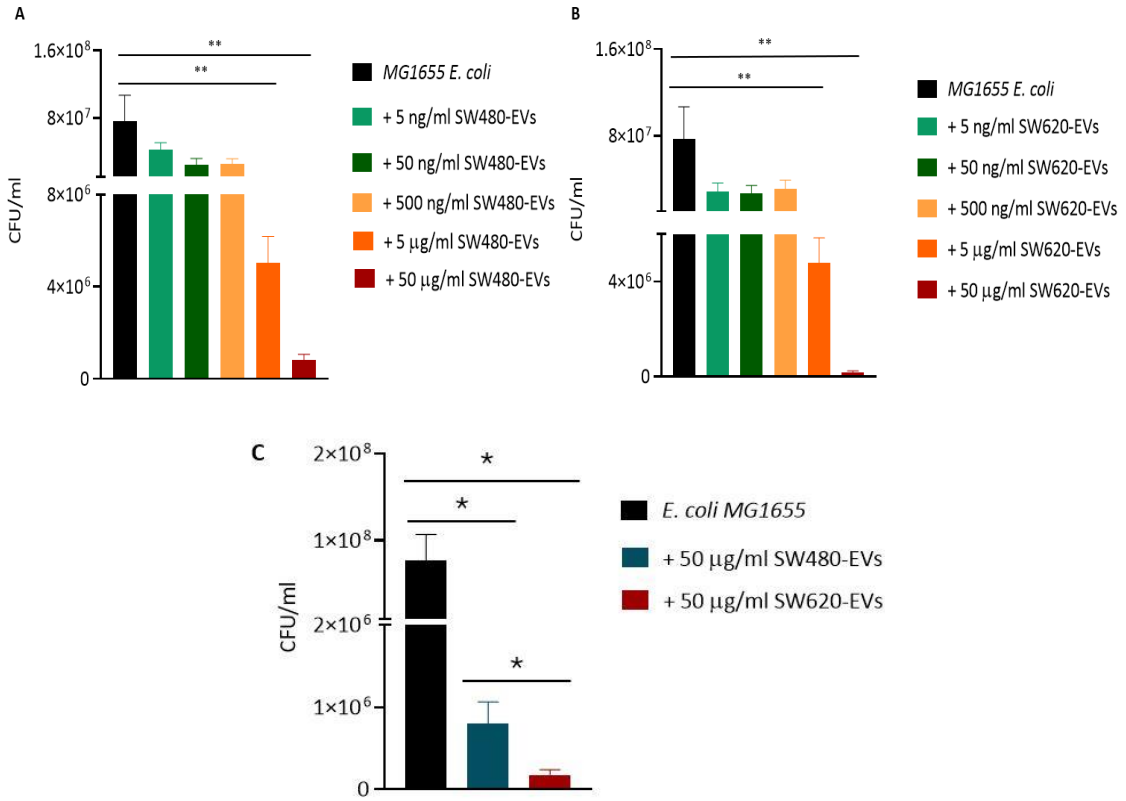

*Figure 4.11: CRC cell lines-derived EVs reduce the ability of E. coli MG1655 to form biofilm under aerobic growth conditions. The number of CFU/ml of E. coli MG1655 biofilm cells treated with different concentrations of SW480-EVs (A) and SW620-EVs (B) (5 ng/ml, 50 ng/ml, 500 ng/ml, 5 µg/ml, and 50 µg/ml). (C) The number of CFU/ml of E. coli MG1655 biofilm cells treated with 50 µg/ml of SW480-EVs and 50 µg/ml SW620-EVs. Error bars represent mean ± SEM, n=3. Statistical analysis by one-way ANOVA test, Brown-forsythe and Bartlett's tests, * p<0.05, **<0.01.*

Similarly, mimicking physiologically relevant conditions, CRC-cell-derived EVs inhibited the ability of *E. coli* MG1655 to form biofilm under anaerobic growth conditions. SW480-EVs significantly decreased the ability of *E. coli* MG1655 to form a biofilm with the highest impact observed due to 50 µg/ml of EVs treatment compared to 5 µg/ml, the number of CFU/ml of biofilm cells decreased from $1.8*10^7$ CFU/ml to $2.5*10^5$ CFU/ml (Figure 4.12A). Also, SW620-EVs significantly decreased the ability of *E. coli* MG1655 to form a biofilm with the highest impact observed with 50 µg/ml of SW620-EVs, the number of CFU/ml of biofilm cells decreased from $2.9*10^7$ CFU/ml to $6.3*10^5$ CFU/ml (Figure 4.12B). Overall, the inhibitory impact of SW620-EVs on the ability of *E. coli* MG1655 to form biofilm was significantly higher than the impact of SW480-EVs (Figure 4.12C).

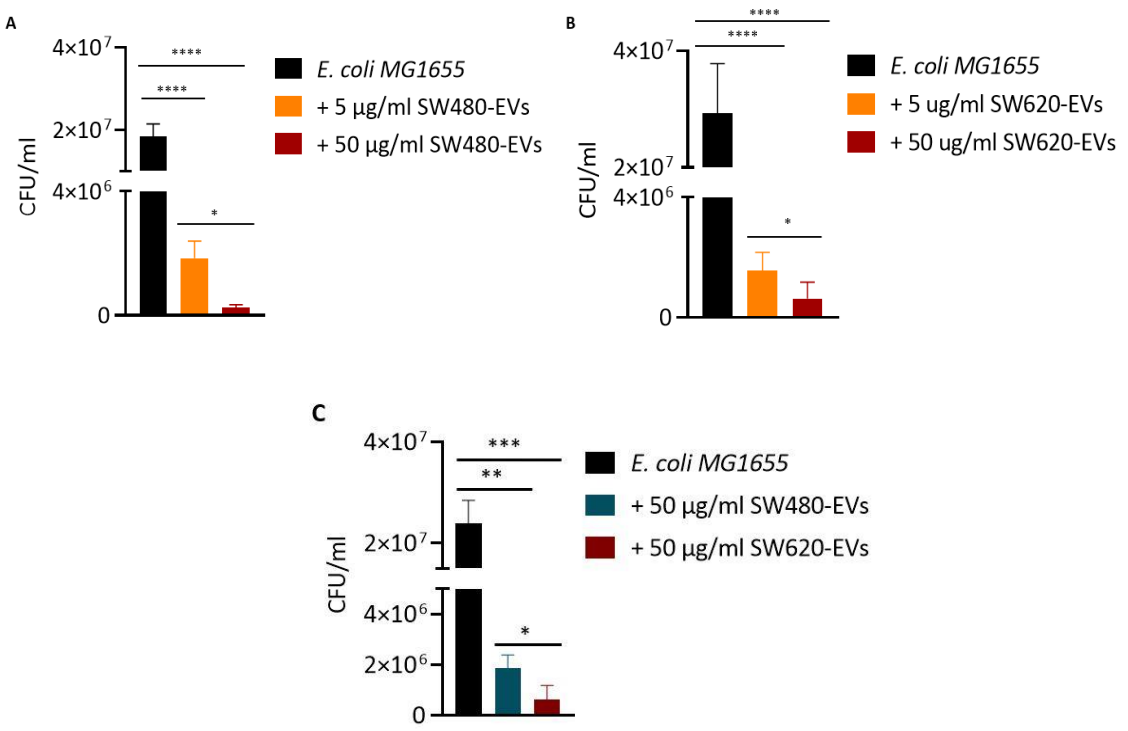

Figure 4.12: CRC cell lines-derived EVs reduce the ability of E. coli MG1655 *to form biofilm under anaerobic growth conditions. The number of CFU/ml of E. coli MG1655 biofilm cells treated with different concentrations (5 µg/ml, and 50 µg/ml) of SW480-EVs (A) and SW620-EVs (B). (C) The number of CFU/ml of E. coli MG1655 biofilm cells treated with 50 µg/ml of SW480-EVs and 50 µg/ml SW620-EVs. Error bars represent mean ± SEM, n=3. Statistical analysis by one-way ANOVA test, Brown-forsythe and Bartlett's tests,* p <0.05, **<0.01, ***<0.001, ****<0.0001.*

Overall, there was a difference in the strength of EV impact on the ability of *E. coli* MG1655 to form biofilm under aerobic and anaerobic growth conditions, the relative change in biofilm formation was 99.8% and 97.8%, respectively. The impact was higher under aerobic growth conditions.

4.3.4 CRC cell line-derived EVs increased the growth of *E. coli* 11G5 under anaerobic growth conditions

The impact on *E. coli* 11G5 was also assessed under aerobic and anaerobic growth conditions, *E. coli* 11G5 were treated with different concentrations of SW480-EVs and SW620-EVs (5 ng/ml, 50 ng/ml, 500 ng/ml, 5 µg/ml, and 50 µg/ml). Both types of EV, SW480 (Figure 4.13A) and SW620 (Figure 4.13B) did not affect the growth of *E. coli* 11G5 under aerobic growth conditions.

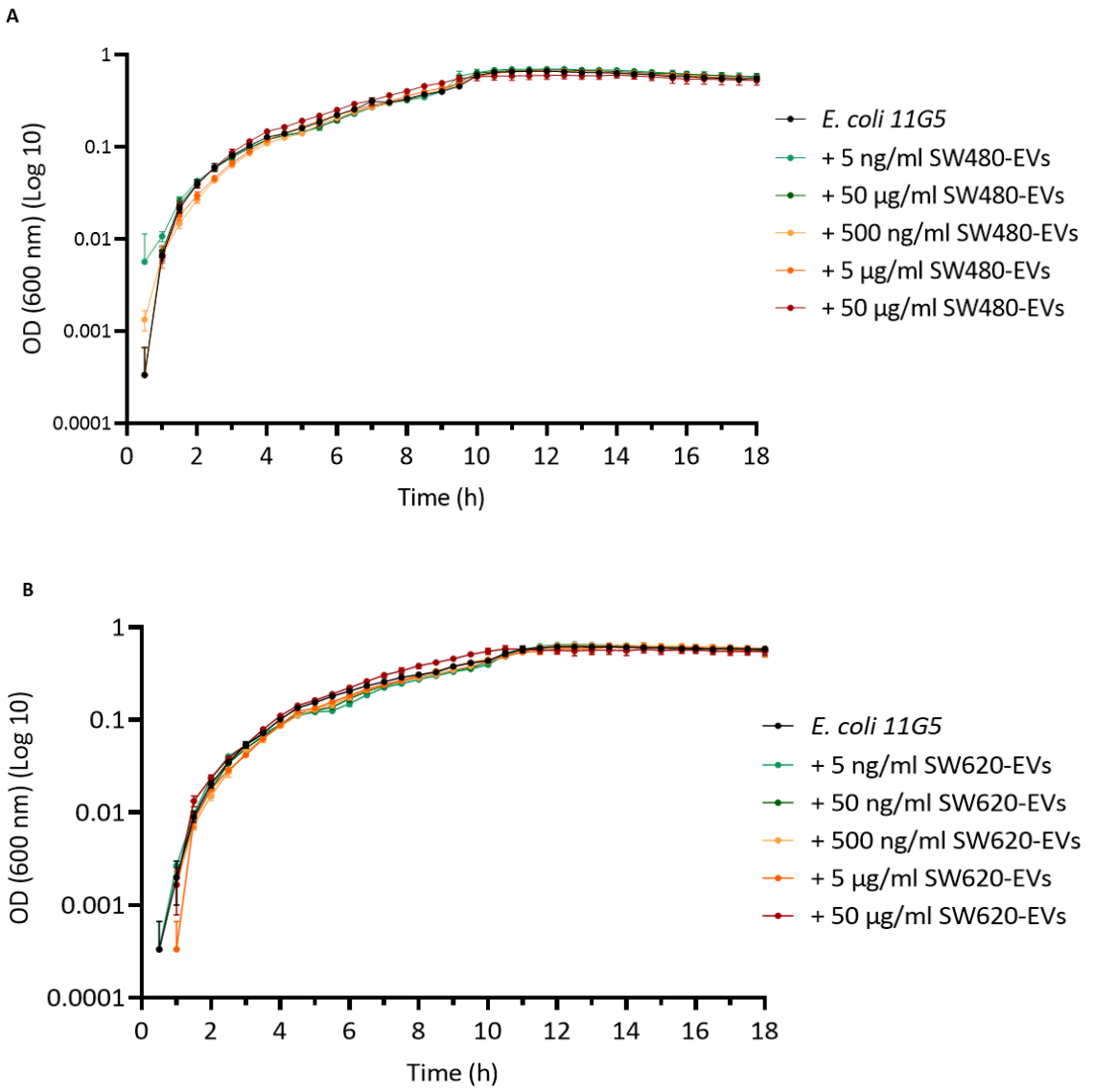

Figure 4.13: Growth curve of E. coli 11G5 treated with CRC-derived EVs under aerobic growth conditions. Absorbance at 600 nm of E. coli 11G5 culture treated with different concentrations of SW480-EVs and SW620-EVs (5 ng/ml, 50 ng/ml, 500 ng/ml, 5 µg/ml, and 50 µg/ml) under aerobic growth conditions for 18 hours. Error bars represent mean ± SEM, n=3.

However, a modest increase in bacterial growth was observed due to SW480-EVs (50 µg/ml) treatment (Figure 4.14A) (Figure 4.15), but SW620-EVs had no impact on the bacterial growth (Figure 4.14B) under anaerobic growth conditions.

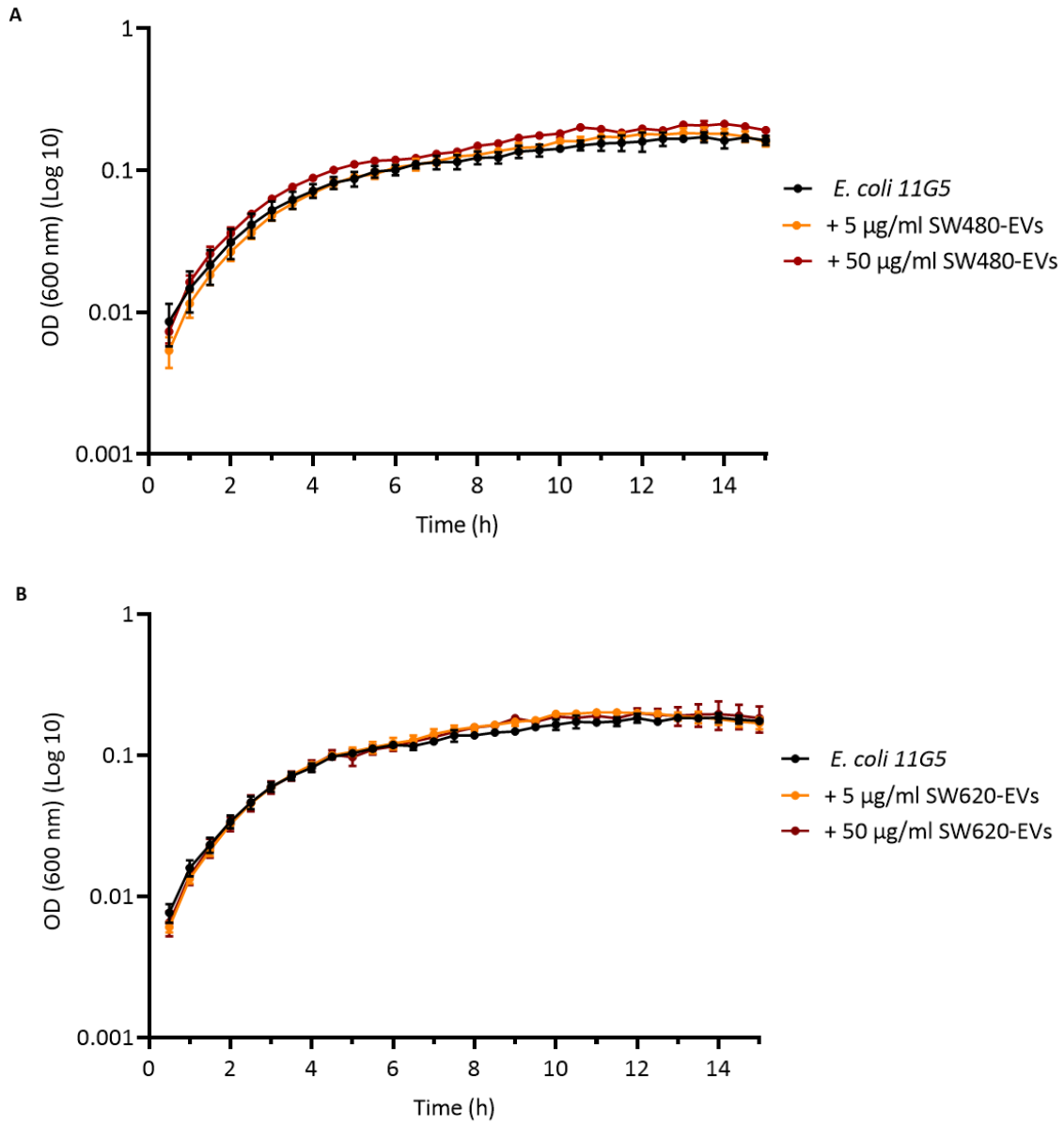

Figure 4.14: Growth curve of E. coli 11G5 treated with CRC-cell line derived-EVs under anaerobic growth conditions. Absorbance at 600 nm of E. coli 11G5 culture treated with SW480-EVs (A) and SW620-EVs (B) (5 µg/ml and 50 µg/ml) under anaerobic growth conditions for 15 hours. Error bars represent mean ± SEM, n=3.

Treating *E. coli* 11G5 with 50 µg/ml of SW480-EVs continuously increased the bacterial growth, OD_{600nm} increased from 0.086 to 0.109, 0.141 to 0.181, and 0.162 to 0.262 after 5 hrs (Figure 4.15A), 10 hrs (Figure 4.15B), and 15 hrs (Figure 4.15C) of incubation with SW480-EVs, respectively. Indeed, the highest impact was observed after 15 hrs of incubation.

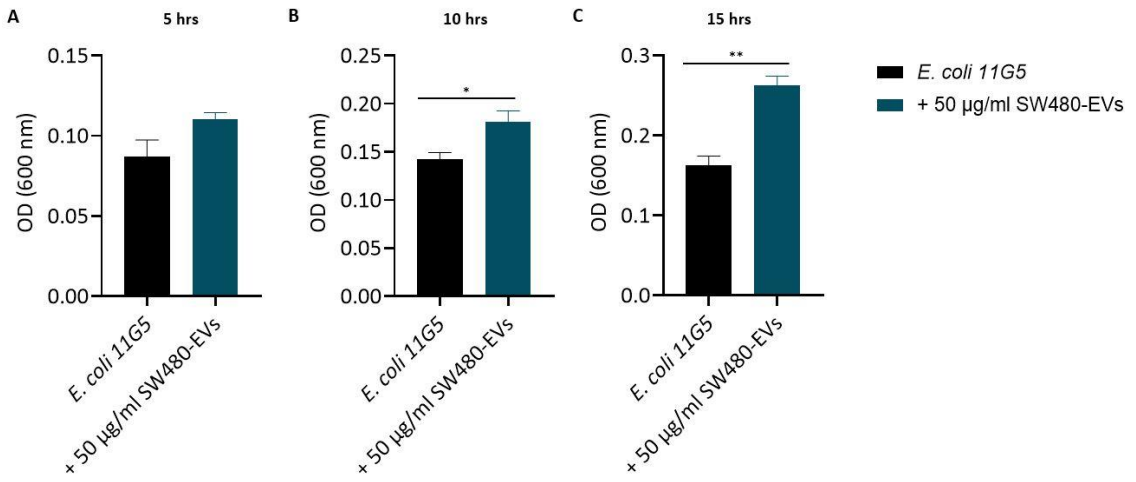

*Figure 4.15: SW480-EVs increased the growth of E. coli 11G5 under anaerobic growth conditions. Absorbance readings at 600 nm of E. coli 11G5 growth at 5 hrs (A), 10 hrs (B), and 15 hrs (C) of incubation with 50 µg/ml of SW480-EVs under anaerobic growth conditions. Error bars represent mean ± SEM, n=3. Statistical analysis by student t-test, * p <0.05, **<0.01.*

Overall, this indicates that both types of EVs can induce the growth of *E. coli* MG1655, the lab strain, but only EVs from the early stages, SW480-EVs, can induce the growth of *E. coli* 11G5, CRC-associated strain, under anaerobic growth conditions

4.3.5 CRC cell line derived-EVs reduced the ability of *E. coli* 11G5 to form a biofilm

Similar to *E. coli* MG1655, the impact on the ability of *E. coli* 11G5 was assessed under aerobic and anaerobic growth conditions. SW480-EVs significantly decreased the ability of *E. coli* 11G5 to form a biofilm with the highest impact observed with 50 µg/ml of EVs, the number of CFU/ml of biofilm cells decreased from $5*10^6$ CFU/ml to $2*10^5$ CFU/ml (Figure 4.16A). SW620-EVs also significantly decreased the ability of *E. coli* 11G5 *to* form a biofilm with the highest impact observed with 50 µg/ml of SW620-EVs, the number of CFU/ml of biofilm cells decreased from $5*10^6$ CFU/ml to $9*10^4$ CFU/ml (Figure 4.16B). In comparison between EV types, the inhibitory impact of SW620-EVs on the ability of *E. coli* 11G5 to form biofilm was significantly higher than the impact of SW480-EVs (Figure 4.16C).

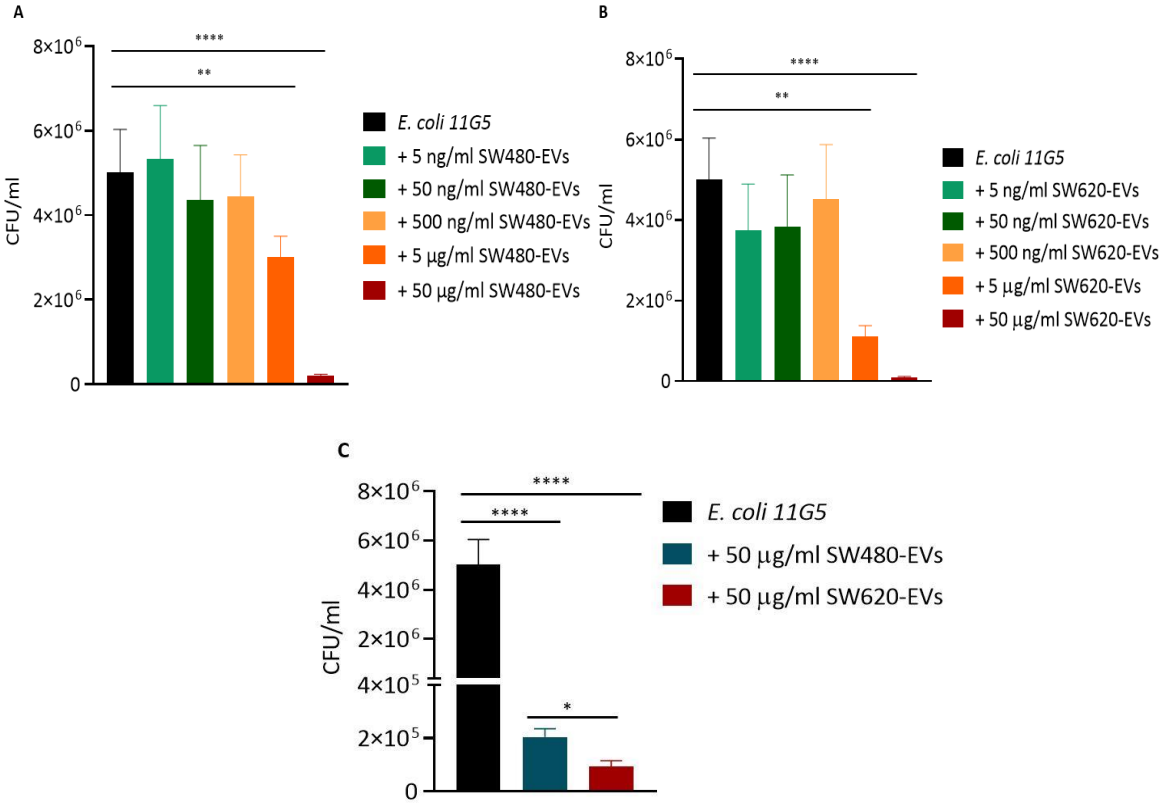

*Figure 4.16: CRC cell line-derived EVs reduced the ability of E. coli 11G5 to form biofilm under aerobic growth conditions. The number of CFU/ml of E. coli 11G5 biofilm cells treated with different concentrations (5 ng/ml, 50 ng/ml, 500 ng/ml, 5 µg/ml, and 50 µg/ml) of SW480-EVs (A) and SW620-EVs (B). (C) The number of CFU/ml of E. coli 11G5 biofilm cells treated with 50 µg/ml of SW480-EVs and 50 µg/ml of SW620-EVs. Error bars represent mean ± SEM, n=3. Statistical analysis by one-way ANNOVA test, Brown-forsythe and Bartlett's tests, ** p<0.01, **** p<0.0001.*

Similarly, CRC-cell line derived-EVs inhibited the ability of *E. coli* 11G5 to form biofilm under anaerobic growth conditions. SW480-EVs significantly decreased the ability of *E. coli* 11G5 to form a biofilm with the highest impact observed with 50 µg/ml of EVs, the number of CFU/ml of biofilm cells decreased from $8*10^6$ CFU/ml to $2*10^4$ CFU/ml (Figure 4.17A). Also, SW620-EVs significantly decreased the ability of *E. coli* 11G5 to form a biofilm with the highest impact observed due to 50 µg/ml of SW620-EVs treatment, the number of CFU/ml of biofilm cells decreased from $8.88*10^6$ CFU/ml to $5.6*10^4$ CFU/ml (Figure 4.17B). The inhibitory impact of SW620-EVs on the ability of *E. coli* 11G5 to form biofilm was significantly higher than the impact of SW480-EVs (Figure 4.17C).

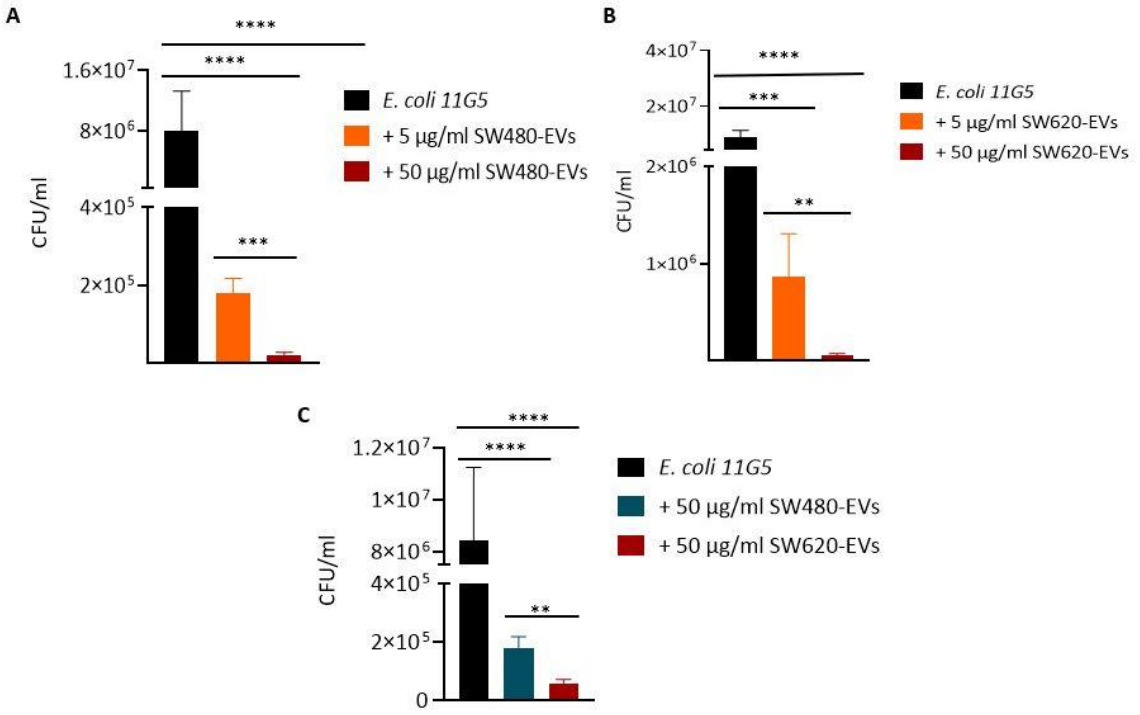

*Figure 4.17: CRC cell line-derived EVs reduced the ability of E. coli 11G5 to form biofilm under anaerobic growth conditions. The number of CFU/ml of E. coli 11G5 biofilm cells treated with different concentrations (5 µg/ml, and 50 µg/ml) of SW480-EVs (A) and SW620-EVs (B). (C) The number of CFU/ml of E. coli 11G5 biofilm cells treated with 50 µg/ml of SW480-EVs and 50 µg/ml of SW620-EVs. Error bars represent mean ± SEM, n=3. Statistical analysis by one-way ANOVA test, Brown-Forsythe and Bartlett's tests, p ***<0.001, ****<0.0001.*

Overall, there was a difference in the strength of EV impact on the ability of *E. coli* 11G5 to form biofilm under aerobic and anaerobic growth conditions, the relative change in biofilm formation was 98.1% and 99.4%, respectively. The impact is higher under anaerobic growth conditions, unlike the impact on *E. coli* MG1655. Under aerobic growth conditions, the impact on *E. coli* MG1655 was higher than the impact on E. coli 11G5 with 99.8% and 98.1%, respectively, the relative change of biofilm formation. However, the impact under anaerobic growth conditions on both strains is quite similar, with the relative change in biofilm formation of 99.8% and 99.4% for *E. coli* MG1655 and *E. coli* 11G5, respectively.

4.3.6 Long-term exposure of *E. coli* MG1655 to CRC cell line-derived EVs had no impact on the bacterial growth

To assess the long-term impact of CRC-cell line derived-EVs on *E. coli* MG1655, bacteria were passaged under anaerobic growth conditions with EVs (5 and 50 µg/ml of SW620-EVs) for 10 days, followed by 5 days without EV-treatment, the passaged bacteria were stored at –80 °C for future analysis. EVs had no impact on bacterial growth following prolonged exposure to EVs, no effect was observed following one day of EV exposure (Figure 4.18A), 5 days (Figure 4.18B), 10 days (Figure 4.18C), and after 5 days without EV treatment following the 10 days of exposure to EVs (Post-treatment day-10) (Figure 4.18D).

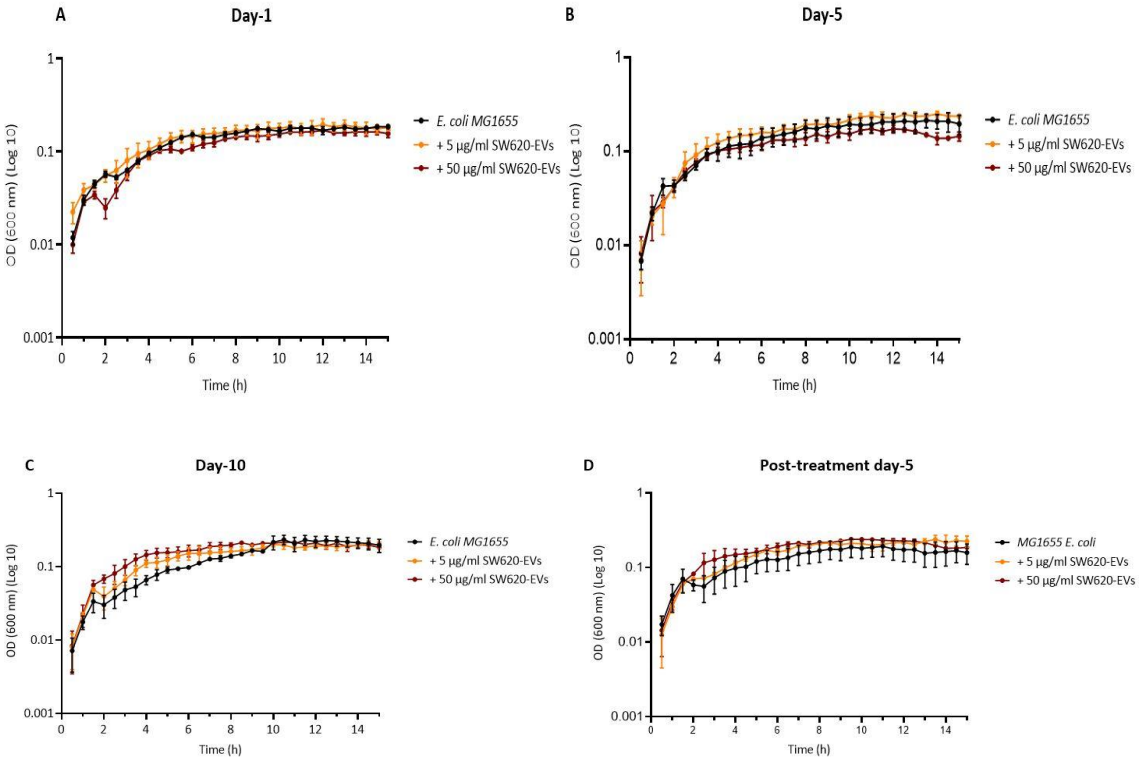

Figure 4.18: Growth curve of passaged E. coli MG1655 with SW620-EV treatment under anaerobic growth conditions. Absorbance at 600 nm of passaged E. coli MG1655 with SW620-EVs treatment (5 µg/ml and 50 µg/ml) under anaerobic growth conditions, stored passaged bacteria were assessed after 1 (A), 5 (B), 10 (C), and 5 days of post-treatment (D). Error bars represent mean ± SEM, n=3.

4.3.7 Long-term exposure of *E. coli* MG1655 to CRC cell line-derived EVs altered the bacterial ability to form biofilm

To assess the long-term impact of CRC-cell line derived-EVs on the ability of *E. coli* MG1655 to form a biofilm, the bacteria were passaged under anaerobic growth conditions with 5 and 50 µg/ml of SW620-EVs for 10 days followed by 5 days without EV-treatment, and passaged bacteria was stored at – 80 °C. As shown in Figure 4.19, the ability of passaged and non-treated *E. coli* MG1655 to form biofilm slightly increased after 1 (from 3.3 $*10^7$ to $5*10^7$ CFU/ml) and 5 days (from $3.3*10^7$ to 5.1 $*10^7$ CFU/ml) of passaging, compared to parental non-passaged bacteria. However, the bacterial ability to form biofilm decreased after 10 (from $3.3*10^7$ to $2.56*10^7$ CFU/ml), and 15 days (from $3.3*10^7$ to $3.14*10^7$ CFU/ml) of passaging.

Passaging with 5 µg/ml of SW620-EVs slightly and non-significantly altered the ability of *E. coli* to form biofilm, the number of CFU/ml of biofilm cells decreased slightly after 1 (from $5*10^7$ to $4.36*10^7$ CFU/ml), 5 days of passaging with EVs (from $5.1*10^7$ to $4*10^7$ CFU/ml), and 5 days after passaging without EVs (from $3.14*10^7$ to $2.4*10^7$ CFU/ml), compared to non-treated *E. coli* MG1655, and increased slightly after 10 days of passaging (from $2.56*10^7$ to $2.66*10^7$ CFU/ml).

Treating with 50 µg/ml of SW620-EVs increased the number of CFU/ml of biofilm after 1 day of passaging (from $5*10^7$ to $7.1*10^7$ CFU/ml), decreased it after 5 days (from $5.1*10^7$ to 3.4 $*10^7$ CFU/ml), increased it after 10 days (from $2.56*10^7$ to $4.08*10^7$ CFU/ml), and had no change on the total number of CFU/ml of biofilm after 5 days without EVs treatment (from $3.14*10^7$ to $3.05*10^7$ CFU/ml).

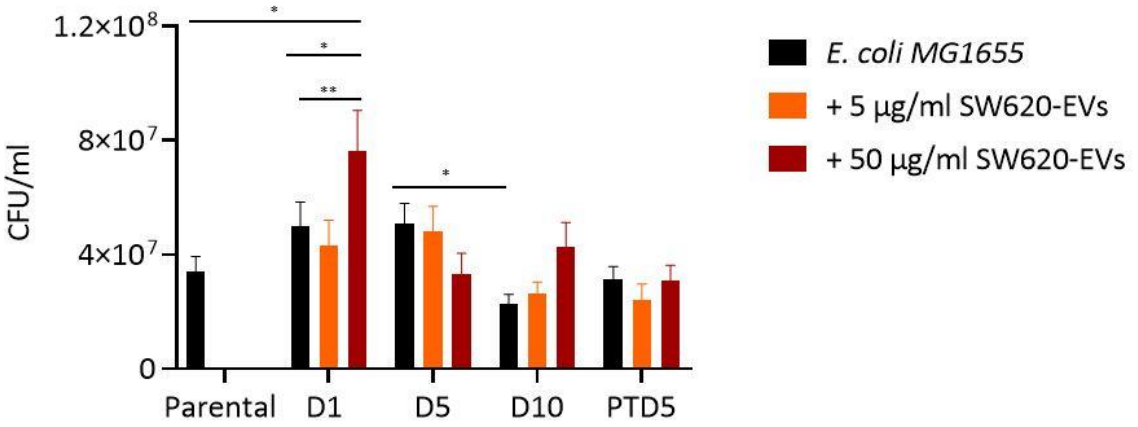

*Figure 4.19: Long-term exposure of E. coli MG1655 to CRC-cell line derived-EVs altered their ability to form biofilm under anaerobic growth conditions. The number of CFU/ml of E. coli MG1655 biofilm cells passaged with SW620-EVs treatment (5 µg/ml and 50 µg/ml), stored pre-passaged bacteria were assessed after 1 (D1), 5 (D5), 10 (D10), and 5 days of post-treatment (PTD5). Error bars represent mean ± SEM, n=3. Statistical analysis by one-way ANOVA test, Brown-forsythe and Bartlett's tests, p *<0.05, **<0.01.*

4.3.8 Long-term exposure of *E. coli* 11G5 to CRC-cell line derived-EVs had no impact on the bacterial growth

Similar to *E. coli* MG1655, the impact of prolonged-term exposure of *E. coli* 11G5 to EVs on bacterial growth was assessed under anaerobic growth conditions. No impact on the bacterial growth was observed after 1 (Figure 4.20A) and 5 (Figure 4.20B) days of passaging with EVs, however, a modest decrease in the bacterial growth was observed after 10 days of passaging with 5 µg/ml of SW620-EVs, and no change was observed with 50 µg/ml of SW620-EVs treatment (Figure 4.20C). Moreover, a decrease in the growth was observed following passaging bacteria without treatment with 50 µg/ml of SW620-EVs for 5 days (Figure 4.20D).

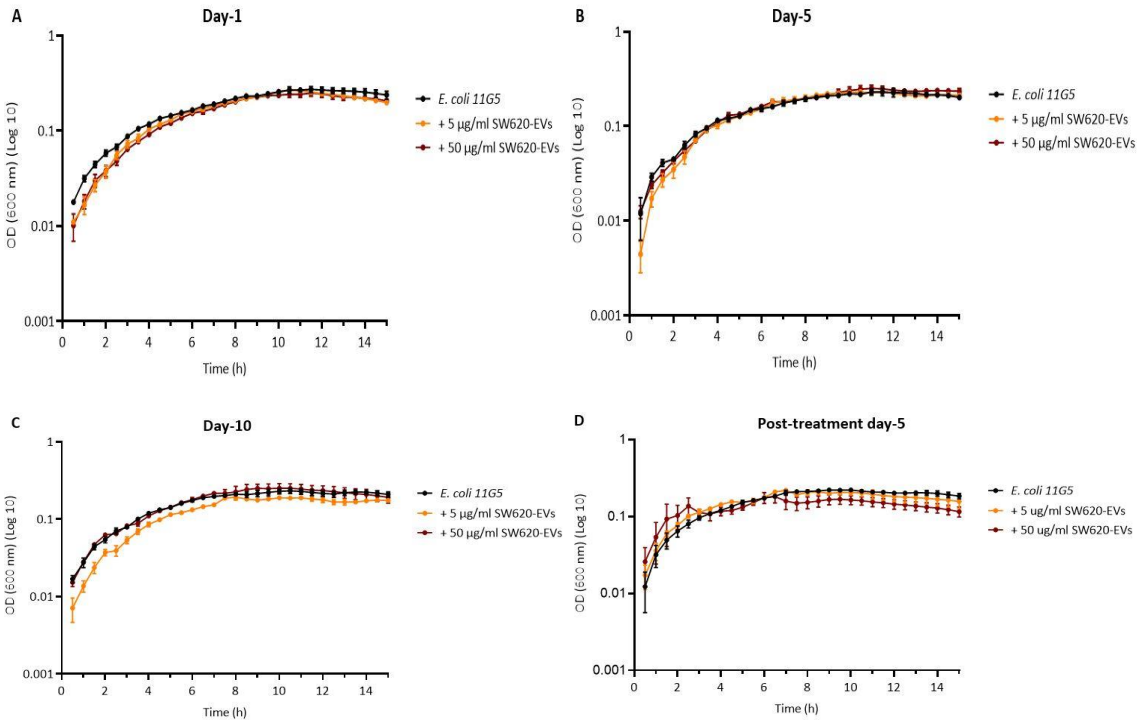

Figure 4.20: Long-term exposure to CRC cell line derived-EVs did not impact E. coli 11G5 growth under anaerobic growth conditions. Absorbance at 600 nm of passaged E. coli 11G5 with SW620-EVs (5 µg/ml and 50 µg/ml) under anaerobic growth after 1 (D1) (A), 5 (D5) (B), 10 (D10) (C), and 5 (PTD5) (D) days of post-treatment. Error bars represent mean ± SEM, n=3.

4.3.9 Long-term exposure of *E. coli* 11G5 to CRC cell line-derived EVs altered the bacterial ability to form biofilm

The impact of prolonged-term exposure to EVs on the ability of *E. coli* 11G5 was also assessed under anaerobic growth conditions. As shown in Figure 4.21, the ability of passaged and non-treated *E. coli* MG1655 to form biofilm increased after 1 (from $2.9*10^6$ to $1*10^7$ CFU/ml), 5 (from $2.9*10^6$ to $1.45*10^7$ CFU/ml), 10 (from $2.9*10^6$ to $1.18*10^7$ CFU/ml), and 15 days of passaging (from $2.9*10^6$ to $1.7*10^7$ CFU/ml), comparing to parental non-passaged bacteria.

However, after 1 day of passaging, their ability decreased when treated with 5 µg/ml of SW620-EVs (from $1*10^7$ to $6.2*10^6$ CFU/ml) and no change was observed when treated with 50 µg/ml of SW620-EVs (from $1*10^7$ to $1.04*10^7$ CFU/ml), compared to non-treated bacteria. After 5 days of passaging, the ability of bacteria to form biofilm increased when treated with 5 µg/ml of SW620-EVs (from $1.45*10^7$ to $1.66*10^7$ CFU/ml) and with 50

µg/ml of SW620-EVs (from 1.45*10^7 to 2.4*10^7 CFU/ml), with higher impact observed when treated with 50 µg/ml of SW620-EVs. Likewise, after 10 days of passaging, the ability of bacteria to form biofilm also increased when treated with 5 µg/ml of SW620-EVs (from 1.18*10^7 to 2*10^7 CFU/ml) and 50 µg/ml of SW620-EVs (from 1.18*10^7 to 2.3*10^7 CFU/ml). This increase in the ability of bacteria to form biofilm was also observed following 5 days (from 1.7*10^7 to 2*10^7 CFU/ml) of passaging without EVs treatment (5 µg/ml of EVs), and from 1.7*10^7 to 2.1*10^7 CFU/ml of passaging without EVs treatment (50 µg/ml).

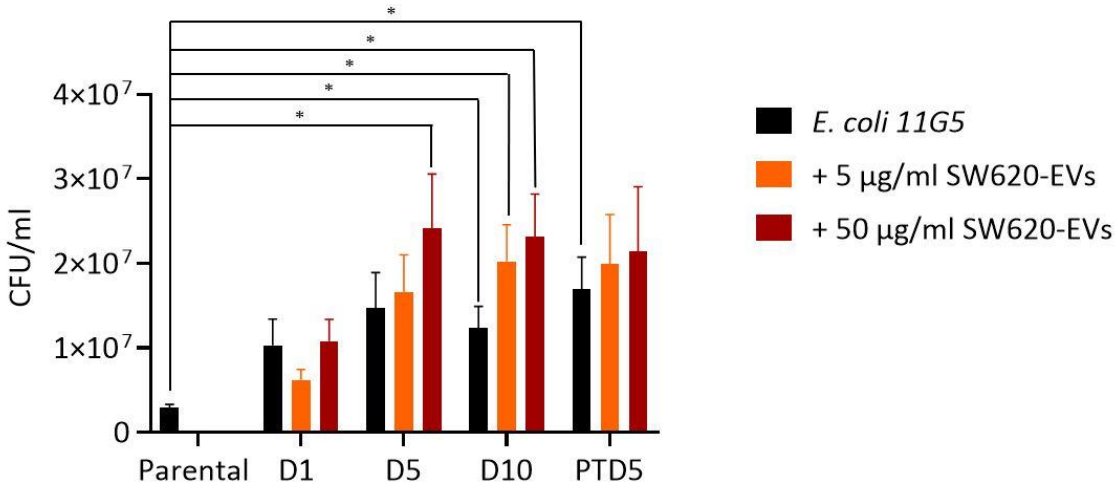

*Figure 4.21: Long-term exposure of E. coli 11G5 to CRC cell line derived-EVs altered the bacterial ability to form biofilm under anaerobic growth conditions. The number of CFU/ml of E. coli 11G5 biofilm cells passaged with SW620-EVs treatment (5 µg/ml and 50 µg/ml) under anaerobic growth conditions, stored pre-passaged bacteria were assessed after 1 (D1) (A), 5 (D5) (B), 10 (D10) (C), and 5 (PTD5) (D) days of post-treatment. Error bars represent mean ± SEM, n=3. Statistical analysis by one-way ANOVA test, Brown-forsythe and Bartlett's tests, p *<0.05.*

4.3.10 Isolated EVs from CRC patients and healthy individuals showed expected characterisation

To assess the impact of clinical sample-derived EVs, blood was collected from CPDs and HDs. EVs were isolated from the blood plasma following the SEC approach. The isolated EVs were characterised following the ISEV guidance (Théry et al., 2018). As shown in Figure 4.22, BCA analysis shows a continuous increase in protein concentration from

fraction 8 to 15, for both CPDs and HDs' blood-plasma EV isolates (Figure 4.22A), and this continuous increase could be due to the presence of lipoproteins contaminants. Also, DELFIA-ELISA showed a fluorescent signal of CD9 (Figure 4.22B), CD63 (Figure 4.22C) and CD81 (Figure 4.22D) from fractions 5 to 12, with the lowest signal in fractions 5 and 6, and the highest in fractions 9-12, indicating the presence of EVs in these latter fractions, therefore, fractions 8-11 were pooled for functional experiments.

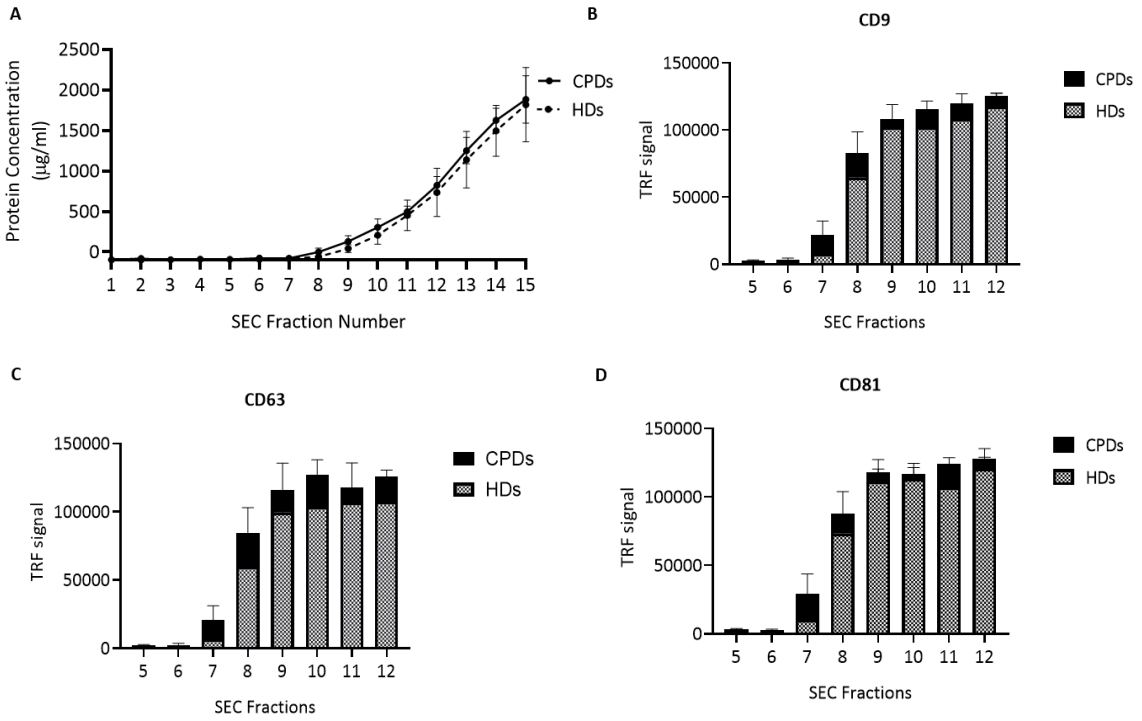

Figure 4.22: EVs were isolated from the blood of CPDs and HDs by SEC. (A) Protein concentration in SEC fraction of CPDs-EVs and HDs-EVs isolates. Detection of EV's tetraspanin CD9 (B), CD63 (C), and CD81 (D) by ELISA; TRF signal (320 nm/ 610 nm) of DELFIA Europium-streptavidin in SEC fractions (F5-F12). Error bars represent mean ± SEM, n=3.

As shown in Figure 4.23, particle size and concentration profile analysis by Nano-analyser confirmed the presence of EVs in the SEC-pool EV-rich fractions, and the average diameter of blood plasma-EVs was 71.3 nm and 73.4 nm for CPDs and HDs, respectively (Figure 4.23A). EV's tetraspanin markers were detected by a nano analyser (NanoFCM) (Figure 4.23B), 0.7 % and 0.8 % of total particles in CPDs-EV and HDs-EV isolates, respectively, were CD9 positive. Also, 3.4 % and 3.2 % of total particles in CPDs-EV and HDs-EV isolates, respectively, were CD63 positive. For CD81 detection, 3 % and 2.5 % of total particles in CPDs-EV and HDs-EV isolates were CD81 positive, respectively.

Indeed, EV's tetraspanin markers were detected in the pool fractions by DELFIA-ELISA (Figure 4.23C), CD9, CD63, and CD81 were detected in CPDs- and HDs-EVs isolates, as well as a low signal of cytosolic TSG101 marker. Lastly, EV's size and morphology were investigated by TEM (Figure 4.23D) which showed a round-double membranous structure, 50 nm in diameter, which follows the typical morphology/size of human EVs.

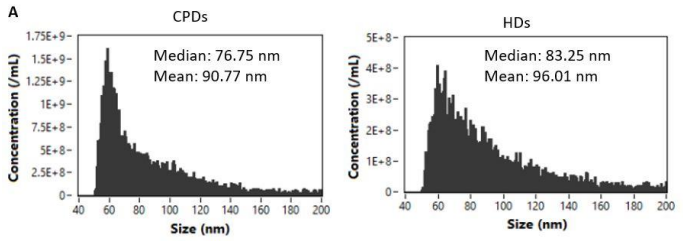

B

Marker	CD9	CD63	CD81
CPDs	0.7%	3.4%	3%
HDs	0.8%	3.2%	2.5%

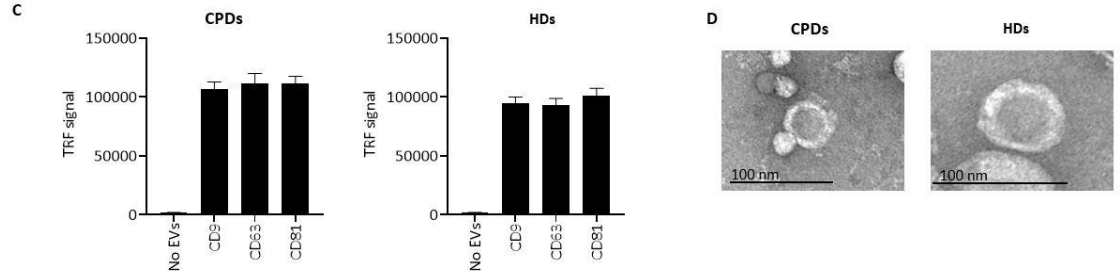

Figure 4.23: Isolated blood plasma EVs showed expected characterisation. (A) A representative analysis of Nano-analyser particle size/concentration profile of CPD's and HD's blood-EV isolates. (B) Tetraspanin detection by nano-analyser, the percentage of CD9, CD63, and CD81 positive particles in the pool fractions of the CPD's and HD's blood-EV isolates. (C) EVs tetraspanin markers (CD9, CD63, and CD81) detection by ELISA in the pool fractions of the CPD's and HD's blood-EV isolates. (D) TEM of blood-EV isolates, scale bar 100 nm. Error bars represent mean ± SEM, n=3.

4.3.11 The impact of CRC-patients-derived EVs on *E. coli* mirrors the impact of CRC cell line-derived EVs

The impact of blood plasma EVs on the bacterial phenotypic characteristics was assessed. EVs from the blood plasma of CPDs and HDs increased the growth of *E. coli* MG1655 (Figure 4.24A); after 8 hours of incubation, OD_{600nm} reading significantly increased from 0.09 to 0.133 and 0.123 when bacteria treated with CPDs-EVs and HDs-EVs, respectively. Despite the increase in the bacterial growth, CPDs-EVs and HDs-EVs significantly decreased the ability of *E. coli* MG1655 to form a biofilm, the total CFU/ml of biofilm cells decreased significantly from $2.3*10^7$ to $1.1*10^6$ and $7.8*10^5$ due to CPDs-

EVs and HDs-EVs treatment, respectively (Figure 4.24B). Therefore, the impact of HDs-EVs on bacterial biofilm was higher than CPDs-EVs, however, this difference is not statistically significant.

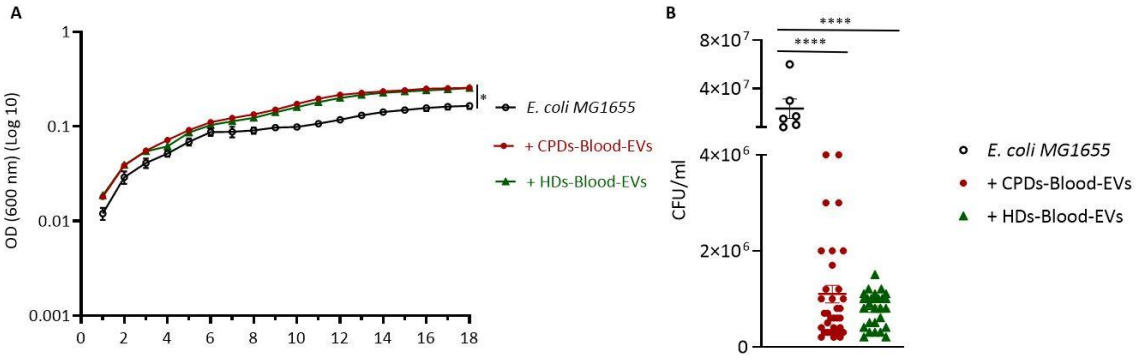

*Figure 4.24: Blood-EVs altered the phenotypic characteristics of E. coli MG1655. (A) Absorbance at 600 nm of E. coli MG1655 culture treated with CPDs-EVs and HDs-EVs for 18 hours. (B) The number of CFU/ml of E. coli MG1655 biofilm cells treated with CPDs-EVs and HDs-EVs. Error bars represent mean ± SEM, n=3. Statistical analysis by one-way ANOVA test, Brown-forsythe and Bartlett's tests, p *<0.05, ****<0.0001.*

Similarly, both CPDs-EVs and HDs-EVs significantly increased the growth of *E. coli* 11G5, OD_{600nm} reading after 8 hours of incubation increased from 0.118 to 0.217 and 0.205 when bacteria treated with CPDs-EVs and HDs-EVs, respectively (Figure 4.25A). Also, CPDs-EVs and HDs-EVs significantly decreased the ability of *E. coli* 11G5 to form a biofilm, the total CFU/ml decreased from $6.5*10^6$ to $6.4*10^5$ and $3.6*10^5$ due to CPDs-EVs and HDs-EVs treatment, respectively (Figure 4.25B), indicating that HDs-EVs have a higher inhibitory impact on the biofilm of *E. coli* 11G5, compared to CPDs-EVs. Overall, this data suggests that the impact of blood EVs on bacterial phenotypic characteristics mirrors the impact of CRC-cell line-derived EVs.

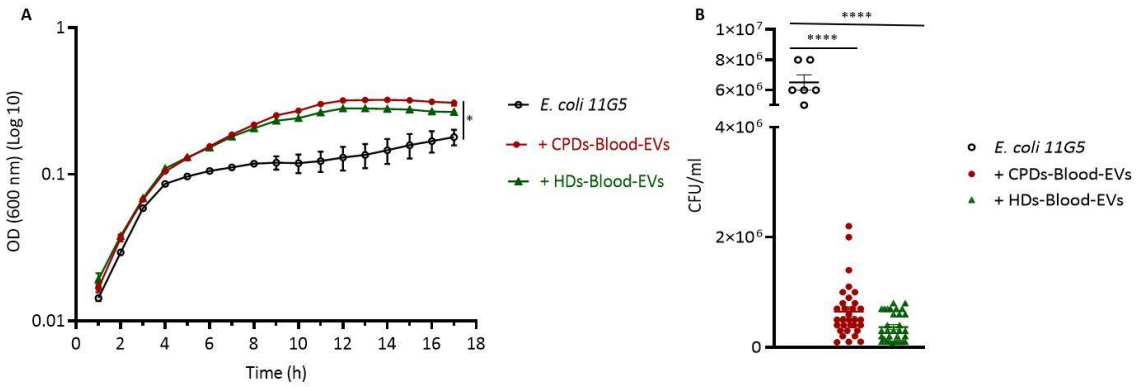

*Figure 4.25: Blood-EVs altered the phenotypic characteristics of E. coli 11G5. (A) Absorbance at 600 nm of E. coli 11G5 culture treated with CPDs-EVs and HDs-EVs for 18 hours. (B) The number of CFU/ml of E. coli 11G5 biofilm cells treated with CPDs-EVs and HDs-EVs. Error bars represent mean ± SEM, n=3. Statistical analysis by one-way ANOVA test, Brown-forsythe and Bartlett's tests, p *<0.05, ****<0.0001.*

4.3.12 Isolated EVs from CRC patient's colon tissue showed expected characterisation

As blood-derived EVs are not specific or local to the tumour, EVs were isolated from CRC-adjacent tissue by SEC chromatography and characterised following MISEV guidelines (Théry et al., 2018). Nano-flow cytometry showed the expected particle size/concentration profile (Figure 4.26A) with a mean size of 76.17 nm and a median of 70.25 nm. EVs tetraspanin markers were detected by ELISA; TRF signal was detected for CD9, CD63, and CD81 (Figure 4.26B). TEM showed the expected double-membranous structure of EVs (Figure 4.26C).

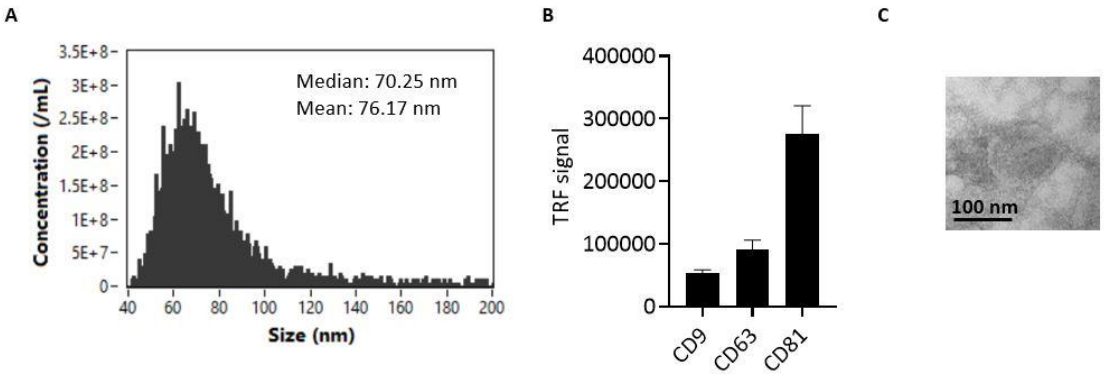

Figure 4.26: Characterisation of CRC-tissue-derived EVs. (A) Particle size/concentration profile by Nano-flow cytometry; particle size median and mean are 70.25 nm and 76.17 nm, respectively. (B) The TRF signal of EV's tetraspanin, CD9, CD63, and CD81 was detected by ELISA. (C) TEM showing double-membranous structures. Error bars represent mean ± SEM, n=3, a representative histogram of the particle's size/concentration profile.

4.3.13 Tissue-derived EVs increased the growth and reduced the ability of *E. coli* MG1655 to form a biofilm

To assess the impact of CRC tissue on *E. coli* growth, EVs were isolated from the bowel tissue of CRC patients by SEC and their impact was assessed. Tissue derived-EVs increased the growth of *E. coli* MG1655, OD_{600nm} increased from 0.249 to 0.322 (Figure 4.27A), and decreased the bacterial ability to form a biofilm, the total CFU/ml of biofilm cells decreased from $5.5*10^6$ to $1.3*10^6$ (Figure 4.27B).

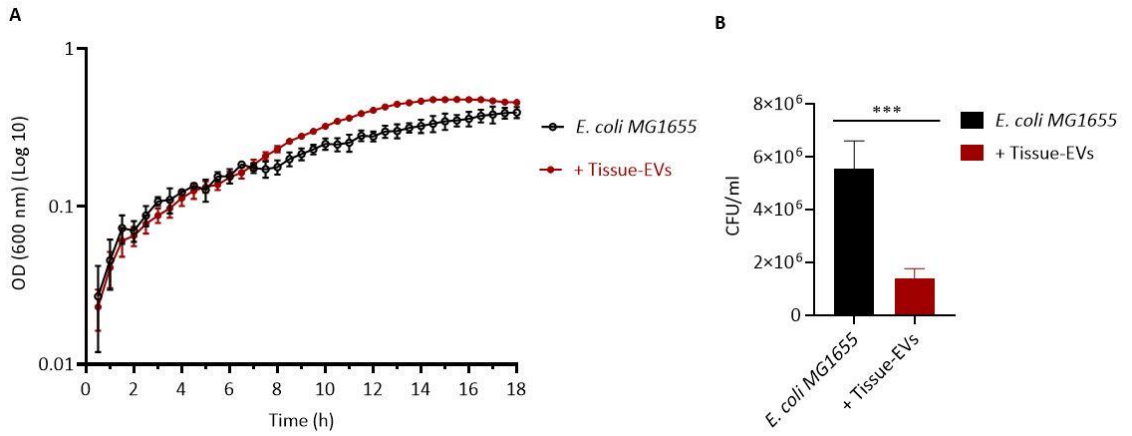

*Figure 4.27: Tissue-derived EVs increased the growth and reduced the ability of E. coli MG1655 to form biofilm. (A) Absorbance at 600 nm of E. coli MG1655 treated with CRC-bowel tissue-EVs for 18 hours under aerobic growth conditions. (B) The number of CFU/ml E. coli MG1655 biofilm cells treated with CRC-bowel tissue-EVs. Error bars represent mean ± SEM, n=3. Statistical analysis by one-way ANOVA test, Brown-forsythe and Bartlett's tests, p ***<0.001.*

However, bowel tissue derived-EVs had no impact on the growth of *E. coli* 11G5 as shown in (Figure 4.28A), but they reduced the ability of *E. coli* 11G5 to form a biofilm (Figure 4.28B), the total number of CFU/ml of biofilm cells was significantly reduced from $9.1*10^6$ to $9.2*10^4$ CFU/ml.

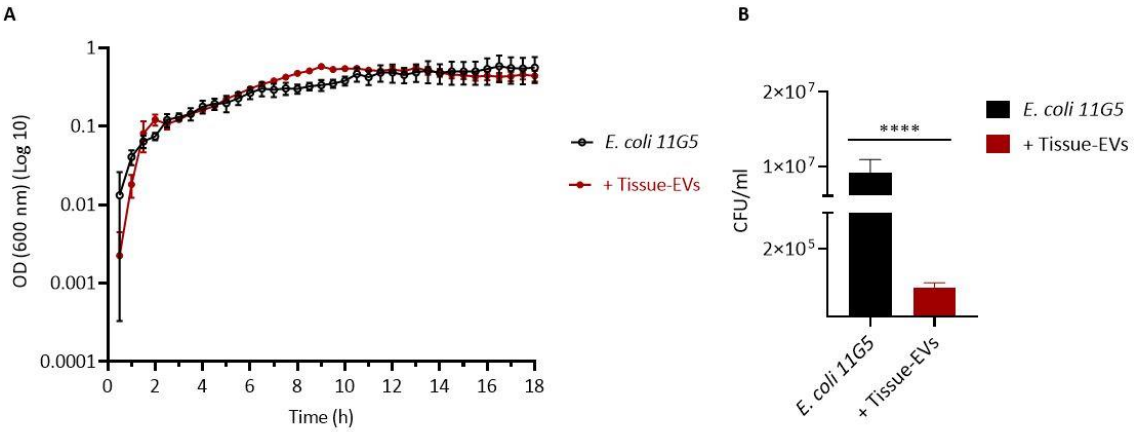

*Figure 4.28: Tissue-derived EVs reduced the ability of E. coli 11G5 to form a biofilm. (A) Absorbance at 600 nm of E. coli 11G5 treated with CRC-bowel tissue-EVs for 18 hours under aerobic growth conditions. (B) The number of CFU/ml of E. coli 11G5 biofilm cells treated with CRC-bowel tissue-EVs. Error bars represent mean ± SEM, n=3. Statistical analysis by one-way ANOVA test, Brown-forsythe and Bartlett's tests, p****<0.0001.*

In comparison between both strains of *E. coli*, tissue-derived EVs have a higher inhibitory impact on *E. coli* 11G5 than *E. coli* MG1655. The relative change in biofilm formation was 74.95% and 99% for *E. coli* MG1655 and *E. coli* 11G5, respectively.

4.3.14 EV-treated *E. coli* had no impact on the proliferation of CRC cells

To test whether EV-treated *E. coli* would have an impact on CRC growth, CRC cells were treated with bacterial culture supernatant (S) of EV-treated *E. coli* (S. trea.) or untreated *E. coli* (S. untrea.) as a control, and the change in CRC-cells proliferation was assessed. The data showed that neither EV-treated nor untreated *E. coli*-produced metabolites had an impact on the proliferation of both types of CRC-cell lines, SW480 (Figure 4.29A) and SW620 (Figure 4.29B).

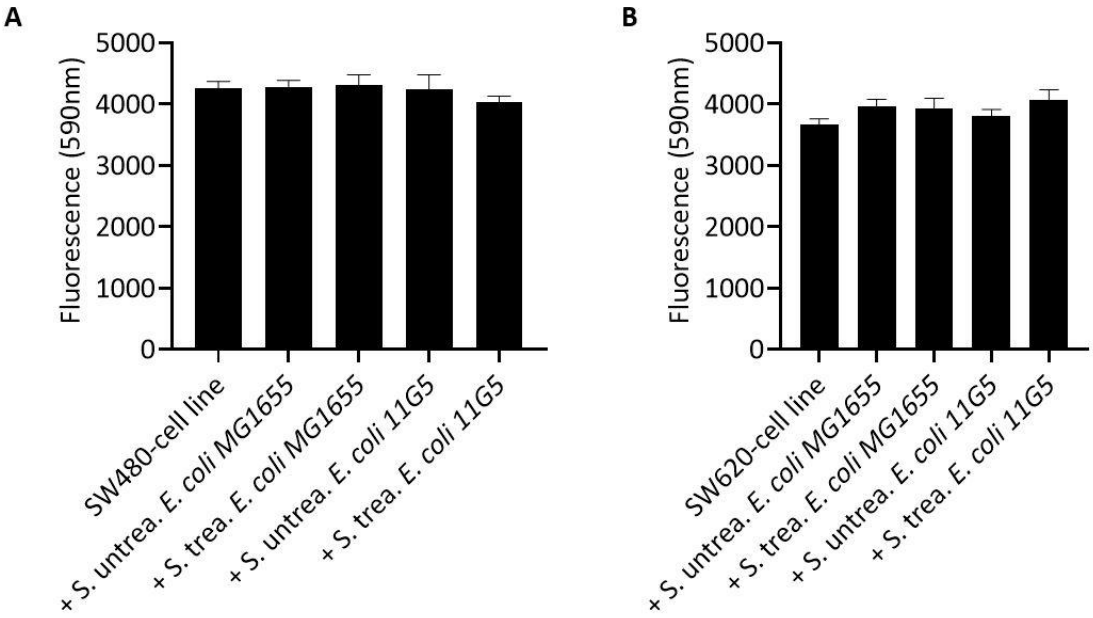

Figure 4.29: EV-treated E. coli had no impact on CRC-cell line proliferation. Fluorescent intensity of Alamar-blue (590 nm) of SW480-cell culture (A) and SW620-cell culture (B) that were treated with EV-treated and EV-untreated E. coli MG1655- and E. coli 11G5-culture supernatant. Error bars represent mean ± SEM, n=3.

4.4 Discussion

The human colon is colonised by around 10^{14} bacteria that under healthy conditions promote intestinal homeostasis and deliver various beneficial functions to the host, such as digestion and immunity. In CRC, various studies revealed the altered structure and hence function of the gut bacteria during tumour initiation and progression, and these bacterial shifts are disease-stage specific (Dougherty & Jobin, 2015). However, the causative mechanisms that drive homeostasis-dysbiosis shift have not been investigated yet, this chapter hypothesised that CRC shapes its surrounding gut microbiome to promote its progression.

4.4.1 Impact of CRC-cell line derived-EVs on *E. coli* growth

It has been shown that specific intestinal cells such as epithelial cells, Paneth cells, and immunity cells secrete antimicrobial peptides (AMPs). These are diverse and bioactive compounds playing crucial roles in host defence and maintaining tolerance to commensal microorganisms in the gut, and alterations in the AMPS are linked to intestinal bowel diseases (Gubatan et al., 2021). For example, the human β-defensin-1 is one of the AMPS constitutively expressed by epithelial cells at the mucosal surface to maintain gut homeostasis, however, its transcription is decreased in CRC (Bonamy et al., 2018). Whereas normal epithelial cells have antimicrobial activity, data from this chapter showed that CRC-derived EVs promote bacterial growth which could be mediated by EVs-protein contents.

It was reported previously that *E. coli* is abnormally prevalent in biopsies of CRC, compared to healthy patients, and is involved in the CRC carcinogenesis process. It invades the colon epithelial cells, promotes cell proliferation, exacerbates inflammation, and induces DNA damage (Buc et al., 2013; Nouri et al., 2021; Raisch et al., 2014). In this chapter, data showed that CRC-EVs alter the phenotypic characteristics of bacteria, CRC-cell line derived-EVs increased bacterial growth, and a disease-stage specific impact on the bacterial growth was observed, treating *E. coli* MG1655 with SW620-EVs (metastatic-stage derived-EVs) increased bacterial growth under aerobic growth conditions, however, SW480-EVs (primary-stage derived-EVs) had no impact on *E. coli* MG1655 growth under aerobic growth conditions.

Under physiologically relevant conditions, EVs from both cell lines, SW480 and SW620, increased the growth of *E. coli* MG1655, and the impact of SW620-EVs on bacterial growth was higher than the impact of SW480-EVs. This data aligns with flow cytometry analysis data in the previous chapter (Chapter 3) that showed the interactions between SW620-EVs and *E. coli* MG1655 were greater than the interactions between SW480-EVs and *E. coli*, this suggests that interaction may be a limiting factor in EV-mediated functional effects. These data support and potentially provide a mechanism for previous findings of higher prevalence of *E. coli* at later stages of CRC, compared to early stages (Bonnet et al., 2014; Swidsinski et al., 1998). Therefore, the impact of CRC-EVs on bacterial growth could promote the progression of CRC.

Interestingly, CRC-cell line derived-EVs did not impact the growth of CRC-associated *E. coli* strain, *E. coli* 11G5, under aerobic growth conditions. However, a modest increase in bacterial growth was observed under anaerobic growth conditions due to SW480-EVs treatment, and no impact was observed due to SW620-EVs treatment. This finding clarifies a previous screening study that showed a higher prevalence of *E. coli* 11G5 in CRC patients at early stage (II), compared to later stages (Stages III and IV) (Iyadorai et al., 2020).Various studies have shown that *E. coli* 11G5 is involved in the CRC carcinogenesis process as it causes carcinogenic DNA mutations, not only in CRC tissues but regionally separated normal colonic tissues from CRC patients, and induces inflammation and ROS production at the early stage of CRC (Buc et al., 2013; Chen, B. et al., 2023; Pleguezuelos-Manzano et al., 2020; Raisch et al., 2014; Veziant et al., 2016; Wassenaar, 2018), the impact of EVs from the early stage of CRC-cell lines on *E. coli* 11G5 growth could be considered a functional mechanism to promote tumour progression and invasion of CRC. It was shown before that EV-derived miRNA could regulate gene expression of *E. coli* inducing bacterial growth, therefore, EV-miRNA contents could mediate the increase in bacterial growth (Liu et al., 2016).

Moreover, TGF-β has been identified as an EV cargo implicating tumorigenesis and metastasis of CRC (Rodrigues-Junior, Tsirigoti, Lim, Heldin, & Moustakas, 2022). It has also been shown that human TGF-β increases the adherence and invasion of *E. coli* to human cells (Zhang, Guang, Khan, Kim, Stins, & Kim, 2002), therefore, EV-TGF-β could also mediate the increase in bacterial growth. Notably, passaging the bacteria with the presence of EVs had no impact on the bacterial growth, this suggests that a direct

exposure of *E. coli* to EVs is needed to alter the phenotypic characteristics of *E. coli*. Also, these alterations in bacterial growth are not permanent and depend upon the presence of the functional cargoes of EVs.

4.4.2 CRC cell line derived-EVs reduce the ability of *E. coli* to form a biofilm

Despite the increase in *E. coli* growth, CRC cell line derived-EVs reduced the bacterial ability to form biofilm. Both SW480-EVs and SW620-EVs reduced the ability of *E. coli* MG1655 and *E. coli* 11G5 under aerobic and anaerobic growth conditions. Notably, the impact of SW620-EVs was higher than SW480-EVs on the ability of both *E. coli* strains to form biofilm. The inhibitory impact of EVs on bacterial biofilm was reported previously by a study that assessed biofilm formation using crystal violet biofilm assay (Koeppen et al., 2021), this assay was recruited in this project as well, however, the binding of crystal violet to EVs-DNA content resulted in a false positive result of the experimental control, therefore, a microtiter-plate assay for biofilm formation assessment was then recruited. Notably, the study showed that human airway cell derived-EVs reduce the biofilm formation of *Pseudomonas aeruginosa* through the delivery of functional miRNA, Let-7b-5p, which was predicted to target genes expressing protein that are essential for biofilm formation, including *PpKA* and *ClpV1-3* (Koeppen et al., 2021). Therefore, EV-miRNA contents could mediate the inhibitory impact on the ability of *E. coli* to form a biofilm. In addition, EVs contain matrix-degrading enzymes, such as MMPs and heparanases that could degrade formed biofilm by targeting biofilm extracellular polymeric substances (EPS) (Nawaz et al., 2018). Also, as data showed the physical binding of EV to *E. coli* surface (Chapter 3), this inhibitory impact could be mediated by the physical binding of EV to *E. coli* which could prevent bacterial cells from attaching to surfaces and each other.

In CRC, previous work detected bacterial biofilms in the colonic epithelium. A study showed that 50% and 67% of CRC and adenoma tissues were biofilm-positive, this indicates lower bacterial biofilm-forming ability at later stages, compared to early stages (Dejea et al., 2014). The study also showed that the bacterial biofilm varies by geographical location along the colonic axis. Interestingly, as a control, the study analysed the paired normal colon tissues obtained from the surgical resection margin furthest from the tumour mass and found that all tissues were bacterial-biofilm positive for both CRC and adenomas without any variations between different colon regions.

Interestingly, sequence analysis revealed substantial overlap between tumours (CRC or adenomas) and paired normal tissue bacterial composition (Dejea et al., 2014). Similarly, a study showed that the ability of *E. coli* 11G5 that was isolated from CRC patients to form biofilm was less than a control biofilm-forming *E. coli* despite its abnormal colonisation of colon mucosa in CRC patients, which indicates that microbiota remodelling enhancing the bacterial colonisation (Raisch et al., 2014).

These variations in bacterial biofilm between tumour tissues and normal adjacent tissues, also between early and later stages of CRC agree with this chapter's data showing higher inhibitory impact of EVs on the ability of bacteria to form biofilm at the later metastatic stage of CRC. Notably, previous work showed that the bacterial biofilm structure in sporadic CRC and familial adenomatous polyposis varies, this suggests that CRC alter the bacterial biofilm. The study also showed that the carcinogenic effects of *E. coli* are enhanced due to the effect of another carcinogenic bacterial strain, *B. fragilis*, that enhanced mucosal exposure to *E. coli* as *B. fragilis* resulted in mucus degradation (Dejea et al., 2018). Therefore, alterations in *E. coli* biofilm could promote the carcinogenic effect of other bacterial species, this could lead to a complementary carcinogenic impact of both species leading to tumour progression.

Moreover, long-term exposure of *E. coli* MG1655 to EVs had no significant permanent impact on the ability of the bacteria to form a biofilm, indicating the need for direct contact with EVs and bacteria to impact its ability to form biofilm. However, a trend of an increase in the ability of *E. coli* 11G5 to form biofilm following long-term exposure to EVs has been observed.

4.4.3 Impact of Blood derived-EVs on the phenotypic characteristics of *E. coli*

To test the impact of EVs from biological samples, EVs were isolated from the blood plasma of HDs and CPDs by SEC and were characterised following the MISEV 2018 guidance (Théry et al., 2018). EV's tetraspanin markers detection in SEC fractions confirmed the presence of EVs in collected SEC fractions, and EVs-rich fractions were pooled for future functional experiments. Indeed, EVs in pooled fractions were characterised, particle size/concentration profile, tetraspanin markers detection by nanoFCM and ELISA, and morphology further confirmed that the isolated particles in pooled fractions were EVs.

EVs from HDs and CPDs altered the phenotypic characteristics of both strains of *E. coli*, increased the bacterial growth and reduced the bacterial ability to form biofilm. Notably, HDs-EVs showed a higher inhibitory impact on the ability of *E. coli* 11G5 to form a biofilm, compared to CPDs-EVs. This unexpected finding could be because blood plasma has EVs from all cell types, not specific to colon EVs, and inhibitory impact on bacterial biofilm could be linked to immunity, as previously described (Koeppen et al., 2021). Overall, the impact of EVs from CPDs mirrors the impact of CRC cell lines on *E. coli* growth and ability to form biofilm.

4.4.4 The impact of CRC tissue derived-EVs on *E. coli* phenotypic characteristics

The role of CRC-EVs in tumour progression has been well investigated with evidence suggesting that EVs are involved in the bidirectional communication between tumour cells and their surrounding microenvironment (Rahmati, Moeinafshar, & Rezaei, 2024). The data showed that CRC tissue-derived-EVs alter the phenotypic characteristics of *E. coli*, they increased the growth of *E. coli* MG1655 and reduced the ability of both *E. coli* strains to form biofilm, this suggests that CRC tissue-derived-EVs alter the gut microbiome to promote tumour progression in CRC.

4.5 Future work

Future work could investigate the impact of CRC-EVs on the pathogenicity of *E. coli* by treating *Galleria Mellonella* larvae with EV-treated *E. coli* and conducting a *Galleria Mellonella* virulence assay (Chen, R. Y. & Keddie, 2021). Also, to assess the impact of CRC-EVs on the phenotypic characteristics of other bacterial strains that are known to be highly prevalent and associated with carcinogenesis such as *F. nucleatum*. Since the gut microbiome is complex, investigating the impact of EVs on the cocultures of two bacterial species and multiple cultures of various bacterial species would be more physiologically relevant than a single bacterial culture. Also, investigating the impact of patients' stool-derived EVs would be more specific to CRC than blood-plasma EVs.

4.6 Conclusions

To conclude, CRC-EVs alter the phenotypic characteristics of *E. coli*, increase bacterial growth and decrease the ability of bacteria to form biofilm. Notably, the inhibitory

impact of metastatic-stage derived EVs on the ability of *E. coli* to form biofilm is higher, compared to early-stage derived EVs.

5 Colorectal cancer extracellular vesicles alter zinc-uptake regulatory genes of *E. coli*

5.1 Abstract

Overview: EV cargoes, including RNA, DNA, proteins, and lipids can be taken up by other cells and elicit various phenotypic responses. Many studies demonstrated the phenotypic effects of specific EVs-associated cargo on target cells, and this has raised interest in EVs as functional mediators. RNA EV-cargo has the potential to alter gene expression and function of recipient cells, therefore, revealing the mechanisms of impact of EVs on *E. coli* and investigating potential EVs-miRNA that could target bacterial genes leading to altered phenotypic characteristics could provide a therapeutic tool for CRC-associated dysbiosis.

Methods: SEC was conducted to isolate CRC cell line-derived EVs. To investigate mechanisms of impact of EVs on *E. coli*, links between *E. coli*-EVs physical interaction and effects were investigated, full transcriptomic analysis of treated *E. coli* was performed to assess the impact of EVs on the bacterial transcriptome, and alignment analysis was performed to determine potential miRNA that could target bacterial genome. Lastly, EVs were lysed, and EV-protein and EV-miRNA contents were then digested to investigate their link to the inhibitory impact on the ability of *E. coli* to form biofilm.

Results: *E. coli-EV's* physical interactions are not necessary to the functional impact, and lysed-EVs also showed an inhibitory impact on the ability of *E. coli* to form biofilm. Transcriptomic analysis revealed that EV treatment resulted in higher expression of motility-associated bacterial genes, EVs also increased the growth and reduced the biofilm formation ability of motility-mutant *E. coli* MG1655. EV treatment resulted in lower expression of bacterial zinc-uptake-associated genes and alignment analysis showed that miR-181 and miR-92 could target these zinc-uptake-associated genes. However, EVs-RNAase treatment showed that EVs-miRNAs are not linked to the inhibitory impact on the ability of bacteria to form biofilm.

5.2 Introduction

5.2.1 *E. coli* biofilm

A biofilm is an aggregate of micro-organisms that live together as a community and are often found attached to surfaces. Microbes in a biofilm secrete various protective substances that enhance their survival. In the gut, *E. coli* biofilms are found to be a major cause of various intestinal infections ((Bai, Xingjian, Nakatsu, & Bhunia, 2021; Sharma et al., 2016). There are four main steps involved in biofilm formation (Figure 5.1).

(i) **Initial adhesion or attachment (reversible)**: Bacterial cells can attach to abiotic such as medical devices made of steel, or biotic surfaces such as epithelial cells. In addition to environmental conditions, such as pH, temperature and ionic surfaces of the surrounding medium, repulsive electrostatic and hydrodynamic forces impact the attachment. However, flagella (bacterial motility structure) help overcome these forces and increases interactions between *E. coli* and surfaces, providing first cell-surface contact for adhesion. Motility is essential for adhesion and biofilm formation, however, non-motile bacteria can also attach to the surfaces with the expression of adhesion factors. (Beloin, Roux, & Ghigo, 2008).

(ii) **Early development of biofilm microcolony (irreversible)**: Following the attachment, the flagella are repressed to shift *E. coli* from a motile to a sessile state. Various molecules mediate this shift such cyclic-diguanylic-acid (c-di-GMP), its concentration is low under a motility state, and it rises for biofilm development. During early development, various adhesive organelles mediate the irreversible attachment to the surface such as type 1 fimbriae or pili, encoded by the *fim* gene whose expression is induced by adhesion and initial development of biofilm. Also, curli fimbriae, encoded by *csg* gene, extracellular structures that attach to the proteins of the extracellular matrix, which provide adhesion to the surface and facilitate cell-to-cell communications.

(iii) **Maturation of the developed biofilm**: Once the bacterial cells are firmly adhered to the surface, they aggregate through cell-to-cell communication. They also produce an extracellular matrix to provide a three-dimensional biofilm structure. Autotransporters, extracellular polymeric substances (EPS), quorum

sensing molecules, and stress resistance genes are major contributors to the maturation stage of biofilm. Autotransporters do not require accessory proteins for their translocation to the outer membrane, Antigen 43 is a key autotransporter encoded by *flu* gene, it promotes cell-to-cell adhesion enhancing auto aggregation and three-dimensional development. The EPS is the medium by which the bacterial cells attach to the surfaces, it also facilitates cell-to-cell interactions providing structure, protection, and shape for the biofilm. EPS is mainly composed of water alongside nucleic acid, metabolites, nutrients, lipids, and polysaccharides. Quorum sensing is a cell density-dependant chemical signalling system in which bacterial cells release small signalling molecules called autoinducers or quormons to their surroundings to promote intraspecies communications (Daniels, Vanderleyden, & Michiels, 2004). Once the concentration of Ais reaches a threshold lever, the bacteria can detect it and alter gene expression. Stress resistance genes are induced during biofilm formation to facilitate the survival of bacteria in harsh conditions.

(iv) **Dispersion:** The final step involves detachment of biofilm cells and their dispersion and transmission into planktonic state which can reattach to different sites and start forming another biofilm. This detachment could result from enzymatic degradation of the matrix and quorum sensing in response to various environmental factors (Sharma et al., 2016).

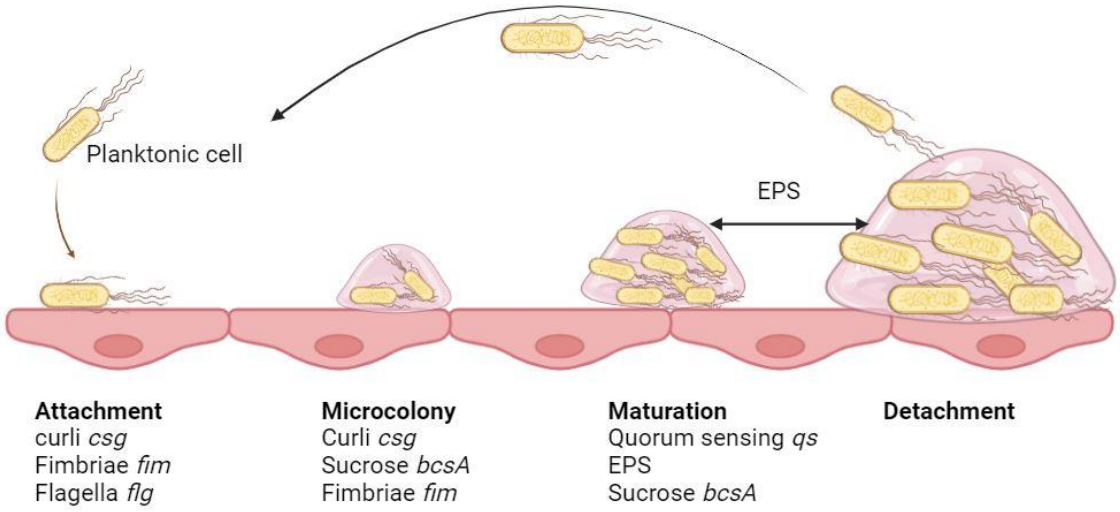

Figure 5.1: Stages of bacterial biofilm formation. There are four stages of biofilm formation: attachment, microcolony, maturation, and detachment. Some genes and factors are involved in promoting each step.

5.2.2 Functional cargoes of EVs and microbiome

The complex host-microbiota interaction involves both host sensing of bacterial metabolites and direct interaction with the bacteria. However, the gut mucus layer separates most gut bacteria from the host cells. Accumulated evidence suggests that EVs are essential for maintaining gut homeostasis (Chu et al., 2016; Jiang et al., 2016), they serve as crucial mediators within intercellular communications, facilitating various physiological and pathological processes. Various types of molecular cargo present in EVs are believed to play specific roles in biological and biomedical processes (Huang et al., 2023). It was also reported that gut dysbiosis is associated with changes in the abundance of EVs and their cargoes (Chang et al., 2020).

5.2.2.1 EV-miRNA as mediators of cross-species regulations

As a vital mediator of intercellular communication, EVs-miRNA can be secreted by and transferred to various target cells, organs, and organisms (Zhao, L. et al., 2021). It was shown that EV nucleic acid contents play a role in microbial structure shaping (Casado-Bedmar & Viennois, 2022; Shen, Huang, Yao, & Jin, 2021). EV-derived miRNAs have been implicated in host-microbiome communications, such as miR-515-5p and miR-1226-5p, they can enter *F. nucleatum* and *E. coli* and regulate gene transcripts increasing bacterial growth (Liu et al., 2016). Notably, targeted deletion of the miRNA biogenesis enzyme, dicer resulted in imbalanced gut microbiota provoking dextran sulfate sodium-induced colitis, which was reversed by faecal miRNA transplantation from wild-type mice, suggesting a crucial role of miRNA in shaping gut microbiota and intestinal homeostasis maintenance (Liu et al., 2016). It was also found that the most abundant faecal miRNAs were also contained within intestinal EVs, suggesting that EVs are the major source of intestinal/faecal miRNAs (Liu et al., 2016).

Other work showed that the gut bacterial composition of mice was shifted following exposure to total abdominal irradiation (cancer radiation treatment) which also resulted in higher expression of miR-34a-5p in small intestine and peripheral blood. Interestingly, gut microbiota composition was retained following miR-34a-5p antagomir injection (Cui et al., 2017). In CRC, various studies have shown distinct faecal or intestinal miRNA expression profiles and their potential link with disease and gut bacterial composition.

Therefore, miRNAs have been considered biomarkers and therapeutic targets (Yuan, Burns, Subramanian, & Blekhman, 2018).

Moreover, it was shown that intestinal miR-21 has an inhibitory impact on the growth of *Lactobacillus*, a key microbiome genus for gut homeostasis (Santos et al., 2020). Mice lacking miR-21 were characterised by an increase in *Lactobacillus*, reduced liver damage, and were protected against gut microbiota dysbiosis resulting in protection against small intestine injury. Whereas induction of miR-21 resulted in a reduction in the abundance of *Lactobacillus*, and supplementation with *Lactobacillus* resulted in reduced liver fibrosis, mimicking the protective effect in miR-21 knockout mice (Santos et al., 2020). Overall, intestinal miRNA could promote diseased conditions by altering gut microbiota.

EVs secreted from airway epithelial cells promoted bacterial growth and biofilm formation of *P. aeruginosa* through delivering transferrin and nutrients to the bacterium (Hendricks et al., 2021). Whereas EVs released from neutrophils or macrophages have been shown to have antimicrobial properties (García-Martínez et al., 2019; Timár et al., 2013). Therefore, EVs-mediated gut microbiome reconstruction is a potential strategy for manipulating the microbiome in diseases including CRC.

5.2.2.2 EVs-matrix metalloproteases

Matrix metalloproteases, MMPs, are a family of zinc-dependent endopeptidases capable of degrading components of ECM. They play a role in various pathological conditions with excessive degradation of ECM, such as periodontitis, rheumatoid arthritis, and tumour invasion and metastasis. In CRC, various studies have demonstrated the role of MMPs in tumour spread (Reunanen & Kähäri, 2013; Yu, J. et al., 2021), and detected MMPs in EVs. A study has found that MMP13 was overexpressed in exosomes derived from nasopharyngeal tumour (You et al., 2015).

Given the crucial role of MMPs in cancer progression and metastasis and their proteolytic activity, they could mediate bacterial biofilm inhibition through the degradation of biofilm components. It was shown that human MMP1 significantly inhibited and disrupted the biofilm of *Enterococcus faecalis* through the degradation of biofilm matrix (Kumar, L., Cox, & Sarkar, 2019).

5.2.3 Hypothesis and aims

This chapter hypothesises that EVs-miRNAs target bacterial genomes and alter their phenotypic characteristics. To test this hypothesis, the following aims will be addressed:

I. To investigate mechanisms of CRC-EVs-*E. coli* interaction
II. Determining potential functional cargoes of EVs that have an impact on *E. coli*
III. To reveal potential genes that could be targeted by EVs-miRNA contents

5.3 Results

5.3.1 EVs-*E. coli* physical interaction had no impact on the bacterial phenotypic characteristics

Data in Chapter 3 showed that EVs-surface proteins are involved in the EVs-*E. coli* interactions. To assess whether EVs-*E. coli* interactions correlate to the functional impact of EVs on *E. coli*, *E. coli* was co-cultured with EVs treated with proteinase-k and trypsin to degrade surface-proteins, and biofilm formation ability was then assessed. The ability of *E. coli* to form biofilm was significantly inhibited by EVs that were treated with proteinase-k and trypsin enzymes (Figure 5.2). The total number of CFU/ml of biofilm cells significantly decreased from $8.3*10^5$ to $2.2*10^5$ due to untreated EVs, and to $9.6*10^4$, $1.3*10^5$, $1.8*10^5$ due to proteinase-k-, trypsin-, and proteinase-k-trypsin-treated EVs, respectively.

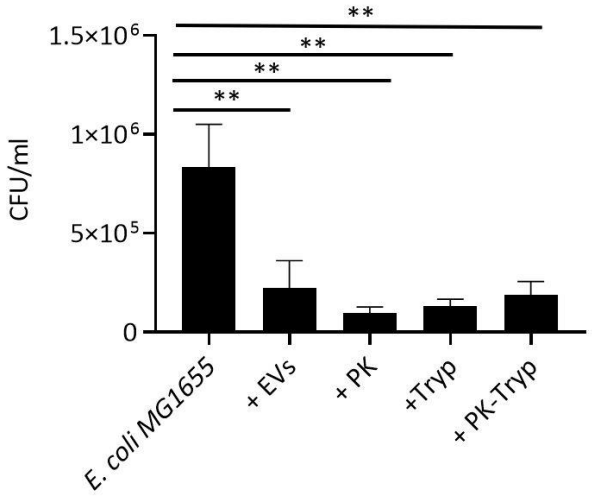

*Figure 5.2: EVs-E. coli physical interactions are not correlated to the biofilm inhibitory impact of EVs on E. coli. The total number of CFU/ml of biofilm cells of E. coli MG1655 treated with 50 µg/ml of SW620-EVs, and PK-, Tryp-, and PK-Tryp- treated SW620-EVs. Error bars represent mean ± SEM, statistical analysis by ANOVA, Brown-forsythe and Bartlett's tests, ** p<0.01, n=3.*

5.3.2 Impact of lysed-EVs mirrors the impact of intact-EVs on *E. coli* biofilm formation ability

Data in Chapter 3, Figure 3.15, showed that *E. coli* lysed EVs. To assess whether lysed-EVs also have an impact on the bacterial phenotypic characteristics, *E. coli* was treated with SW620-EVs that were lysed by RIPA lysis buffer, and bacterial phenotypic characteristics were then assessed (growth, and ability to form biofilm). As shown in Figure 5.3, lysed EVs have also an inhibitory impact on the bacterial ability to form biofilm (A), the total number of CFU/ml of biofilm cells of *E. coli* MG1655 decreased from $4.7*10^6$ to $6.7*10^4$, $3.7*10^5$, and $1.7*10^6$ due to lysed-EVs, intact-EVs, and RIPA lysis buffer (as a control), respectively, and the impact of lysed-EVs is higher than intact-EVs. Contrarily, EVs have increased the growth of *E. coli* (B), however, this increase in not statistically significant, the absorbance reading at 600_{nm} of bacterial culture increased from 0.232 to 0.331, 0.682, and 0.447 after 18 hours of co-culturing with EVs, lysed-EVs, and RIPA lysis buffer, respectively, and lysed-EVs have also a higher impact on the bacterial growth, however, this difference is not statistically significant.

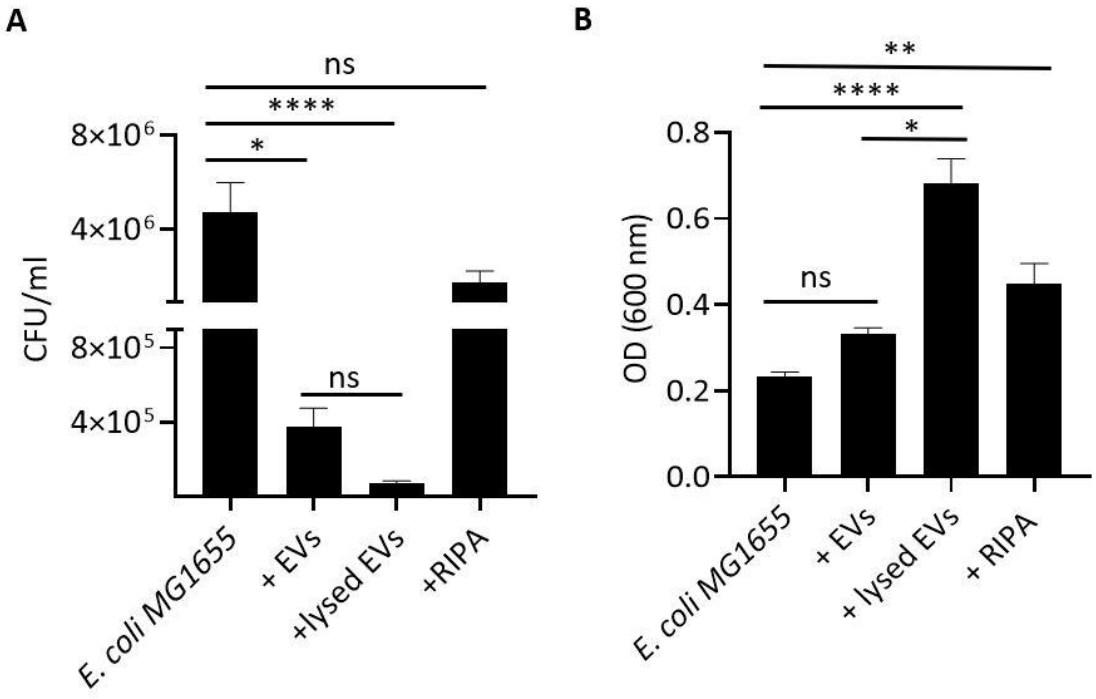

*Figure 5.3: lysed-EVs increased the growth and decreased the ability of E. coli to form biofilm. (A) the total number of CFU/ml of E. coli MG1655 biofilm treated with 50 µg/ml of intact and lysed SW620-EVs, and RIPA buffer, as a control. (B) Absorbance at 600 nm of E. coli MG1655 at 18 hours culturing with intact and lysed SW620-EVs, and RIPA lysis buffer, as a control. Error bars represent mean ± SEM, statistical analysis by ANOVA, Brown-forsythe and Bartlett's tests, * p<0.05, ** p<0.01, *** p<0.001, **** p<0.0001, n=3.*

5.3.3 CRC cell line derived-EVs altered the expression of bacterial genes involved in the bacterial motility and zinc-ion uptake

To investigate EV-mediated altered bacterial mechanisms, a full transcriptome analysis was performed for *E. coli* MG1655 which *was* treated with SW620-EVs. As shown in Figure 5.4, 13 genes were differentially expressed, 3 were significantly upregulated in EV-treated bacteria, *ppsA*, *fliA*, and *mdtJ*, and 10 were significantly downregulated, *zinT*, *znuA*, *znuC*, *ykgM*, *yodB*, *msrQ*, *uxaA*, *pliG*, *uxaC*, and *rspB*.

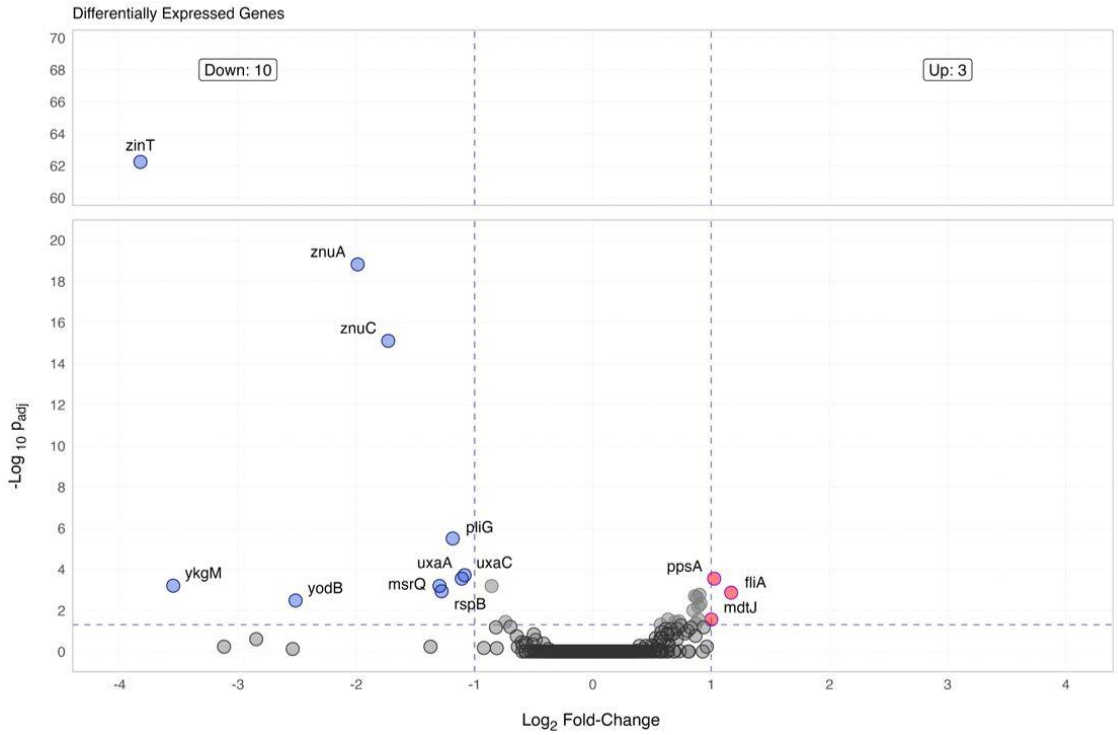

Figure 5.4: Differentially expressed genes in SW620-EVs treated E. coli MG1655 vs non-treated E. coli MG1655. The volcano plot of differentially expressed genes represents a log 2-fold change on the x-axis and log 10 adjusted p-value on the y-axis. Single genes are represented as dots, the upregulated genes are in blue, and the downregulated ones are in red. P<0.05, n=3.

To investigate the biological functions of the differentially expressed genes, gene ontology (GO) analysis was performed (Figure 5.5). Across the upregulated genes, GO analysis showed that motility, particularly the flagellar motility structure of *E. coli* is the most altered mechanism in EV-treated bacteria.

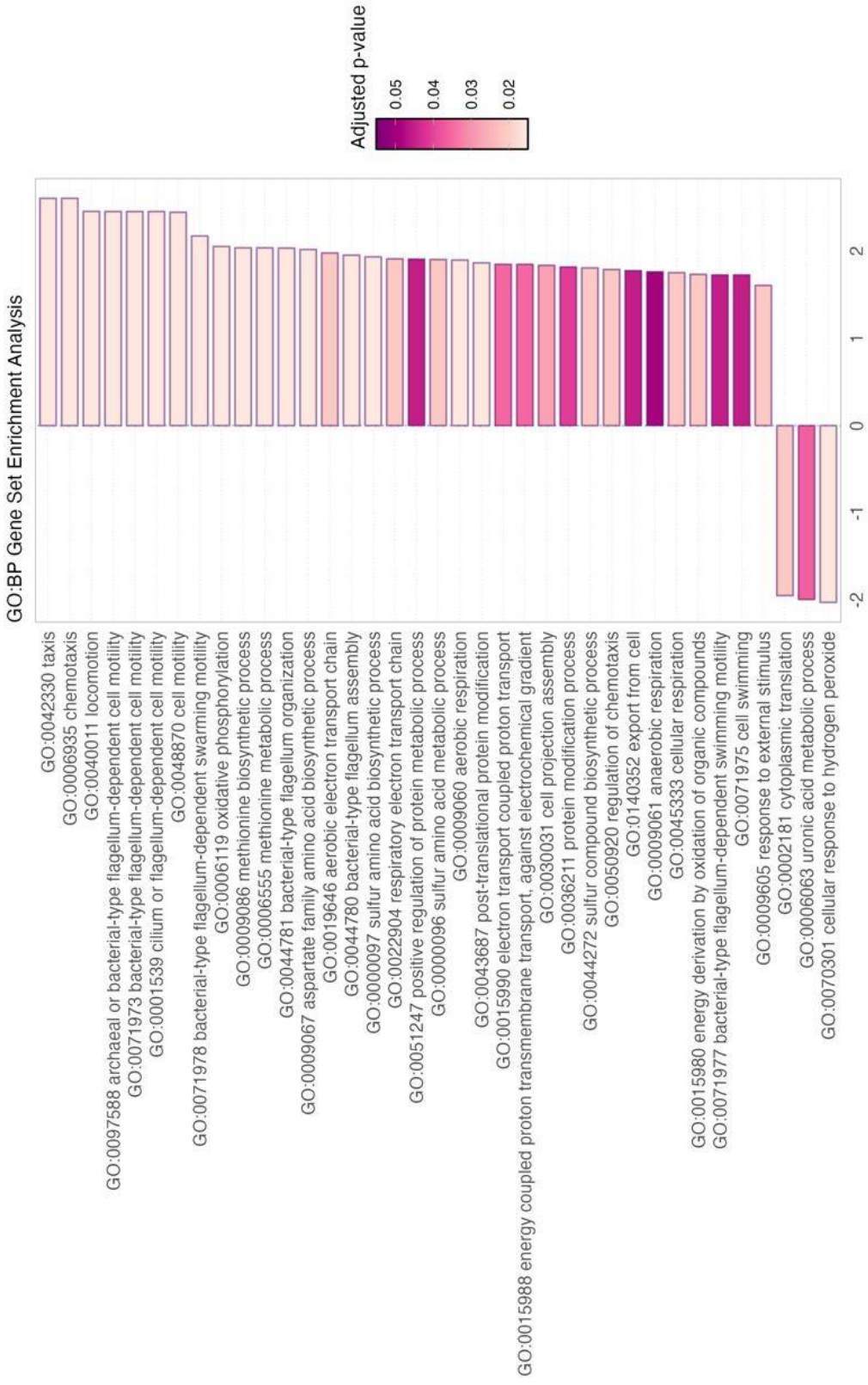

Figure 5.5: Gene ontology analysis of differentially expressed genes. Analysis showing enrichment of biological function of differentially expressed genes in EV-treated vs non-treated E. coli MG1655.

Out of the 13 downregulated genes, 6 genes are associated with zinc ion uptake: *zinT*, *znuA*, *znuC*, *ykgO*, *rspB*, and *yodB*, as listed in Table 5.1.

Table 5.1: Gene ontology terms of the downregulated genes that are linked to zinc ion uptake

Downregulated gene	Biological process	Molecular function
zinT	Intracellular zinc ion homeostasis	Zinc ion binding
znuA	Zinc ion transport	Zinc ion binding
znuC	Zinc ion transport	ABC-type zinc transporter activity
ykgO	Translation	Structural constituent of ribosome
rspB	Zinc ion binding	Metal ion binding
yodB	Respiratory electron transport chain	Metal ion binding

5.3.4 CRC cell line derived-EVs increased the growth and reduced the biofilm formation ability of motility-mutant *E. coli* MG1655

To investigate the impact of SW620-EVs on motility-associated genes, motility-mutated *E. coli* MG1655 strains, Δ*pdeh*, Δ*FliC*, and Δ*Flh*, were treated with SW620-EVs, and their growth and biofilm formation ability were assessed. As shown in Figure 5.6, EVs treatment increased the growth of the parental *E. coli* MG1655 strain (Figure 5.6A), Δ*pdeh* (Figure 5.6B), Δ*FliC* (Figure 5.6C), and Δ*Flh* (Figure 5.6D) strains. At 12 hours incubation time, absorbance at 600 nm increased from 0.125 to 0.201, 0.154 to 0.211, 0.154 to 0.235, and 0.156 to 0.230 of parental, Δ*pdeh*, Δ*FliC*, and Δ*Flh*, respectively.

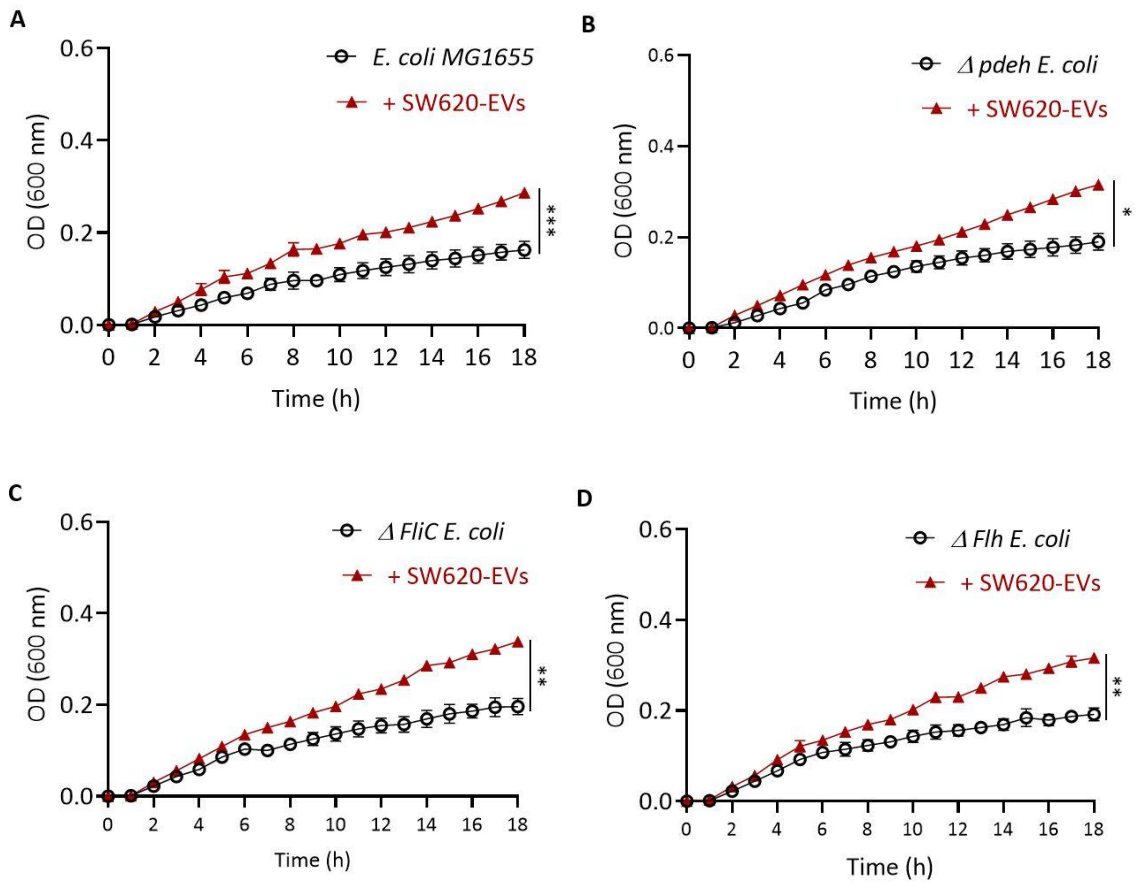

*Figure 5.6: SW620-EVs increased the growth rate of motility-mutant E. coli MG1655. Absorbance at 600 nm of parental E. coli MG1655 (A) and motility-mutants (Δpdeh (B), ΔFliC (C), and ΔFlh (D)) treated with SW620-EVs and incubated at 37 °C for 18 hrs. Representative replicate, error bars represent mean ± SEM, p *<0.05, **<0.01, ***<0.001.*

However, EV treatment significantly reduced the ability of parental and motility-mutant *E. coli* MG1655 strains to form a biofilm (Figure 5.7). The total number of CFU/ml decreased from $3.4*10^6$ to $1.7*10^5$, $1.3*10^6$ to $2.9*10^4$, $5.6*10$ to $6.8*10^3$, and $8.2*10^5$ to $1.3*10^4$ of parental, Δ*pdeh*, Δ*FliC*, and Δ*Flh*, respectively.

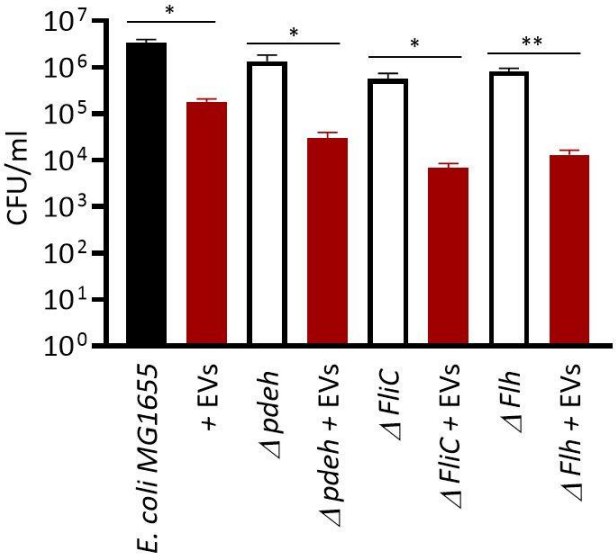

*Figure 5.7: EVs reduced the ability of E. coli MG1655 motility-mutant strains to form biofilm. The total number of CFU/ml of biofilm cells of parental E. coli MG1655 and motility-mutant strains, Δpdeh, ΔFliC, and ΔFlh, treated with SW620-EVs. Error bars represent mean ± SEM, p *<0.05, **<0.01. N=3.*

In comparison, the inhibitory impact on motility-mutant strains is higher than the impact on parental strain, the relative change in biofilm formation was 94.8%, 97.7%, 98.7%, and 98.4% for parental non-mutated *E. coli* MG1655, Δ*pdeh*, Δ*FliC*, and Δ*Flh*, respectively. Moreover, as shown in Figure 5.8, the normalised data to untreated conditions showed that the impact of SW620-EVs on mutated *E. coli* strains is significantly higher than their impact on parental strain.

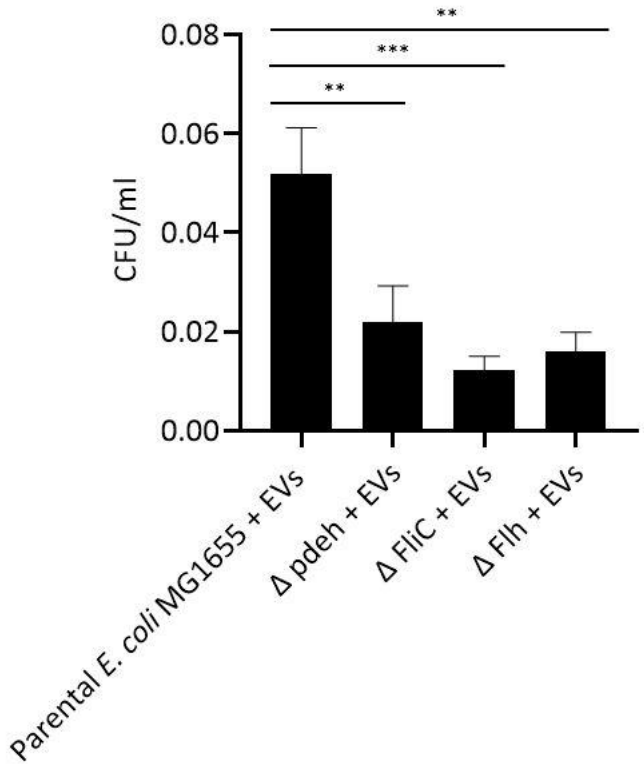

*Figure 5.8: CRC cell line-derived EVs have a higher inhibitory impact on motility-mutated E. coli MG1655 strains compared to their impact on parental E. coli MG1655. The bar chart represents CFU/ml of biofilm cells of parental E. coli MG1655 and motility mutated E. coli MG1655 strains treated with SW620-EVs. Data was normalised data to the untreated condition of each E. coli strain. Error bars represent the mean ± SEM, One-way ANOVA, Brown-forsythe and Bartlett's tests, p *<0.05, **<0.01. N=3.*

5.3.5 EV treatment reduced the ability of *E. coli* to invade CRC cells

To assess whether the increase in motility-related gene expression is correlated to an increase in the invasive ability of *E. coli*, SW480-cells and SW620-CRC cells were incubated with EV-treated and non-treated *E. coli* MG1655, and the total number of invaded bacterial cells was assessed. As shown in Figure 5.9, the percentage of invaded *E. coli* MG1655 cells reduced due to SW620-EV treatment. For SW620-cells, the percentage of invaded bacterial cells decreased from 0.007% to 0.004% due to SW620-EV treatment of *E. coli* MG1655. For SW480-cells, the percentage of invaded bacterial cells decreased from 0.004% to 0.003% due to SW620-EV treatment, however, this was not statistically significant. Overall, *E. coli* MG1655 could invade SW620-cells more than SW480-cells.

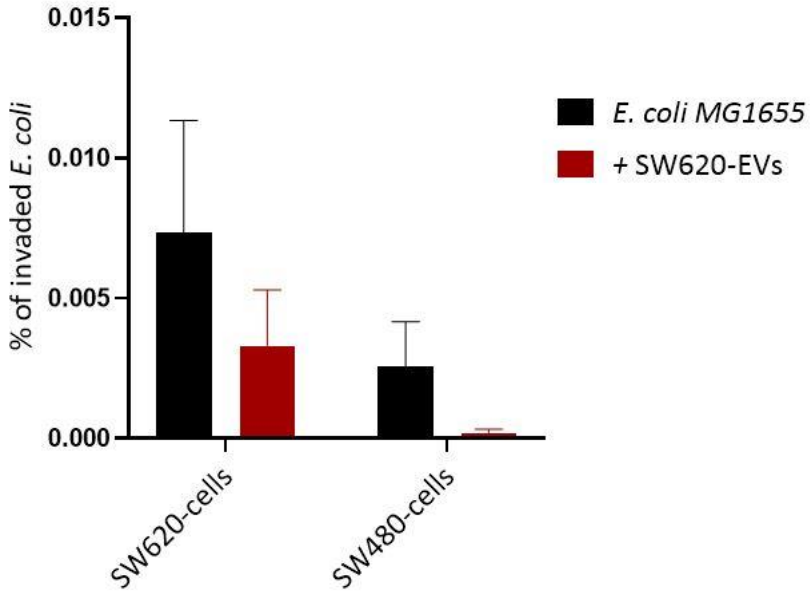

Figure 5.9: EV treatment reduced the ability of E. coli MG1655 to invade CRC cells. The percentage of invaded E. coli MG1655 treated with SW620-EVs and incubated with SW620-cells and SW480-cells. Error bars represent mean ± SEM, n=3.

5.3.6 EVs-miRNA could target bacterial zinc-uptake genes

Numerous studies have found that miRNAs are differentially regulated in CRC tumours and adjacent normal colon tissue, and these miRNAs are correlated with the abundance of specific microbiota in the tumour microenvironment (Yuan, Burns, Subramanian, & Blekhman, 2018). Therefore, an alignment analysis was performed using BLASTN tool to investigate potential EV-miRNA that targets the downregulated genes. Out of 186 miRNAs that are expressed in both SW480- and SW620-EVs, 27 are over-expressed in SW620-EVs, compared to SW40-EVs, and these were aligned against the *E. coli* MG1655 genome since SW620-EVs have more effect on bacteria compared to SW480-EVs, as shown in previous data (Figure 4.11). Table 5.2 shows the list of miRNAs that could potentially target downregulated genes such as *znuA* and *pliG*, it also shows potential targeted genes that are located adjacent to the downregulated genes such as *msrP* which position is adjacent to *msrQ*, *zinT*, and *yodB* that are significantly downregulated in EV-treated *E. coli* MG1655.

Table 5.2: List of targeted E. coli MG1655 genes by SW620-EVs miRNAs

Downregulated gene	miR	Adjacent downregulated genes
znuA	miR-92a-1-5p	
pliG	miR-181a-5p	
Potential targeted genes	**miR**	**Adjacent downregulated genes**
msrP	miR-181a-3p	*msrQ, ZinT, yodB*

miR-92a-1-5p could potentially target *znuA* gene that encodes for periplasmic zinc-binding protein. Alignment analysis showed sequence similarities between miR-92a-1-5p and *znuA* gene (Figure 5.10A), 10 nucleotides of miR-92a-1-5p match 10 nucleotides of *znuA* gene (Figure 5.10B). *znuA* is part of the zinc uptake znuABC transporter system (Figure 5.10C), binds to zinc with high affinity and specificity and delivers it to the membrane permease for translocation into cytoplasm.

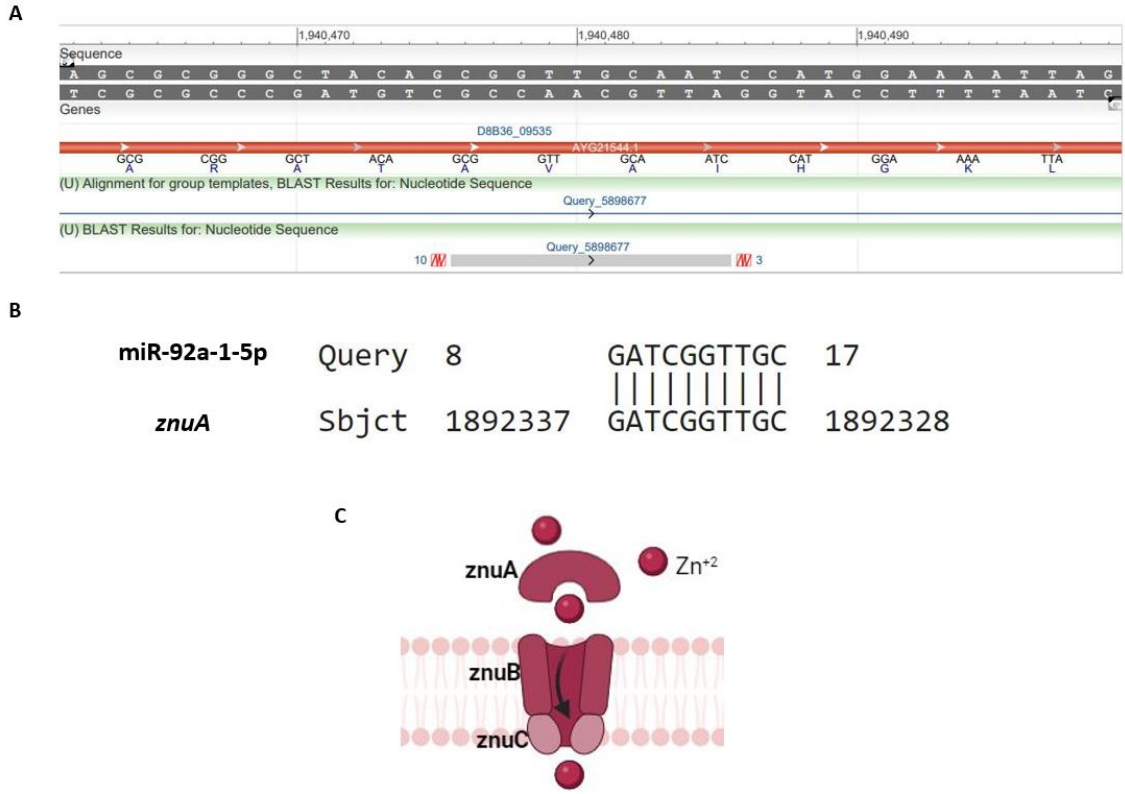

Figure 5.10: Schematic illustration of potential miRNA targeting znuA gene. A. graphics of alignment of miR-92a-1-5p sequence to the genome of E. coli MG1655 znuA gene. B. Aligned nucleotide sequences of miR-92a-1-5p and znuA gene. C. The structure of the zinc-uptake ABC transporter consists of periplasmic zinc-binding protein (znuA), ATPase (znuB), and integral membrane protein (znuC).

Moreover, has-miR-181a-3p could potentially target the *msrP* gene as shown in Figure 5.11. BLAST graphic alignment analysis showed the similarities between the miR sequence and bacterial genome sequence (Figure 5.11A), 10 nucleotides of miR-181a-3p match the bacterial genome sequence across *msrP* gene (Figure 5.11B), this gene is adjacent to *msrQ*, *zinT*, and *yodB* genes that are significantly downregulated due to SW620-EVs treatment (Figure 5.11C).

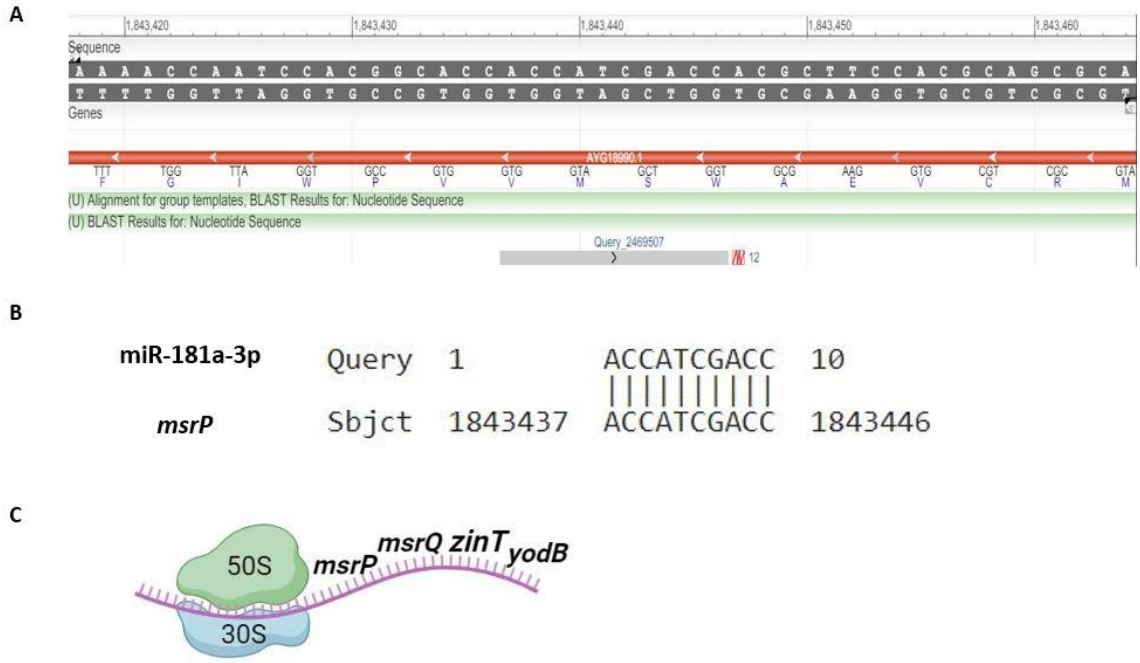

Figure 5.11: Schematic illustration of potential miRNA targeting msrP gene. A. graphics of alignment of miR-181a-3p sequence to the genome of E. coli MG1655 msrP gene. B. Aligned nucleotide sequences of miR-181a-3p and msrP gene. C. Gene location of msrP, msrQ, zinT, and yodB genes.

5.3.7 EVs-miRNAs had no impact on the ability of *E. coli* MG1655 to form a biofilm

To investigate if either EVs-protein or EVs-miRNAs or both mediate the inhibitory impact on the bacterial ability to form a biofilm, *E. coli* MG1655 was treated with EVs that were lysed and treated with either PK to digest EVs-proteins, RNAase to digest EVs-RNA, or MMPsi to digest EVs-MMPs, and the impact on biofilm was assessed. As shown in Figure 5.12, there was a slight not statistically significant recovery of biofilm due to treatment with lysed EVs that were treated with PK and MMPsi; the total number of CFU/ml increased from $1.9*10^5$ to $3.1*10^5$ and $3.5*10^5$ following PK-EV and MMPsi-EV treatment, respectively. However, no change in the total CFU/ml of biofilm cells was observed following the EV treatment with RNAase.

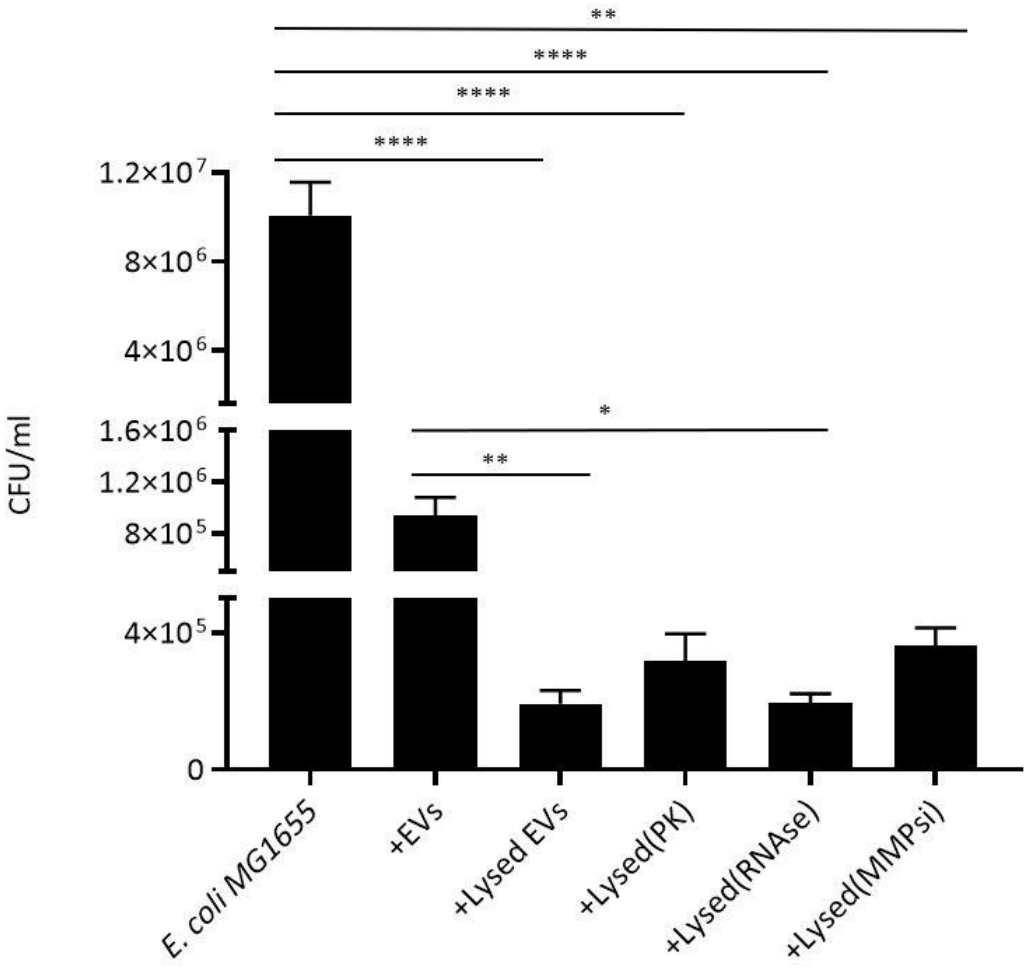

*Figure 5.12: EVs-miRNAs are not involved in the altered bacterial biofilm formation ability. Total CFU/ml of E. coli MG1655 biofilm cells treated with lysed SW620-EVs treated with PK, RNAases, and MMPsi. Error bars represent mean ± SEM, statistical analysis by ANOVA, Brown-forsythe and Bartlett's tests, * p<0.05, ** p<0.01, *** p<0.001, **** p<0.00001, n=3.*

5.4 Discussion

5.4.1 Impact of EVs-*E. coli* physical interactions

Data in Chapter 3 showed that *E. coli* interacts with human CRC-derived EVs through EVs-surface protein-mediated interactions. In this chapter, data showed that these physical interactions are not necessary for the inhibitory impact of EVs on the ability of *E. coli* to form biofilm, EVs had a significant inhibitory impact on the ability of *E. coli* to form biofilm following the digestion of EV-surface proteins but this does not mean no EV-*E. coli* interaction. This suggests that the actual binding of EVs to *E. coli* surfaces is not related to altered biofilm formation ability, and the EVs contents are mediating this inhibitory impact. Data also showed that bacterial degrading enzymes lyse EVs releasing their contents that could be taken up by bacteria, these lysed EVs significantly inhibited the ability of *E. coli* to form biofilm.

5.4.2 CRC-EVs alter motility-related gene expression

At the early stages of biofilm formation, bacteria change from a motile to a sessile state by switching motility genes off. EVs significantly increased the expression of the flagella-associated gene, *fliA*, thus enhancing motility, and enhancing motility would disrupt the early mechanism of biofilm formation. Notably, EVs have a higher inhibitory impact on the ability of motility-mutant *E. coli* strains compared to non-mutant parent *E. coli* strain, this suggests that the mechanism of EV action is not limited only to their impact on motility but to their impact on other pathways related to biofilm formation processes. Notably, increased motility was not correlated to bacterial invasion of CRC cells, EV treatment decreased the ability of *E. coli* MG1655 to invade CRC cells, although the percentage of invaded bacterial cells was very low.

5.4.3 CRC-EVs downregulate bacterial zinc ion-uptake-related genes

EVs significantly downregulated zinc-ion uptake genes (*zinT*, *znuA*, *znuC*, *ykgO*, *rspB*, and *yodB*). The bacterial zinc uptake system is crucial for the survival and biofilm formation of many enteric pathogens under zinc-deficient conditions (Quan, Xia, Lian, Wu, & Zhu, 2020). Zinc-uptake genes are tightly regulated and are expressed upon its scarcity, it was reported that ZnuABC plays a critical role in zinc uptake in *E. coli* and ZinT contributes to the ZnuA-mediated recruitment of zinc in the periplasmic space. Also, a functional zinc

uptake system is essential for bacterial adhesion to epithelial cells and colonisation of intestinal epithelial (Gabbianelli et al., 2011; Graham et al., 2009). Another study reported that *ykgM* and *zinT* genes are regulated by Zur (zinc uptake regulator) which is highly induced under zinc shortage conditions. Both genes were found highly expressed in *E. coli* biofilm and are required for maintaining optimal intracellular zinc concentration. Mutations in *ykgM* and *zinT* genes lead to the inhibition of curli biosynthesis impacting biofilm formation. *ZintT* and *ykgM* mutants contained lower concentrations of zinc than wild type and bot mutants were less able to attach to the surfaces, including epithelial cells surface (Lim et al., 2011). Data from this chapter showed that EV treatment significantly downregulated the *ZinT* gene, therefore, EV treatment alters zinc-uptake systems impacting the ability of *E. coli* to form biofilm.

Notably, zinc-bound Zur repressor acts as a repressor for genes encoding high-affinity zinc importer (*znuABC*) in the presence of zinc, it responds to zinc at a femtomolar range (Choi et al., 2017) (Figure 5.13), and EVs are rich in zinc (Piacenza et al., 2018). Therefore, EV's zinc content could mediate the downregulation of zinc-uptake genes through the Zur repressor-mediated zinc-homeostasis system.

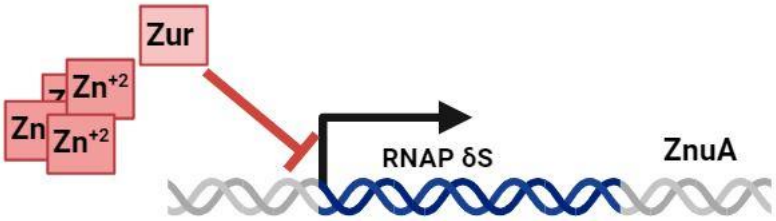

Figure 5.13: Zinc-bound Zur repressor mediates bacterial zinc-homeostasis. Under the presence of zinc, Zur repressor responds (binds) to zinc to repress zinc uptake genes fully by binding to RNA polymerase sigma S (RNAP σS).

Interestingly, the alignment analysis showed that *znuA* could be targeted by miR-92, which is found in EVs, however, RNAase treatment of lysed-EVs showed that EV-miRNAs contents did not seem to be mediating the inhibitory impact on the bacterial ability to form biofilm. The antibacterial activity of zinc could clarify the impact mechanism by which EV-zinc content could mediate the biofilm inhibition and altered expression of zinc uptake genes, it was shown before that zinc could penetrate biofilm to inhibit bacterial growth and subsequently inhibit biofilm formation (Kumar, V. B., Lahav, &

Gazit, 2024). Therefore, EVs-zinc content could be the reason for biofilm inhibition and a decrease in the expression of zinc-uptake genes.

5.5 Future work

Future work could investigate the link between EV-zinc content and their inhibitory impact on bacterial biofilm formation through the EV-zinc depletion process using zinc chelators. Data showed that EVs treatment reduced the expression of zinc-uptake genes, this could potentially be due to EVs-zinc content, therefore, EVs-zinc content could be depleted, and the impact of zinc-free EVs on the bacterial phenotypic characteristics could be assessed.

5.6 Conclusion

CRC-EVs alter the gene expression of zinc-ion uptake genes which are crucial for zinc-ion homeostasis, and the downregulation of zinc-uptake genes could be linked to the inhibitory impact of EVs on the ability of *E. coli* to form biofilm.

6 Discussion

Several decades ago, CRC was infrequently diagnosed. Nowadays, it is the third most diagnosed cancer and the fourth leading cause of cancer-related mortality. Although the risk of CRC increases with age, approximately 10% of newly diagnosed cases occur in adults younger than 50 years, called early-onset CRC (EoCRC). Whereas the incidence of CRC has decreased among the older age group for whom the early screening is recommended, an opposite trend has been observed in the younger age group, EoCRC, for whom the early screening is not recommended (O'Sullivan et al., 2022), and the incidence is estimated to increase by more than 140% by 2030 (Hofseth et al., 2020; Siegel et al., 2017). In the United Kingdom, CRC is the second most common cause of cancer death, more than 16,800 people die from CRC each year (Morgan et al., 2023). The survival rate is closely related to tumour stage, approximately 90%, 85%, 65%, and 10% of patients with CRC stage I, II, III, and IV, respectively, survive their cancer for 5 years or more following their diagnosis (National Statistics, 2023). Notably, only 10-15% of CRC cases are hereditary, therefore, new primary prevention strategies are crucial to reduce the disease burden.

Various epidemiological studies have identified several risk factors for CRC, such as age, environmental factors, alcohol intake, and smoking. In the past decade, the gut microbiome has been identified as one of the etiological factors for CRC, development and progression of CRC have been closely linked to the gut microbiome (Wong, S. H. & Yu, 2019). Gut dysbiosis that results in the altered microbiome structure; decreased diversity and higher abundance of pathogenic species has been closely linked to CRC (Rebersek, 2021). It has been reported that pathogenic intestinal bacteria such as *F. nucleatum*, *E. coli*, and *B. fragilis* play a vital role in CRC progression (Cheng, Ling, & Li, 2020; Zhou, P., Yang, Sun, & Zhou, 2022). Many studies have revealed the differences in the abundance of these gut microbiota species at various stages of CRC; the number of these pathogenic species increases during the development and progression of the disease (Liang, J. Q. et al., 2021; Yachida et al., 2019; Zhang, Xinyu et al., 2019).

FMT emerged as an intervention protocol for IBD, to reverse the pathogenic shift of gut bacterial species and restore healthy gut bacterial structure. Despite the success of FMT in treating *clostridium difficile* infection, studies have shown the shift in the bacterial structure of the donated microbiome into the original pathogenic state after some time following FMT, with the need for repeating the FMT procedure and re-administration of

a healthy microbiome, however, studies showed that the efficacy of FMT after second administration of microbiota is significantly lower than the initial FMT. Another study has shown the reverting back of specific pro-inflammatory species into the original pathogenic state (Angelberger et al., 2013; Ianiro et al., 2022). These previous findings suggest underlying host-control mechanisms contributing to the shift of a healthy gut into a diseased state, and these mechanisms have not been investigated yet.

In CRC, EVs have been considered functional entities that play crucial roles in tumour progression through functional cell-cell cargo transfer and cell-EV interactions, activating various tumorigenic signalling pathways. It is also evident that CRC cells release EVs into the tumour microenvironment to modulate the surrounding cells for cancer promotion and progression (Glass & Coffey, 2022; Tao & Guo, 2020). Particularly, EVs have been involved in the shift of various stromal cells, such as fibroblasts and immune cells, into a carcinogenic state (Valenti et al., 2006; Webber, Steadman, Mason, Tabi, & Clayton, 2010). Therefore, EVs could also be suggested to mediate the microbiome shifts in CRC. Most previous studies have focused on analysing the changes in the gut microbiota structure and consider these changes as useful tools for early screening of CRC. However, mechanisms mediating the shift of gut microbiome in CRC have not been investigated yet, and this project hypothesises that CRC-EVs alter the gut microbiome leading to dysbiosis and tumour progression.

6.1 High-yield generation and isolation of EVs

Over the last decade, the interest in EV research has exponentially grown due to their close relation with their cellular origin, and their links to various diseases. EVs are heterogenous entities with different nomenclature based on their cellular origin, biogenesis, and size, however, ISEV recommended the use of the general term ''Extracellular vesicles'' (Théry et al., 2018). There are various EV isolation and enrichment techniques in the literature that depend on size such as SEC, differential ultracentrifugation, ultrafiltration, sequential filtration, density such as density gradient centrifugation (DGC), solubility charge such as polymer-based precipitation, expression of surface proteins such as immunoaffinity, or combination of these techniques (Konoshenko, Lekchnov, Vlassov, & Laktionov, 2018). However, reproducibility and low yield of EVs make EV research challenging (Allelein et al., 2021)

In this project, bioreactor flasks were utilised for large-scale production of EVs, as previously described (Suwakulsiri et al., 2019). CRC cell lines, SW480 and SW620, were used as a model of different stages of CRC and the progression of the tumour, ultrafiltration followed by SEC was the conducted efficient EVs isolation approach, as previously described (Jamaludin et al., 2019). A comparative analysis between the different EV isolation approaches showed that the DGC technique has the highest EV yield and purity (Allelein et al., 2021), and another study found that ultrafiltration followed by the SEC EV isolation approach is comparable to DGC in terms of yield and purity (Lobb et al., 2015).

A high yield of SW480- and SW620- EVs was obtained, and isolated EVs were characterised by multiple complementary techniques, following the MISEV 2018 (Théry et al., 2018). Specific characteristics of the isolated EVs were shown, such as morphology (double membranous structure), quantification and particle size distribution, and EV's surface protein markers (CD9, CD63, and CD81). As ELISA is a cell surface-antigen detection method (Bishop & Hwang, 1992), the fluorescent signal indicating the presence of TSG101, cytosolic protein, was not detected. Therefore, the bioreactor flasks cell culture model and SEC isolation method are highly reliable procedures to generate reproducible high yield of EVs.

Studies have reported an increased level of blood circulating EVs in CRC patients compared to healthy individuals, due to increased EV release by cancer cells and enhanced tumour-induced EV secretion in non-malignant cells as well (Titu et al., 2023). Previous analysis of blood circulating EV cargo revealed cancer-specific molecules including proteins and miRNAs that may be employed for CRC early detection (Brocco et al., 2022). Although EVs can be isolated from all blood fluids, it was reported that blood provides the richest EV source (Palviainen et al., 2020). Therefore, mimicking physiological relevant conditions, blood was collected from CRC patients and healthy individuals using EDTA collection tubes as EDTA has less effect on downstream applications compared to other anti-coagulants such as heparin (Diehl et al., 2023). Separation of EV-containing plasma from whole blood allows for long-term storage (Diehl et al., 2023). EVs were successfully isolated from blood-plasma of CRC patients and healthy individuals following the SEC isolation approach (Diehl et al., 2023), and isolated EVs showed the expected characterisation; double membranous structure,

density and size distribution, EV's surface protein markers (CD9, CD63, and CD81). Although NanoFCM particle concentration analysis showed a high particle count, the percentages of CD9-positive, CD63-positive, and CD81-positive particles were low. This indicates the presence of lipoproteins in the EV isolates. Lipoproteins are biological particles that transport lipids throughout the body and are more abundant in blood than EVs, an additional isolation step would improve the purity of EV isolates, as suggested before (Karimi et al., 2018), or by following different isolation methods such as DGC that separates EVs from lipoprotein contaminants, however, it is a technically challenging technique (Onódi et al., 2018)

However, EVs in blood plasma originate from various sources, including blood cells, tissues, and tumour cells (Alberro, Iparraguirre, Fernandes, & Otaegui, 2021). Therefore, EVs were isolated from CRC-tissue, so EV harvest is less confounded by non-tumour entities as would be the case in blood-plasma EV harvest. Also, tissue-derived EVs are more organ-specific and more relevant to the disease compared to the cell line-derived EVs (Cvjetkovic et al., 2024). Enzymatic tissue digestion was performed as previously described (Jeppesen et al., 2019), with some modification, and EVs were isolated by the SEC. Isolated EVs showed expected characterisation, double membranous structure, density and size distribution, and EV surface protein markers (CD9, CD63, and CD81). Obtaining colon tissues from healthy individuals, as a control, was not possible and that was the limitation for assessing the impact of tissue-derived EVs on *E. coli*.

6.2 EVs mediated *E. coli*–CRC cross-kingdom interactions

Cellular communication is crucial for organisms to maintain homeostasis and to respond to various physiological and pathological conditions. Various pathways are involved in cellular communication, such as direct cell contact, molecular transfer, and EV transfer (Munhoz da Rocha, Amatuzzi, Lucena, Faoro, & Alves, 2020). Comprehensive research has been done on host cell-cell interactions through EV uptake and internalisation by various mechanisms resulting in functional cargo transfer or degradation of EV contents. The fate of EVs might be determined by cell-specific ligands/receptors that direct the cellular response. The mode of EV uptake/entry determines the functional impact on the recipient cell, endocytosis is thought to be the most common mode of EV entry into recipient cells, and fusion with cell membrane can result in direct entry of EV into

cytoplasm. EVs could also trigger functional impact without entering recipient cells through ligand/receptor interaction on cell and EV surfaces (Abels & Breakefield, 2016). The main functions of EVs related to cellular communication include gene expression alteration, functional molecular transfer, and cell surface rearrangement (Raeven, Zipperle, & Drechsler, 2018).

The interest in EVs as mediators of cross-kingdom interactions has risen recently. Since dysbiosis is closely linked to CRC, investigating gut microbiome-CRC interactions which are mediated by EVs could clarify the cause of dysbiosis associated with CRC. In 1985, electron microscopy imaging of the gut luminal surface showed a layer of EVs between the microvilli and mucous, suggesting that this EV layer can act as an additional barrier to limit adherence by both commensal and pathogenic bacteria (Hill, 1985). Enteropathogenic infection results in inflammation, epithelial injury and barrier disruption, and immune activation is required at this stage to protect against pathogens and help with barrier integrity restoration. Interestingly, studies showed that epithelial cells-derived EVs can act at a distance in the gut to activate immunity responses, thus limiting bacterial spreading. It was noted that the release of epithelial-EVs increased following infection by protozoan parasite, these EVs carry antimicrobial peptides and were found to bind to the surface of invading pathogens (Hu et al., 2013). Also, EVs were found to have an antifungal property, infection with the human pathogenic fungus *Aspergillus fumigatus* triggered the release of a distinct set of antifungal EVs from polymorphonuclear leukocytes, a type of white blood cell playing a key role in human immunity (Shopova et al., 2020).

It is known that *E. coli* interact with mucosa, by either attaching to the epithelial cells' surface and/or invading the epithelial cells (Kalita, Hu, & Torres, 2014). Data in chapter 3 showed that CRC-derived EV binds to the surface of *E. coli* and attaches to the motility structure of *E. coli* (fimbriae), suggesting physical interactions that could lead to the internalisation of EVs by *E. coli* and delivery of their contents or trigger functional impact through surface binding. Within the gut environment, host EVs have been reported to enter microorganisms altering their gene expression (Lee, 2019), faecal miRNA, which were also present in gut EVs, were taken up by *E. coli* and *F. nucleatum* (Liu et al., 2016). It was also reported that EVs secreted by human airway cells deliver miRNA to bacteria, *P. aeruginosa*, altering their phenotypic characteristics (Koeppen et al., 2021).

Moreover, a study showed the binding of faecal exosomes to the surface of *E. coli* (Kumar, A. et al., 2021). However, the mechanism by which miRNA enters bacteria was not investigated, this project data could propose that binding and interactions of EVs with *E. coli* resulted in miRNA delivery.

Interestingly, exposure of *E. coli* to different cell types-derived EVs, SW480- and SW620-EVs, showed that EVs-*E. coli* interactions are disease-stage specific, interactions with SW620-EVs are greater than SW480-EVs which means that the functional impact of EVs on the bacteria could be higher at later-metastatic stage of CRC. Also, these interactions are microorganisms-specific, the strength of interactions between SW620-EVs and *E. coli* 11G5 is higher than their interactions with *E. coli* MG1655. This *E. coli* strain-specific interactions support the hypothesis that CRC mediate dysbiosis as EVs interaction is higher with the non-pathogenic strain which suggests that these interactions could result in higher impact on the bacterial phenotypic characteristics. Also, these disease-stage-specific interactions could clarify the higher prevalence of pathogenic microbiota at later-metastatic stage of CRC, compared to their prevalence at the early stages of tumour (Russo et al., 2023). Previous proteomic analysis of SW480-EVs and SW620-EVs showed the relative abundance of vesicular proteins varies between SW480-EVs and SW620-EVs (Choi, Dong-Sic et al., 2012), therefore, variations in the strength of *E. coli*-EVs interaction at different stage of the disease could be due to variations in the abundance of specific EV receptor(s) on the surface of SW480-EVs and SW620-EVs that could mediate these cross kingdom interactions.

Various EV protein and glycoprotein receptors were identified as mediators for cell-cell interactions, such as EV surface integrins and glypicans, facilitating EV cellular binding and uptake (Buzás, Tóth, Sódar, & Szabó-Taylor, 2018). Therefore, to investigate potential EV surface receptors mediating the binding of EVs to *E. coli* surfaces facilitating cross-kingdom interactions, EV surface proteins and sugars were enzymatically digested. Treatment of EVs surface proteins and sugars indicated that *E. coli*-EVs interactions are protein-mediated, the loss of flow cytometry signal indicating the *E. coli*-EVs interaction following EVs-surface protein digestion suggesting that EVs-surface proteins mediating the binding of EVs to *E. coli* surfaces. However, glycosylation treatment of EVs had no impact on the *E. coli*-EVs interaction suggesting that EVs surface sugars are not involved in the binding of EVs to *E. coli* surfaces.

Lastly, to further investigate the mode of interactions between *E. coli* and EVs, it was feasible to assess mechanisms by which *E. coli* could be involved in these interactions and data showed that *E. coli* degrades EVs, and this could facilitate the delivery and uptake of EV contents. Similarly, at cell-cell interactions, EVs are degraded once they are taken up by cells to maintain homeostasis of cellular communication. It was reported that the degradation of EVs is an essential step for the release of their content at the cell-cell interactions (Amarasinghe et al., 2023). Revealing that *E. coli* has an impact on the host-EVs integrity further demonstrates host-microbiome interactions through EVs, however, it is still unknown whether different degradation processes are required depending on EVs size and contents, or whether *E. coli* target specific populations of EVs depending on size and EV surface structure.

6.3 CRC-EVs mediate phenotypic alteration of *E. coli*

Many studies have investigated the causative links between the gut microbiota and CRC, revealing the differences in gut composition between patients and healthy individuals, and the mechanisms by which the gut microbiome induces and promotes tumorigenesis. These microbiome alterations have been found at the early stages of CRC, adenoma, therefore they could be used as biomarkers for early CRC detection. Moreover, it was suggested that modulation of the gut microbiome could be considered a new strategy for CRC prevention (Cheng, Ling, & Li, 2020)Given that tumours alter their surrounding microenvironment to promote progression, this suggests that CRC may also shape their surrounding gut microbiota to further induce a dysbiotic and inflamed environment that favours tumour progression. However, the impact of CRC on the gut microbiome has not been investigated yet.

In CRC, proteins, lipids, and miRNAs that are shuttled by EVs among neighbouring cells act as crucial secondary messengers that trigger cellular responses promoting tumour progression, therefore, CRC-EVs could also shuttle their functional cargoes to bacteria and induce functional modulations that contribute to gut dysbiosis associated with CRC. Data in Chapter 4 showed that EVs which are derived from CRC-cell lines, CRC patient's blood, and CRC patient's tissue can alter the phenotypic characteristics of *E. coli*, EVs increased the bacterial growth and significantly decreased the bacterial ability to form biofilm. Under aerobic growth conditions, SW620-EVs significantly increased the growth

of *E. coli* MG1655 but SW480-EVs had no impact on the bacterial growth, also, SW620-EVs induced the bacterial growth after 8 hours of incubation with *E. coli*. However, under anaerobic growth conditions which mimic physiologically relevant conditions, both types of EVs significantly increased the growth of *E. coli* MG1655 with a higher impact on the bacterial growth observed when treated with SW620-EVs. Moreover, these data align with the interaction data that also showed a higher strength of interactions between *E. coli* and SW620-EVs. This suggests that higher interactions between *E. coli* and SW620-EVs could lead to the delivery of a higher dose of functional EV content that triggered the increase in bacterial growth.

However, both types of EVs showed no impact on *E. coli* 11G5 growth under aerobic growth conditions, and only a modest non-significant increase in bacterial growth was observed under anaerobic growth condition due to only SW480-EVs treatment. This strain-specific impact on *E. coli* growth suggests selective mechanisms of CRC which could be linked to the altered gut bacterial structure associated with the disease. Although *E. coli* MG1655 is a non-pathogenic strain, it was reported that the outgrowth of commensal *E. coli* within the gut has been linked to immune-mediated diseases such as IBD (Ellermann & Sperandio, 2020). A previous study has shown that faecal miRNA, which was found to be also enriched in intestinal-derived EVs, increased the growth of *E. coli* (Liu et al., 2016).

Despite the increase in bacterial growth, both types of EVs significantly reduced the ability of *E. coli* MG1655 to form biofilm under aerobic and anaerobic growth conditions with higher impact observed when bacteria were treated with SW620-EVs. Also, both types significantly decreased the ability of *E. coli* 11G5 to form biofilm. Similarly, EVs-miRNA derived from human airway cells reduced the ability of *P. aeruginosa* to form biofilm (Koeppen et al., 2021). Contrarily, a study showed that infection with respiratory syncytial virus increased the release of host-EVs containing host iron-binding protein transferrin that interacts with *P. aeruginosa* biofilm to transfer nutrients promoting bacterial biofilm growth. Therefore, data of this project suggests that EVs could alter the prevalence of bacteria by increasing the total number of planktonic cells and decreasing the total number of biofilm cells. Notably, passaging bacteria with EV treatment showed no impact on *E. coli* growth, and no inhibitory impact on bacterial biofilm formation

ability, indicating that the presence of functional EV cargo is needed to induce functional impact on the bacterial phenotypic characteristics.

Interestingly, EVs from CRC patient's blood and tissue also increase *E. coli* growth and decrease their ability to form biofilm. No differential impact was observed due to blood plasma EVs derived from cancer patients and healthy individuals; blood EVs originate from various resources. Additionally, since all cells release EVs, inter-species communication through host-EVs could not be limited to the gut microbiota, and commensal bacteria which represent an enormous number and range of bacteria could also be affected/regulated by host-EVs. Lastly, EVs from CRC tissue are more representative to the disease, and their functional impact on bacterial growth mirrors the impact of CRC-cell line derived EVs; increased the growth of *E. coli* MG1655 and had no impact on the growth of *E. coli* 11G5. Moreover, the inhibitory impact of tissue-EVs on *E. coli* 11G5 biofilm formation ability is higher than their impact on *E. coli* MG1655.

6.4 CRC- EVs mediate genomic alteration of *E. coli*

To begin to understand the mechanisms by which EVs reduce the bacterial ability to form a biofilm, a causative link between EV binding to the bacterial surface and biofilm formation was investigated first. Data showed that physical binding is not correlated to biofilm formation inhibition, digesting EVs-surface proteins decreased the interaction strength between EVs and *E. coli* but had no change on the bacterial biofilm formation inhibitory impact of EVs, also, both intact and lysed-EVs had an inhibitory impact on the ability of bacteria to form biofilm. This indicates that EVs contents mediate the inhibitory impact on biofilm regardless of EV uptake or physical interaction with *E. coli*.

While EVs carry different types of molecules such as proteins, nucleic acids, and lipids, investigating whether EVs-miRNA contents are mediating the biofilm inhibition impact was the first feasible EV-cargo to be investigated since targeting predictions can be made based miRNA-mRNA interactions suggesting possible mechanisms. Additionally, miRNA associated with various bacterial species are differentially expressed in CRC patients (Yuan, Burns, Subramanian, & Blekhman, 2018), suggesting that CRC may contribute to the altered bacterial structure through host miRNA-mediated communication. Recently, studies started to explore mechanisms by which host miRNA regulates bacterial gene expression, RNA delivery to bacteria through EVs was shown

recently (Koeppen et al., 2021).Therefore, RNA sequencing and alignment analysis were performed, exposure to EV significantly decreased the expression of zinc-ion uptake-related genes, and it is well evident that the zinc-uptake system is crucial for bacterial biofilm formation (Lim et al., 2011).

Alignment analysis determined potential miRNA that could target one of the downregulated zinc-uptake related genes, *zinT*, however, digesting EV-RNA content had no change on the inhibitory impact indicating that EV-miRNA contents are not correlated to the inhibitory impact on the biofilm. Contrarily, a previous study showed that EV deliver miRNA to bacterial resulting in a decrease in proteins essential for biofilm formation in lung infection conditions (Koeppen et al., 2021), and another study predicted, using RNA alignment analysis, that host-miRNA alters bacterial gene expression through targeting genes that are involved in bacterial growth (Kumar, A. et al., 2021). Similar to EV-miRNA, EVs-protein contents are not correlated to the inhibitory impact of EVs on bacterial biofilm as digestion of EVs-protein had no change in the inhibitory impact. However, this result reflects only on proteins that are sensitive to proteinase-k and trypsin digestion, previous studies showed the insensitivity of some EVs-protein content to proteinase-k and trypsin treatment (Choi, Dongsic et al., 2020; Moon et al., 2019; Tang et al., 2019).

One of the potential mechanisms of impact is through the delivery of zinc ions to *E. coli.* Zinc is a crucial element for organisms' homeostasis including humans and bacteria, in humans, it is involved in various physiological processes such as neurotransmission, protein synthesis, and DNA repair. It is tightly regulated, imbalance in zinc metabolism is associated with various diseases such as neurodegenerative diseases (Fan et al., 2024) and CRC (Wan & Zhang, 2022). The intestine is the main site for zinc absorption and excretion and plays a role in the structure and function of the intestinal mucosal barrier (Wan & Zhang, 2022). Notably, EVs contain labile zinc ion which was found to be upregulated under oxidative stress and inflammation (Piacenza et al., 2018). In bacteria, exposure to zinc promotes commensal-to-pathogen transition leading to mucosal inflammation (Wu, T. et al., 2021). Many metals are known to have antimicrobial properties including zinc, it was shown before that zinc could penetrate biofilm to inhibit bacterial growth and subsequently inhibit biofilm formation (Kumar, V. B., Lahav, & Gazit, 2024). Therefore, EVs-zinc content could be the reason for biofilm inhibition and

decrease in expression of zinc-uptake genes. However, this mechanism needs to be validated and detailed process by which this occurs requires further study.

6.5 Future work

This work has shown the interactions between *E. coli*-CRC tumour through EVs. Investigating mechanisms of interactions and identifying potential binding partners between *E. coli* and CRC would facilitate further functional analysis such as blocking these interactions and using EVs as drug delivery entities to bacteria.

In addition, this work revealed the functional impact of CRC-EVs on *E. coli* phenotypic characteristics, such as growth and biofilm. Investigating the impact of EVs on *E. coli* pathogenicity would be a future experiment to assess whether EVs could mediate the commensal-to-pathogen shift associated with the disease. Also, testing interactions and impact of EVs with other bacterial strains which are highly linked to CRC, such as *F. nucleatum*. Since the gut microbiome is complex and dynamic, assessing the impact of EVs on co-culture or multiple bacterial cultures would be more physiologically relevant than a single bacterial culture. Lastly, mechanisms of impact have not been investigated yet, and assessing zinc-mediated EV impact on *E. coli* would reveal a novel mechanism by which EV deliver zinc to *E. coli* altering their phenotypic characteristics.

6.6 Conclusions

To conclude, CRC-EVs interact with *E. coli* in a disease-stage manner, and alter the phenotypic characteristics of *E. coli*, increasing bacterial growth and decreasing their ability to form biofilm. This impact could be mediated through the delivery of zinc to bacteria.

7 Appendices

7.1 Supplementary data

7.1.1 Genomic analysis of *E. coli* strains

Table 7.1: Mutations identified by genomic sequencing across E. coli MG1655

Mutation type	*Ref.*	*Alt.*	*Gene Symbol*
DEL	GCCCCC	GCCCC	betT
SNV	C	T	yfdH

Table 7.2: Mutations identified by genomic sequencing across E. coli 11G

Mutation type	***Ref.***	***Alt.***	***Gene Symbol***
SNV	G	A	aas
SNV	C	T	accC
SNV	T	C	aceA
SNV	A	G	acnA
SNV	T	C	acnA
SNV	C	T	acnA
SNV	C	T	acnA
SNV	T	G	acnA
SNV	T	C	acnA
SNV	C	T	acrR
SNV	C	G	actP
SNV	G	A	actP
SNV	T	C	actP
SNV	T	C	actP
SNV	G	A	actP
SNV	C	T	actP
SNV	A	C	actP
SNV	G	A	actP
SNV	C	A	actP
SNV	A	G	actP
SNV	A	T	agaR
SNV	T	C	agaS
SNV	A	G	agaS
SNV	A	C	agaS
SNV	A	G	agaS
SNV	G	A	agaS
SNV	A	G	agaS
SNV	A	G	allC
SNV	A	G	allC
SNV	C	T	alr
SNV	T	C	alr
SNV	A	G	amiD
SNV	T	C	amiD
SNV	A	G	amiD
SNV	T	G	amn
SNV	C	T	amn
SNV	G	T	amn
SNV	C	G	amn
SNV	C	T	amn
SNV	T	A	amn
SNV	G	A	amn
SNV	C	T	amn
SNV	T	C	amn
SNV	T	C	ampD
SNV	T	C	ampD
SNV	G	A	ampG
SNV	T	C	ampG
SNV	G	A	ampG
SNV	T	C	arcB
SNV	A	G	arcB
SNV	G	A	arcB
SNV	G	A	arcB
SNV	T	C	argB
SNV	C	A	argB
SNV	A	T	argB
SNV	C	T	argH
SNV	C	T	arnB
SNV	T	G	arnB
SNV	G	A	arnB
SNV	T	G	arnB
SNV	G	A	arnB
SNV	A	G	arnB
SNV	T	C	aroA
SNV	G	A	aroL
SNV	C	T	aroL
SNV	G	A	aroM
SNV	T	C	aroM
SNV	T	C	aroM
SNV	C	A	aroM
SNV	C	T	aroM
SNV	T	A	aroM
SNV	G	A	aroM
SNV	T	C	aroM
SNV	T	A	aroM
SNV	A	G	aroM
SNV	T	C	aroM
SNV	C	T	aroP
SNV	T	G	aroP
SNV	G	T	artQ
SNV	A	G	artQ
SNV	T	G	artQ
SNV	C	T	artQ
SNV	T	G	ascG
SNV	G	A	ascG
SNV	C	T	ascG
SNV	G	C	ascG
SNV	G	A	ascG
SNV	T	G	ascG
SNV	G	A	aslA
SNV	C	T	aslA
SNV	A	G	aslA
SNV	G	A	aslA

SNV	T	C	aslB
SNV	T	G	asnB
SNV	A	C	aspC
SNV	A	G	aspC
SNV	A	G	aspS
SNV	G	C	astC
SNV	T	C	astC
SNV	C	A	astC
SNV	G	A	atoC
SNV	T	C	atoS
SNV	C	T	atoS
SNV	T	C	atoS
SNV	C	A	atoS
SNV	C	T	atoS
SNV	T	C	atoS
SNV	A	G	bcsA
SNV	G	A	bcsA
SNV	T	C	bcsA
SNV	T	C	bcsA
SNV	C	T	bcsA
SNV	G	A	bcsA
SNV	C	A	bcsA
SNV	T	C	bcsA
SNV	C	G	bcsA
SNV	C	T	bcsA
SNV	T	C	bcsB
SNV	C	A	bcsB
SNV	T	C	bcsB
SNV	T	C	bcsB
SNV	A	G	bcsB
SNV	C	G	bcsB
SNV	G	A	bcsE
SNV	T	C	bcsE
SNV	G	A	bcsE
SNV	T	C	bcsE
SNV	C	T	bglB
SNV	A	G	bglB
SNV	G	A	bglB
SNV	C	T	bglB
SNV	G	A	bglB
SNV	G	T	bglB
SNV	G	A	bglB
SNV	A	C	bglB
SNV	C	T	bglB
SNV	T	C	bglB
SNV	A	G	bglB
SNV	T	C	bglF
SNV	T	A	bglF
SNV	C	T	bglF
SNV	G	A	bglF
SNV	G	T	bglF
SNV	C	A	bglF
SNV	G	A	bglF
SNV	C	T	bglF
SNV	C	T	btuB
SNV	A	G	btuB
SNV	C	T	btuB
SNV	C	T	btuB
SNV	A	C	caiE
SNV	A	G	caiE
SNV	T	C	caiE
SNV	A	G	carB
SNV	C	T	carB
SNV	A	G	ccmH
SNV	C	T	ccmH
SNV	G	A	cdaR
SNV	A	G	cdaR
SNV	A	G	cdaR
SNV	C	T	cdaR
SNV	T	C	cdaR
SNV	A	G	cfa
SNV	A	G	cheB
SNV	C	T	cheZ
SNV	C	G	chiA
SNV	C	T	chiA
SNV	A	G	chiA
SNV	C	T	chiA
SNV	G	A	clcB
SNV	C	T	clcB
SNV	T	C	clcB
SNV	G	T	clcB
SNV	G	A	clsB
SNV	A	G	clsB
SNV	T	A	clsB
SNV	C	T	clsB
SNV	A	G	clsB
SNV	A	G	clsB
SNV	G	A	clsB
SNV	A	G	clsB
SNV	A	T	clsB
SNV	T	C	clsB
SNV	A	T	clsB
SNV	G	A	cobS
SNV	C	T	codB
SNV	T	C	codB
SNV	C	T	codB
SNV	T	C	codB
SNV	T	C	comR

SNV	C	T	corA
SNV	A	G	cpdB
SNV	C	T	cpxA
SNV	T	G	cpxA
SNV	C	T	cstA
SNV	T	C	cstA
SNV	C	T	cstA
SNV	A	G	cstA
SNV	C	T	cstA
SNV	C	T	cstA
SNV	G	C	cstA
SNV	C	T	cstA
SNV	T	C	cstA
SNV	A	G	cstA
SNV	G	T	cstA
SNV	T	G	cstA
SNV	G	A	cstA
SNV	A	G	cstA
SNV	A	G	cstA
SNV	C	T	cstA
SNV	C	G	cstA
SNV	C	T	cstA
SNV	C	G	cstA
SNV	C	T	cueO
SNV	T	C	cusA
SNV	C	T	cusA
SNV	C	T	cusA
SNV	C	G	cusA
SNV	T	C	cusA
SNV	G	A	cusA
SNV	C	T	cusA
SNV	G	A	cusA
SNV	T	G	cusA
SNV	A	G	cusA
SNV	C	A	cusA
SNV	A	G	cusA
SNV	C	T	cusA
SNV	T	C	cusA
SNV	C	T	cusA
SNV	C	T	cusA
SNV	G	T	cusC
SNV	G	A	cusC
SNV	T	C	cusC
SNV	A	G	cusC
SNV	C	A	cyoB
SNV	A	G	dcuS
SNV	A	G	dcuS
SNV	A	G	dcuS
SNV	G	A	deaD
SNV	A	G	degP
SNV	G	A	degP
SNV	T	C	degP
SNV	T	C	dgcE
SNV	G	A	dgcE
SNV	C	T	dgcI
SNV	G	A	dgcI
SNV	G	T	dgcI
SNV	A	G	dgcI
SNV	A	G	dgcQ
SNV	T	C	dgcQ
SNV	A	G	dgt
SNV	C	T	dgt
SNV	A	C	dgt
SNV	A	G	diaA
SNV	T	A	diaA
SNV	C	T	diaA
SNV	G	A	diaA
SNV	C	T	diaA
SNV	T	C	diaA
SNV	T	A	diaA
SNV	G	T	dnaE
SNV	C	T	dnaE
SNV	C	T	dnaE
SNV	G	A	dnaE
SNV	C	G	dnaN
SNV	A	G	dnaN
SNV	A	G	dosP
SNV	C	T	dosP
SNV	G	T	dosP
SNV	T	C	dpiA
SNV	G	A	dppA
SNV	T	C	dppA
SNV	A	G	dppA
SNV	A	G	dppA
SNV	G	A	dppC
SNV	A	G	dppC
SNV	C	T	dppC
SNV	G	A	dsbG
SNV	A	G	dsbG
SNV	A	G	dtpB
SNV	C	A	dtpD
SNV	C	T	dtpD
SNV	G	A	dtpD
SNV	T	C	dtpD
SNV	C	T	dtpD
SNV	A	G	dtpD
SNV	C	T	dusA
SNV	C	T	dusA

SNV	T	C	dusA
SNV	C	T	dusA
SNV	G	T	dusA
SNV	C	T	dusA
SNV	G	T	ebgA
SNV	G	A	ebgA
SNV	A	G	ebgA
SNV	T	C	ebgA
SNV	T	C	ebgA
SNV	C	A	ebgA
SNV	C	T	ebgA
SNV	C	T	ebgA
SNV	T	C	ebgA
SNV	T	C	ecpC
SNV	C	T	ecpC
SNV	C	T	efeO
SNV	T	C	efeO
SNV	T	A	emrK
SNV	T	G	entB
SNV	G	A	entB
SNV	G	A	entB
SNV	C	T	entB
SNV	T	C	epd
SNV	G	A	epd
SNV	G	A	epd
SNV	A	T	epd
SNV	T	C	eptA
SNV	T	C	eptA
SNV	A	G	eptA
SNV	C	T	eptA
SNV	C	T	eptA
SNV	G	A	eptA
SNV	A	G	eptA
SNV	A	G	eptA
SNV	G	C	eptA
SNV	C	T	eptA
SNV	G	A	eptA
SNV	A	G	eptA
SNV	A	G	eptA
SNV	A	G	eptA
SNV	A	G	eptA
SNV	T	C	eptC
SNV	G	A	eptC
SNV	T	C	eptC
SNV	T	C	eptC
SNV	A	G	eptC
SNV	A	C	eptC
SNV	G	A	eptC
SNV	G	A	eptC
SNV	C	T	eptC

SNV	C	T	eptC
SNV	A	G	eptC
SNV	T	C	eptC
SNV	A	G	eptC
SNV	A	G	eptC
SNV	A	T	eptC
SNV	A	C	eutB
SNV	G	A	eutB
SNV	C	T	eutQ
SNV	A	G	eutQ
SNV	T	A	exoX
SNV	T	G	exuT
SNV	A	C	exuT
SNV	C	T	exuT
SNV	C	T	exuT
SNV	G	A	fabB
SNV	A	T	fabB
SNV	G	T	fabB
SNV	T	A	fabB
SNV	T	C	fabB
SNV	A	G	fadB
SNV	G	A	fadB
SNV	G	A	fadB
SNV	G	A	fadB
SNV	C	G	fadB
SNV	G	A	fadB
SNV	A	G	fadB
SNV	A	G	fadB
SNV	A	G	fadB
SNV	G	A	fadE
SNV	T	C	fadE
SNV	A	G	fadE
SNV	A	T	fadE
SNV	T	C	fadE
SNV	T	C	fadJ
SNV	G	A	fadJ
SNV	A	C	fadJ
SNV	C	T	fadJ
SNV	G	A	fadJ
SNV	T	G	fadJ
SNV	C	T	fadJ
SNV	A	G	fadJ
SNV	T	C	fadJ
SNV	A	T	fadJ
SNV	G	A	fadJ
SNV	A	G	fadJ
SNV	A	G	fadJ
SNV	A	G	fadJ
SNV	G	A	fadJ

SNV	A	C	fadJ
SNV	G	A	fadJ
SNV	G	T	fadJ
SNV	C	A	fadJ
SNV	T	G	fadJ
SNV	A	G	fbaB
SNV	A	G	fdoG
SNV	T	C	fdoG
SNV	C	T	fdoG
SNV	G	A	fdoG
SNV	G	A	fdoH
SNV	A	G	fdoH
SNV	G	A	fdoH
SNV	G	A	fes
SNV	T	C	fhuE
SNV	T	C	fhuE
SNV	G	A	fhuE
SNV	A	G	fimD
SNV	C	T	fimD
SNV	A	G	fimD
SNV	C	T	fimD
SNV	C	T	fimD
SNV	A	T	flgE
SNV	C	A	flgE
SNV	G	C	flgE
SNV	C	T	flgE
SNV	A	G	flgE
SNV	G	A	flgE
SNV	C	T	flgE
SNV	C	T	flgE
SNV	C	T	flgE
SNV	A	G	flgI
SNV	A	T	flgI
SNV	A	G	flgI
SNV	T	C	flgI
SNV	C	T	flgI
SNV	A	T	flgI
SNV	C	T	flgI
SNV	T	C	flgJ
SNV	G	T	flgJ
SNV	G	A	flgJ
SNV	C	T	flgJ
SNV	G	A	flgJ
SNV	C	T	fliD
SNV	T	C	fliF
SNV	G	A	fliF
SNV	G	A	fliF
SNV	C	T	fliF
SNV	C	T	fliF
SNV	A	C	fliF
SNV	A	G	fliF
SNV	A	G	fliF
SNV	T	G	fliF
SNV	T	C	flk
SNV	G	A	flk
SNV	T	C	frwB
SNV	T	C	frwC
SNV	C	T	fryA
SNV	T	C	fryA
SNV	G	A	fryA
SNV	G	A	fryA
SNV	A	T	fryA
SNV	G	A	ftsH
SNV	A	T	ftsH
SNV	C	T	ftsH
SNV	C	T	ftsP
SNV	C	T	ftsP
SNV	G	A	ftsP
SNV	G	A	ftsP
SNV	T	A	ftsP
SNV	G	A	ftsP
SNV	A	G	ftsY
SNV	C	A	ftsY
SNV	C	T	fucA
SNV	A	G	fucO
SNV	A	C	fucO
SNV	C	T	fucO
SNV	G	A	fucO
SNV	C	T	fucO
SNV	C	T	fucO
SNV	A	C	fucO
SNV	G	A	fucO
SNV	A	C	fucO
SNV	A	G	fumB
SNV	A	G	fumB
SNV	G	T	fumB
SNV	G	T	gabP
SNV	C	T	gabP
SNV	T	C	gabP
SNV	A	G	gabP
SNV	A	G	galF
SNV	G	T	galF
SNV	A	C	galF
SNV	C	T	galF
SNV	G	A	galF
SNV	G	A	galF
SNV	G	A	galF
SNV	A	T	galF

SNV	C	T	galF
SNV	T	C	galF
SNV	C	A	galF
SNV	A	G	gcvP
SNV	G	A	gcvP
SNV	A	G	gcvP
SNV	G	A	gcvP
SNV	G	A	gcvP
SNV	G	A	ghxQ
SNV	T	C	ghxQ
SNV	A	G	ghxQ
SNV	G	A	glaR
SNV	C	T	glaR
SNV	G	T	glaR
SNV	C	T	glaR
SNV	T	C	glcB
SNV	A	G	glcB
SNV	G	A	glcB
SNV	T	C	glcB
SNV	A	G	glcB
SNV	T	C	glcB
SNV	T	C	glcE
SNV	C	G	glcE
SNV	C	T	glcE
SNV	G	A	glcE
SNV	A	G	glgP
SNV	T	C	glgP
SNV	T	G	glgP
SNV	C	T	glgP
SNV	A	G	glgP
SNV	A	G	glgP
SNV	T	C	glgP
SNV	A	C	glgP
SNV	A	G	glmS
SNV	A	G	glmS
SNV	T	G	glmS
SNV	T	C	glmS
SNV	C	G	glmS
SNV	T	C	glmS
SNV	T	C	glmS
SNV	C	A	glmS
SNV	G	A	glmS
SNV	G	T	glmS
SNV	C	T	glnS
SNV	T	C	glnS
SNV	G	A	glnS
SNV	T	C	glnS
SNV	T	C	glnS
SNV	T	C	glpF
SNV	G	A	glpF
SNV	A	T	glsA
SNV	T	A	glsA
SNV	A	T	glsA
SNV	A	G	glsA
SNV	C	T	glsA
SNV	C	T	gltA
SNV	G	A	gltA
SNV	T	C	gmhA
SNV	T	C	gmhA
SNV	A	G	gnd
SNV	T	A	gnd
SNV	A	C	gnd
SNV	A	G	gnd
SNV	G	C	gnd
SNV	C	T	gnd
SNV	T	C	gnd
SNV	A	G	gnd
SNV	T	C	gnd
SNV	A	G	gnd
SNV	A	T	gnd
SNV	A	G	gnd
SNV	A	T	gnd
SNV	C	T	gnd
SNV	G	A	gnd
SNV	G	A	gpmM
SNV	G	A	gpmM
SNV	A	C	gpsA
SNV	G	T	gpsA
SNV	G	A	gpsA
SNV	A	G	gpsA
SNV	C	T	gpsA
SNV	A	G	gpsA
SNV	T	C	gshA
SNV	T	C	gsiB
SNV	A	G	gsiB
SNV	G	A	gsiB
SNV	A	T	gsiB
SNV	T	C	gsk
SNV	T	C	gsk
SNV	T	C	gsk
SNV	T	A	gspI
SNV	G	A	gspI
SNV	T	C	guaB
SNV	G	A	guaB
SNV	A	C	guaB
SNV	A	G	guaB
SNV	C	G	guaB
SNV	G	A	guaB

SNV	A	G	guaB
SNV	A	G	guaB
SNV	G	A	gyrA
SNV	A	G	gyrA
SNV	C	T	gyrA
SNV	C	G	hcp
SNV	C	T	hcp
SNV	T	C	helD
SNV	C	T	helD
SNV	T	C	helD
SNV	G	A	helD
SNV	G	A	helD
SNV	C	T	helD
SNV	A	G	helD
SNV	T	C	helD
SNV	A	G	helD
SNV	A	T	helD
SNV	G	A	helD
SNV	A	T	hemA
SNV	T	C	hemA
SNV	G	A	hemC
SNV	T	G	hemC
SNV	A	G	hemC
SNV	A	C	hemC
SNV	T	C	hemN
SNV	C	T	hemN
SNV	T	C	hemN
SNV	T	A	hflK
SNV	T	C	hisA
SNV	T	C	hisA
SNV	G	A	hisA
SNV	T	C	hisA
SNV	G	T	hisA
SNV	G	T	hisA
SNV	T	A	hisA
SNV	C	T	hisA
SNV	G	A	hisD
SNV	C	T	hisF
SNV	G	A	hisS
SNV	A	G	hisS
SNV	A	G	hisS
SNV	C	A	hisS
SNV	C	T	hofB
SNV	T	C	hprR
SNV	C	T	hprS
SNV	T	A	hprS
SNV	T	C	hprS
SNV	A	G	hprS
SNV	G	A	hprS
SNV	C	G	hprS
SNV	C	T	hprS
SNV	C	A	hrpA
SNV	T	C	hrpA
SNV	G	A	hrpA
SNV	A	T	hsrA
SNV	T	A	hsrA
SNV	T	C	hsrA
SNV	A	G	hsrA
SNV	A	C	hsrA
SNV	G	A	hyaF
SNV	A	C	hyaF
SNV	G	A	hyaF
SNV	T	C	hyaF
SNV	A	T	hyaF
SNV	G	A	hyaF
SNV	A	G	hybB
SNV	A	G	hybB
SNV	G	A	hycC
SNV	T	C	hycC
SNV	C	T	hycC
SNV	A	G	hycE
SNV	A	G	hycE
SNV	A	G	iclR
SNV	A	G	iclR
SNV	T	A	iclR
SNV	A	G	iclR
SNV	C	T	ileS
SNV	T	C	ileS
SNV	C	T	ileS
SNV	C	T	ileS
SNV	C	T	ileS
SNV	C	T	ileS
SNV	A	G	ileS
SNV	C	T	ilvB
SNV	T	C	ilvB
SNV	G	A	ilvB
SNV	A	G	ilvB
SNV	G	A	ilvB
SNV	A	G	ilvB
SNV	G	A	ilvB
SNV	G	T	ilvB
SNV	G	A	ispH
SNV	C	T	ispH
SNV	C	T	ispH
SNV	A	G	ispH
SNV	T	C	ispH
SNV	T	C	kbaY

SNV	A	G	kbaY
SNV	G	A	kdgK
SNV	A	G	kdgK
SNV	C	A	kdgK
SNV	G	T	kdgK
SNV	G	A	kdgK
SNV	T	C	kdgK
SNV	A	G	kdgR
SNV	C	T	kefC
SNV	G	A	kefC
SNV	G	A	kefC
SNV	A	G	kefC
SNV	T	C	kefF
SNV	C	A	kup
SNV	C	T	kup
SNV	G	C	kup
SNV	T	C	lamB
SNV	C	T	letB
SNV	C	T	leuO
SNV	A	G	leuO
SNV	C	T	leuO
SNV	A	G	leuO
SNV	A	G	leuO
SNV	T	C	leuO
SNV	G	C	ligA
SNV	C	T	lldP
SNV	A	G	loiP
SNV	C	T	loiP
SNV	C	A	loiP
SNV	C	A	loiP
SNV	T	C	loiP
SNV	G	A	loiP
SNV	C	T	loiP
SNV	A	G	loiP
SNV	C	T	lpoB
SNV	C	A	lpoB
SNV	C	A	lpoB
SNV	T	C	lptD
SNV	A	C	lptD
SNV	A	T	lptD
SNV	A	G	lptD
SNV	G	T	lptD
SNV	C	T	lptD
SNV	C	T	lptD
SNV	G	A	lptD
SNV	A	G	lptD
SNV	C	T	lptD
SNV	C	T	lptD
SNV	T	C	lptD
SNV	A	G	lptD
SNV	A	C	lptD
SNV	G	A	lptD
SNV	T	C	lptD
SNV	A	G	lptD
SNV	T	C	lptD
SNV	G	A	lptD
SNV	A	T	lptD
SNV	T	C	lptD
SNV	T	C	lptD
SNV	G	A	lptD
SNV	A	G	lptD
SNV	T	C	lptD
SNV	G	T	lptD
SNV	T	G	lptD
SNV	T	C	lptD
SNV	G	A	lptD
SNV	A	G	lptD
SNV	G	A	lptD
SNV	T	C	lptD
SNV	A	T	lptD
SNV	G	A	lptD
SNV	A	G	lptD
SNV	T	C	lptD
SNV	A	G	lptD
SNV	A	G	lptD
SNV	G	C	lptD
SNV	C	T	lptF
SNV	A	G	lptF
SNV	T	C	lpxL
SNV	C	A	lpxP
SNV	A	G	lpxP
SNV	A	G	lpxP
SNV	T	C	lpxP
SNV	G	A	lpxP
SNV	C	T	lysA
SNV	T	C	lysA
SNV	G	A	lysA
SNV	G	A	lysA
SNV	A	C	lysC
SNV	C	T	lysC
SNV	A	G	lysC
SNV	C	T	lysC
SNV	C	T	lysP
SNV	A	T	lysP
SNV	G	A	lysP
SNV	G	A	lysP
SNV	A	C	lysP

SNV	G	A	lysS
SNV	G	A	lysS
SNV	A	C	maeB
SNV	G	C	maeB
SNV	A	G	map
SNV	A	G	map
SNV	G	A	mdtB
SNV	C	T	mdtB
SNV	T	C	mdtB
SNV	A	G	mdtB
SNV	C	A	mdtB
SNV	T	C	mdtK
SNV	T	C	mdtK
SNV	C	A	mdtK
SNV	G	A	mdtK
SNV	G	A	mdtK
SNV	A	G	mdtO
SNV	T	A	mdtO
SNV	T	C	mdtO
SNV	C	T	mdtO
SNV	G	T	metA
SNV	C	T	metA
SNV	A	G	mglC
SNV	G	A	mglC
SNV	A	G	mglC
SNV	T	C	mgtA
SNV	G	A	mltA
SNV	A	G	mltB
SNV	G	A	mltB
SNV	C	T	mltG
SNV	T	G	mltG
SNV	T	C	mltG
SNV	C	T	mltG
SNV	A	G	mnmA
SNV	T	G	mnmA
SNV	A	G	mnmA
SNV	G	A	mnmA
SNV	C	T	mnmA
SNV	A	G	mnmA
SNV	C	T	mnmG
SNV	T	C	mnmG
SNV	T	C	moeB
SNV	G	A	mrdB
SNV	A	G	mrdB
SNV	C	T	mrdB
SNV	A	G	mrdB
SNV	A	T	mscK
SNV	G	A	mscK
SNV	A	G	mscK
SNV	C	T	mscK
SNV	C	T	mscK
SNV	T	C	mscS
SNV	G	A	mscS
SNV	G	T	mscS
SNV	A	G	mscS
SNV	A	T	mscS
SNV	A	T	mscS
SNV	A	G	mtr
SNV	T	C	mtr
SNV	C	T	mtr
SNV	G	C	mtr
SNV	A	G	mtr
SNV	A	G	mtr
SNV	C	T	mukF
SNV	A	G	mukF
SNV	T	C	mukF
SNV	T	C	murE
SNV	C	T	murE
SNV	T	C	murE
SNV	C	T	murE
SNV	A	G	murE
SNV	G	T	murE
SNV	T	C	NA
SNV	C	T	NA
SNV	T	C	NA
SNV	T	C	NA
SNV	A	G	NA
SNV	G	C	NA
SNV	C	T	NA
SNV	T	C	NA
SNV	C	T	NA
SNV	T	C	NA
SNV	C	A	NA
SNV	T	C	NA
SNV	G	A	NA
SNV	A	G	NA
SNV	A	G	NA
SNV	T	C	NA
SNV	T	G	NA
DEL	ACCC	ACC	NA
DEL	CTTTTT	CTTTT	NA
SNV	G	A	NA
SNV	A	C	NA
SNV	A	G	NA
SNV	C	G	NA
SNV	C	A	NA
SNV	C	T	NA
SNV	G	A	NA

SNV	A	G	NA
SNV	A	G	NA
SNV	G	A	NA
SNV	G	A	NA
SNV	G	A	NA
SNV	C	T	NA
SNV	G	C	NA
SNV	G	A	NA
SNV	C	T	NA
SNV	C	T	NA
SNV	C	T	NA
SNV	C	G	NA
SNV	T	G	NA
SNV	T	G	NA
SNV	G	A	NA
SNV	C	T	NA
SNV	T	C	NA
SNV	C	T	NA
SNV	G	A	NA
SNV	T	G	NA
SNV	T	G	NA
SNV	G	A	NA
SNV	C	G	NA
SNV	A	G	NA
SNV	A	T	NA
SNV	A	G	NA
SNV	C	A	NA
SNV	T	C	NA
SNV	G	T	NA
SNV	A	G	NA
SNV	G	A	NA
SNV	C	T	NA
SNV	C	T	NA
SNV	C	G	NA
SNV	T	G	NA
SNV	G	C	NA
SNV	C	G	NA
SNV	A	T	NA
SNV	T	C	NA
SNV	G	A	NA
SNV	T	C	NA
SNV	A	T	NA
SNV	T	A	NA
SNV	A	G	nadB
SNV	G	A	nadB
SNV	G	A	nadB
SNV	A	T	nagA
SNV	G	A	nagA
SNV	T	C	nagK
SNV	G	C	nagK
SNV	C	T	nagK
SNV	T	C	napA
SNV	T	G	napA
SNV	G	A	narG
SNV	A	G	narG
SNV	C	T	narG
SNV	C	T	narG
SNV	A	G	narG
SNV	C	T	narG
SNV	C	T	narG
SNV	C	T	narG
SNV	T	C	narG
SNV	A	G	narG
SNV	C	T	narG
SNV	T	C	narG
SNV	G	T	narG
SNV	A	G	narG
SNV	A	G	narY
SNV	A	G	narY
SNV	T	C	narY
SNV	G	A	narY
SNV	T	C	narY
SNV	G	T	narY
SNV	T	A	narZ
SNV	G	A	nemA
SNV	A	G	nemA
SNV	T	C	nemA
SNV	G	T	nemA
SNV	A	G	nemA
SNV	T	C	nemA
SNV	G	A	nemA
SNV	G	A	nemA
SNV	T	A	nfrA
SNV	C	A	nfrA
SNV	T	C	nfrA
SNV	G	A	nfrA
SNV	G	T	nfrA
SNV	T	C	nfrA
SNV	C	T	nirC
SNV	G	C	nirC
SNV	T	A	nnr
SNV	C	T	nnr
SNV	T	C	nnr
SNV	G	T	nnr
SNV	T	C	nnr
SNV	G	A	nnr
SNV	T	C	nrdB
SNV	C	T	nrdB

SNV	C	T	nrdB
SNV	T	C	nrdB
SNV	T	C	nrdE
SNV	G	T	nrdE
SNV	A	G	nrdE
SNV	C	T	nrdE
SNV	C	T	nrfB
SNV	G	A	nuoC
SNV	A	G	nuoC
SNV	G	A	nuoC
SNV	A	G	nuoC
SNV	A	G	nuoC
SNV	A	G	nuoC
SNV	G	A	nuoC
SNV	C	A	nuoC
SNV	A	G	nuoC
SNV	T	C	nuoL
SNV	G	A	nuoL
SNV	G	A	nuoL
SNV	C	G	nuoL
SNV	G	T	nusA
SNV	A	G	nusA
SNV	G	A	nusA
SNV	A	T	nusA
SNV	G	A	nusA
SNV	C	G	obgE
SNV	G	A	obgE
SNV	T	C	opgE
SNV	A	C	opgE
SNV	T	C	opgE
SNV	A	C	oppB
SNV	C	T	oppB
SNV	C	T	oppB
SNV	C	T	oppB
SNV	A	G	oppB
SNV	T	A	oxc
SNV	G	A	oxc
SNV	T	C	pabB
SNV	T	C	pabB
SNV	A	G	panB
SNV	A	G	panB
SNV	T	C	panB
SNV	C	T	panB
SNV	T	C	panB
SNV	A	G	panB
SNV	C	T	panB
SNV	C	T	panB
SNV	T	G	panB
SNV	A	G	panB

SNV	T	A	panB
SNV	T	A	panB
SNV	C	A	parC
SNV	G	A	parC
SNV	G	A	patA
SNV	T	C	patA
SNV	A	G	patA
SNV	G	A	patA
SNV	C	G	patA
SNV	C	T	patA
SNV	G	T	patA
SNV	T	C	patA
SNV	G	A	patA
SNV	A	G	patA
SNV	A	G	patA
SNV	C	T	patA
SNV	C	T	patZ
SNV	G	A	patZ
SNV	T	G	patZ
SNV	T	C	patZ
SNV	A	G	patZ
SNV	C	T	pck
SNV	A	G	pck
SNV	G	A	pck
SNV	T	C	pck
SNV	A	G	pck
SNV	C	T	pck
SNV	T	C	pcnB
SNV	G	A	pcnB
SNV	C	G	pcnB
SNV	G	A	pcnB
SNV	C	T	pcnB
SNV	T	C	pcnB
SNV	T	G	pcnB
SNV	T	C	pcnB
SNV	G	A	pcnB
SNV	C	G	pcnB
SNV	C	T	pcnB
SNV	A	G	pcnB
SNV	C	T	pdeF
SNV	A	C	pdeK
SNV	G	T	pdeN
SNV	C	A	pdeN
SNV	G	T	pdeN
SNV	C	T	pdeN
SNV	G	A	pdeN
SNV	G	T	pdeN
SNV	A	G	pdeN
SNV	A	G	pdeN

SNV	G	A	pdeN
SNV	T	C	pdeN
SNV	C	T	pdeN
SNV	C	A	pdeN
SNV	C	T	pdeN
SNV	G	A	pdeN
SNV	G	A	pdeN
SNV	G	A	pdeN
SNV	C	T	pdeN
SNV	A	G	pdeN
SNV	A	G	pdxA
SNV	C	A	pdxB
SNV	C	T	pepA
SNV	A	G	pepA
SNV	T	G	pepA
SNV	C	T	pepA
SNV	G	A	pepA
SNV	T	C	pepA
SNV	A	G	pepA
SNV	C	T	pepA
SNV	A	C	pepA
SNV	T	C	pflC
SNV	T	C	pflC
SNV	C	T	pflD
SNV	C	T	pflD
SNV	A	G	pflD
SNV	A	G	pflD
SNV	G	A	pflD
SNV	A	T	pgaA
SNV	T	C	pgaA
SNV	C	G	pgl
SNV	T	C	pgrR
SNV	T	C	pheT
SNV	G	A	pheT
SNV	A	G	pheT
SNV	T	C	pheT
SNV	C	A	pheT
SNV	G	A	pheT
SNV	G	A	pheT
SNV	G	A	pheT
SNV	A	C	pheT
SNV	G	A	pheT
SNV	A	G	pheT
SNV	C	A	pheT
SNV	C	A	pheT
SNV	A	G	pheT
SNV	G	A	pheT
SNV	G	A	phnJ
SNV	A	G	phnJ
SNV	G	A	phnJ
SNV	C	G	phnJ
SNV	C	T	phnJ
SNV	C	A	phoA
SNV	A	G	phoA
SNV	C	G	phoB
SNV	A	G	phoB
SNV	G	A	phoB
SNV	A	G	php
SNV	T	C	php
SNV	C	T	plsB
SNV	A	G	plsB
SNV	A	C	pnp
SNV	G	A	pnp
SNV	A	G	pnp
SNV	G	T	pnp
SNV	G	A	potA
SNV	G	C	potA
SNV	T	C	potG
SNV	T	G	potG
SNV	C	T	potG
SNV	T	C	potG
SNV	C	T	potG
SNV	T	C	potG
SNV	C	T	potG
SNV	A	T	potG
SNV	C	T	potG
SNV	C	T	potG
SNV	C	T	potG
SNV	G	T	potG
SNV	T	C	potG
SNV	C	T	potG
SNV	G	A	potG
SNV	C	T	potG
SNV	G	A	potG
SNV	C	T	potG
SNV	T	C	potG
SNV	G	A	potG
SNV	C	T	potG
SNV	T	C	potG
SNV	G	A	potG
SNV	T	C	ppc
SNV	G	A	ppc
SNV	C	T	ppc
SNV	T	C	ppc
SNV	G	A	ppc
SNV	C	T	ppdD
SNV	T	C	ppiD
SNV	T	C	ppiD

SNV	C	T	ppiD
SNV	C	T	ppsA
SNV	A	G	ppsA
SNV	A	G	ppsA
SNV	G	A	ppsA
SNV	T	C	ppsA
SNV	A	G	ppsA
SNV	C	G	ppsA
SNV	G	A	ppsA
SNV	T	A	ppsA
SNV	C	G	ppsA
SNV	C	A	pqqL
SNV	T	A	pqqL
SNV	C	T	pqqL
SNV	T	C	preA
SNV	T	C	preA
SNV	C	T	preA
SNV	G	A	preA
SNV	G	T	preA
SNV	C	T	prfB
SNV	G	A	prfB
SNV	A	G	prfB
SNV	T	A	prfB
SNV	A	G	prlC
SNV	T	C	prlC
SNV	A	G	prlC
SNV	C	T	prmA
SNV	G	T	prmA
SNV	C	T	prmA
SNV	A	G	prmA
SNV	A	G	prmA
SNV	T	A	prmA
SNV	T	C	prmA
SNV	C	T	prmA
SNV	T	C	prmA
SNV	C	T	prmA
SNV	A	G	prpB
SNV	G	A	prpB
SNV	C	T	pssA
SNV	A	G	pstB
SNV	C	T	pstB
SNV	T	C	pstC
SNV	A	T	pta
SNV	T	C	pta
SNV	A	G	pth
SNV	A	T	pth
SNV	A	G	ptsP
SNV	A	G	purA
SNV	G	T	purA
SNV	T	C	purA
SNV	A	G	purA
SNV	T	C	purT
SNV	A	C	purT
SNV	T	C	purT
SNV	G	A	pxpB
SNV	C	T	pxpB
SNV	G	A	pxpB
SNV	G	C	pxpB
SNV	T	C	pyrG
SNV	G	A	pyrG
SNV	A	G	pyrG
SNV	G	A	pyrG
SNV	G	T	pyrG
SNV	G	A	pyrG
SNV	A	G	pyrG
SNV	C	T	qseC
SNV	T	C	qseC
SNV	A	G	qseC
SNV	T	C	qseC
SNV	T	C	rapA
SNV	A	G	rapA
SNV	T	C	rapA
SNV	A	C	rbbA
SNV	T	C	rbbA
SNV	G	C	rbbA
SNV	G	A	rbbA
SNV	A	G	rcdA
SNV	A	G	rcdB
SNV	G	A	rcdB
SNV	A	G	rcdB
SNV	C	T	rcdB
SNV	A	G	rcsC
SNV	C	T	rcsC
SNV	C	A	rcsC
SNV	C	T	rcsC
SNV	T	C	rcsD
SNV	T	A	rcsD
SNV	C	T	rcsD
SNV	A	C	rcsD
SNV	T	C	rcsD
SNV	C	G	rcsD
SNV	A	G	rcsD
SNV	G	A	rdcA
SNV	C	T	rdcA
SNV	C	T	rdcA
SNV	G	A	rdcA
SNV	G	A	recB
SNV	A	G	recB

SNV	G	A	recC
SNV	T	C	recC
SNV	C	T	recN
SNV	G	C	recN
SNV	T	C	recN
SNV	C	T	recN
SNV	A	G	recN
SNV	C	T	rhlE
SNV	T	C	rhlE
SNV	G	A	rhlE
SNV	T	C	rhlE
SNV	C	T	rhlE
SNV	A	G	rhlE
SNV	C	T	rhlE
SNV	G	A	rhlE
SNV	T	G	rhlE
SNV	C	T	rhlE
SNV	C	T	rhlE
SNV	T	C	rhlE
SNV	T	G	rhlE
SNV	T	A	rhlE
SNV	C	T	rhlE
SNV	C	G	rlmG
SNV	T	C	rlmG
SNV	G	A	rlmG
SNV	G	A	rlmG
SNV	C	T	rlmI
SNV	T	C	rlmN
SNV	A	G	rluA
SNV	A	G	rluA
SNV	T	C	rluA
SNV	C	T	rluD
SNV	A	T	rnb
SNV	T	C	rnb
SNV	T	C	rnr
SNV	G	A	rnr
SNV	G	C	rnr
SNV	T	C	rob
SNV	G	A	rob
SNV	G	A	rob
SNV	G	A	rob
SNV	A	G	rplC
SNV	C	T	rpoB
SNV	C	G	rpoB
SNV	T	A	rpoB
SNV	T	C	rpoB
SNV	C	T	rpoB
SNV	G	A	rpoB
SNV	G	T	rpoC
SNV	T	G	rseB
SNV	T	C	rseB
SNV	T	C	rstB
SNV	C	T	rstB
SNV	G	A	rsxG
SNV	T	C	rsxG
SNV	A	T	rsxG
SNV	G	A	rsxG
SNV	T	C	rtcA
SNV	T	C	sbcD
SNV	G	A	sbcD
SNV	C	A	sbcD
SNV	G	A	sbcD
SNV	T	A	sdaB
SNV	T	A	sdaB
SNV	C	T	sdaB
SNV	C	T	sdaB
SNV	A	G	sdaB
SNV	C	A	sdaC
SNV	A	G	secA
SNV	T	C	secA
SNV	T	C	secA
SNV	A	C	secA
SNV	A	G	secA
SNV	T	C	secA
SNV	A	G	secD
SNV	T	C	secD
SNV	C	T	secD
SNV	C	T	secD
SNV	C	T	secD
SNV	C	T	secD
SNV	G	A	secD
SNV	A	G	secD
SNV	C	G	secD
SNV	G	T	secD
SNV	A	G	secD
SNV	C	T	secD
SNV	T	C	secF
SNV	T	C	secF
SNV	A	G	secF
SNV	T	C	secF
SNV	G	T	secM
SNV	G	A	serA
SNV	A	G	serS
SNV	G	A	sgrR
SNV	A	G	sgrR
SNV	C	T	slt
SNV	T	C	slt
SNV	G	T	slt

SNV	C	T	slt
SNV	T	C	slt
SNV	A	G	slt
SNV	C	A	slt
SNV	G	C	smf
SNV	G	A	smf
SNV	C	A	smf
SNV	C	T	smf
SNV	T	C	smf
SNV	C	T	smf
SNV	T	C	smf
SNV	A	G	speF
SNV	A	G	speF
SNV	G	A	speF
SNV	G	A	speF
SNV	A	G	speF
SNV	T	A	speF
SNV	T	C	speF
SNV	G	A	speF
SNV	G	A	speF
SNV	C	T	speF
SNV	G	A	speF
SNV	C	T	speF
SNV	T	C	spoT
SNV	A	G	spoT
SNV	C	A	spoT
SNV	G	A	sppA
SNV	G	A	sppA
SNV	T	C	sppA
SNV	C	T	sppA
SNV	A	G	srlA
SNV	C	T	srlA
SNV	G	A	srlA
SNV	C	T	srlA
SNV	T	C	srlA
SNV	G	A	srlA
SNV	A	G	srlE
SNV	A	C	srlE
SNV	A	G	srlE
SNV	T	G	srlE
SNV	C	T	srlE
SNV	C	T	srlE
SNV	A	G	srlE
SNV	G	C	srlE
SNV	C	T	srlE
SNV	T	C	srlE
SNV	T	G	ssuD
SNV	T	G	ssuD
SNV	T	C	sucA
SNV	A	C	sucA
SNV	A	C	sucA
SNV	T	C	sucA
SNV	T	G	sufB
SNV	G	A	sufD
SNV	C	A	sufD
SNV	G	A	sufD
SNV	A	G	sufD
SNV	T	A	surA
SNV	T	C	surA
SNV	C	T	surA
SNV	T	C	tamB
SNV	A	T	tamB
SNV	G	T	tamB
SNV	A	C	tamB
SNV	C	A	tamB
SNV	G	C	tamB
SNV	T	C	tamB
SNV	C	T	tamB
SNV	C	T	tamB
SNV	C	T	tamB
SNV	A	G	tamB
SNV	A	G	tcyP
SNV	C	T	tcyP
SNV	T	G	tcyP
SNV	A	G	tcyP
SNV	T	C	tcyP
SNV	C	T	tcyP
SNV	C	A	thiB
SNV	A	G	thiE
SNV	T	C	thiE
SNV	T	G	thiE
SNV	G	C	thiF
SNV	C	T	thiF
SNV	C	A	thiF
SNV	G	A	thiF
SNV	T	C	thiL
SNV	G	T	thpR
SNV	C	G	thpR
SNV	A	G	thpR
SNV	T	C	thpR
SNV	A	C	thpR
SNV	T	C	tktA
SNV	A	G	tktA
SNV	G	A	tktA
SNV	T	C	tolB
SNV	C	T	tolB
SNV	C	A	torZ
SNV	G	A	torZ

SNV	C	T	torZ
SNV	T	C	torZ
SNV	G	A	torZ
SNV	T	G	torZ
SNV	G	A	torZ
SNV	G	A	torZ
SNV	A	G	torZ
SNV	C	A	trpC
SNV	G	C	trpC
SNV	C	A	trpC
SNV	G	A	trpC
SNV	G	A	trpC
SNV	T	C	trpC
SNV	A	G	trpC
SNV	A	G	trpC
SNV	T	C	trpC
SNV	C	A	trpC
SNV	G	T	trpC
SNV	A	G	trpC
SNV	T	A	trpC
SNV	A	G	trpR
SNV	C	T	trpR
SNV	G	C	trpR
SNV	A	G	tsx
SNV	A	T	tusD
SNV	G	A	tyrB
SNV	G	A	tyrB
SNV	T	C	tyrR
SNV	C	T	tyrR
SNV	C	T	tyrR
SNV	G	A	ubiF
SNV	A	T	ubiF
SNV	G	T	ubiF
SNV	T	C	ubiF
SNV	A	G	ubiF
SNV	C	T	ubiF
SNV	G	A	ubiF
SNV	A	C	ubiF
SNV	T	C	ubiX
SNV	T	C	udp
SNV	G	A	uidA
SNV	G	A	uidA
SNV	T	A	uidA
SNV	T	C	uidA
SNV	A	G	uidA
SNV	A	G	uidA
SNV	G	A	uidA
SNV	G	A	uidA
SNV	A	C	uidA
SNV	G	A	uidA
SNV	A	G	uidA
SNV	G	T	uidA
SNV	C	G	ulaA
SNV	G	C	ulaA
SNV	G	C	ulaA
SNV	T	C	ulaA
SNV	C	T	ulaA
SNV	T	C	ulaA
SNV	C	T	ulaA
SNV	G	A	ulaA
SNV	G	T	ulaD
SNV	G	A	ulaD
SNV	C	G	ulaD
SNV	C	T	ulaG
SNV	T	C	uvrA
SNV	G	A	uvrA
SNV	A	G	uvrA
SNV	C	T	uvrA
SNV	A	G	uvrA
SNV	G	A	uxaC
SNV	G	A	uxaC
SNV	G	A	uxaC
SNV	A	G	uxaC
SNV	T	C	uxaC
SNV	G	A	uxaC
SNV	A	G	uxuB
SNV	A	G	uxuB
SNV	T	C	uxuB
SNV	G	A	uxuB
SNV	A	C	wcaF
SNV	T	C	wcaF
SNV	A	G	wcaM
SNV	C	T	wcaM
SNV	G	A	wcaM
SNV	C	G	wcaM
SNV	G	A	wcaM
SNV	C	T	wcaM
SNV	G	A	wcaM
SNV	G	A	wcaM
SNV	A	G	wcaM
SNV	T	G	wcaM
SNV	A	G	wcaM
SNV	C	T	wcaM
SNV	C	T	wcaM
SNV	C	T	wcaM
SNV	G	A	wcaM
SNV	C	A	xapB
SNV	A	G	xdhA

SNV	A	G	xdhA
SNV	G	A	xdhA
SNV	A	G	xdhA
SNV	G	A	xdhA
SNV	G	A	xdhA
SNV	A	G	xdhD
SNV	T	C	xseA
SNV	G	A	xylB
SNV	A	G	yadV
SNV	C	T	yafP
SNV	A	C	yafP
SNV	A	C	yafP
SNV	C	G	yafP
SNV	C	G	yafP
SNV	T	C	yafP
SNV	A	T	yafP
SNV	A	G	yafP
SNV	T	G	yafP
SNV	T	C	yafP
SNV	G	A	yafP
SNV	A	G	yafP
SNV	C	T	yafP
SNV	T	A	yafP
SNV	A	G	yafP
SNV	C	T	yahC
SNV	A	G	yaiP
SNV	G	A	yaiP
SNV	G	A	yaiP
SNV	A	G	yaiP
SNV	G	A	yaiP
SNV	G	A	yaiP
SNV	A	G	yaiP
SNV	T	C	yaiP
SNV	A	G	yaiP
SNV	T	A	yaiP
SNV	C	T	yaiP
SNV	C	A	yaiP
SNV	T	G	yaiP
SNV	A	T	yajG
SNV	A	T	ybaP
SNV	T	C	ybaP
SNV	G	A	ybaP
SNV	G	A	ybaP
SNV	A	G	ybaP
SNV	T	C	ybbP
SNV	T	C	ybbP
SNV	A	G	ybbP
SNV	T	C	ybbP
SNV	A	G	ybbP
SNV	C	G	ybbP
SNV	T	C	ybbP
SNV	C	T	ybbP
SNV	T	C	ybbP
SNV	T	C	ybbP
SNV	G	A	ybdN
SNV	T	C	ybdN
SNV	C	T	ybgI
SNV	A	C	ybgI
SNV	G	A	ybgI
SNV	T	C	ybgI
SNV	G	A	ybgI
SNV	C	T	ybgI
SNV	G	A	ybhG
SNV	A	G	ybhG
SNV	G	A	ybhI
SNV	A	C	ybhI
SNV	A	G	ybhI
SNV	G	T	ybhK
SNV	G	A	ybjS
SNV	A	G	ycaD
SNV	A	T	ycaO
SNV	T	C	ycaO
SNV	C	T	ycaO
SNV	G	C	ycaO
SNV	T	C	ycaO
SNV	C	T	ycaO
SNV	C	T	ycaO
SNV	A	G	ycaO
SNV	C	T	yccS
SNV	T	C	yccS
SNV	C	A	ycdX
SNV	C	T	ycdX
SNV	A	C	ycdX
SNV	T	C	ycdX
SNV	C	T	ycdX
SNV	G	T	ycdX
SNV	A	G	ycgM
SNV	A	G	ycgM
SNV	T	C	ycgR
SNV	T	C	ycgR
SNV	A	G	ycgR
SNV	G	A	ycgR
SNV	A	T	ycgR
SNV	A	G	ycgR
SNV	G	T	ycgR
SNV	T	C	ycjX
SNV	A	G	ycjX
SNV	T	C	ycjX

SNV	C	A	ydbA
SNV	T	C	ydbA
SNV	T	G	ydbA
SNV	C	T	ydbA
SNV	A	G	ydbK
SNV	G	A	ydbK
SNV	C	T	ydbK
SNV	C	T	ydbK
SNV	A	G	ydbK
SNV	T	C	ydbK
SNV	T	C	ydbK
SNV	G	T	ydbK
SNV	A	T	ydbK
SNV	T	C	ydbK
SNV	A	C	ydbK
SNV	C	T	ydbK
SNV	A	G	ydcI
SNV	G	T	ydcI
SNV	A	G	ydeP
SNV	G	T	ydeP
SNV	G	A	ydeP
SNV	G	T	ydeP
SNV	G	A	ydeP
SNV	C	A	ydeP
SNV	A	C	ydeP
SNV	C	T	ydeP
SNV	A	C	ydeP
SNV	A	G	ydeP
SNV	C	T	ydeP
SNV	C	T	ydeP
SNV	T	C	ydeP
SNV	T	G	ydgI
SNV	T	G	ydhK
SNV	C	T	ydhK
SNV	A	G	ydiN
SNV	G	A	ydiN
SNV	A	T	ydiN
SNV	C	T	ydiN
SNV	C	T	ydiN
SNV	A	G	ydjA
SNV	C	T	ydjI
SNV	A	G	ydjI
SNV	G	A	ydjI
SNV	G	A	ydjI
SNV	A	G	ydjI
SNV	A	G	ydjI
SNV	C	A	ydjY
SNV	G	T	ydjY
SNV	A	G	yeaO
SNV	G	A	yeaO
SNV	C	T	yebQ
SNV	T	C	yeeJ
SNV	A	G	yeeS
SNV	T	C	yegD
SNV	A	G	yehB
SNV	T	C	yehF
SNV	A	C	yehF
SNV	A	T	yehM
SNV	T	C	yehM
SNV	C	T	yehM
SNV	A	G	yehM
SNV	G	C	yehM
SNV	G	A	yehM
SNV	G	A	yehM
SNV	A	G	yehM
SNV	G	A	yehM
SNV	A	G	yehM
SNV	G	A	yehM
SNV	T	C	yehP
SNV	G	A	yehP
SNV	G	A	yehP
SNV	A	G	yehP
SNV	T	C	yehP
SNV	G	A	yehP
SNV	T	C	yehP
SNV	C	T	yehP
SNV	T	A	yehQ
SNV	T	C	yehQ
SNV	G	A	yehQ
SNV	T	A	yehQ
SNV	T	C	yehQ
SNV	T	C	yehQ
SNV	T	G	yehQ
SNV	C	T	yehQ
SNV	T	C	yehQ
SNV	G	A	yejF
SNV	A	G	yejF
SNV	A	G	yfbL
SNV	A	G	yfbL
SNV	A	C	yfhM
SNV	C	A	ygcQ
SNV	G	T	ygcQ
SNV	C	T	ygcQ
SNV	G	C	ygcQ
SNV	C	T	ygcU
SNV	C	T	ygcU
SNV	T	C	ygcU
SNV	T	A	ygeV

SNV	A	G	ygeV
SNV	C	T	ygeV
SNV	T	C	ygeV
SNV	G	A	ygeV
SNV	T	C	ygeV
SNV	C	G	ygeY
SNV	T	A	ygeY
SNV	C	T	ygeY
SNV	T	C	ygeY
SNV	G	T	ygeY
SNV	C	A	ygfK
SNV	C	T	ygfK
SNV	G	A	ygfK
SNV	A	G	ygfK
SNV	G	A	ygfK
SNV	T	C	ygfK
SNV	T	C	ygfK
SNV	C	T	ygfK
SNV	C	T	ygfM
SNV	G	A	ygfM
SNV	C	T	ygfM
SNV	T	C	ygfM
SNV	C	T	ygfM
SNV	C	A	ygfM
SNV	G	A	ygfX
SNV	A	T	ygfX
SNV	C	T	ygfX
SNV	A	G	ygfX
SNV	G	A	yggR
SNV	T	C	yggR
SNV	C	T	yggR
SNV	G	A	yggR
SNV	C	T	yggR
SNV	A	G	yghJ
SNV	A	G	yghJ
SNV	C	T	yghJ
SNV	A	C	yghJ
SNV	A	G	yghJ
SNV	A	C	yghJ
SNV	T	A	yghJ
SNV	T	C	yghJ
SNV	A	T	yghJ
SNV	C	T	yghJ
SNV	C	A	yghJ
SNV	A	G	yghJ
SNV	C	A	yghJ
SNV	C	T	yghJ
SNV	G	A	yghJ
SNV	A	T	yghJ
SNV	A	T	yghT
SNV	C	A	ygiD
SNV	T	C	ygiD
SNV	C	T	ygiD
SNV	A	G	ygiQ
SNV	G	A	ygiQ
SNV	A	G	ygiQ
SNV	C	T	ygiQ
SNV	G	A	ygiQ
SNV	T	A	ygiQ
SNV	C	T	ygiQ
SNV	A	G	ygiQ
SNV	T	C	ygiQ
SNV	A	T	ygiQ
SNV	T	C	ygiS
SNV	C	A	ygjQ
SNV	C	T	yhgE
SNV	A	C	yhgE
SNV	C	T	yhgE
SNV	G	A	yhjJ
SNV	A	G	yhjJ
SNV	G	A	yhjJ
SNV	A	G	yhjJ
SNV	A	G	yhjJ
SNV	T	C	yhjJ
SNV	G	A	yhjJ
SNV	A	G	yhjJ
SNV	A	G	yhjJ
SNV	T	C	yhjJ
SNV	G	C	yhjJ
SNV	G	A	yhjJ
SNV	G	A	yicH
SNV	A	C	yicI
SNV	A	G	yicJ
SNV	T	C	yicR
SNV	T	A	yidE
SNV	A	C	yidE
SNV	G	A	yidE
SNV	T	C	yidE
SNV	G	A	yidR
SNV	C	T	yidR
SNV	G	A	yidR
SNV	C	T	yidR
SNV	C	T	yidR
SNV	G	A	yidR
SNV	C	T	yidR
SNV	A	G	yidR
SNV	C	T	yidR
SNV	A	G	yidR

SNV	G	A	yidR
SNV	T	C	yidR
SNV	C	T	yidR
SNV	G	A	yidR
SNV	A	G	yidR
SNV	T	C	yidR
SNV	G	A	yidR
SNV	A	T	yieP
SNV	A	G	yieP
SNV	A	T	yjcS
SNV	A	G	yjcS
SNV	T	C	yjcS
SNV	T	A	yjcS
SNV	G	A	yjcS
SNV	C	T	yjcS
SNV	C	T	yjcS
SNV	G	A	yjcS
SNV	T	C	yjeH
SNV	G	A	yjeH
SNV	C	T	yjfP
SNV	A	G	yjfP
SNV	A	G	yjfP
SNV	A	G	yjgR
SNV	A	G	yjgR
SNV	T	C	yjgR
SNV	C	G	yjiH
SNV	T	C	yjiH
SNV	T	A	yjiH
SNV	A	G	yjiN
SNV	A	G	yjiN
SNV	A	G	yjiN
SNV	A	G	yjiN
SNV	A	G	yjiN
SNV	G	A	yjiR
SNV	T	C	ykgF
SNV	C	G	ykgF
SNV	T	C	ykgF
SNV	A	C	ykgF
SNV	C	T	ykgF
SNV	C	A	ykgF
SNV	T	G	ykgF
SNV	C	T	ykgF
SNV	C	T	ykgM
SNV	A	G	ynfC
SNV	C	T	ynfC
SNV	A	T	ynfC
SNV	G	A	ynfH
SNV	G	T	ynfH
SNV	G	A	ynfH
SNV	T	A	ynfH
SNV	G	A	ynfL
SNV	G	T	ynjB
SNV	T	A	ynjB
SNV	C	T	yobB
SNV	T	A	yobB
SNV	A	G	yphE
SNV	C	T	yphE
SNV	A	G	yphE
SNV	A	G	yphE
SNV	G	A	yphG
SNV	C	T	yphG
SNV	C	T	yphG
SNV	G	A	yphG
SNV	C	T	yphG
SNV	G	A	yphG
SNV	C	A	yphG
SNV	T	C	yphG
SNV	T	G	yphG
SNV	C	A	yphG
SNV	G	A	yphG
SNV	G	A	yphG
SNV	G	A	yphG
SNV	T	C	yphG
SNV	G	A	yphG
SNV	A	G	yphG
SNV	G	T	yphG
SNV	G	A	yphG
SNV	T	C	yphG
SNV	A	C	yphG
SNV	T	G	yphG
SNV	G	A	yphG
SNV	C	T	yphG
SNV	T	C	yphG
SNV	C	T	yqjD
SNV	T	A	ytfQ
SNV	G	A	zapE
SNV	T	C	zapE
SNV	T	C	zapE
SNV	T	C	zapE
SNV	G	C	zitB
SNV	G	A	zitB
SNV	T	G	zitB
SNV	G	T	zitB
SNV	A	G	zitB
SNV	C	T	zitB
SNV	C	G	zitB
SNV	G	T	znuB
SNV	C	A	zur

SNV	A	G	zur
SNV	T	A	zur
SNV	C	T	zur
SNV	T	C	zur

7.2 Publications and presentations

7.2.1 Published papers

Maani, R. (2023). Exosomes: A potential new system of communication between microbes, gut, and brain. *Neurodigest, News and Views from the Neurology Community,* Retrieved from https://neurodigest.co.uk/articles/exosomes-a-potential-new-system-of-communication-between-microbes-gut-and-brain/

Brealey, J., Lees, R., Tempest, R., Law, A., Guarnerio, S., **Maani, R**., . . . Peacock, B. (2024). Shining a light on fluorescent EV dyes: Evaluating efficacy, specificity and suitability by nano-flow cytometry. Journal of Extracellular Biology, 3(10), e70006. doi:10.1002/jex2.70006

Chandler, K., Millar, J., Ward, G., Boyall, C., White, T., Ready, J. D., **Maani, R.**, . . . Peake, N. (2023). Imaging of light-enhanced extracellular vesicle-mediated delivery of oxaliplatin to colorectal cancer cells via laser ablation, inductively coupled plasma mass spectrometry. *Cells, 13*(1), 24. doi:10.3390/cells13010024

Guarnerio, S., Tempest, R., **Maani, R.**, Hunt, S., Cole, L. M., Le Maitre, C. L., . . . Peake, N. (2023). Cellular responses to extracellular vesicles as potential markers of colorectal cancer progression. *International Journal of Molecular Sciences, 24*(23), 16755. doi:10.3390/ijms242316755

Tempest, R., Guarnerio, S., **Maani, R.**, Cooper, J., & Peake, N. (2021). The biological and biomechanical role of transglutaminase-2 in the tumour microenvironment. *Cancers, 13*(11), 2788. doi:10.3390/cancers13112788

7.2.2 Oral presentations

Extracellular vesicles shaping the colorectal cancer microbiome. 1st Symposium of MOVE (MObility for Vesicles research in Europe), Malaga, Spain, October 2023.

Extracellular vesicles shaping the colorectal cancer microbiome. UKEV annual meeting, Edinburgh, UK, December 2022.

7.2.3 Poster presentations

Extracellular vesicles alter colorectal cancer-linked *E. coli* through protein-mediated surface binding and uptake. ISEV annual meeting, Seattle, USA, May 2023.

Extracellular vesicles alter colorectal cancer-linked *E. coli* through direct surface binding and uptake. Microbiology Society annual meeting, Birmingham, UK, April 2023.

Colorectal cancer-extracellular vesicles alter flagella-associated gene expression of *E. coli*. UKEV annual meeting, Cambridge, UK, December 2023.

Extracellular vesicles shaping the colorectal cancer microbiome. Microbiology Society-Early Career Microbiologist Forum, Sheffield, UK, July 2022.

Extracellular vesicles shaping the colorectal cancer microbiome. Microbiology Society annual meeting, Belfast, UK, April 2022.

7.3 Ethics approval letter

Ymchwil Iechyd a Gofal Cymru
Health and Care Research Wales

NHS
Health Research Authority

Dr Nick Peake
Senior Lecturer
Sheffield Hallam University
Biomolecular Research Centre
Faculty of Health & Wellbeing
Howard Street, Sheffield
S1 1WB

Email: approvals@hra.nhs.uk
HCRW.approvals@wales.nhs.uk

20 May 2020

Dear Dr Peake

HRA and Health and Care Research Wales (HCRW) Approval Letter

Study title:	**Extracellular vesicles - key mediators and potential biomarkers in colorectal cancer patients.**
IRAS project ID:	**244453**
REC reference:	**19/NI/0221**
Sponsor	**Sheffield Teaching Hospitals NHS FT**

I am pleased to confirm that HRA and Health and Care Research Wales (HCRW) Approval has been given for the above referenced study, on the basis described in the application form, protocol, supporting documentation and any clarifications received. You should not expect to receive anything further relating to this application.

Please now work with participating NHS organisations to confirm capacity and capability, in line with the instructions provided in the "Information to support study set up" section towards the end of this letter.

How should I work with participating NHS/HSC organisations in Northern Ireland and Scotland?
HRA and HCRW Approval does not apply to NHS/HSC organisations within Northern Ireland and Scotland.

If you indicated in your IRAS form that you do have participating organisations in either of these devolved administrations, the final document set and the study wide governance report (including this letter) have been sent to the coordinating centre of each participating nation. The relevant national coordinating function/s will contact you as appropriate.

8 References

Abdouh, M., Floris, M., Gao, Z., Arena, V., Arena, M., & Arena, G. O. (2019). Colorectal cancer-derived extracellular vesicles induce transformation of fibroblasts into colon carcinoma cells. *Journal of Experimental & Clinical Cancer Research: CR, 38*(1), 257. doi:10.1186/s13046-019-1248-2

Abels, & Breakefield. (2016). Introduction to extracellular vesicles: Biogenesis, RNA cargo selection, content, release, and uptake. *Cellular and Molecular Neurobiology, 36*(3), 301–312. doi:10.1007/s10571-016-0366-z

Addington, E., Sandalli, S., & Roe, A. J. (2024). Current understandings of colibactin regulation. *Microbiology (Reading, England), 170*(2), 001427. doi:10.1099/mic.0.001427

Alberro, A., Iparraguirre, L., Fernandes, A., & Otaegui, D. (2021). Extracellular vesicles in blood: Sources, effects, and applications. *International Journal of Molecular Sciences, 22*(15), 8163. doi:10.3390/ijms22158163

Allelein, S., Medina-Perez, P., Lopes, A. L. H., Rau, S., Hause, G., Kölsch, A., & Kuhlmeier, D. (2021). Potential and challenges of specifically isolating extracellular vesicles from heterogeneous populations. *Scientific Reports, 11*(1), 11585. doi:10.1038/s41598-021-91129-y

Amarasinghe, I., Phillips, W., Hill, A. F., Cheng, L., Helbig, K. J., Willms, E., & Monson, E. A. (2023). Cellular communication through extracellular vesicles and lipid droplets. *Journal of Extracellular Biology, 2*(3), e77. doi:10.1002/jex2.77

Anderson, E. C., Hessman, C., Levin, T. G., Monroe, M. M., & Wong, M. H. (2011). The role of colorectal cancer stem cells in metastatic disease and therapeutic response. *Cancers, 3*(1), 319–339. doi:10.3390/cancers3010319

Angelberger, S., Reinisch, W., Makristathis, A., Lichtenberger, C., Dejaco, C., Papay, P., . . . Berry, D. (2013). Temporal bacterial community dynamics vary among ulcerative colitis patients after fecal microbiota transplantation. *The American Journal of Gastroenterology, 108*(10), 1620–1630. doi:10.1038/ajg.2013.257

Arthur, J. C., Gharaibeh, R. Z., Mühlbauer, M., Perez-Chanona, E., Uronis, J. M., McCafferty, J., . . . Jobin, C. (2014). Microbial genomic analysis reveals the essential role of inflammation in bacteria-induced colorectal cancer. *Nature Communications, 5*, 4724. doi:10.1038/ncomms5724

Arthur, J. C., Perez-Chanona, E., Mühlbauer, M., Tomkovich, S., Uronis, J. M., Fan, T., . . . Jobin, C. (2012). Intestinal inflammation targets cancer-inducing activity of the microbiota. *Science (New York, N.Y.), 338*(6103), 120–123. doi:10.1126/science.1224820

Baranyai, T., Herczeg, K., Onódi, Z., Voszka, I., Módos, K., Marton, N., . . . Giricz, Z. (2015). Isolation of exosomes from blood plasma: Qualitative and quantitative comparison of ultracentrifugation and size exclusion chromatography methods. *PloS One, 10*(12), e0145686. doi:10.1371/journal.pone.0145686

Bonamy, C., Sechet, E., Amiot, A., Alam, A., Mourez, M., Fraisse, L., . . . Sperandio, B. (2018). Expression of the human antimicrobial peptide β-defensin-1 is repressed by the EGFR-ERK-MYC axis in colonic epithelial cells. *Scientific Reports, 8*(1), 18043. doi:10.1038/s41598-018-36387-z

Bonnet, M., Buc, E., Sauvanet, P., Darcha, C., Dubois, D., Pereira, B., . . . Darfeuille-Michaud, A. (2014). Colonization of the human gut by E. coli and colorectal cancer risk. *Clinical Cancer Research: An Official Journal of the American Association for Cancer Research, 20*(4), 859–867. doi:10.1158/1078-0432.CCR-13-1343

Bonsergent, E., Grisard, E., Buchrieser, J., Schwartz, O., Théry, C., & Lavieu, G. (2021). Quantitative characterization of extracellular vesicle uptake and content delivery within mammalian cells. *Nature Communications, 12*, 1864. doi:10.1038/s41467-021-22126-y

Bonsergent, E., & Lavieu, G. (2019). Content release of extracellular vesicles in a cell-free extract. *FEBS Letters, 593*(15), 1983–1992. doi:10.1002/1873-3468.13472

Borges-Canha, M., Portela-Cidade, J. P., Dinis-Ribeiro, M., Leite-Moreira, A. F., & Pimentel-Nunes, P. (2015). Role of colonic microbiota in colorectal carcinogenesis: A systematic review. *Revista Espanola De Enfermedades Digestivas, 107*(11), 659–671. doi:10.17235/reed.2015.3830/2015

Brocco, Simeone, Buca, Marino, De Tursi, Grassadonia, . . . Tinari. (2022). Blood circulating CD133+ extracellular vesicles predict clinical outcomes in patients with metastatic colorectal cancer. *Cancers, 14*(5), 1357. doi:10.3390/cancers14051357

Bui, T., Mascarenhas, L., & Sumagin, R. (2018). Extracellular vesicles regulate immune responses and cellular function in intestinal inflammation and repair. *Tissue Barriers, 6*, 0. doi:10.1080/21688370.2018.1431038

Bull, M. J., & Plummer, N. T. (2014). Part 1: The human gut microbiome in health and disease. *Integrative Medicine: A Clinician's Journal, 13*(6), 17–22. Retrieved from https://www.ncbi.nlm.nih.gov/pmc/articles/PMC4566439/

Buzás, E. I., Tóth, E. Á, Sódar, B. W., & Szabó-Taylor, K. É. (2018). Molecular interactions at the surface of extracellular vesicles. *Seminars in Immunopathology, 40*(5), 453–464. doi:10.1007/s00281-018-0682-0

Canani, R. B., Costanzo, M. D., Leone, L., Pedata, M., Meli, R., & Calignano, A. (2011). Potential beneficial effects of butyrate in intestinal and extraintestinal diseases. *World Journal of Gastroenterology : WJG, 17*(12), 1519–1528. doi:10.3748/wjg.v17.i12.1519

Cañas, M., Giménez, R., Fábrega, M., Toloza, L., Baldomà, L., & Badia, J. (2016). Outer membrane vesicles from the probiotic escherichia coli nissle 1917 and the commensal ECOR12 enter intestinal epithelial cells via clathrin-dependent endocytosis and elicit differential effects on DNA damage. *PloS One, 11*(8), e0160374. doi:10.1371/journal.pone.0160374

Casasanta, M. A., Yoo, C. C., Udayasuryan, B., Sanders, B. E., Umaña, A., Zhang, Y., . . . Slade, D. J. (2020). Fusobacterium nucleatum host-cell binding and invasion induces IL-8 and CXCL1 secretion that drives colorectal cancer cell migration. *Science Signaling, 13*(641), eaba9157. doi:10.1126/scisignal.aba9157

Cevallos, S. A., Lee, J., Tiffany, C. R., Byndloss, A. J., Johnston, L., Byndloss, M. X., & Bäumler, A. J. (2019). Increased epithelial oxygenation links colitis to an expansion of tumorigenic bacteria. *mBio, 10*(5), 2244. doi:10.1128/mBio.02244-19

Cha, B. S., Park, K. S., & Park, J. S. (2020). Signature mRNA markers in extracellular vesicles for the accurate diagnosis of colorectal cancer. *Journal of Biological Engineering, 14*, 4. doi:10.1186/s13036-020-0225-9

Chen, B., Ramazzotti, D., Heide, T., Spiteri, I., Fernandez-Mateos, J., James, C., . . . Sottoriva, A. (2023). Contribution of pks+ E. coli mutations to colorectal carcinogenesis. *Nature Communications, 14*(1), 7827. doi:10.1038/s41467-023-43329-5

Chen, R. Y., & Keddie, B. A. (2021). The galleria mellonella-enteropathogenic escherichia coli model system: Characterization of pathogen virulence and insect immune responses. *Journal of Insect Science, 21*(4), 7. doi:10.1093/jisesa/ieab046

Cho, I., & Blaser, M. J. (2012). The human microbiome: At the interface of health and disease. *Nature Reviews. Genetics, 13*(4), 260–270. doi:10.1038/nrg3182

Choi, D., Choi, D., Hong, B. S., Jang, S. C., Kim, D., Lee, J., . . . Gho, Y. S. (2012). Quantitative proteomics of extracellular vesicles derived from human primary and metastatic colorectal cancer cells. *Journal of Extracellular Vesicles, 1* doi:10.3402/jev.v1i0.18704

Choi, D., Go, G., Kim, D., Lee, J., Park, S., Di Vizio, D., & Gho, Y. S. (2020). Quantitative proteomic analysis of trypsin-treated extracellular vesicles to identify the real-vesicular proteins. *Journal of Extracellular Vesicles, 9*(1), 1757209. doi:10.1080/20013078.2020.1757209

Choi, Lee, Shin, Cho, Cha, & Roe. (2017). Zinc-dependent regulation of zinc import and export genes by zur. *Nature Communications, 8*(1), 15812. doi:10.1038/ncomms15812

Clay, S. L., Fonseca-Pereira, D., & Garrett, W. S. (2022). Colorectal cancer: The facts in the case of the microbiota. *The Journal of Clinical Investigation, 132*(4), e155101. doi:10.1172/JCI155101

Contursi, A., Fullone, R., Szklanna-Koszalinska, P., Marcone, S., Lanuti, P., Taus, F., . . . Patrignani, P. (2023). Tumor-educated platelet extracellular vesicles: Proteomic profiling and crosstalk with colorectal cancer cells. *Cancers, 15*(2), 350. doi:10.3390/cancers15020350

Cougnoux, A., Dalmasso, G., Martinez, R., Buc, E., Delmas, J., Gibold, L., . . . Bonnet, R. (2014). Bacterial genotoxin colibactin promotes colon tumour growth by inducing a senescence-associated secretory phenotype. *Gut, 63*(12), 1932–1942. doi:10.1136/gutjnl-2013-305257

Cuevas-Ramos, G., Petit, C. R., Marcq, I., Boury, M., Oswald, E., & Nougayrède, J. (2010). Escherichia coli induces DNA damage in vivo and triggers genomic instability in mammalian cells. *Proceedings of the National Academy of Sciences of the United States of America, 107*(25), 11537–11542. doi:10.1073/pnas.1001261107

Cui, M., Xiao, H., Li, Y., Dong, J., Luo, D., Li, H., . . . Fan, S. (2017). Total abdominal irradiation exposure impairs cognitive function involving miR-34a-5p/BDNF axis. *Biochimica Et Biophysica Acta. Molecular Basis of Disease, 1863*(9), 2333–2341. doi:10.1016/j.bbadis.2017.06.021

Cvjetkovic, A., Karimi, N., Crescitelli, R., Thorsell, A., Taflin, H., Lässer, C., & Lötvall, J. (2024). Proteomic profiling of tumour tissue-derived extracellular vesicles in colon cancer. *Journal of Extracellular Biology, 3*(2), e127. doi:10.1002/jex2.127

Dang, Yin, Sun, & Yang. (2020). Recurrence of moderate to severe ulcerative colitis after fecal microbiota transplantation treatment and the efficacy of re-FMT: A case series. *BMC Gastroenterology, 20*(1), 401. doi:10.1186/s12876-020-01548-w

David, L. A., Maurice, C. F., Carmody, R. N., Gootenberg, D. B., Button, J. E., Wolfe, B. E., . . . Turnbaugh, P. J. (2014). Diet rapidly and reproducibly alters the human gut microbiome. *Nature, 505*(7484), 559–563. doi:10.1038/nature12820

de Jonge, N., Carlsen, B., Christensen, M. H., Pertoldi, C., & Nielsen, J. L. (2022). The gut microbiome of 54 mammalian species. *Frontiers in Microbiology, 13* doi:10.3389/fmicb.2022.886252

de Vos, W. M., Tilg, H., Van Hul, M., & Cani, P. D. (2022). Gut microbiome and health: Mechanistic insights. *Gut, 71*(5), 1020–1032. doi:10.1136/gutjnl-2021-326789

Dejea, C. M., Fathi, P., Craig, J. M., Boleij, A., Taddese, R., Geis, A. L., . . . Sears, C. L. (2018). Patients with familial adenomatous polyposis harbor colonic biofilms containing tumorigenic bacteria. *Science (New York, N.Y.), 359*(6375), 592–597. doi:10.1126/science.aah3648

Dejea, C. M., Wick, E. C., Hechenbleikner, E. M., White, J. R., Mark Welch, J. L., Rossetti, B. J., . . . Sears, C. L. (2014). Microbiota organization is a distinct feature of proximal colorectal cancers. *Proceedings of the National Academy of Sciences of the United States of America, 111*(51), 18321–18326. doi:10.1073/pnas.1406199111

Diaz, G., Bridges, C., Lucas, M., Cheng, Y., Schorey, J. S., Dobos, K. M., & Kruh-Garcia, N. A. (2018). Protein digestion, ultrafiltration, and size exclusion chromatography to optimize the isolation of exosomes from human blood plasma and serum. *Journal of Visualized Experiments: JoVE,* (134), 57467. doi:10.3791/57467

Diehl, J. N., Ray, A., Collins, L. B., Peterson, A., Alexander, K. C., Boutros, J. G., . . . Akerman, A. W. (2023). A standardized method for plasma extracellular vesicle isolation and size distribution analysis. *Plos One, 18*(4), e0284875. doi:10.1371/journal.pone.0284875

Dougherty, M. W., & Jobin, C. (2015). Intestinal bacteria and colorectal cancer: Etiology and treatment. *Gut Microbes, 15*(1), 2185028. doi:10.1080/19490976.2023.2185028

Dougherty, M. W., & Jobin, C. (2021). Shining a light on colibactin biology. *Toxins, 13*(5), 346. doi:10.3390/toxins13050346

Duan, B., Zhao, Y., Bai, J., Wang, J., Duan, X., Luo, X., . . . Yang, S. (2022). Colorectal cancer: An overview. In J. A. Morgado-Diaz (Ed.), *Gastrointestinal cancers* . Brisbane (AU): Exon Publications. Retrieved from http://www.ncbi.nlm.nih.gov/books/NBK586003/

Dziubańska-Kusibab, P. J., Berger, H., Battistini, F., Bouwman, B. A. M., Iftekhar, A., Katainen, R., . . . Meyer, T. F. (2020). Colibactin DNA-damage signature indicates mutational impact in colorectal cancer. *Nature Medicine, 26*(7), 1063–1069. doi:10.1038/s41591-020-0908-2

Ellermann, M., & Sperandio, V. (2020). Bacterial signaling as an antimicrobial target. *Current Opinion in Microbiology, 57*, 78–86. doi:10.1016/j.mib.2020.08.001

Engen, P. A., Green, S. J., Voigt, R. M., Forsyth, C. B., & Keshavarzian, A. (2015). The gastrointestinal microbiome: Alcohol effects on the composition of intestinal microbiota. *Alcohol Research: Current Reviews, 37*(2), 223–236.

Fan, Y., Wu, T., Zhao, L., Jia, R., Ren, H., Hou, W., & Wang, Z. (2024). From zinc homeostasis to disease progression: Unveiling the neurodegenerative puzzle. *Pharmacological Research, 199*, 107039. doi:10.1016/j.phrs.2023.107039

Fearon, E. R., & Vogelstein, B. (1990). A genetic model for colorectal tumorigenesis. *Cell, 61*(5), 759–767. doi:10.1016/0092-8674(90)90186-i

Flemer, B., Lynch, D. B., Brown, J. M. R., Jeffery, I. B., Ryan, F. J., Claesson, M. J., . . . O'Toole, P. W. (2017). Tumour-associated and non-tumour-associated microbiota in colorectal cancer. *Gut, 66*(4), 633–643. doi:10.1136/gutjnl-2015-309595

Fuentes, P., Sesé, M., Guijarro, P. J., Emperador, M., Sánchez-Redondo, S., Peinado, H., . . . Ramón Y Cajal, S. (2020). ITGB3-mediated uptake of small extracellular vesicles facilitates intercellular communication in breast cancer

cells. *Nature Communications, 11*(1), 4261. doi:10.1038/s41467-020-18081-9

Gabbianelli, R., Scotti, R., Ammendola, S., Petrarca, P., Nicolini, L., & Battistoni, A. (2011). Role of ZnuABC and ZinT in escherichia coli O157:H7 zinc acquisition and interaction with epithelial cells. *BMC Microbiology, 11*, 36. doi:10.1186/1471-2180-11-36

Gagnière, J., Raisch, J., Veziant, J., Barnich, N., Bonnet, R., Buc, E., . . . Bonnet, M. (2016). Gut microbiota imbalance and colorectal cancer. *World Journal of Gastroenterology, 22*(2), 501–518. doi:10.3748/wjg.v22.i2.501

Geuking, M. B., Köller, Y., Rupp, S., & McCoy, K. D. (2014). The interplay between the gut microbiota and the immune system. *Gut Microbes, 5*(3), 411–418. doi:10.4161/gmic.29330

Gilbert, J., Blaser, M. J., Caporaso, J. G., Jansson, J., Lynch, S. V., & Knight, R. (2018). Current understanding of the human microbiome. *Nature Medicine, 24*(4), 392–400. doi:10.1038/nm.4517

Graham, A. I., Hunt, S., Stokes, S. L., Bramall, N., Bunch, J., Cox, A. G., . . . Poole, R. K. (2009). Severe zinc depletion of escherichia coli: Roles for high affinity zinc binding by ZinT, zinc transport and zinc-independent proteins. *The Journal of Biological Chemistry, 284*(27), 18377–18389. doi:10.1074/jbc.M109.001503

Gubatan, J., Holman, D. R., Puntasecca, C. J., Polevoi, D., Rubin, S. J., & Rogalla, S. (2021). Antimicrobial peptides and the gut microbiome in inflammatory bowel disease. *World Journal of Gastroenterology, 27*(43), 7402–7422. doi:10.3748/wjg.v27.i43.7402

Gur, C., Ibrahim, Y., Isaacson, B., Yamin, R., Abed, J., Gamliel, M., . . . Mandelboim, O. (2015). Binding of the Fap2 protein of fusobacterium nucleatum to human inhibitory receptor TIGIT protects tumors from immune cell attack. *Immunity, 42*(2), 344–355. doi:10.1016/j.immuni.2015.01.010

Hewitt, R. E., McMarlin, A., Kleiner, D., Wersto, R., Martin, P., Tsokos, M., . . . Stetler-Stevenson, W. G. (2000). Validation of a model of colon cancer

progression. *The Journal of Pathology, 192*(4), 446–454. doi:10.1002/1096-9896(2000)9999:9999<::AID-PATH775>3.0.CO;2-K

Hill, R. H. (1985). Prevention of adhesion by indigenous bacteria to rabbit cecum epithelium by a barrier of microvesicles. *Infection and Immunity, 47*(2), 540–543. doi:10.1128/iai.47.2.540-543.1985

Hossain, M. S., Karuniawati, H., Jairoun, A. A., Urbi, Z., Ooi, D. J., John, A., . . . Hadi, M. A. (2022). Colorectal cancer: A review of carcinogenesis, global epidemiology, current challenges, risk factors, preventive and treatment strategies. *Cancers, 14*(7), 1732. doi:10.3390/cancers14071732

Hung, R. J., Ulrich, C. M., Goode, E. L., Brhane, Y., Muir, K., Chan, A. T., . . . Henderson, B. (2015). Cross cancer genomic investigation of inflammation pathway for five common cancers: Lung, ovary, prostate, breast, and colorectal cancer. *Journal of the National Cancer Institute, 107*(11), djv246. doi:10.1093/jnci/djv246

Ianiro, Punčochář, Karcher, Porcari, Armanini, Asnicar, . . . Segata. (2022). Variability of strain engraftment and predictability of microbiome composition after fecal microbiota transplantation across different diseases. *Nature Medicine, 28*(9), 1913–1923. doi:10.1038/s41591-022-01964-3

Inder, K. L., Ruelcke, J. E., Petelin, L., Moon, H., Choi, E., Rae, J., . . . Hill, M. M. (2014). Cavin-1/PTRF alters prostate cancer cell-derived extracellular vesicle content and internalization to attenuate extracellular vesicle-mediated osteoclastogenesis and osteoblast proliferation. *Journal of Extracellular Vesicles, 3* doi:10.3402/jev.v3.23784

Isaac, R., Reis, F. C. G., Ying, W., & Olefsky, J. M. (2021). Exosomes as mediators of intercellular crosstalk in metabolism. *Cell Metabolism, 33*(9), 1744–1762. doi:10.1016/j.cmet.2021.08.006

Iyadorai, T., Mariappan, V., Vellasamy, K. M., Wanyiri, J. W., Roslani, A. C., Lee, G. K., . . . Vadivelu, J. (2020). Prevalence and association of pks+ Escherichia coli with colorectal cancer in patients at the university

malaya medical centre, malaysia. *PloS One, 15*(1), e0228217. doi:10.1371/journal.pone.0228217

Jandhyala, Talukdar, Subramanyam, Vuyyuru, Sasikala, & Reddy. (2015). Role of the normal gut microbiota. *World Journal of Gastroenterology : WJG, 21*(29), 8787–8803. doi:10.3748/wjg.v21.i29.8787

Jennifer, B., Berg, V., Modak, M., Puck, A., Seyerl-Jiresch, M., Künig, S., . . . Stöckl, J. (2020). Transferrin receptor 1 is a cellular receptor for human heme-albumin. *Communications Biology, 3*(1), 1–13. doi:10.1038/s42003-020-01294-5

Jeppesen, D. K., Fenix, A. M., Franklin, J. L., Higginbotham, J. N., Zhang, Q., Zimmerman, L. J., . . . Coffey, R. J. (2019). Reassessment of exosome composition. *Cell, 177*(2), 428–445.e18. doi:10.1016/j.cell.2019.02.029

Jiang, L., Shen, Y., Guo, D., Yang, D., Liu, J., Fei, X., . . . Cai, Z. (2016). EpCAM-dependent extracellular vesicles from intestinal epithelial cells maintain intestinal tract immune balance. *Nature Communications, 7*, 13045. doi:10.1038/ncomms13045

Johansson, M. E. V., Larsson, J. M. H., & Hansson, G. C. (2011). The two mucus layers of colon are organized by the MUC2 mucin, whereas the outer layer is a legislator of host-microbial interactions. *Proceedings of the National Academy of Sciences of the United States of America, 108 Suppl 1*(Suppl 1), 4659–4665. doi:10.1073/pnas.1006451107

Jones, E. J., Booth, C., Fonseca, S., Parker, A., Cross, K., Miquel-Clopés, A., . . . Carding, S. R. (2020). The uptake, trafficking, and biodistribution of bacteroides thetaiotaomicron generated outer membrane vesicles. *Frontiers in Microbiology, 11*, 57. doi:10.3389/fmicb.2020.00057

Kalita, A., Hu, J., & Torres, A. G. (2014). Recent advances in adherence and invasion of pathogenic escherichia coli. *Current Opinion in Infectious Diseases, 27*(5), 459–464. doi:10.1097/QCO.0000000000000092

Karampoga, A., Tzaferi, K., Koutsakis, C., Kyriakopoulou, K., & Karamanos, N. K. (2022). Exosomes and the extracellular matrix: A dynamic

interplay in cancer progression. *The International Journal of Developmental Biology, 66*(1-2-3), 97–102. doi:10.1387/ijdb.210120nk

Karimi, N., Cvjetkovic, A., Jang, S. C., Crescitelli, R., Hosseinpour Feizi, M. A., Nieuwland, R., . . . Lässer, C. (2018). Detailed analysis of the plasma extracellular vesicle proteome after separation from lipoproteins. *Cellular and Molecular Life Sciences: CMLS, 75*(15), 2873–2886. doi:10.1007/s00018-018-2773-4

Kashyap, P. C., Marcobal, A., Ursell, L. K., Smits, S. A., Sonnenburg, E. D., Costello, E. K., . . . Sonnenburg, J. L. (2013). Genetically dictated change in host mucus carbohydrate landscape exerts a diet-dependent effect on the gut microbiota. *Proceedings of the National Academy of Sciences of the United States of America, 110*(42), 17059–17064. doi:10.1073/pnas.1306070110

Kho, Z. Y., & Lal, S. K. (2018). The human gut microbiome – A potential controller of wellness and disease. *Frontiers in Microbiology, 9* doi:10.3389/fmicb.2018.01835

Kim, C. H. (2023). Complex regulatory effects of gut microbial short-chain fatty acids on immune tolerance and autoimmunity. *Cellular & Molecular Immunology, 20*(4), 341–350. doi:10.1038/s41423-023-00987-1

Kimiz-Gebologlu, I., & Oncel, S. S. (2022). Exosomes: Large-scale production, isolation, drug loading efficiency, and biodistribution and uptake. *Journal of Controlled Release: Official Journal of the Controlled Release Society, 347*, 533–543. doi:10.1016/j.jconrel.2022.05.027

Kohoutova, D., Smajs, D., Moravkova, P., Cyrany, J., Moravkova, M., Forstlova, M., . . . Bures, J. (2014). Escherichia coli strains of phylogenetic group B2 and D and bacteriocin production are associated with advanced colorectal neoplasia. *BMC Infectious Diseases, 14*, 733. doi:10.1186/s12879-014-0733-7

Koliarakis, I., Messaritakis, I., Nikolouzakis, T. K., Hamilos, G., Souglakos, J., & Tsiaoussis, J. (2019). Oral bacteria and intestinal dysbiosis

in colorectal cancer. *International Journal of Molecular Sciences, 20*(17), 4146. doi:10.3390/ijms20174146

Konoshenko, M. Y., Lekchnov, E. A., Vlassov, A. V., & Laktionov, P. P. (2018). Isolation of extracellular vesicles: General methodologies and latest trends. *BioMed Research International, 2018*, 8545347. doi:10.1155/2018/8545347

Krieg, A. M. (2002). CpG motifs in bacterial DNA and their immune effects*. *Annual Review of Immunology, 20*(Volume 20, 2002), 709–760. doi:10.1146/annurev.immunol.20.100301.064842

Krishnan, S., Alden, N., & Lee, K. (2015). Pathways and functions of gut microbiota metabolism impacting host physiology. *Current Opinion in Biotechnology, 36*, 137–145. doi:10.1016/j.copbio.2015.08.015

Kumar, L., Cox, C. R., & Sarkar, S. K. (2019). Matrix metalloprotease-1 inhibits and disrupts enterococcus faecalis biofilms. *PLoS ONE, 14*(1), e0210218. doi:10.1371/journal.pone.0210218

Kumar, V. B., Lahav, M., & Gazit, E. (2024). Preventing biofilm formation and eradicating pathogenic bacteria by zn doped histidine derived carbon quantum dots. *Journal of Materials Chemistry. B, 12*(11), 2855–2868. doi:10.1039/d3tb02488a

Kunde, S., Pham, A., Bonczyk, S., Crumb, T., Duba, M., Conrad, H., . . . Kugathasan, S. (2013). Safety, tolerability, and clinical response after fecal transplantation in children and young adults with ulcerative colitis. *Journal of Pediatric Gastroenterology and Nutrition, 56*(6), 597–601. doi:10.1097/MPG.0b013e318292fa0d

Kurtjak, M., Kereïche, S., Klepac, D., Križan, H., Perčić, M., Krušić Alić, V., . . . Malenica, M. (2022). Unveiling the native morphology of extracellular vesicles from human cerebrospinal fluid by atomic force and cryogenic electron microscopy. *Biomedicines, 10*(6), 1251. doi:10.3390/biomedicines10061251

Lan, J., Sun, L., Xu, F., Liu, L., Hu, F., Song, D., . . . Wang, G. (2019). M2 macrophage-derived exosomes promote cell migration and invasion in colon

cancer. *Cancer Research, 79*(1), 146–158. doi:10.1158/0008-5472.CAN-18-0014

Lee, H. (2019). Microbe-host communication by small RNAs in extracellular vesicles: Vehicles for transkingdom RNA transportation. *International Journal of Molecular Sciences, 20*(6), 1487. doi:10.3390/ijms20061487

Lee-Six, H., Olafsson, S., Ellis, P., Osborne, R. J., Sanders, M. A., Moore, L., . . . Stratton, M. R. (2019). The landscape of somatic mutation in normal colorectal epithelial cells. *Nature, 574*(7779), 532–537. doi:10.1038/s41586-019-1672-7

Li, H., Limenitakis, J. P., Fuhrer, T., Geuking, M. B., Lawson, M. A., Wyss, M., . . . Macpherson, A. J. (2015). The outer mucus layer hosts a distinct intestinal microbial niche. *Nature Communications, 6*, 8292. doi:10.1038/ncomms9292

Li, S., Konstantinov, S. R., Smits, R., & Peppelenbosch, M. P. (2017). Bacterial biofilms in colorectal cancer initiation and progression. *Trends in Molecular Medicine, 23*(1), 18–30. doi:10.1016/j.molmed.2016.11.004

Liang, G., Zhu, Y., Ali, D. J., Tian, T., Xu, H., Si, K., . . . Xiao, Z. (2020). Engineered exosomes for targeted co-delivery of miR-21 inhibitor and chemotherapeutics to reverse drug resistance in colon cancer. *Journal of Nanobiotechnology, 18*(1), 10. doi:10.1186/s12951-019-0563-2

Liang, J. Q., Li, T., Nakatsu, G., Chen, Y., Yau, T. O., Chu, E., . . . Yu, J. (2020). A novel faecal lachnoclostridium marker for the non-invasive diagnosis of colorectal adenoma and cancer. *Gut, 69*(7), 1248–1257. doi:10.1136/gutjnl-2019-318532

Liang, Z., Liu, H., Wang, F., Xiong, L., Zhou, C., Hu, T., . . . Lan, P. (2019). LncRNA RPPH1 promotes colorectal cancer metastasis by interacting with TUBB3 and by promoting exosomes-mediated macrophage M2 polarization. *Cell Death & Disease, 10*(11), 829. doi:10.1038/s41419-019-2077-0

Lim, J., Lee, K., Kim, S. H., Kim, Y., Kim, S., Park, W., & Park, S. (2011). YkgM and ZinT proteins are required for maintaining intracellular zinc concentration and producing curli in enterohemorrhagic escherichia coli (EHEC) O157:H7 under zinc deficient conditions. *International Journal of Food Microbiology, 149*(2), 159–170. doi:10.1016/j.ijfoodmicro.2011.06.017

Lin, & Zhang. (2017). Role of intestinal microbiota and metabolites on gut homeostasis and human diseases. *BMC Immunology, 18*(1), 2. doi:10.1186/s12865-016-0187-3

Lobb, R. J., Becker, M., Wen Wen, S., Wong, C. S. F., Wiegmans, A. P., Leimgruber, A., & Möller, A. (2015). Optimized exosome isolation protocol for cell culture supernatant and human plasma. *Journal of Extracellular Vesicles, 4*, 10.3402/jev.v4.27031. doi:10.3402/jev.v4.27031

Long, X., Wong, C. C., Tong, L., Chu, E. S. H., Ho Szeto, C., Go, M. Y. Y., . . . Yu, J. (2019). Peptostreptococcus anaerobius promotes colorectal carcinogenesis and modulates tumour immunity. *Nature Microbiology, 4*(12), 2319–2330. doi:10.1038/s41564-019-0541-3

Lynch, H. T., & de la Chapelle, A. (2003). Hereditary colorectal cancer. *The New England Journal of Medicine, 348*(10), 919–932. doi:10.1056/NEJMra012242

Maddocks, O. D. K., Short, A. J., Donnenberg, M. S., Bader, S., & Harrison, D. J. (2009). Attaching and effacing escherichia coli downregulate DNA mismatch repair protein in vitro and are associated with colorectal adenocarcinomas in humans. *PloS One, 4*(5), e5517. doi:10.1371/journal.pone.0005517

Majka, M., Janowska-Wieczorek, A., Ratajczak, J., Ehrenman, K., Pietrzkowski, Z., Kowalska, M. A., . . . Ratajczak, M. Z. (2001). Numerous growth factors, cytokines, and chemokines are secreted by human CD34(+) cells, myeloblasts, erythroblasts, and megakaryoblasts and regulate normal hematopoiesis in an autocrine/paracrine manner. *Blood, 97*(10), 3075–3085. doi:10.1182/blood.v97.10.3075

McLoughlin, K., Schluter, J., Rakoff-Nahoum, S., Smith, A. L., & Foster, K. R. (2016). Host selection of microbiota via differential adhesion. *Cell Host & Microbe, 19*(4), 550–559. doi:10.1016/j.chom.2016.02.021

Minciacchi, Freeman, & Di Vizio. (2015). Extracellular vesicles in cancer: Exosomes, microvesicles and the emerging role of large oncosomes. *Seminars in Cell & Developmental Biology, 40*, 41–51. doi:10.1016/j.semcdb.2015.02.010

Moon, S., Shin, D. W., Kim, S., Lee, Y., Mankhong, S., Yang, S. W., . . . Kang, J. (2019). Enrichment of exosome-like extracellular vesicles from plasma suitable for clinical vesicular miRNA biomarker research. *Journal of Clinical Medicine, 8*(11), 1995. doi:10.3390/jcm8111995

Moraes, J. A., Encarnação, C., Franco, V. A., Xavier Botelho, L. G., Rodrigues, G. P., Ramos-Andrade, I., . . . Renovato-Martins, M. (2021). Adipose tissue-derived extracellular vesicles and the tumor microenvironment: Revisiting the hallmarks of cancer. *Cancers, 13*(13), 3328. doi:10.3390/cancers13133328

Mulcahy, L. A., Pink, R. C., & Carter, D. R. F. (2014). Routes and mechanisms of extracellular vesicle uptake. *Journal of Extracellular Vesicles, 3*, 10.3402/jev.v3.24641. doi:10.3402/jev.v3.24641

Munhoz da Rocha, I. F., Amatuzzi, R. F., Lucena, A. C. R., Faoro, H., & Alves, L. R. (2020). Cross-kingdom extracellular vesicles EV-RNA communication as a mechanism for Host–Pathogen interaction. *Frontiers in Cellular and Infection Microbiology, 10*, 593160. doi:10.3389/fcimb.2020.593160

Nagao-Kitamoto, H., Kitamoto, S., Kuffa, P., & Kamada, N. (2016). Pathogenic role of the gut microbiota in gastrointestinal diseases. *Intestinal Research, 14*(2), 127–138. doi:10.5217/ir.2016.14.2.127

National Statistics. (2023). Cancer survival: Index for sub-integrated care boards, 2005 to 2020. Retrieved from https://digital.nhs.uk/data-and-information/publications/statistical/cancer-survival-in-england/index-for-sub-integrated-care-boards-2005-to-2020

Nawaz, M., Shah, N., Zanetti, B. R., Maugeri, M., Silvestre, R. N., Fatima, F., . . . Valadi, H. (2018). Extracellular vesicles and matrix remodeling enzymes: The emerging roles in extracellular matrix remodeling, progression of diseases and tissue repair. *Cells, 7*(10), 167. doi:10.3390/cells7100167

Nishida, A., Inoue, R., Inatomi, O., Bamba, S., Naito, Y., & Andoh, A. (2018). Gut microbiota in the pathogenesis of inflammatory bowel disease. *Clinical Journal of Gastroenterology, 11*(1), 1–10. doi:10.1007/s12328-017-0813-5

Nougayrède, J., Homburg, S., Taieb, F., Boury, M., Brzuszkiewicz, E., Gottschalk, G., . . . Oswald, E. (2006). Escherichia coli induces DNA double-strand breaks in eukaryotic cells. *Science (New York, N.Y.), 313*(5788), 848–851. doi:10.1126/science.1127059

Ocansey, D. K. W., Zhang, L., Wang, Y., Yan, Y., Qian, H., Zhang, X., . . . Mao, F. (2020). Exosome-mediated effects and applications in inflammatory bowel disease. *Biological Reviews of the Cambridge Philosophical Society, 95*(5), 1287–1307. doi:10.1111/brv.12608

Ogata-Kawata, H., Izumiya, M., Kurioka, D., Honma, Y., Yamada, Y., Furuta, K., . . . Tsuchiya, N. (2014). Circulating exosomal microRNAs as biomarkers of colon cancer. *PloS One, 9*(4), e92921. doi:10.1371/journal.pone.0092921

Onfroy-Roy, L., Hamel, D., Foncy, J., Malaquin, L., & Ferrand, A. (2020). Extracellular matrix mechanical properties and regulation of the intestinal stem cells: When mechanics control fate. *Cells, 9*(12), 2629. doi:10.3390/cells9122629

Onódi, Z., Pelyhe, C., Terézia Nagy, C., Brenner, G. B., Almási, L., Kittel, Á, . . . Giricz, Z. (2018). Isolation of high-purity extracellular vesicles by the combination of iodixanol density gradient ultracentrifugation and bind-elute chromatography from blood plasma. *Frontiers in Physiology, 9* doi:10.3389/fphys.2018.01479

O'Sullivan, D. E., Sutherland, R. L., Town, S., Chow, K., Fan, J., Forbes, N., . . . Brenner, D. R. (2022). Risk factors for early-onset colorectal cancer: A

systematic review and meta-analysis. *Clinical Gastroenterology and Hepatology: The Official Clinical Practice Journal of the American Gastroenterological Association, 20*(6), 1229–1240.e5. doi:10.1016/j.cgh.2021.01.037

Palviainen, M., Saraswat, M., Varga, Z., Kitka, D., Neuvonen, M., Puhka, M., . . . Siljander, P. R. M. (2020). Extracellular vesicles from human plasma and serum are carriers of extravesicular cargo—Implications for biomarker discovery. *PLoS ONE, 15*(8), e0236439. doi:10.1371/journal.pone.0236439

Peterson, L. W., & Artis, D. (2014). Intestinal epithelial cells: Regulators of barrier function and immune homeostasis. *Nature Reviews. Immunology, 14*(3), 141–153. doi:10.1038/nri3608

Piacenza, F., Biesemeier, A., Farina, M., Piva, F., Jin, X., Pavoni, E., . . . Malavolta, M. (2018). Measuring zinc in biological nanovesicles by multiple analytical approaches. *Journal of Trace Elements in Medicine and Biology, 48*, 58–66. doi:10.1016/j.jtemb.2018.03.010

Pino, M. S., & Chung, D. C. (2010). The chromosomal instability pathway in colon cancer. *Gastroenterology, 138*(6), 2059–2072. doi:10.1053/j.gastro.2009.12.065

Popēna, I., Ābols, A., Saulīte, L., Pleiko, K., Zandberga, E., Jēkabsons, K., . . . Riekstiņa, U. (2018). Effect of colorectal cancer-derived extracellular vesicles on the immunophenotype and cytokine secretion profile of monocytes and macrophages. *Cell Communication and Signaling: CCS, 16*(1), 17. doi:10.1186/s12964-018-0229-y

Proença, M. A., Biselli, J. M., Succi, M., Severino, F. E., Berardinelli, G. N., Caetano, A., . . . Silva, A. E. (2018). Relationship between fusobacterium nucleatum, inflammatory mediators and microRNAs in colorectal carcinogenesis. *World Journal of Gastroenterology, 24*(47), 5351–5365. doi:10.3748/wjg.v24.i47.5351

Quan, G., Xia, P., Lian, S., Wu, Y., & Zhu, G. (2020). Zinc uptake system ZnuACB is essential for maintaining pathogenic phenotype of F4ac+

enterotoxigenic E. coli (ETEC) under a zinc restricted environment. *Veterinary Research, 51*(1), 127. doi:10.1186/s13567-020-00854-1

Raeven, P., Zipperle, J., & Drechsler, S. (2018). Extracellular vesicles as markers and mediators in sepsis. *Theranostics, 8*(12), 3348–3365. doi:10.7150/thno.23453

Rahmati, Moeinafshar, & Rezaei. (2024). The multifaceted role of extracellular vesicles (EVs) in colorectal cancer: Metastasis, immune suppression, therapy resistance, and autophagy crosstalk. *Journal of Translational Medicine, 22*(1), 452. doi:10.1186/s12967-024-05267-8

Ramachandran, R. P., Vences-Catalán, F., Wiseman, D., Zlotkin-Rivkin, E., Shteyer, E., Melamed-Book, N., . . . Aroeti, B. (2018). EspH suppresses erk by spatial segregation from CD81 tetraspanin microdomains. *Infection and Immunity, 86*(10), 303. doi:10.1128/IAI.00303-18

Ranjbar, M., Salehi, R., Haghjooy Javanmard, S., Rafiee, L., Faraji, H., Jafarpor, S., . . . Nedaeinia, R. (2021). The dysbiosis signature of fusobacterium nucleatum in colorectal cancer-cause or consequences? A systematic review. *Cancer Cell International, 21*(1), 194. doi:10.1186/s12935-021-01886-z

Raskov, H., Kragh, K. N., Bjarnsholt, T., Alamili, M., & Gögenur, I. (2018). Bacterial biofilm formation inside colonic crypts may accelerate colorectal carcinogenesis. *Clinical and Translational Medicine, 7*(1), 30. doi:10.1186/s40169-018-0209-2

Rawls, J. F., Mahowald, M. A., Ley, R. E., & Gordon, J. I. (2006). Reciprocal gut microbiota transplants from zebrafish and mice to germ-free recipients reveal host habitat selection. *Cell, 127*(2), 423–433. doi:10.1016/j.cell.2006.08.043

Ren, J., Ding, L., Zhang, D., Shi, G., Xu, Q., Shen, S., . . . Hou, Y. (2018). Carcinoma-associated fibroblasts promote the stemness and chemoresistance of colorectal cancer by transferring exosomal lncRNA H19. *Theranostics, 8*(14), 3932–3948. doi:10.7150/thno.25541

Reunanen, N., & Kähäri, V. (2013). Matrix metalloproteinases in cancer cell invasion. *Madame curie bioscience database [internet]* Landes Bioscience. Retrieved from https://www.ncbi.nlm.nih.gov/books/NBK6598/

Rizzatti, G., Lopetuso, L. R., Gibiino, G., Binda, C., & Gasbarrini, A. (2017). Proteobacteria: A common factor in human diseases. *BioMed Research International, 2017*, 9351507. doi:10.1155/2017/9351507

Rodrigues-Junior, D. M., Tsirigoti, C., Lim, S. K., Heldin, C., & Moustakas, A. (2022). Extracellular vesicles and transforming growth factor β signaling in cancer. *Frontiers in Cell and Developmental Biology, 10*, 849938. doi:10.3389/fcell.2022.849938

Rubinstein, M. R., Wang, X., Liu, W., Hao, Y., Cai, G., & Han, Y. W. (2013). Fusobacterium nucleatum promotes colorectal carcinogenesis by modulating E-cadherin/β-catenin signaling via its FadA adhesin. *Cell Host & Microbe, 14*(2), 195–206. doi:10.1016/j.chom.2013.07.012

Runova, O. L., & Golubkov, V. I. (2002). [Protein of escherichia coli interacting specifically with human low density lipoproteins]. *Vestnik Rossiiskoi Akademii Meditsinskikh Nauk,* (12), 39–41. Retrieved from https://pubmed.ncbi.nlm.nih.gov/12611175/

Russo, Gloria, Nannini, Meoni, Niccolai, Ringressi, . . . Amedei. (2023). From adenoma to CRC stages: The oral-gut microbiome axis as a source of potential microbial and metabolic biomarkers of malignancy. *Neoplasia (New York, N.Y.), 40*, 100901. doi:10.1016/j.neo.2023.100901

Saus, E., Iraola-Guzmán, S., Willis, J. R., Brunet-Vega, A., & Gabaldón, T. (2019). Microbiome and colorectal cancer: Roles in carcinogenesis and clinical potential. *Molecular Aspects of Medicine, 69*, 93–106. doi:10.1016/j.mam.2019.05.001

Schippa, S., & Conte, M. P. (2014). Dysbiotic events in gut microbiota: Impact on human health. *Nutrients, 6*(12), 5786–5805. doi:10.3390/nu6125786

Schluter, J., & Foster, K. R. (2012). The evolution of mutualism in gut microbiota via host epithelial selection. *PLoS Biology, 10*(11), e1001424. doi:10.1371/journal.pbio.1001424

Secher, T., Samba-Louaka, A., Oswald, E., & Nougayrède, J. (2013). Escherichia coli producing colibactin triggers premature and transmissible senescence in mammalian cells. *PloS One, 8*(10), e77157. doi:10.1371/journal.pone.0077157

Sender, R., Fuchs, S., & Milo, R. (2016). Revised estimates for the number of human and bacteria cells in the body. *PLoS Biology, 14*(8), e1002533. doi:10.1371/journal.pbio.1002533

Shah, S. C., & Itzkowitz, S. H. (2022). Colorectal cancer in inflammatory bowel disease: Mechanisms and management. *Gastroenterology, 162*(3), 715–730.e3. doi:10.1053/j.gastro.2021.10.035

Sharp, C., & Foster, K. R. (2022). Host control and the evolution of cooperation in host microbiomes. *Nature Communications, 13*(1), 3567. doi:10.1038/s41467-022-30971-8

Shen, Q., Huang, Z., Yao, J., & Jin, Y. (2022). Extracellular vesicles-mediated interaction within intestinal microenvironment in inflammatory bowel disease. *Journal of Advanced Research, 37*, 221–233. doi:10.1016/j.jare.2021.07.002

Shoaie, S., & Nielsen, J. (2014). Elucidating the interactions between the human gut microbiota and its host through metabolic modeling. *Frontiers in Genetics, 5*, 86. doi:10.3389/fgene.2014.00086

Shopova, I. A., Belyaev, I., Dasari, P., Jahreis, S., Stroe, M. C., Cseresnyés, Z., . . . Brakhage, A. A. (2020). Human neutrophils produce antifungal extracellular vesicles against aspergillus fumigatus. *mBio, 11*(2), 596. doi:10.1128/mBio.00596-20

Silva, Y. P., Bernardi, A., & Frozza, R. L. (2020). The role of short-chain fatty acids from gut microbiota in gut-brain communication. *Frontiers in Endocrinology, 11* doi:10.3389/fendo.2020.00025

Skalitzky, M. K., Zhou, P. P., Goffredo, P., Guyton, K., Sherman, S. K., Gribovskaja-Rupp, I., . . . Hrabe, J. E. (2023). Characteristics and symptomatology of colorectal cancer in the young. *Surgery, 173*(5), 1137–1143. doi:10.1016/j.surg.2023.01.018

Smyth, T. J., Redzic, J. S., Graner, M. W., & Anchordoquy, T. J. (2014). Examination of the specificity of tumor cell derived exosomes with tumor cells in vitro. *Biochimica Et Biophysica Acta, 1838*(11), 2954–2965. doi:10.1016/j.bbamem.2014.07.026

Sobhani, I., Amiot, A., Le Baleur, Y., Levy, M., Auriault, M., Van Nhieu, J. T., & Delchier, J. C. (2013). Microbial dysbiosis and colon carcinogenesis: Could colon cancer be considered a bacteria-related disease? *Therapeutic Advances in Gastroenterology, 6*(3), 215–229. doi:10.1177/1756283X12473674

Stoffel, E. M., & Kastrinos, F. (2014). Familial colorectal cancer, beyond lynch syndrome. *Clinical Gastroenterology and Hepatology: The Official Clinical Practice Journal of the American Gastroenterological Association, 12*(7), 1059–1068. doi:10.1016/j.cgh.2013.08.015

Strofilas, A., Lagoudianakis, E. E., Seretis, C., Pappas, A., Koronakis, N., Keramidaris, D., . . . Manouras, A. (2012). Association of helicobacter pylori infection and colon cancer. *Journal of Clinical Medicine Research, 4*(3), 172–176. doi:10.4021/jocmr880w

Suwakulsiri, W., Xu, R., Rai, A., Shafiq, A., Chen, M., Greening, D. W., & Simpson, R. J. (2024). Comparative proteomic analysis of three major extracellular vesicle classes secreted from human primary and metastatic colorectal cancer cells: Exosomes, microparticles, and shed midbody remnants. *Proteomics, 24*(11), e2300057. doi:10.1002/pmic.202300057

Suzuki, K., Meek, B., Doi, Y., Muramatsu, M., Chiba, T., Honjo, T., & Fagarasan, S. (2004). Aberrant expansion of segmented filamentous bacteria in IgA-deficient gut. *Proceedings of the National Academy of Sciences of the United States of America, 101*(7), 1981–1986. doi:10.1073/pnas.0307317101

Tang, X., Chang, C., Guo, J., Lincoln, V., Liang, C., Chen, M., . . . Li, W. (2019). Tumour-secreted Hsp90α on external surface of exosomes mediates tumour - stromal cell communication via autocrine and paracrine mechanisms. *Scientific Reports, 9*(1), 1–13. doi:10.1038/s41598-019-51704-w

Tao, & Guo. (2020). Role of extracellular vesicles in tumour microenvironment. *Cell Communication and Signaling : CCS, 18*, 163. doi:10.1186/s12964-020-00643-5

Théry, C., Witwer, K. W., Aikawa, E., Alcaraz, M. J., Anderson, J. D., Andriantsitohaina, R., . . . Zuba-Surma, E. K. (2018). Minimal information for studies of extracellular vesicles 2018 (MISEV2018): A position statement of the international society for extracellular vesicles and update of the MISEV2014 guidelines. *Journal of Extracellular Vesicles, 7*(1), 1535750. doi:10.1080/20013078.2018.1535750

Titu, S., Gata, V. A., Decea, R. M., Mocan, T., Dina, C., Irimie, A., & Lisencu, C. I. (2023). Exosomes in colorectal cancer: From physiology to clinical applications. *International Journal of Molecular Sciences, 24*(5), 4382. doi:10.3390/ijms24054382

Tomasello, G., Tralongo, P., Damiani, P., Sinagra, E., Di Trapani, B., Zeenny, M. N., . . . Leone, A. (2014). Dismicrobism in inflammatory bowel disease and colorectal cancer: Changes in response of colocytes. *World Journal of Gastroenterology, 20*(48), 18121–18130. doi:10.3748/wjg.v20.i48.18121

Tomkovich, S., Dejea, C. M., Winglee, K., Drewes, J. L., Chung, L., Housseau, F., . . . Sears, C. L. (2019). Human colon mucosal biofilms from healthy or colon cancer hosts are carcinogenic. *The Journal of Clinical Investigation, 129*(4), 1699–1712. doi:10.1172/JCI124196

Toyofuku, M., Nomura, N., & Eberl, L. (2019). Types and origins of bacterial membrane vesicles. *Nature Reviews. Microbiology, 17*(1), 13–24. doi:10.1038/s41579-018-0112-2

Toyota, M., Ahuja, N., Ohe-Toyota, M., Herman, J. G., Baylin, S. B., & Issa, J. J. (1999). CpG island methylator phenotype in colorectal cancer. *Proceedings of the National Academy of Sciences of the United States of America, 96*(15), 8681–8686. Retrieved from https://www.ncbi.nlm.nih.gov/pmc/articles/PMC17576/

Tytgat, H. L. P., Nobrega, F. L., van der Oost, J., & de Vos, W. M. (2019). Bowel biofilms: Tipping points between a healthy and compromised gut? *Trends in Microbiology, 27*(1), 17–25. doi:10.1016/j.tim.2018.08.009

Umwali, Y., Yue, C., Gabriel, A. N. A., Zhang, Y., & Zhang, X. (2021). Roles of exosomes in diagnosis and treatment of colorectal cancer. *World Journal of Clinical Cases, 9*(18), 4467–4479. doi:10.12998/wjcc.v9.i18.4467

Urabe, F., Kosaka, N., Ito, K., Kimura, T., Egawa, S., & Ochiya, T. (2020). Extracellular vesicles as biomarkers and therapeutic targets for cancer. *American Journal of Physiology. Cell Physiology, 318*(1), C29–C39. doi:10.1152/ajpcell.00280.2019

Ursell, L. K., Metcalf, J. L., Parfrey, L. W., & Knight, R. (2012). Defining the human microbiome. *Nutrition Reviews, 70 Suppl 1*(Suppl 1), 38. doi:10.1111/j.1753-4887.2012.00493.x

Valenti, R., Huber, V., Filipazzi, P., Pilla, L., Sovena, G., Villa, A., . . . Rivoltini, L. (2006). Human tumor-released microvesicles promote the differentiation of myeloid cells with transforming growth factor-beta-mediated suppressive activity on T lymphocytes. *Cancer Research, 66*(18), 9290–9298. doi:10.1158/0008-5472.CAN-06-1819

Valter, M., Verstockt, S., Finalet Ferreiro, J. A., & Cleynen, I. (2021). Extracellular vesicles in inflammatory bowel disease: Small particles, big players. *Journal of Crohn's & Colitis, 15*(3), 499–510. doi:10.1093/ecco-jcc/jjaa179

van Bergenhenegouwen, J., Kraneveld, A. D., Rutten, L., Kettelarij, N., Garssen, J., & Vos, A. P. (2014). Extracellular vesicles modulate host-microbe responses by altering TLR2 activity and phagocytosis. *PloS One, 9*(2), e89121. doi:10.1371/journal.pone.0089121

van Niel, G., D'Angelo, G., & Raposo, G. (2018). Shedding light on the cell biology of extracellular vesicles. *Nature Reviews. Molecular Cell Biology, 19*(4), 213–228. doi:10.1038/nrm.2017.125

Veziant, J., Gagnière, J., Jouberton, E., Bonnin, V., Sauvanet, P., Pezet, D., . . . Bonnet, M. (2016). Association of colorectal cancer with pathogenic escherichia coli: Focus on mechanisms using optical imaging. *World Journal of Clinical Oncology, 7*(3), 293–301. doi:10.5306/wjco.v7.i3.293

Wan, Y., & Zhang, B. (2022). The impact of zinc and zinc homeostasis on the intestinal mucosal barrier and intestinal diseases. *Biomolecules, 12*(7), 900. doi:10.3390/biom12070900

Wang, D., Wang, X., Song, Y., Si, M., Sun, Y., Liu, X., . . . Yu, X. (2022). Exosomal miR-146a-5p and miR-155-5p promote CXCL12/CXCR7-induced metastasis of colorectal cancer by crosstalk with cancer-associated fibroblasts. *Cell Death & Disease, 13*(4), 380. doi:10.1038/s41419-022-04825-6

Wang, M., Su, Z., & Amoah Barnie, P. (2020). Crosstalk among colon cancer-derived exosomes, fibroblast-derived exosomes, and macrophage phenotypes in colon cancer metastasis. *International Immunopharmacology, 81*, 106298. doi:10.1016/j.intimp.2020.106298

Wang, T., Cai, G., Qiu, Y., Fei, N., Zhang, M., Pang, X., . . . Zhao, L. (2012). Structural segregation of gut microbiota between colorectal cancer patients and healthy volunteers. *The ISME Journal, 6*(2), 320–329. doi:10.1038/ismej.2011.109

Wang, Y., & Fu, K. (2023). Genotoxins: The mechanistic links between escherichia coli and colorectal cancer. *Cancers, 15*(4), 1152. doi:10.3390/cancers15041152

Wassenaar, T. M. (2018). E. coli and colorectal cancer: A complex relationship that deserves a critical mindset. *Critical Reviews in Microbiology, 44*(5), 619–632. doi:10.1080/1040841X.2018.1481013

Webber, J., Steadman, R., Mason, M. D., Tabi, Z., & Clayton, A. (2010). Cancer exosomes trigger fibroblast to myofibroblast differentiation. *Cancer Research, 70*(23), 9621–9630. doi:10.1158/0008-5472.CAN-10-1722

Weiland-Bräuer, N., Neulinger, S. C., Pinnow, N., Künzel, S., Baines, J. F., & Schmitz, R. A. (2015). Composition of bacterial communities associated with aurelia aurita changes with compartment, life stage, and population. *Applied and Environmental Microbiology, 81*(17), 6038–6052. doi:10.1128/AEM.01601-15

Williams, C., Pazos, R., Royo, F., González, E., Roura-Ferrer, M., Martinez, A., . . . Falcón-Pérez, J. M. (2019). Assessing the role of surface glycans of extracellular vesicles on cellular uptake. *Scientific Reports, 9*(1), 11920. doi:10.1038/s41598-019-48499-1

Wilson, M. R., Jiang, Y., Villalta, P. W., Stornetta, A., Boudreau, P. D., Carrá, A., . . . Balskus, E. P. (2019). The human gut bacterial genotoxin colibactin alkylates DNA. *Science (New York, N.Y.), 363*(6428), eaar7785. doi:10.1126/science.aar7785

Winter, S. E., Winter, M. G., Xavier, M. N., Thiennimitr, P., Poon, V., Keestra, A. M., . . . Bäumler, A. J. (2013). Host-derived nitrate boosts growth of E. coli in the inflamed gut. *Science (New York, N.Y.), 339*(6120), 708–711. doi:10.1126/science.1232467

Wong, W., Lee, M. M., Chan, B. D., Kam, R. K., Zhang, G., Lu, A., & Tai, W. C. (2016). Proteomic profiling of dextran sulfate sodium induced acute ulcerative colitis mice serum exosomes and their immunomodulatory impact on macrophages. *Proteomics, 16*(7), 1131–1145. doi:10.1002/pmic.201500174

Wu, J., Dong, W., Pan, Y., Wang, J., Wu, M., & Yu, Y. (2023). Crosstalk between gut microbiota and metastasis in colorectal cancer: Implication of neutrophil extracellular traps. *Frontiers in Immunology, 14*, 1296783. doi:10.3389/fimmu.2023.1296783

Wu, L., & Gao, C. (2023). Comprehensive overview the role of glycosylation of extracellular vesicles in cancers. *ACS Omega, 8*(50), 47380–47392. doi:10.1021/acsomega.3c07441

Wu, N., Feng, Y., Lyu, N., Wang, D., Yu, W., & Hu, Y. (2022). Fusobacterium nucleatum promotes colon cancer progression by changing the mucosal microbiota and colon transcriptome in a mouse model. *World Journal of Gastroenterology, 28*(18), 1981–1995. doi:10.3748/wjg.v28.i18.1981

Wu, N., Yang, X., Zhang, R., Li, J., Xiao, X., Hu, Y., . . . Zhu, B. (2013). Dysbiosis signature of fecal microbiota in colorectal cancer patients. *Microbial Ecology, 66*(2), 462–470. doi:10.1007/s00248-013-0245-9

Wu, S., Rhee, K., Zhang, M., Franco, A., & Sears, C. L. (2007). Bacteroides fragilis toxin stimulates intestinal epithelial cell shedding and gamma-secretase-dependent E-cadherin cleavage. *Journal of Cell Science, 120*(Pt 11), 1944–1952. doi:10.1242/jcs.03455

Wu, T., Gagnon, A., McGourty, K., DosSantos, R., Chanetsa, L., Zhang, B., . . . Kelleher, S. L. (2021). Zinc exposure promotes commensal-to-pathogen transition in pseudomonas aeruginosa leading to mucosal inflammation and illness in mice. *International Journal of Molecular Sciences, 22*(24), 13321. doi:10.3390/ijms222413321

Xiao, Y., Zhong, J., Zhong, B., Huang, J., Jiang, L., Jiang, Y., . . . Zhong, T. (2020). Exosomes as potential sources of biomarkers in colorectal cancer. *Cancer Letters, 476*, 13–22. doi:10.1016/j.canlet.2020.01.033

Xu, R., Greening, D. W., Chen, M., Rai, A., Ji, H., Takahashi, N., & Simpson, R. J. (2019). Surfaceome of exosomes secreted from the colorectal cancer cell line SW480: Peripheral and integral membrane proteins analyzed by proteolysis and TX114. *Proteomics, 19*(8), e1700453. doi:10.1002/pmic.201700453

Yadav, D., Ghosh, T. S., & Mande, S. S. (2016). Global investigation of composition and interaction networks in gut microbiomes of individuals

belonging to diverse geographies and age-groups. *Gut Pathogens, 8*, 17. doi:10.1186/s13099-016-0099-z

Yan. (2020). Mechanistic understanding of the symbiotic relationship between the gut microbiota and the host. *Cellular and Molecular Gastroenterology and Hepatology, 10*(4), 853–854. doi:10.1016/j.jcmgh.2020.05.003

Yang, J., Wei, H., Zhou, Y., Szeto, C., Li, C., Lin, Y., . . . Yu, J. (2022). High-fat diet promotes colorectal tumorigenesis through modulating gut microbiota and metabolites. *Gastroenterology, 162*(1), 135–149.e2. doi:10.1053/j.gastro.2021.08.041

Yang, Y., Weng, W., Peng, J., Hong, L., Yang, L., Toiyama, Y., . . . Ma, Y. (2017). Fusobacterium nucleatum increases proliferation of colorectal cancer cells and tumor development in mice by activating toll-like receptor 4 signaling to nuclear factor-κB, and up-regulating expression of MicroRNA-21. *Gastroenterology, 152*(4), 851–866.e24. doi:10.1053/j.gastro.2016.11.018

Yin, Y., Liu, B., Cao, Y., Yao, S., Liu, Y., Jin, G., . . . Huang, Z. (2022). Colorectal cancer-derived small extracellular vesicles promote tumor immune evasion by upregulating PD-L1 expression in tumor-associated macrophages. *Advanced Science (Weinheim, Baden-Wurttemberg, Germany), 9*(9), 2102620. doi:10.1002/advs.202102620

You, Y., Shan, Y., Chen, J., Yue, H., You, B., Shi, S., . . . Cao, X. (2015). Matrix metalloproteinase 13-containing exosomes promote nasopharyngeal carcinoma metastasis. *Cancer Science, 106*(12), 1669–1677. doi:10.1111/cas.12818

Yu, J., He, Z., He, X., Luo, Z., Lian, L., Wu, B., . . . Chen, H. (2021). Comprehensive analysis of the expression and prognosis for MMPs in human colorectal cancer. *Frontiers in Oncology, 11* doi:10.3389/fonc.2021.771099

Yuan, C., Burns, M. B., Subramanian, S., & Blekhman, R. (2018). Interaction between host MicroRNAs and the gut microbiota in colorectal cancer. *mSystems, 3*(3), 205. doi:10.1128/mSystems.00205-17

Yusuf, Sampath, & Umar. (2023). Bacterial infections and cancer: Exploring this association and its implications for cancer patients. *International Journal of Molecular Sciences, 24*(4), 3110. doi:10.3390/ijms24043110

Zhang, G., Khan, N., Kim, K., Stins, M., & Kim, K. (2002). Transforming growth factor-β increases escherichia coli K1 adherence, invasion, and transcytosis in human brain microvascular endothelial cells. *Cell and Tissue Research, 309*(2), 281–286. doi:10.1007/s00441-002-0549-4

Zhang, Y., Li, S., Gan, R., Zhou, T., Xu, D., & Li, H. (2015). Impacts of gut bacteria on human health and diseases. *International Journal of Molecular Sciences, 16*(4), 7493–7519. doi:10.3390/ijms16047493

Zhao, S., Mi, Y., Guan, B., Zheng, B., Wei, P., Gu, Y., . . . Li, D. (2020). Tumor-derived exosomal miR-934 induces macrophage M2 polarization to promote liver metastasis of colorectal cancer. *Journal of Hematology & Oncology, 13*(1), 156. doi:10.1186/s13045-020-00991-2

Zhao, S., Mi, Y., Zheng, B., Wei, P., Gu, Y., Zhang, Z., . . . Li, D. (2022). Highly-metastatic colorectal cancer cell released miR-181a-5p-rich extracellular vesicles promote liver metastasis by activating hepatic stellate cells and remodelling the tumour microenvironment. *Journal of Extracellular Vesicles, 11*(1), e12186. doi:10.1002/jev2.12186

Zhou, P., Yang, D., Sun, D., & Zhou, Y. (2022). Gut microbiome: New biomarkers in early screening of colorectal cancer. *Journal of Clinical Laboratory Analysis, 36*(5), e24359. doi:10.1002/jcla.24359